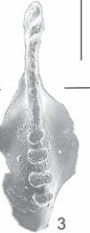




Permophiles

International Commission on Stratigraphy



Asselian Stage		Sakmarian Stage		Artinskian Stage	
Conodont Zone					
<i>postfusus</i>	<i>aff. merrilli</i>	<i>binodosus</i>	<i>anceps</i>	<i>asymmetricus</i>	
					
1	2	3	4	5	6



**Newsletter of the
Subcommission on
Permian Stratigraphy
Number 72
ISSN 1684-5927
January 2022**

Table of Contents

Notes from SPS Secretary Yichun Zhang	3
Notes from SPS Chair Lucia Angiolini	4
Annual Report 2021	5
Henderson's Harangue #9 Charles M. Henderson	8
Answers to comments on Artinskian Proposal	9
Final proposal for the Global Stratotype Section and Point (GSSP) for the base-Artinskian Stage (Lower Permian) Valery V. Chernykh, Charles M. Henderson, Ruslan V. Kutygin, Tatiana V. Filimonova, Guzal M. Sungatullina, Marina S. Afanasieva, Tatiana N. Isakova, Rafael Kh. Sungatullin, Michael H. Stephenson, Lucia Angiolini, Boris I. Chuvashov	14
Middle Kungurian (Early Permian) seaways in the southwestern USA Spencer G. Lucas, Charles Henderson, James E. Barrick, Karl Krainer	48
Update: improved palynological resolution in the latest Permian of the Levant Michael H. Stephenson	52
Call to the Permian community: Identifying an enigmatic sedimentary structure from the Bromacker Frank Scholze, Anna Pint, Peter Frenzel	53
Celebrating the 180th anniversary of the establishment of the Permian System –report on Kazan Golovkinsky Stratigraphic Meeting 2021 Joerg W. Schneider, Vladimir V. Silantiev, Milyausha N. Urazaeva, Veronika V. Zharinova, Ilja Kogan	57
Extended abstracts of the projects funded by SPS	
Correlating the continental end-Permian biome collapse (Lopingian) across eastern Australia Chris Mays	60
Correlation between the Cisuralian successions of the Robledo Mountains (New Mexico) and the Carnic Alps (Austria) integrating conodont and foraminifer biostratigraphy Daniel Calvo Gonzalez	61
Everything on track(s): Upcoming excavation for an exceptional Middle to Upper Permian ichnofauna in central Germany Daniel Falk	67
Stratigraphic gap associated with the Permian-Triassic succession in the continental deposits of SW Europe: time constraints, stratigraphic correlations and paleogeography inferences Joan Lloret	69
Memorial to Claude Spinosa 17 July 1937 – 5 September 2021 Tamra A. Schiappa, Walter Snyder	
SUBMISSION GUIDELINES FOR ISSUE 73	

Fig. 1. Outcrop sections photographs of the still active quarry in the Bromacker area, Scholze et al., this issue.

Fig. 2. Selected outcrops of Kungurian strata in New Mexico and Arizona, Lucas et al., this issue.

Fig. 3. The evolutionary lineage of conodonts from Asselian to Artinskian stages, Chernykh et al., this issue.

Fig. 4. Claude Spinosa with Brian Glenister, Tatyana Leonova, and a student, in Aktubinsk, during summer 1991 field conference, Schiappa and Snyder, this issue.

72

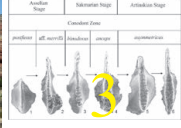


Permophiles

International Commission on Stratigraphy











Newsletter of the
Subcommission on
Permian Stratigraphy
Number 72
ISSN 1684-5927
January 2022

Notes from the SPS secretary

Yichun Zhang

Introduction and thanks

Time flies, and, it's time for me to edit a new issue of *Permophiles*. Covid-19 pandemic was continuing to be a threat to public health that hampers, to some extent, on-site meetings, international collaborations and joint fieldworks. However, during the past half year, under the leadership of Profs. Lucia Angiolini and Michael Stephenson, SPS has done many works including webinar meetings, small projects funding and voting to base-Artinskian GSSP. Thanks to Lucia and Mike for their great efforts.

Many thanks to the contributors of this issue: Charles M. Henderson, Valery V. Chernykh and co-authors, Spencer G. Lucas and co-authors, Michael H. Stephenson, Frank Scholze and co-authors, Joerg W. Schneider and co-authors, Tamra A. Schiappa and Walter Snyder and four small project winners, Chris Mays, Daniel Calvo Gonzalez, Daniel Falk and Lloret Joan.

Finally, I would like to keep drawing your attention to the new SPS website <https://permian.stratigraphy.org/>, where you can find all issues of *Permophiles*, updated Permian Timescales, presentation videos and news about the Permian subcommission.

Permophiles 72

This issue of *Permophiles* contains fruitful contributions including comments and replies on the proposed base-Artinskian GSSP proposal, an updated proposal, extended abstracts by four small project winners, and enquiries about an interesting trace fossil. As I have repeated frequently, *Permophiles* is always an open platform for free discussions on Permian topics.

As usual, this issue starts with the ninth harangue by Charles M. Henderson. He still highlights to our Permian community the significance of integrating the sequence stratigraphy in defining a GSSP. This is significant in defining current base-Artinskian GSSP and future base-Kungurian GSSP.

Since the publication of the base-Artinskian GSSP proposal in last issue of *Permophiles*, an email discussion was opened among SPS voting members for one month since 18 August 2021. Shuzhong Shen, Charles M. Henderson, Guang, Shi, Joerg Schneider and a SPS corresponding member (Dr. Micha Horacek) had a heated discussion on several key questions with respect to the proposal including (1) correlations between the conodonts and fusulines; (2) the application of the proposed GSSP in Gondwana sections and (3) the geochemical data correlations between Dal'ny Tulkas sections and those sections in South China. Those comments and replies are provided in this issue. After the open discussion, a formal vote on the GSSP of base-Artinskian stage was conducted among SPS voting members. The proposal has been accepted by a majority of support. The result of vote is reported here (see below).

Spencer Lucas and his colleagues reviewed the Artinskian-Kungurian strata in the Delaware, Orogrande, Pedregosa basins and Arizona shelf in North America. Based on the correlations, a seaway was reconstructed from Arizona to the Delaware basin. Also, a significant transgression was recognized across the

American Southwest during middle Kungurian times.

Michael H. Stephenson introduced his recent work on the palynology in Israel and Levant. *Pretricolpipollenites bharadwajii* in the Arqov Formation indicates a Changhsingian age for part of this formation.

Frank Scholze and co-authors reported an enigmatic sedimentary structure from the Tambach sandstone in the Thuringian Forest Basin, Germany. They thought it might be a drag mark by a drifting object in shallow water above soft sediment. They ask trace fossils experts to give answers or comments on this special trace.

Joerg W. Schneider and his colleagues reported the contents of the Kazan Golovkinsky Stratigraphic Meeting, which was dedicated to the 180 anniversary of the establishment of the Permian system.

SPS has funded small projects of young researchers on Permian studies. In this issue of *Permophiles*, extended abstracts of their projects are provided by four winners, respectively Chris Mays, Daniel Calvo Gonzalez, Daniel Falk and Joan Lloret. Chris Mays's project aims at comparing the timing and amplitude of end-Permian mass extinction event in eastern Australia in order to test "Polar refugium" and "diachronous aridification" and establish the correlations of uppermost Permian and lowermost Triassic strata across Antarctica, India and southern Africa. Daniel Calvo Gonzalez's project focuses on the correlations of the Cisuralian (Lower Permian) successions in the Robledo Mountains of New Mexico and Carnic Alps of Austria based on biostratigraphy of both conodont and foraminifers. Daniel Falk's project deals with the study of the ichnofauna from the Hornburg Formation in the Hornburg Basin, central Germany. Joan Lloret's project aims to estimate and constrain the duration and age of the unconformity in selected key sections in SW Europe and to understand the evolution of Pangea. Those four projects are expected to bring new insights into focus including intercontinental correlations, and end-Permian mass extinction patterns.

Finally, very sadly, Prof. Claude Spinosa, honorary member of SPS, a famous ammonoid paleontologist, passed away on 5 September 2021. A memorial article was provided by Tamra A. Schiappa and Walter Snyder.

Report on the vote on the Global Stratotype Section and Point (GSSP) defining the base of the Artinskian stage of the Permian system

A call to vote on the Global Stratotype Section and Point (GSSP) defining the base of the Artinskian Stage of the Permian System has been sent to the SPS Voting Members on 18th October 2021, with the request of returning the vote by the 18th November 2021.

Proposal

The Global Stratotype Section and Point (GSSP) for the base of the Artinskian Stage (Permian System) is proposed at the point indicated by the FAD of *Sweetognathus asymmetricus* at 0.6 m above the base of bed 4b at the Dal'ny Tulkas section in the southern Urals of Russia. An interpolated geochronologic age

between 290.1 Ma \pm 0.2 Ma and 290.5 Ma \pm 0.4 Ma, strontium isotope values near 0.70767, and many additional fossils groups, particularly ammonoids and fusulines, serve as additional markers to correlate the boundary.

The record of voting by 17 SPS voting members is as follows:

Prof. Lucia Angiolini (SPS Chair) Dipartimento di Scienze Terra "A. Desio" Via Mangiagalli 34, 20133 Milano, Italy E-mail: lucia.angiolini@unimi.it, **Yes**

Dr. Alexander Biakov Northeast Interdisciplinary Scientific Research Institute, Far East Branch, Russian Academy of Sciences, Portovaya ul. 16, Magadan, 685000 Russia E-mail: abiakov@mail.ru, **Yes**

Dr. Valery Chernykh Institute of Geology and Geochemistry Urals Branch of Russian Academy of Science Pochtovy per 7 Ekaterinburg 620154 Russia E-mail: vtschernich@mail.ru, **Yes**

Dr. Valeriy K. Golubev Borissiak Paleontological Institute Russian Academy of Sciences Profsoyuznaya str. 123, Moscow, 117997 Russia E-mail: vg@paleo.ru, **Yes**

Prof. Charles M. Henderson Dept. of Geoscience University of Calgary Calgary, Alberta Canada T2N1N4 E-mail: cmhender@ucalgary.ca, **Yes**

Prof. Spencer G. Lucas New Mexico Museum of Natural History and Science 1801 Mountain Road N. W. Albuquerque, New Mexico 87104-1375 USA E-mail: spencer.lucas@state.nm.us, **Yes**

Prof. Ausonio Ronchi Dipartimento di Scienze della Terra e dell'Ambiente Università di Pavia - Via Ferrata 1, 27100 PV, ITALY voice +39-0382-985856 E-mail: ausonio.ronchi@unipv.it, **Yes**

Prof. Tamra A. Schiappa Department of Geography, Geology and the Environment Slippery Rock University Slippery Rock, PA 16057 USA E-mail: tamra.schiappa@sru.edu, **Yes**

Prof. Mark D. Schmitz Isotope Geology Laboratory Department of Geosciences Boise State University 1910 University Drive Boise, ID 83725-1535 E-mail: markschmitz@boisestate.edu, **Yes**

Prof. Joerg W. Schneider Freiberg University of Mining and Technology Institute of Geology, Dept. of Palaeontology, Bernhard-von-Cotta-Str.2 Freiberg, D-09596, Germany E-mail: Joerg.Schneider@geo.tu-freiberg.de, **Yes**

Prof. Shuzhong Shen. School of Earth Sciences and Engineering Nanjing University, 163 Xianlin Avenue, Nanjing, Jiangsu 210023, P.R.China E-mail: szshen@nju.edu.cn, **Yes**

Prof. Guang R. Shi School of Earth, Atmospheric and Life Sciences University of Wollongong Northfields Avenue, NSW 2522, Australia E-mail: guang@uow.edu.au, **Yes**

Prof. Michael H. Stephenson (SPS Vice-Chairman) British Geological Survey Kingsley Dunham Centre Keyworth, Nottingham NG12 5GG United Kingdom E-mail: mhste@bgs.ac.uk, **Yes**

Prof. Katsumi Ueno Department of Earth System Science, Fukuoka University, Fukuoka 814-0180 Japan email: kasumi@fukuoka-u.ac.jp, **No**

Prof. Yue Wang Nanjing Institute of Geology and Palaeontology, 39 East Beijing Rd. Nanjing, Jiangsu 210008, China E-mail: yuewang@nigpas.ac.cn, **Yes**

Prof. Yichun Zhang State Key laboratory of Palaeobiology and Stratigraphy Nanjing Institute of Geology and Palaeontology 39 East Beijing Road Nanjing, Jiangsu 210008, China E-mail: yczhang@nigpas.ac.cn, **Yes**

One voting member did not respond to the call and to the reminder for it: **Dr. Nestor R. Cuneo Museo** Paleontologico Egidio Feruglio (U9100GYO) Av. Fontana 140, Trelew, Chubut, Patagonia Argentina E-mail: rcuneo@mef.org.ar

The result is a 15-1 vote in favour (**93.75%**). The proposal for the Global Stratotype Section and Point (GSSP) for the base of the Artinskian Stage (Permian System) at the point indicated by the FAD of *Sweetognathus asymmetricus* at 0.6 m above the base of bed 4b at the Dal'ny Tulkas section in the southern Urals of Russia has been accepted by the Subcommittee on Permian Stratigraphy and then forwarded to ICS.

Future issues of Permophiles

The next issue of Permophiles will be the 73rd issue.

We welcome contributions related to Permian studies around the world. So, I kindly invite our colleagues to contribute harangues, papers, reports, comments and communications.

The deadline for submission to Issue 73 is 31 July 2022.

Manuscripts and figures can be submitted via email address (yczhang@nigpas.ac.cn) as attachment.

To format the manuscript, please follow the TEMPLATE on SPS website.

Notes from the SPS Chair

Lucia Angiolini

In the last few months we have been working hard on the proposal for the Global Stratotype Section and Point (GSSP) for the base of the Artinskian Stage (Lower Permian), a preliminary version of which was published in the SPS Newsletter *Permophiles* 71 by Chernykh et al. (2021). The proposal concerns the siting of the Global Boundary Stratotype Section and Point (GSSP) at 0.6 m above the base of bed 4b at the Dal'ny Tulkas section in the southern Urals of Russia. This point corresponds to the First Appearance Datum of the conodont *Sweetognathus asymmetricus*, which is part of a well defined and widely distributed lineage. An interpolated geochronologic age between 290.1 Ma \pm 0.2 Ma and 290.5 Ma \pm 0.4 Ma, a strontium isotope value of approximately 0.70767, and many additional fossils groups, particularly ammonoids and fusulines, serve as additional markers to correlate the boundary.

The proposal was discussed within the Permian community (see the report of the discussion in this issue of *Permophiles*) and then a call to vote on the Global Stratotype Section and Point (GSSP) defining the base of the Artinskian Stage of the Permian System has been sent to the SPS Voting Members in October 2021. The Artinskian Stage GSSP proposal was approved by SPS on 18th November 2021, based on the large majority of positive votes (see the Secretary Notes for more details).

A formal proposal of the Artinskian-base GSSP was then submitted to the International Commission on Stratigraphy (ICS) on 23 November 2021. Phil Gibbard, Secretary General of ICS, invited the voting members of ICS to formally approve

the proposal, following a period for e-mail discussion of the topic. The allotted period for discussion ended on 22 December 2021, after which formal voting has taken place, with the closing deadline on 26 January 2022. The proposal received very constructive questions and comments by several ICS voting members, which were answered and addressed and included in the final version of the proposal published in this issue of *Permophiles*.

I want to thank Charles Henderson and Mike Stephenson who helped to answer the comments of the SPS and ICS voting members, the dedication of Valery Chernykh and Guzel Sungatullina who constantly provided answers and data, and the work of Marina Afanasieva, Tatiana Isakova and Tatiana Filimonova. Many Thanks also to Fabio Franceschi who did the proposal drawings.

To increase the audience of the Permian Community and promote discussion, on the 11 November 2021, the webinar “Everything You Always Wanted to Know About Paleogeography (But Were Afraid to Ask)” by Giovanni Muttoni was organized live online through MS Teams:

<https://permian.stratigraphy.org/Interests/Giovanni>

This was followed by a lively discussion on Permian palaeogeographic reconstructions on 9 December 2021. A new webinar is scheduled for April 2022 by Prof Mike Simmons of Halliburton. This seminar will show how we can build stratigraphy using biostratigraphically constrained sequence stratigraphy, Earth systems science, and the relatively new technique of forward stratigraphic modelling.

We also organized a call to fund small projects of young researchers on Permian correlation. Four projects have been selected out of nine received and these obtained SPS funding. The projects were proposed by the following: Daniel Calvo Gonzalez, University of Calgary, Canada, Daniel Falk, University College Cork, School of Biological, Earth, and Environmental Sciences, Ireland, Joan Lloret, Instituto de Geociencias (IGEO), CSIC-UCM, Madrid, Spain, and Chris Mays, Swedish Museum of Natural History, Stockholm, Sweden. An extended summary of each project is published in this issue of *Permophiles*.

Shuzhong Shen and his research group are working on the replacement section for the previously-defined base of the Lopingian GSSP at the Penglaitan section in Guangxi, South China that has been permanently flooded due to a dam. They are studying a new outcrop at Penglaitan which is very close to the GSSP section, but also an additional section, the Fengshan section, which may represent an auxiliary section. Shuzhong Shen will provide more information to the Permian community in the next few months.

As always, I conclude my notes asking all of you to contribute to the discussion on Permian topics and to *Permophiles* and urging your comments and opinions which are very important to move Permian studies forward.

Finally, I want to warmly thank the SPS Secretary Yichun Zhang, who is very efficient in dealing with the work of the subcommission and in preparing *Permophiles*.

ANNUAL REPORT 2021

1. TITLE OF CONSTITUENT BODY and NAME OF REPORTER

International Subcommission on Permian Stratigraphy (SPS)
Submitted by: Lucia Angiolini, SPS Chair
Dipartimento di Scienze della Terra “A. Desio”, Via
Mangiagalli 34, 20133 Milano, Italy, E-mail: lucia.angiolini@unimi.it

2. OVERALL OBJECTIVES, AND FIT WITHIN IUGS SCIENCE POLICY

Subcommission Objectives: The Subcommission’s primary objective is to define the series and stages of the Permian by means of internationally agreed GSSPs and establish a high-resolution temporal framework based on multidisciplinary (biostratigraphical, geochronologic, chemostratigraphical, magnetostratigraphical etc.) approaches, and to provide the international forum for scientific discussion and interchange on all aspects of the Permian, but specifically on refined intercontinental and regional correlations.

Fit within IUGS Science Policy: The objectives of the Subcommission involve two main aspects of IUGS policy: 1) The development of an internationally agreed chronostratigraphic scale with units defined by GSSPs where appropriate and related to a hierarchy of units to maximize relative time resolution within the Permian System; and 2) the establishment of framework and systems to encourage international collaboration in understanding the evolution of the Earth and life during the Permian Period.

3 ORGANISATION - interface with other international projects / groups

3a. Officers for 2020-2024 period:

Prof. Lucia Angiolini (SPS Chair)

Dipartimento di Scienze della Terra “A. Desio”. Via Mangiagalli 34, 20133 Milano, Italy, E-mail: lucia.angiolini@unimi.it

Prof. Michael H. Stephenson (SPS Vice-chair)

British Geological Survey. Keyworth, Nottingham NG12 5GG, United Kingdom, E-mail: mhste@bgs.ac.uk

Prof. Yichun Zhang (SPS Secretary)

State Key laboratory of Palaeobiology and Stratigraphy. Nanjing Institute of Geology and Palaeontology
39 East Beijing Road, Nanjing, Jiangsu 210008, China, E-mail: yczhang@nigpas.ac.cn

4. EXTENT OF NATIONAL/REGIONAL/GLOBAL SUPPORT FROM SOURCES OTHER THAN IUGS

Shuzhong Shen and Michael Stephenson are investigating the possibility of support for SPS through the Deep-time Digital Earth (DDE) Big Science Program of IUGS focused on informatics support for biostratigraphic data management and palaeogeographic reconstructions.

5. CHIEF ACCOMPLISHMENTS IN 2021 (including any

relevant publications arising from ICS working groups)

•The proposal for the Global Stratotype Section and Point (GSSP) for the base-Artinskian Stage (Lower Permian) has been published in the SPS Newsletters Permophiles 71 by Chernykh et al. (2021). A call to vote on this GSSP was sent to the SPS Voting Members on October 2021. Based on the large majority of positive votes (15 out of 16), the proposal for the GSSP for the base of the Artinskian Stage at the point indicated by the FAD of the conodont *Sweetognathus asymmetricus* at the Dal'ny Tulkas section, Russia was accepted by the Subcommittee on Permian Stratigraphy. A formal proposal of the Artinskian-base GSSP has been submitted to the International Commission on Stratigraphy.

•A professional video was produced to advertise SPS at <https://www.youtube.com/watch?v=s2f1647pCpI> and two webinars were organized live online through zoom <https://www.youtube.com/watch?v=dzkjP84kvfI> <https://permian.stratigraphy.org/Interests/Giovanni>

•A call to fund small projects of young researchers on Permian correlation was organized and four projects were selected <https://permian.stratigraphy.org/news/2021-11-07>

•The Permian Time Scale was updated <https://permian.stratigraphy.org/gssps> and two issues of Permophiles were published (SPS Newsletters *Permophiles* 70 and 71).

6. SUMMARY OF EXPENDITURE IN 2021

An amount of Euros 5410 (= USD 6153,3) was spent for video preparation, literature compilation, Dal'ny Tulkas GSSP proposal preparation, and for funding projects of young researchers on Permian correlation. Due to Covid restrictions, it was not possible to do field work in Dal'ny Tulkas and Mechetlino as scheduled.

7. SUMMARY OF INCOME IN 2021

An amount of Euros 2963,39 was allocated from ICS. An additional amount of Euros 4112,79 was received for the Special Project: Turbocharging Permian GSSPs.

8. BUDGET REQUESTED FROM ICS IN 2022***

We apply for 4500 US\$ from ICS for SPS activities in 2022. This will be mainly for the activities to finalize the base-Artinskian GSSP at Dal'ny Tulkas section, establish the base-Kungurian GSSP at Mechetlino, Russia, and to organize a voting members field trip in the area.

9. WORK PLAN, CRITICAL MILESTONES, ANTICIPATED RESULTS AND COMMUNICATIONS TO BE ACHIEVED NEXT YEAR:

•We plan to have the base Artinskian GSSP ratified and start to work on the base Kungurian GSSP.

•We plan to organize several webinars.

•We plan to start a new working group on Gondwana Correlatin.

10. KEY OBJECTIVES AND WORK PLAN FOR THE PERIOD 2020-2024

•Establish the Artinskian and Kungurian GSSPs.

•Revise the Permian timescale where it needs to be improved (Guadalupian stages, replacement GSSP section of the base-

Lopingian).

•Establish a robust palaeogeographic frameworks for the Permian and focus on N-S correlations.

•Propose DDE-sponsored informatics support for biostratigraphic data management and palaeogeographic reconstructions.

•Organize webinars to increase the size, diversity and international coverage of the Permian Community

•Publish at least two *Permophiles* issues each year.

APPENDIX [Names and Addresses of Current Officers and Voting Members)

Prof. Lucia Angiolini (SPS Chair)

Dipartimento di Scienze della Terra "A. DEsio"
Via Mangiagalli 34, 20133, Milano, Italy
E-mail: lucia.angiolini@unimi.it

Dr. Alexander Biakov

Northeast Interdisciplinary Scientific Research Institute
Far East Branch, Russian Academy of Sciences,
Portovaya ul. 16, Magadan, 685000 Russia
E-mail: abiakov@mail.ru

Dr. Valery Chernykh

Institute of Geology and Geochemistry
Urals Branch of Russian Academy of Science
Pochtovy per 7, Ekaterinburg 620154 Russia
E-mail: vtschernich@mail.ru

Dr. Nestor R. Cuneo

Museo Paleontologico Egidio Feruglio
(U9100GYO) Av. Fontana 140,
Trelew, Chubut, Patagonia Argentina
E-mail: rcuneo@mef.org.ar

Dr. Valeriy K. Golubev

Borissiak Paleontological Institute, Russian Academy of Sciences
Profsoyuznaya str. 123, Moscow, 117997 Russia
E-mail: vg@paleo.ru

Prof. Charles M. Henderson

Dept. of Geoscience, University of Calgary
Calgary, Alberta, Canada T2N1N4
E-mail: cmhender@ucalgary.ca

Prof. Spencer G. Lucas

New Mexico Museum of Natural History and Science
1801 Mountain Road N. W., Albuquerque, New Mexico 87104-1375 USA
E-mail: spencer.lucas@state.nm.us

Prof. Ausonio Ronchi

Dipartimento di Scienze della Terra e dell'Ambiente
Università di Pavia - Via Ferrata 1, 27100 PV, ITALY
voce +39-0382-985856
E-mail: ausonio.ronchi@unipv.it

Dr. Tamra A. Schiappa

Department of Geography, Geology and the Environment
Slippery Rock University, Slippery Rock, PA 16057 USA
E-mail: tamra.schiappa@sru.edu

Prof. Mark D. Schmitz

Isotope Geology Laboratory
Department of Geosciences
Boise State University, 1910 University Drive
Boise, ID 83725-1535, USA
E-mail: markschmitz@boisestate.edu

Prof. Joerg W. Schneider

Freiburg University of Mining and Technology
Institute of Geology, Dept. of Palaeontology,
Bernhard-von-Cotta-Str.2, Freiberg, D-09596, Germany
E-mail: Joerg.Schneider@geo.tu-freiberg.de

Prof. Shuzhong Shen

School of Earth Sciences and Engineering
Nanjing University, 163 Xianlin Avenue,
Nanjing, Jiangsu 210023, P.R. China
E-mail: szshen@nju.edu.cn

Prof. Guang R. Shi

School of Earth, Atmospheric and Life Sciences
University of Wollongong,
Northfields Avenue, NSW 2522, Australia
E-mail: guang@uow.edu.au

Prof. Michael H. Stephenson (SPS Vice-Chair)

British Geological Survey, Kingsley Dunham Centre
Keyworth, Nottingham NG12 5GG
United Kingdom
E-mail: mhste@bgs.ac.uk

Prof. Katsumi Ueno

Department of Earth System Science
Fukuoka University, Fukuoka 814-0180 JAPAN
E-mail: katsumi@fukuoka-u.ac.jp

Prof. Yue Wang

Nanjing Institute of Geology and Palaeontology,
39 East Beijing Rd. Nanjing, Jiangsu 210008, China
E-mail: yuewang@nigpas.ac.cn

Prof. Yichun Zhang (SPS Secretary)

Nanjing Institute of Geology and Palaeontology
39 East Beijing Road, Nanjing, Jiangsu 210008, China
E-mail: yczhang@nigpas.ac.cn

Working group leaders

1) Artinskian-base and Kungurian-base GSSP Working Group;
Chair-Valery Chernykh.

2) Correlation between marine and continental Guadalupian
Working Group; Chair-Charles Henderson.

3) Carboniferous-Permian-Triassic Nonmarine-Marine
Correlation Working Group ; Chair-Joerg Schneider.

Honorary Members

Prof. Giuseppe Cassinis

Dipartimento di Scienze della Terra e dell'Ambiente
Università di Pavia
Via Ferrata 1, 27100 PV, Italy
E-mail: cassinis@unipv.it

Dr. Boris I. Chuvashov

Institute of Geology and Geochemistry Urals Branch of
Russian Academy of Science
Pochtovy per 7
Ekaterinburg 620154 Russia
E-mail: chuvashov@igg.uran.ru

Prof. Ernst Ya. Leven

Geological Institute
Russian Academy of Sciences
Pyjevskiy 7
Moscow 109017 Russia
E-mail: erleven@yandex.ru

Dr. Galina Kotlyar

All-Russian Geological Research Institute
Sredny pr. 74
St. Petersburg 199206 Russia
E-mail: Galina_Kotlyar@vsegei.ru

Henderson's Harangue #9

Charles M. Henderson

Department of Geoscience, University of Calgary, Calgary, Alberta, Canada T2N 1N4

It is time to 'finish' and start testing the Permian!

As an attempt to stimulate debate or perhaps simply because something smells fishy, I deliver my ninth harangue. In Italian, it would be "L'arringa di Henderson" (the double "r" is important).

This harangue will touch on several points from sequence biostratigraphy to GSSPs, as made in previous harangues from Permophiles 63 to 71. This 72nd issue of *Permophiles* includes the revised version of the base-Artinskian GSSP proposal – the penultimate GSSP needed to complete the Permian. To my knowledge, at least two other articles in this issue, including by Lucas et al., and by Calvo Gonzalez, discuss some of the correlation changes necessary as we start testing the Permian as now defined.

The base-Artinskian proposal was produced and vetted by many different geoscientists, which serves to strengthen the chosen definition. In *Permophiles* 64, I discussed the democratic process associated with defining a chronostratigraphic unit that moves from a working group, to a subcommission vote, to ICS and then IUGS. This is cause for celebration, in contrast to some of the challenges faced by democracies in our modern world. The result is not perfect, but a definition provides an avenue for scientific testing around the world. One of the key physical attributes of the chosen Artinskian boundary is that it occurs within or at the top (MFS) of a transgressive systems tract. This is also true of the recently ratified Sakmarian Stage. I highlighted the importance of considering sequence biostratigraphic signatures in my first harangue in *Permophiles* 63. There is one more stage boundary to define, at the base of the Kungurian. It looks like it too will be defined within a transgressive systems tract, but perhaps a transgression not as significant as that for the Artinskian. In the Lucas et al. paper in this issue, the importance of a flooding surface within the Kungurian (marking mid-Kungurian) is highlighted as a correlation tool. This is a nice development, since one of the consequences of the GSSP process is that we know more about each boundary interval, than we do about the succession between boundaries. This limits our understanding about various events, including climatic and extinction events. This is one reason I think it is important to 'finish' the Permian – to ensure the base-Kungurian is ratified in 2022. Then we can concentrate on testing these definitions by looking at the entire succession.

Returning to the point about boundary intervals, I'd like to highlight a couple of directions my current collaborative research is taking. I have been working primarily with Spencer Lucas to characterize the Leonardian (more or less equals upper Artinskian through Kungurian) in the US southwest. The base of the Kungurian, associated with the first appearance of *Neostreptognathodus pnevi* is relatively straightforward, but internal Kungurian (mid-upper Leonardian) biostratigraphy is

incompletely known. Environmental considerations and relative sea-level lowstand during this interval also affect biostratigraphic correlation potential. Some of the pieces of the puzzle are coming together, based on recent work on the Fort Apache Limestone of Arizona, the Yeso of New Mexico, the Blaine in north-central Texas and the Bone Springs Formation in West Texas. Stay tuned. While working on the Sakmarian and Artinskian GSSPs, I was reminded of how poorly the full Sakmarian succession is characterized. For example, the full range of some taxa occurring within the Artinskian boundary interval is not clear, including (among others) *Sweetognathus obliquidentatus*, *Sw. aff. ruzhencevi*, *Sw. transitus*, *Sw. naviformis* and *Sw. primus*. This does not detract from the definition of the appearance of *Sw. asymmetricus* – this is a good datum. I am starting to think that the answers to this question may be found in two very different regions – in the Aktastinian succession at the Aktasty section in Kazakhstan, and in a succession at a place called Secret Canyon, Nevada. Stay tuned for the secret to be revealed. Maybe others have recognized this issue too?

One of the most astute comments that we received regarding the base-Artinskian GSSP proposal was to better detail the emendations to the diagnosis and description of *Sweetognathus asymmetricus*. It was suggested that this emendation was non-trivial and critical to clearly delineate definition and global correlation of the Artinskian. This was addressed in the proposal printed in this issue. It is possible that this individual was thinking (at least in part) of rocks exposed from Kansas to north-central Texas. The recognition of the distinctiveness of this taxon from the true *Sweetognathus whitei* is most certainly non-trivial and will necessitate chronostratigraphic revisions in this region and elsewhere. But I think if we make a concerted effort we will get to a place where we can understand the Permian better and where "big data analyses" have a chance of revealing temporally constrained patterns, particularly as associated with the Late Paleozoic Ice Age and Permian extinctions. Maybe we need to reconsider the ranges of taxa such as *Uraloceras* and *Pamirina* and *Geinitzina* and *Streptognathodus* as well as others. For example, previous correlations suggested that Kansas was the only place in the world where *Sweetognathus* and *Streptognathodus* lived in abundance, side-by-side, in Artinskian cyclothem. The new definitions mean that these cyclothem are late Asselian (to early Sakmarian?) and that different species of *Sweetognathus* migrated globally and proliferated as an ecologic replacement in many niches, following the extinction of *Streptognathodus* during the early Sakmarian. Figure 4 in the paper by Calvo Gonzalez in this issue shows what some of these correlation changes might look like – he has been influenced to an extent by his supervisors. I have been making some similar changes to my own previous published work – some are highlighted in the base-Sakmarian and base-Artinskian proposals. It is a humbling experience to point out how often I have been wrong. I am reassured that I have also been partly right, and argue that this is the normal situation for geoscientists. The rock record is cryptic and hard to interpret, and at best we can expect to be right a little bit more than we are wrong. I think this is why so many of us love this game called "geology".

This is the time of year many of us make resolutions that time will reveal we did not keep. I almost certainly will continue to enjoy a glass of wine or a shot of single malt and I probably won't exercise as much as I should. But maybe there is a resolution Permian workers can make and keep. Let's finish the Permian (ie. the Kungurian) and let's start testing these definitions more rigorously, while investigating the full succession between boundaries as well as into the continental realm. Best wishes to all for 2022!

Answers to comments on Artinskian Proposal

COMMENTS BY VOTING MEMBERS

COMMENT BY SHUZHONG SHEN

I hope every friend is ok with the Covid-19 and Delta. It has been a long time for us to discuss something together last time in Cologne. I hope my message will raise your interest to discuss the base-Artinskian GSSP issue.

It's really timing for us to move forward the GSSP work in the Permian, I appreciate the hard work by SPS executive committee. Thanks also give to our Russian colleagues, they excavated the Dalny Tulkas section and it looks good now. The Dalny Tulkas is a good section with multiple markers, particularly the high-precision dates done by Mark Schmitz and Vladmir Davydov will be very useful for calibration of the base-Artinskian. Conodonts are not very abundant, but look ok based on Valery's collections. The section also contains fusulines (not very useful for correlation) and ammonoids (useful). Carbon isotopes were very likely altered.

The most concern problem for me is the index species *Sweetognathus asymmetricus* we plan to use. This species was named by Sun et al. (2017, paper attached) based on the specimens from the lower part of the Chihhsia Formation at the Tieqiao section in South China, which is associated with the fusuline *Misellina claudiae* Zone (Shen et al., 2007, fig. 3, paper attached). The *Misellina claudiae* Zone is underlain by the *Pamirina-Eoparafusulina* Zone in the Liangshan Member of the basal Chihhsia Formation and the upper part of the underlying Maping Formation at the Tieqiao section. So, *Sweetognathus asymmetricus* was named from the Kungurian specimens in South China based on fusulines. The problem is if we think the index species *Sw. asymmetricus* at the Dalny Tulkas section is the same species of South China, then this species has an extremely long range at least from the supposed FAD at the base of Artinskian at Dalny Tulkas to early Kungurian in South China. Therefore, it will be hard to use such a long-range species for global correlation of the base of Artinskian Stage.

In addition, Charles recognized two lineages of "*Sw. whitei*", the American *Sw. whitei* is from Asselian to Sakmarian, and the Russian *Sw. aff. whitei* (now *Sw. asymmetricus*) is from Artinskian (see *Permophiles* 70, p. 10). This probably needs to be clarified in the proposal.

I would suggest that the proposal may add a section on how to use this GSSP candidate for correlation in different continents.

Hope my opinions are useful to improve the proposal.

ANSWER BY CHARLES HENDERSON

The answer to Shuzhong Shen's comment is contained in part by my comment below. Shuzhong and I have also had many email exchanges recently to find a consensus regarding this issue. The following represents our consensus on correlation with South China. There remain some issues, but this revised text that will be added to the proposal clearly demonstrates that the defining lineage is present in south China.

To be added to the proposal:

The chronomorphocline *Sw. binodosus* - *Sw. anceps* - *Sw. asymmetricus* can also be recognized in transgressive facies of uppermost Raanes and lower Great Bear Cape formations (Beauchamp et al., 2021; Chernykh et al., 2020), southwest Ellesmere Island, Canadian Arctic (Henderson, 1988; Henderson, 1999; Beauchamp and Henderson, 1994; Mei et al., 2002), Riepetown Formation, Moorman Ranch, Nevada (Ritter, 1986), upper Riepe Springs Limestone, Elko County, Nevada (Read and Nestell, 2018), Buckskin Mountain Formation in Carlin Canyon, Nevada (Dehari, 2016), Ross Creek Formation in southeastern British Columbia (Henderson and McGugan, 1986), and many other regions. In South China, the chronomorphocline can be recognized in condensed and continuously deposited, thin beds of slope carbonates, organic-rich mudstone or shale and wackestone in the Luodian (NSC) and Ziyun (Houhongchong or HHC) sections of Guizhou province. These slope deposits are correlated with the Liangshan Formation (or Liangshan Member in the basal part of the Chihhsia Formation) and the time represented by a hiatus between the Liangshan Formation and the Maping Formation in more proximal sections in South China. Jun Chen (2011) illustrated well preserved specimens of *Sweetognathus binodosus* and *Sw. anceps* from 347 to 362 metres above the Luodian section base. Wang Zhi-hao and Higgins (1989) and Wang Zhi-hao (1994) also illustrated *Sw. binodosus* and *Sw. asymmetricus* from the Luodian section. Jun Chen (2011) illustrated *Sw. asymmetricus* (*Sw. whitei* in his thesis) from -533 to -548 metres at the Houhongchong section in Ziyun. *Sweetognathus asymmetricus* was named based on its occurrence in beds 18-23 at the Tieqiao section (Guangxi Province) of south China, but this level near the lithologic boundary between the Liangshan Member and the lower part of the main Chihhsia Formation, seems to be high in the range of the species (Wang et al., 1987; Shen et al., 2007; Sun et al., 2017; Zhang et al., 1988). The species, as currently understood, may have a long range, but the FAD level of *Sw. asymmetricus* is clearly recognized by being proximal to the *Sw. binodosus*-*Sw. anceps* lineage with transitional forms between *Sw. anceps* and *Sw. asymmetricus* overlapping the boundary.

COMMENT BY CHARLES HENDERSON

Dear SPS voting member colleagues:

First, the proposal in the most recent issue of *Permophiles* (#71), was completed to generate the kind of remarks and comments that Shuzhong has provided. So thanks, Shuzhong, for initiating this discussion. There is also another comment from a corresponding member on the carbon isotopes. Do we delete the entire section on carbon isotopes or emphasize even more than

we have that they are diagenetically altered.

As we consider this and hopefully other comments we could also consider how much do we need to understand before voting on a proposal? The work will actually never be done. There is always more to learn. And there are places in which the FAD of *Sw. asymmetricus* (or any other name) will never apply, but the radiometric ages and Sr signature will likely be useful. Right Guang (Guang Shi)? Maybe a decision will allow even more exciting research work to test the correlations! I think we are looking at a very important level that is broadly correlatable and many tools are offered to correlate!

The Tieqiao section is a very important section, and the discussion could be expanded in the proposal. It is interesting how thick the 'Kungurian' is in this section (also Luodian) compared to the rest of the Cisuralian. It seems that tectonic subsidence initiates at this time, providing significant accommodation space. The point is that the rest of the lower Cisuralian is somewhat condensed. The FO of *Sweetognathus asymmetricus* (formerly *Sw. whitei* and *Sw. aff. whitei*) is below the FO of *Misellina claudiae*, but they do overlap a little. It is clear that the Tieqiao FO is younger than the FAD. How much is not so clear?

It would be nice if there were lower occurrences of *Sweetognathus* at this section, but the Liangshan Member is mostly barren. The Liangshan Member constitutes a major transgression and the proposal refers to the importance of this signature, as do some of my recent harangues. This change is so profound that a long, long, time ago (when I was a PhD student) this was considered the base-Permian in China. The time scale has evolved, but the question remains regarding the exact correlation of this major change?

I have demonstrated that there are two lineages of *Sweetognathus* (I attach the paper) and the FO's of the two "whitei" species are separated by 4.4 million years. One occurs during the LPIA (in cyclothems and with the conodont *Streptognathodus*) and the other after the LPIA (above major cyclothems and above the extinction of *Streptognathodus*) and yet these two points have been more-or-less equated in much of the literature. It is almost like 4.4 million years does not exist in some sections or at least how we think of those sections? It is such a critical interval of time that we really need to get this right. This so-called "gap" is critical and has affected many correlations including of tetrapods and tetrapod trackways. Getting this right is critical to integrating with the non-marine succession.

We also need to keep in mind that the Kungurian is not yet defined so when we say *M. claudiae* is Kungurian, how is that decided? Is it? Could it be upper Artinskian? It does not occur in the proposed type region for the Kungurian. The Kungurian has evolved too. The current candidate level (FAD of *N. pnevi*) occurs in the Saraninian substage - this was originally considered part of the Artinskian. This lower base-Kungurian level is proposed because it has a good marine signature and above, in Russia, it is restricted marine and non-marine. With which Kungurian is *Misellina* correlated?

Other fusulinids are important to update for the base-Artinskian. For example, the genus *Biwaella* (see Shen et al., 2007) is indicated in our 2007 paper as mid-upper Artinskian,

but Read and Nestell (2019) show that the acme of this genus is lower than previously considered - it is upper Asselian and Sakmarian. In addition, the genus *Eoparafusulina* seems to have very different ranges in South China and NA. In North America it is largely Sakmarian. Why are the occurrences in the Maping and lower Liangshan Member (Shen et al., 2007) Artinskian? What if they were Sakmarian?

I agree with Shuzhong that we should add more information about correlation to other regions - some are already provided. I agree that the proposal could document South China correlation better. Comments anyone?

COMMENT BY GUANG SHI

In my view, the proposal has outlined some excellent information for the proposed base-Artinskian GSSP, which I have found very useful for my consideration. I have not been to the section, so am not qualified to offer too much insights into this discussion.

Nevertheless, I think the proposal would be considerably strengthened if some discussions could be included on how the proposed GSSP might be applied to Gondwanan sections given the challenge of their highly endemic faunas/floras. Correlation via radiometric ages, C and Sr isotope profiles potentially will help but, to my knowledge, published information of these vital indicators for the Lower Permian part of Gondwana are still very limited, so what else then? I appreciate this challenge is not unique to the base-Artinskian and therefore should not be held as a legitimate reason for halting the discussion, but for the proposal to proceed I do think some elaboration/guidance on its application to Gondwana would be useful - e.g., this may include a reference to some Gondwanan sections where radiometric isotope ages or other correlation tools are known to exist and can be tied to the Dalny Tulkas section with reasonable confidence?

Also, I do think we need to resolve the apparent conflict (inconsistency) in age between *Sweetognathus asymmetricus* and *Misellina claudiae* Zone.

Concerning the question of when is the best time to make the call (i.e. to propose/ratify the GSSP), my humble view is that we should not rush; instead, we should consider all available evidence and seek to account for known differences in a diligent and scientific manner. To this end, it appears to me that the apparent conflict in age between *Sweetognathus asymmetricus* and *Misellina claudiae* Zone and the apparent significant time difference between the two *Sweetognathus* lineages is a matter of concern to me (although I am not qualified to comment on this one way or another, or offer a suggestion for the way forward).

ANSWER

The question about *Sweetognathus asymmetricus* vs *Misellina claudiae* and also the question on the two conodont lineages have been replied above and have been resolved in the revised paragraph on conodont issues and correlation with South China written by Charles Henderson and Shuzhong Shen and included into the revised proposal of the base-Artinskian GSSP.

Mike Stephenson has already replied that he has agreed to add some details on possible links to Gondwana, based on radiometric isotope ages or other correlation tools. The revised version of

the GSSP proposal will contain a paragraph on correlation with Gondwana.

COMMENT BY JOERG SCHNEIDER

I could made it very, very short, because I'm a non-marine. The high-precision radioisotopic ages are of great value for correlations to the non-marine Permian sections globally. And they are of course valuable for correlation with other marine biotic provinces, e.g. of Gondwana.

Attached the Fig. 2 of Schneider et al. 2020 in the updated version of August 2021 with radioisotopic ages (red stars).

ANSWER

As said above, a paragraph focused on radiometric ages based correlation is in preparation for the revised version of the GSSP proposal as it is a very important topic. The radiometric age dates will be very important for corelation with the terrestrial realm. To be addressed.

COMMENTS BY SPS CORRESPONDING MEMBERS

We received only one comment from the corresponding members which is reported below.

As the issues Micha Horacek pointed out are numerous, the answers are given separately under each point raised by him.

COMMENT BY MICHA HORACEK, Department of Lithospheric Research, Vienna University, Vienna, Austria

I have noted with interest the proposal by Chernykh et al., 2021. Being neither too familiar with the Lower Permian biochronology nor the proposed section I only want to raise a few points that attracted my attention and might be worth considering before a decision on the announced proposal is made:

-Being a geochemist, to see the Dal'ny Tulkas section carbon isotope curve in Chernykh et al., 2021, fig. 19 (Fig. 1) and to read that it is regarded as on the one hand diagenetically overprinted, but on the other hand comparable (because showing a similar trend) to synchronous other ¹³C-isotope curves (interpreted to

indicate the marine ¹³C-evolution), makes my hair stand on end. As the ¹³C-values in the Dal'ny Tulkas section seem to be depleted by at least 8‰ and most of them more than 12‰ with respect to the compared Naqing section, China (Fig. 2; Buggisch et al., 2011), any potentially observed similarity in trends is most certainly completely coincidental, as a diagenetic alteration of that extent causing an exactly identical shift in ¹³C throughout the section would depend on too many assumptions to be regarded as likely. Also, concurrent trends in C- and O-isotopes (as noted by Chernykh et al., 2021) are usually regarded as further indicators for diagenesis (Marshall 1992, Horacek et al., 2007). Furthermore, by comparing the Dal'ny Tulkas section isotope curve (Fig. 1) with the mentioned other section(s), I cannot see the similarity in trends noted by Chernykh et al., 2021, (Fig. 2). It is to be noted that the isotope curve of the Dal'ny Tulkas section covers a larger interval than the interval which is

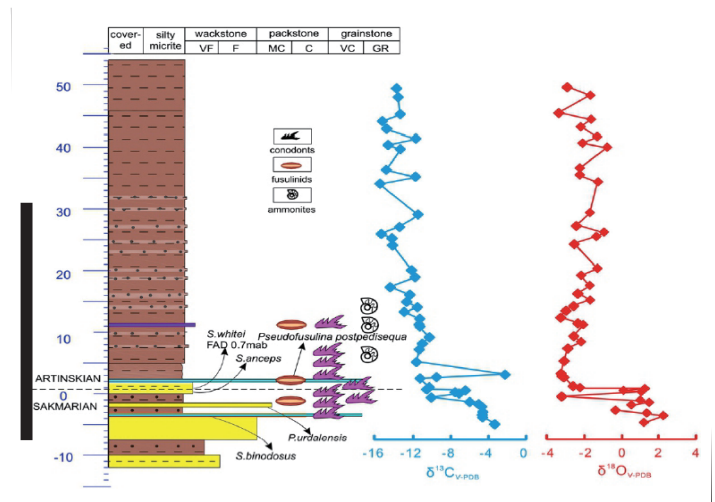


Fig. 1. Carbonate ¹³C- and ¹⁸O-isotope curves of the Dal'ny Tulkas section modified after Zeng et al., 2012. Black bar on the left marks the part of the section investigated in Chernykh et al., 2021.

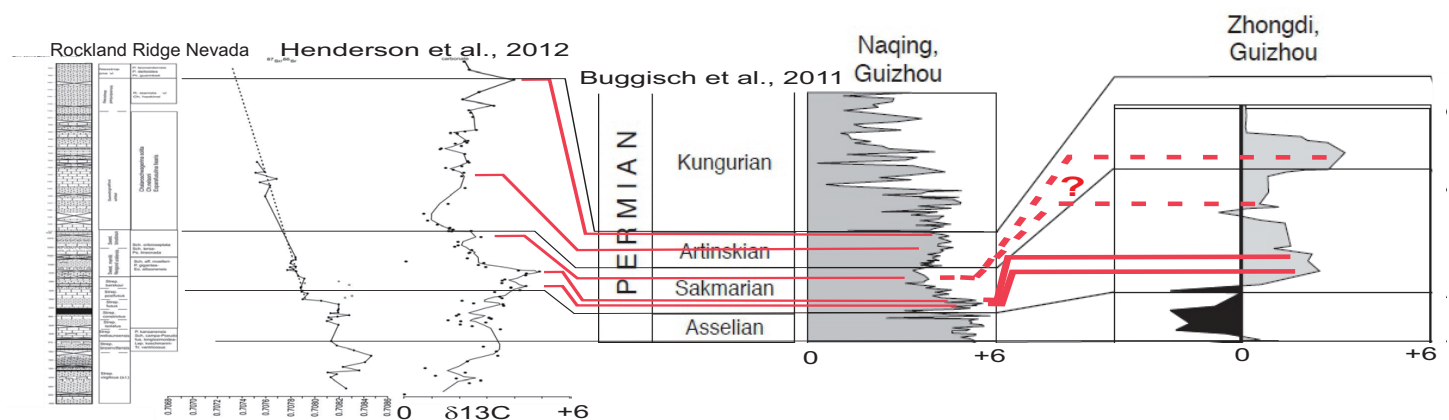


Fig. 2. Correlation of Rockland Ridge section, Nevada (USA; Henderson et al., 2012), Naqing and Zhongdi sections (China; Buggisch et al., 2011) carbon isotope curves, based solely on similarities in the ¹³C-curve shape (red correlation lines), which might be coincidental. No long-lasting ¹³C-minimum interval (as shown for the Dal'ny Tulkas section) can be found in the Naqing and Zhongdi sections at the base of the Artinskian, however, a short-time minimum is present in the Rockland Ridge section, Nevada, in that interval. If the ¹³C-curves should represent global ¹³C-trends, the curves point towards slight differences in definition and drawing of boundaries, or asynchronous appearance of marker fossils.

otherwise described in the article by Chernykh et al., 2021 (Fig. 1). Concerning carbon isotopes, it should be tested, if the trench also gives these low ^{13}C values (rather likely), and if C_{org} isotope data might circumvent the problem of carbonate diagenesis, even though to my knowledge there currently aren't much other synchronous Corg isotope data published.

ANSWER

We agree that the $\delta^{18}\text{O}$ and $\delta^{13}\text{C}$ values from Dal'ny Tulkas are the result of diagenetic alteration and that the correlation presented by Zeng et al. (2012) of the Dalny Tulkas carbon shift with the isotopic curves from South China sections of Buggish et al. (2011) is not supported, as clearly shown by M. Horacek in his fig. 2 included in his comment. So the revised proposal reports the data published by Zeng et al. 2012 and underline the fact that they are diagenetically altered. Furthermore a comment on their lack of correspondence with data from other sections (South China) is underscored.

The strontium data of the Dal'ny Tulkas section has not been properly published. From the publications by Schmitz et al., 2009, Chernykh et al., 2012, and Henderson et al., 2012, can be extracted that there exist Sr-isotope data of conodonts from the upper Carboniferous and the Lower Permian from Uralian sections, but it cannot be seen (only assumed) from which section the individual samples come from. Also the resolution is limited: in the extended SAB "boundary interval" there are only 3 points, with one point lying approximately on the SAB and the next neighbouring ones on each side almost two million years afar. Even though the Uralian Lower Permian Sr-isotope trend appears to be quite consistent and in agreement with the results from Nevada/USA (which also are rather incomplete in this interval: Henderson et al., 2012; see Fig. 2), the data are limited and should be improved with respect to sample density, to enable reliable age calculations based on the Sr-isotope values.

ANSWER

We agree that the Sr isotope data are of low resolution, but as said by M. Horacek, they are consistent, and although we hope that more data will be gathered in the near future we think it is important to include them in the proposal.

Problematic are observed discrepancies between publications and within the publication, which are not explained. In Chernykh 2020 the Sakmarian-Artinskian Boundary (SAB) is drawn at the base of section bed 4b, in Chernykh et al., 2021, it is in the middle of 4b, see their figs. 3 and 7. Most probably this difference results from the new identification and discrimination of a transitional form from *Sweetognathus anceps* to *Sweetognathus asymmetricus*, found in Dal'ny Tulkas section bed 4b. As in bed 4b also the index fossil *Sweetognathus asymmetricus* (marker for the base of the Artinskian) was identified and in this bed only two conodont bearing levels have been found, the lower one must be the one hosting the transitional form, whereas the upper level must contain the "real" *Sweetognathus asymmetricus*. In between, obviously, the boundary was drawn by Chernykh et al., 2021, alas, in contradiction to their own fig. 8, which classifies

the transitional form as already Artinskian. Perhaps the authors themselves are still uncertain about where exactly to place the boundary?

ANSWER

The authors are not uncertain of the position of the boundary, but in fact there was a mistake in Fig. 3 and Fig. 7 and in the final paragraph of the proposal. The base-Artinskian GSSP is defined at 0.6 m above the base of bed 4b (and so near the base of 4b as in Chernykh 2020) and not at 1.2 m above the base, as erroneously reported in the proposal. In the sample collected at 0.6 m there is the FAD of *Sweetognathus asymmetricus* along with the occurrence of transitional forms from *Sweetognathus anceps* to *Sweetognathus asymmetricus*. *Sweetognathus asymmetricus* and the transitional forms coexist and this coexistence is normal and expected in conodont sample-population based taxonomy. In the revised proposal the base-Artinskian GSSP is correctly placed at 0.6 m above the base of bed 4b.

Further unsatisfying details, even though probably not directly relevant concerning consideration of proposal:

In Chernykh et al., 2021, the correlation between Dal'ny Tulkas section and trench is shown, but not explained how it was achieved in detail, nor how the SAB was identified in the Dal'ny Tulkas trench. In the chapter "Interpreted Sequence Stratigraphy" Chernykh et al., 2021, correlate trench beds 3 and 4 with section bed 2 (as they contain "...noncalcareous algae, plant remains, and Calamites..."), but this is in contradiction with their fig. 7, where they correlate trench beds 7-1 with section beds 3 and lower part of bed 4. The SAB is drawn below trench bed 8 and within the middle of section bed 4b. Theoretically, these neighbouring section and trench should be an example how to reliably and easy-to-understand correlate them and identify the SAB in the field. At least for me, the descriptions and explanations fail to convincingly tell me how that correlation was achieved. To me it seems that this "correlation" was achieved by the interpretation of top of section bed 5 (limestone layer) being identical with trench limestone bed 10 (10-1 and 10-2) and the same distance from the defined boundary in Dal'ny Tulkas section to this limestone layer was subtracted from trench bed 10 to find the boundary there in the trench. Should this be the case, it is not the kind of correlation I would expect. Thus, at present the dug trench does not add much valuable data to the section. As I assume that the trench might have been produced to better conserve the golden spike of the boundary, investigations should be continued and completed (with unequivocal identification of the SAB in the trench by biochronological evidence) to confirm the findings in the Dal'ny Tulkas section.

ANSWER

In the proposal, trench beds 3 and 4 are not at all correlated with section bed 2. There is simply the description of their content in terms of plant debris. The most important correlation line is the dotted line drawn at the base of bed 7-1 in the trench and bed 3 in the section which represents a sequence boundary followed by a transgressive systems tract. Both terrigenous sedimentation and plant debris input end with beds 6 in the trench

and bed 2 in the section, to be replaced by carbonate mudstone sedimentation. This is a very important signal. The subsequent correlation line is based on fusuline content. The SAB is drawn based on the FO of Artinskian fusulines in the trench bed 8 and the FAD of *Sweetognathus asymmetricus* at 0.6 m above the base of bed 4b in the section. The three following correlation lines are based on ammonoid and fusuline contents.

Thus the correlation was not achieved as presumed by Micha Horacek (and in fact the thicknesses do not correspond exactly) but based on lithology and fossil content.

Finally Micha Horacek is right: the trench has been produced to better display and conserve the GSSP. It is also worth noting that the trench and section are only about 30 metres apart.

Further disappointing to me is the incomplete presentation of data. In the article the authors state that no ammonoids have been found in Dal'ny Tulkas section and trench below the SAB, but the figures indicate such a datum in bed 1 of the section. In bed 1 of the trench is indicated the only conodont sample position so far in the trench, but the information about the species remains unsaid (it might be *Sweetognathus binodosus* according to their fig. 19 from Zeng et al., 2012 (Fig. 1)). Also further fossil levels (e.g. fusulinids from trench bed 7-2, and section bed 3) remain undescribed in the article, which I find a bit unsatisfying, even though perhaps these data are not this relevant.

ANSWER

The proposal has been revised in order to better explain that there are rare unidentifiable ammonoids in bed 1 of the section, and rare unidentifiable fusulines in bed 7-2 of the trench and bed 3 of the section, but no identifications are available.

In relation to the occurrence of *Sweetognathus binodosus* reported by Zeng et al 2012, this was not replicated, but it is known to co-occur with *Sw. obliquidentatus* common below and above the SAB.

The fragmentary conodont from bed 1 of the trench belongs to an undetermined species of *Mesogondolella*, as reported in the proposal.

Furthermore missing are the paleomagnetism (Balabanov et al., 2018), further (C- and O-) isotope (Nurgaliev et al., 2018) and geochemistry (Sungatullin et al., 2018) data, which seemingly only have been published in a conference volume that is not publicly available on the internet (at least I could not find it). A geochemical study by Mizens et al., 2018 (in Russian), apparently shows an investigation of the Dal'ny Tulkas trench (see their fig. 2), with the SAB drawn exactly as in Chernykh et al., 2021. Thus, it seems to me that the correlation of section and trench (returning to my concern about this point above) cannot be correct, as the trench SAB probably represents the boundary before the consideration of the transitional *Sweetognathus anceps* to *Sweetognathus asymmetricus* form (although it remains obscure how the boundary was defined there), whereas the section SAB in Chernykh et al., 2021, was drawn by considering this transitional form, if its position in the middle of section bed 4b is indeed the proposed boundary. At least such a situation should falsify my assumption that the distance to the next

overlying carbonate layer was used for identification of the SAB in the trench.

ANSWER

The missing data have been added in the revised proposal. The paper by Hounslow and Balabanov (2018) will be quoted regarding paleomag. The SAB occurs within the long Kiaman superchron. They report a short normal polarity (C12n) within the upper Artinskian.

The SAB position has been revised as explained in the answer to the comment above. The same holds true for the correlation.

Transitional forms of conodont species do not affect correlation consideration. The speciation event is determined when there are forms within a sample-population that clearly include all characters of the species.

The SAB in the trench was located at bed 8 based on the FO of Artinskian fusulines.

The distance between beds was not used for the correlation.

Conclusions

The proposal published by Chernykh et al., 2021, occurs to me as having been written and submitted in haste, as it shows to me some signs of inconsistency (e.g. exact definition and position of SAB). Also, many data are not included, which to date have not been published properly but should be part of such a relevant proposal. Parameters that do "not work well" in the proposed GSSP section (e.g. C-isotopes) should be honestly/critically addressed.

ANSWER

Dr. Horacek is warmly thanked for his detailed revision, which will improve the proposal. The proposal was not prepared in haste. On the contrary many versions have been produced and many separate data on Dal'ny Tulkas section have been published over the years. This makes the synthesis difficult, but it was decided that it was time to finalize the proposal and vote for it.

References:

- Balabanov Y., Sungatullin R., Sungatullina G. and Kosareva L., 2018. A Paleomagnetic Study of the Section of Dal'ny Tulkas, Lower Permian. Proceedings Kazan Golovkinsky Stratigraphic Meeting «Advances in Devonian, Carboniferous and Permian Research: Stratigraphy, Environments, Climate and Resources». Kazan, Russian Federation, 19-23 September 2017. Filodiritto Publisher, Bologna, p. 44–50.
- Buggisch, W., Wang, X. D, Alekseev, A. S., Joachimski, M. M., 2011. Carboniferous–Permian carbon isotope stratigraphy of successions from China (Yangtze platform), USA (Kansas) and Russia (Moscow Basin and Urals). Palaeogeography, Palaeoclimatology, Palaeoecology, v. 301, p. 18–38.
- Chernykh, V.V., 2020. A brief review of the Dal'ny Tulkas Section (southern Urals, Russia) – potential candidate for a GSSP to define the base of the Artinskian stage in the global chronostratigraphic scale. Permophiles, no. 69, p. 9–14.
- Chernykh, V. V., Chuvashov, B. I., Davydov, V. I. and Schmitz, M. D., 2012, Mechetlino Section: A candidate for the Global Stratotype and Point (GSSP) of the Kungurian Stage

- (Cisuralian, Lower Permian). *Permophiles*, no. 56, p. 21–34.
- Chernykh, V.V., Henderson, C.M., Kutugin, R.V., Filimonova, T.V., Sungatullina, G.M., Afanasieva, M.S., Isakova, T.N., Sungatullin, R.K., Stephenson, M.H., Angiolini, L., Chuvashov, B.I., 2021, Proposal for the Global Stratotype Section and Point (GSSP) for the base-Artinskian Stage (Lower Permian). *Permophiles*, no. 71, p. 45–72.
- Henderson, C. M., Wardlaw, B. R., Davydov, W. I., Schmitz, M. D., Schiappa, T. A., Tierney, K. E., 2012, Proposal for base-Kungurian GSSP. *Permophiles*, no. 56, p. 8–21.
- Horacek M., Brandner, R., Abart, R., 2007. Carbon isotope record of the P/T boundary and the Lower Traissic in the Southern Alps: evidence for rapid changes in storage of organic carbon, correlation with magnetostratigraphy and biostratigraphy. *Palaeogeography, Palaeoclimatology, Palaeoecology*, v. 252, p. 347–354.
- Marshall, J.D., 1992. Climatic and oceanographic isotopic signals from the carbonate rock record and their preservation. *Geological Magazine*, v. 129, p. 143–160.
- Mizens G.A., Sungatullin R.Kh., Sungatullina G.M., Gareev B.I., Batalin G.A., Sadriev F.F. (2018) Reference sections of Cisuralian Series (Permian System): geochemical features. *Litosfera*, v. 18, no. 6, p. 819–838. DOI: 10.24930/1681-9004-2018-18-6-819-838.
- Nurgalieva N., Gareev B. and Batalin G. 2018. Dal'ny Tulkas and Mechetlino Lower Permian Sections: Carbonate Carbon and Oxygen isotopes. In: Nurgaliev D., Barclay M., Nikolaeva S. and Silantiev V.(Eds.), *Proceedings Kazan Golovkinsky Stratigraphic Meeting, 2017: Advances in Devonian, Carboniferous and Permian Research: Stratigraphy, Environments, Climate and Resources Kazan, Russian Federation, 19-23 September 2017*, p. 202–205.
- Schmitz, M. D., Davydov, V. I., and Snyder, W. S., 2009. PermoCarboniferous Conodonts and Tuffs: High precision marine Sr isotope geochronology. *Permophiles*, no. 53, Supplement 1 (ICOS 2009 Abstracts edited by C.M. Henderson and C. MacLean), p. 48.
- Sungatullin R., Mizens G., Sungatullina G., Gareev B., and Batalin G., 2018. Geochemistry of the Lower Permian Mechetlino and Dal'ny Tulkas Sections, Southern Urals. *Proceedings Kazan Golovkinsky Stratigraphic Meeting «Advances in Devonian, Carboniferous and Permian Research: Stratigraphy, Environments, Climate and Resources»*. Kazan, Russian Federation, 19-23 September 2017. Filodiritto Publisher, Bologna, p. 216–223.
- Zeng, J., Cao, C. Q., Davydov, V. I. and Shen, S. Z., 2012. Carbon isotope chemostratigraphy and implications of paleoclimatic changes during the Cisuralian (Early Permian) in the southern Urals, Russia. *Gondwana Research*, v. 21, p. 601–610.

Final proposal for the Global Stratotype Section and Point (GSSP) for the base-Artinskian Stage (Lower Permian)

Valery V. Chernykh

Zavaritskii Institute of Geology and Geochemistry, Ural Branch, Russian Academy of Sciences, Pochtovyi per. 7, Yekaterinburg, 620219, Russia

Email: chernykh@igg.uran.ru

Charles M. Henderson

Department of Geoscience, University of Calgary, Calgary, Alberta, Canada T2N 1N4

Email: cmhender@ucalgary.ca

Ruslan V. Kutugin

Diamond and Precious Metal Geology Institute, Siberian Branch of the Russian Academy of Sciences (DPMGI SB RAS), Lenina ave., 39, Yakutsk, 677007, Russia

Email: rkutugin@mail.ru

Tatiana V. Filimonova

Geological Institute of the Russian Academy of Sciences (GIN RAS), Pyzhevsky lane, 7, Moscow, 119017, Russia

Email: filimonova@ginras.ru

Guzal M. Sungatullina

Kazan Federal University (KFU), Kremlyovskaya str, 18, Kazan 420008, Russia

Email: Guzel.Sungatullina@kpfu.ru

Marina S. Afanasieva

Paleontological Institute of Russian Academy of Sciences (PIN PAS), Profsoyuznaya, str. 123, Moscow, 117647, Russia

Email: afanasieva-marina@mail.ru

Tatiana N. Isakova

Geological Institute of the Russian Academy of Sciences (GIN RAS), Pyzhevsky lane, 7, Moscow, 119017, Russia

Email: isakova@ginras.ru

Rafael Kh. Sungatullin

Kazan Federal University (KFU), Kremlyovskaya str, 18, Kazan, 420008, Russia

Email: Rafael.Sungatullin@kpfu.ru

Michael H. Stephenson

British Geological Survey, Keyworth, Nottingham NG12 5GG, UK

Email: mhste@bgs.ac.uk

Lucia Angiolini

Dipartimento di Scienze della Terra “A. Desio”, Università degli Studi di Milano, 20133 Milano, Italy

Email: lucia.angiolini@unimi.it

Boris I. Chuvashov

Zavaritskii Institute of Geology and Geochemistry, Ural Branch,

Russian Academy of Sciences, Pochtovyi per. 7, Yekaterinburg, 620219, Russia

Introduction

Considerable new data have been generated and understanding has considerably improved regarding a potential GSSP level for the base-Artinskian since the reports provided in *Permophiles* 41 (Chuvashov et al., 2002a, b) and *Permophiles* 58 (Chuvashov et al., 2013). Work has focused on the Dal’ny Tulkas Section in Russia and the FAD position of *Sweetognathus* aff. *whitei*, but the uncertain taxonomy delayed final completion. The fact that this process took time is simply a reflection of the careful study needed to resolve this issue. The taxon is very distinct and an appropriate marker for the base-Artinskian. Kotlyar et al. (2016) showed additional progress at Dal’ny Tulkas, as did Chernykh (2020). Henderson (2020) indicated that the base-Artinskian GSSP should be ready to go. Finally, it was reported in *Permophiles* 70 that there is now an agreement (Henderson and Chernykh, 2021) that the defining conodont species is *Sweetognathus asymmetricus* Sun and Lai. The SPS voting members voted 15-1 (and one no reply) in favour (*Permophiles* 72). The Dal’ny Tulkas section is data-rich, making it an excellent GSSP site. It also includes, ammonoids, fusulines, small foraminifers, palynology, radiolarians, geochronologic ages, and Sr isotopic data that provide additional constraints on how to

correlate the GSSP into other regions and realms. A proposal for the GSSP definition is provided to conclude this paper.

Acknowledgements

Lucia Angiolini thanks the International Commission on Stratigraphy for financial support to complete this GSSP proposal. Charles Henderson acknowledges research support from NSERC Discovery Grant program. Mike Stephenson publishes with the permission of the Director of the British Geological Survey (NERC). The foraminiferal study was made as a part of the research on the State Program of Geological Institute of RAS No. 0135-2019-0062. Additional work to complete the GSSP proposal was supported by research grant RFBR N 16-o5-0036a. Valery Chernykh and Boris Chuvashov acknowledge support from the Russian Academy of Sciences.

Historical Considerations and Lithologic Succession

The boundary deposits of Sakmarian and Artinskian are represented most fully in the section on the stream Dal’ny Tulkas, located on the southern end of the Usolka anticline near the eastern outskirts of the settlement Krasnousol’sky, Bashkortostan (Fig. 1). The Kurort suite includes predominantly the

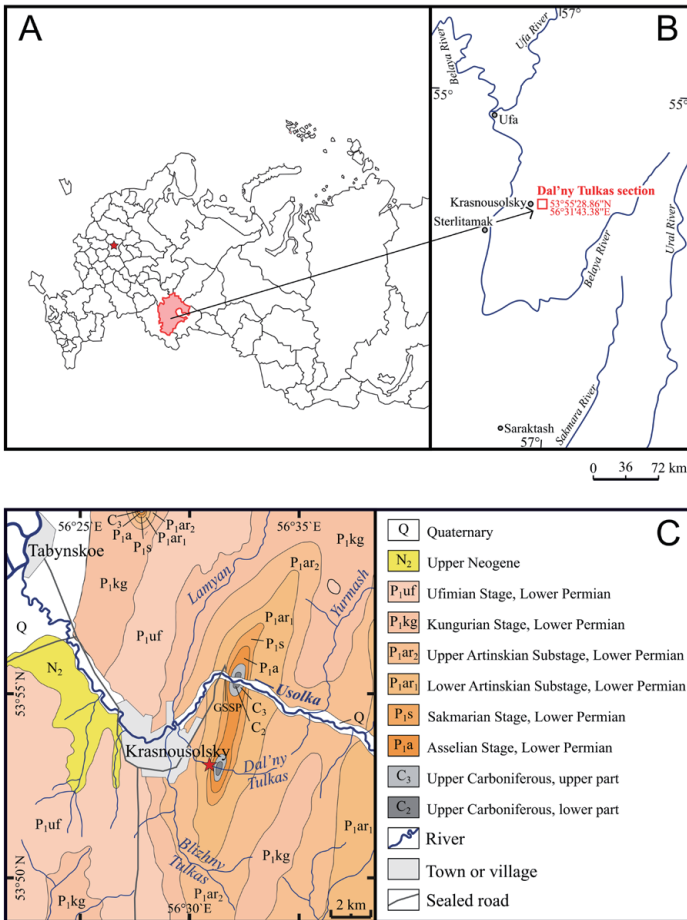


Fig. 1. Geology location map of the Dal’ny Tulkas section. Base of section is 53.88847N and 056.51615E.

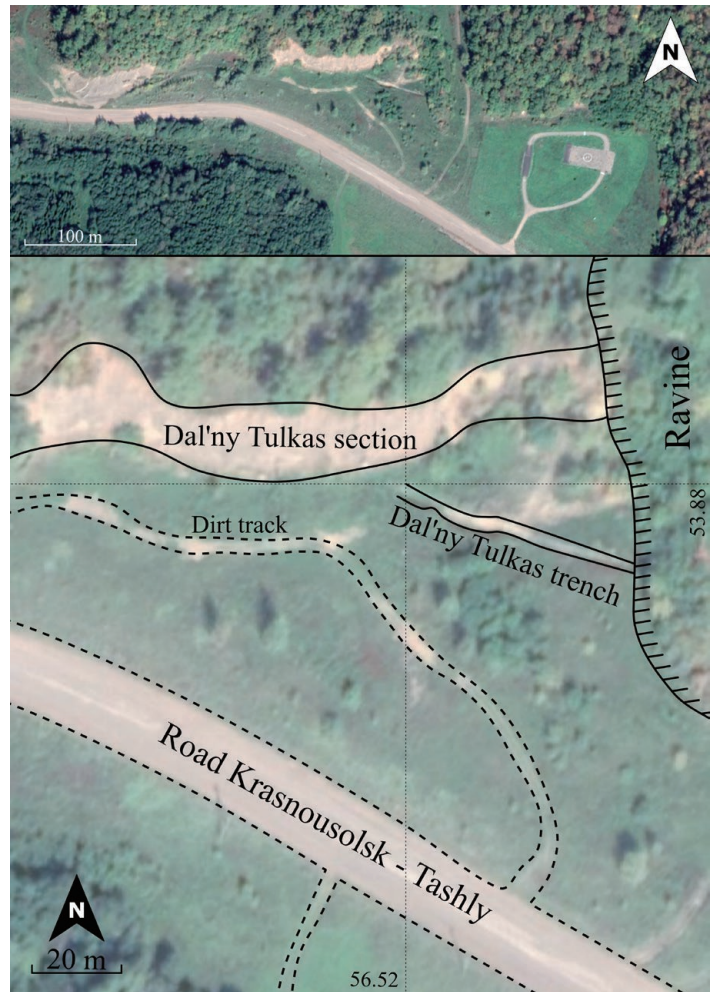


Fig. 2. Air photo of the Dal’ny Tulkas section and trench.

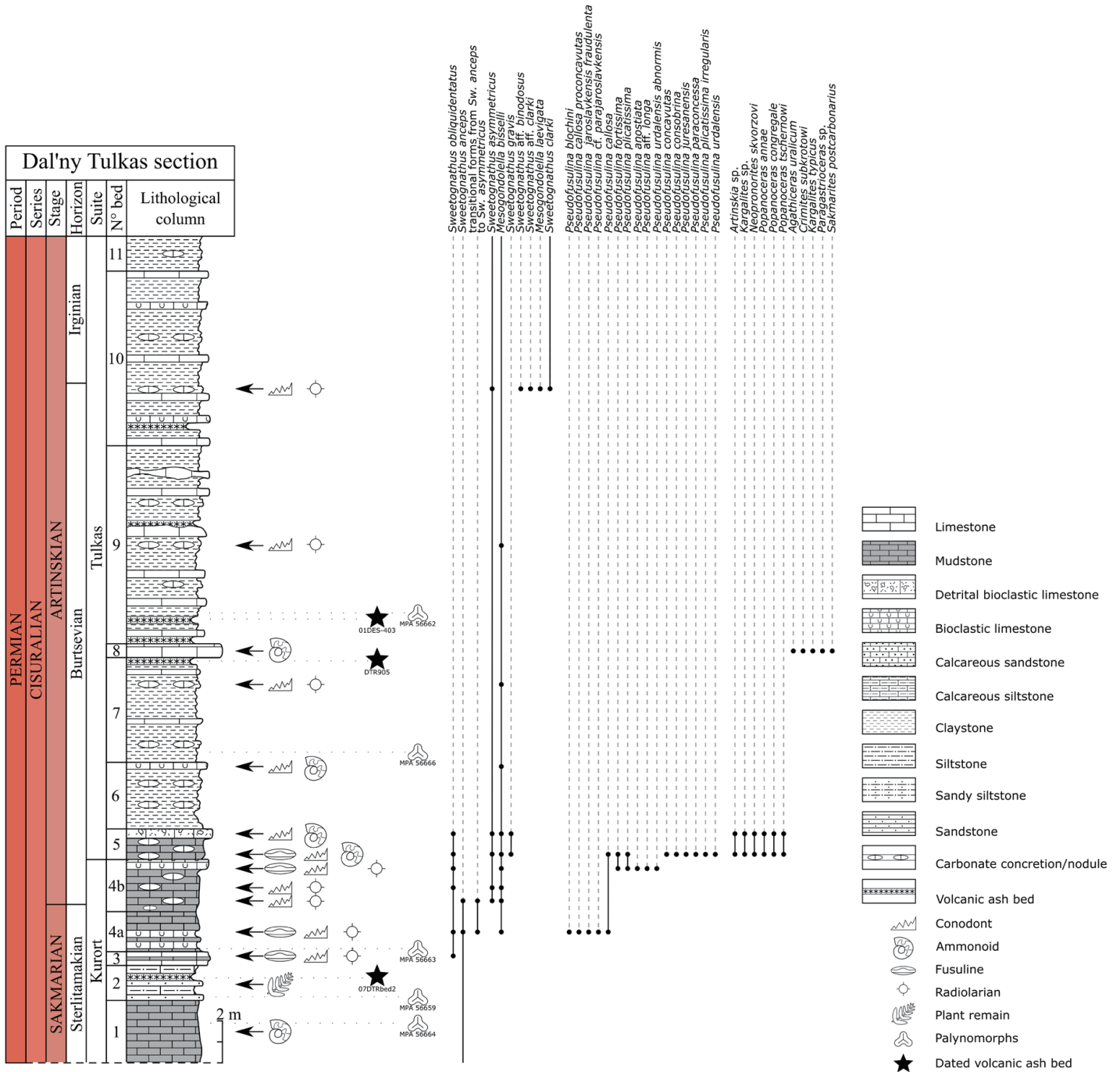


Fig.3. Stratigraphic column with distribution of samples collected for conodonts, ammonoids, fusulines, and radiolarians in the Dal'ny Tulkas section. See legend for lithology and fossil symbols.

Sterlitamakian horizon of Sakmarian Stage and the Tulkas suite includes the Artinskian Stage (Chuvashov et al., 1990) within the Dal'ny Tulkas section boundary interval. The Kurort suite comprises beds of dark-coloured carbonate mudstone, argillite, sandstone, and occasional bioclastic limestone with fusulines, rare ammonoids, radiolarians, palynology, and a few bivalves. The Sterlitamakian horizon is transitional to the Artinskian Stage and is typically poorly exposed. In 2003 a bulldozer cleared this part of the section and exposed all beds (Fig. 2), which include resistant beds of sandy-argillaceous limestone with rare interbeds of detrital limestone and carbonate-clay concretions; all beds have been sampled for fusulines, ammonoids and conodonts.

Most of the conodont samples of the Dal'ny Tulkas section proved to be productive. In the Artinskian part of the section there are four ash tuff layers.

The lower boundary of the Artinskian Stage is determined by the level of the appearance in bed 4b of the cosmopolitan conodont *Sweetognathus asymmetricus* in the phylogenetic lineage – *Sw. expansus* to *Sw. aff. merrilli* to *Sw. binodosus* to *Sw. anceps* to *Sw. asymmetricus* to *Sw. clarki*. The first Artinskian complex of fusulines is noted in the section 2.5 m higher, in the lower part of bed 5, which also includes Artinskian ammonoids and conodonts. The first appearance datum of *Sw. asymmetricus* in the Dal'ny Tulkas section is used for definition, but everywhere else, the base-Artinskian will be correlated primarily with various fossils including conodonts, as well as a variety of stratigraphic signals including geochronologic age and strontium isotopes.

The schematic lithologic column of the Dal'ny Tulkas section with indications of the paleontologic samples is given below (Figs. 3, 4), including detailed description and lists of identified ammonoids, fusulines, conodonts, small foraminifers and radiolarians (Table 1). There is also a depiction of a trench, which is only about 30 metres from the main section (Figs. 2, 5-6). The correlation between the trench and main section is provided in Figure 7 and it is based on lithology and fossil content. The bed numbers and description of the main section and trench vary because different teams measured the respective sites and because fresh beds vary in appearance from the same beds when weathered. The trench was dug to recover fresh lithologic material and additional fossils; it was not dug to test correlation, but rather to enrich the paleontological characteristics of the interval, mostly of radiolaria and palynomorphs. Many other sections in the world will be correlated without conodonts, especially all those from the terrestrial realm.

Section Description

Sakmarian Stage

Sterlitamakian horizon

Kurort suite

Bed 1. Monotonous silty mudstone, grey on fresh fracture, brownish-grey on altered surface, microlayered (2 to 5 cm-thick). Fossil content: rare ammonoids, fish-scales, non-calcareous algae. Thickness: 3 m.

Bed 2. Calcareous clayey siltstone and fine-grained sandstone in 15-20 cm-thick beds. Fossil content: noncalcareous algae and plant remains. Thickness: 1.7 m.



Fig. 4. Photos of the Dal'ny Tulkas section. A: general view of the section, the arrow indicates bed 8; B: beds at the transition Sakmarian-Artinskian; C: lower Artinskian part of the succession, arrow points to bed 5.

Bed 3. Brownish-grey limestone in 10-15 cm-thick beds with mudstone in the middle part of the bed. Carbonate concretions in the upper part of the bed. Fossil content: unidentified radiolarians (in sections), rare unidentifiable fusulines, conodonts [*Sweetognathus cf. obliquidentatus* (Chernykh)]. Thickness: 0.7 m.

Bed 4a. Monotonous brownish-dark grey platy mudstone, with some interbeds of siltstone. In the lower part of the layer, there are 5-7 cm-thick beds of recessive bioclastic limestone with fusulines (*Pseudofusulina callosa* Rauser, *P. callosa proconcavatas* Rauser, *P. jaroslavkensis fraudulentata* Kireeva, *P. cf. parajaroslavkensis* Kireeva, *P. blochini* Korzhenevski), unidentified radiolarians (in sections), bryozoans, crinoids, conodonts [*Mesogondolella bisselli* (Clark and Behnken), *Sweetognathus anceps* Chernykh, *Sw. obliquidentatus* (Chernykh)], transitional forms from *Sw. anceps* Chern. to *Sw. asymmetricus* Sun and Lai). Thickness: 1.8 m.

Artinskian Stage

Burtsevian horizon

Kurort suite

Bed 4b. Mudstone with carbonate concretions at 0.6 m with conodonts [*Mesogondolella bisselli* (Clark and Behnken), *Sweetognathus anceps* Chernykh., transitional forms from *Sw. anceps* Chernykh to *Sw. asymmetricus* Sun

and Lai, *Sw. asymmetricus* Sun and Lai]. 1.2 m above along the section, a level with small carbonate concretions yields conodonts [*Mesogondolella bisselli* (Clark and Behnken), *Sw. obliquidentatus* (Chernykh), *Sw. asymmetricus* Sun and Lai]. The upper part of the unit consists of a 42 cm-thick tempestite composed of coarse-grained graded bed of bioclastic limestone with fusulines (*Pseudofusulina* aff. *longa* Kireeva, *P. fortissima* Kireeva, *P. anostiata* Kireeva, *P. plicatissima* Rauser, *P. urdalensis abnormis* Rauser), bryozoans, crinoids, conodonts [*Mesogondolella bisselli* (Clark and Behnken), *Sw. obliquidentatus* (Chernykh)]. Concretions with unidentified radiolarians (in sections). Thickness: 2.6 m

Tulkas suite

Bed 5. Brownish-grey silty mudstone in the lower part of the layer (60 cm) with numerous mudstone concretions. The upper part of the bed consists of laminar mudstone with lenses of detrital bioclastic limestone. Fossil content: fusulines in the lower part of the bed (*Pseudofusulina callosa* Rauser, *P. plicatissima* Rauser, *P. plicatissima irregularis* Rauser, *P. urdalensis* Rauser, *P. fortissima* Kireeva, *P. concavatus* Vissarionova, *P. juresanensis* Rauser, *P. consobrina* Rauser, *P. paraconcessa* Rauser), ammonoids in the lower and upper parts of the bed (*Popanoceras annae* Ruzhencev, *P. tschernowi* Maximova, *P. congregale* Ruzhencev, *Kargalites* sp., *Neopronorites skvorzovi* Tschernow, rare *Artinskia* sp.), conodonts in the lower and upper parts of the bed [*Mesogondolella bisselli* (Clark et Behnken), *Sweetognathus asymmetricus* Sun and Lai, *Sw. obliquidentatus* (Chernykh), *Sw. gravis* Chernykh]. Thickness: 1.5 m

Bed 6. Dark-greenish-grey claystone with carbonate concretions and with 20 cm-thick interbeds of bluish-grey mudstone, locally bioclastic at the top. Fossil content: ammonoids (as in bed 5), conodonts [*Mesogondolella bisselli* (Clark and Behnken)]. Thickness: 3.2 m.

Bed 7. Claystone, dark-brownish-grey on fresh fracture, greenish-grey on altered surface, with thin interbeds of marly limestone in the upper part. At 1.1 m below the top of the unit a large (0,5 x 20 cm) concretion of mudstone yields numerous unidentified radiolarians (in sections) and conodonts [*Mesogondolella bisselli* (Clark and Behnken)]. Thickness: 5 m.

Bed 8. Limestone, bluish-grey on fresh fracture, whitish on altered surface, locally bioclastic. In the lower 20 cm, 4 cm-thick clayey interbeds occur. At the base and top of the bed, yellowish silicified tuffs up to 10 cm-thick.

Fossil content: ammonoids [*Sakmarites postcarbonarius* (Karpinsky), *Agathiceras uralicum* (Karpinsky), *Kargalites typicus* (Ruzhencev), *Paragastrioceras* sp., and *Crimites subkrotowi* Ruzhencev)]. Thickness (decreasing westwards): 0.7-0.5 m.

Bed 9. Claystone with periodically repeated (about every 1-2.5 m) 5-10 cm-thick interbeds of steel-grey marly limestone and frequent yellowish-light grey 1-5 cm-thick silicified tuffs. Lenticular concretions of steel-grey marly limestone. In the middle part of the bed, one of the concretions yields numerous unidentified radiolarians (in sections) and conodonts [*Mesogondolella bisselli* (Clark and Behnken)]. Thickness: 9.4 m

Artinskian Stage

Irginian horizon

Bed 10. Claystone as below, but with more frequent and thicker (15-20 cm) limestone interbeds and concretions and bioclastic limestone accompanied by 3-10 cm-thick yellowish-light grey silicified tuffs. Fossil content: unidentified radiolarians (in sections), conodonts [*Sweetognathus asymmetricus* Sun and Lai, *Sw. clarki* (Kozur), *Sw. aff. binodosus* Chernykh, *Mesogondolella bisselli* (Clark and Behnken), and *M. laevigata* Chernykh]. Thickness: 8.3 m.

Bed 11. Claystone with rare small carbonate concretions. Thickness: 1.7 m

Trench description (Fig. 5, 6)

Sakmarian Stage

Sterlitamakian horizon

Bed 1. Sandy siltstone, grey, unevenly thin-bedded, with interbeds of clayey mudstone, with a large amount of scattered bioclasts. Fossil content: conodonts (*Mesogondolella* sp.). Thickness: 0.6 m.

Bed 2. Sandy siltstone, microlayered, separated by interbeds of claystone; in the lower part the bedding is poorly expressed, at the top the bedding is very thin. Fossil content: abundant unidentified radiolarians (in sections) and algae. Thickness: 2.1 m.

Bed 3. Sandy siltstone, grey, microlayered with interbeds of clayey sandstone. Fossil content: calamite trunks, algae, fish scales. Thickness: 1.2 m.

Bed 4. Dark grey, thin-bedded siltstone with an interbed of red tuff at the base. Fossil content: algae, unidentified radiolarians (in sections), and fish scales. Thickness: 0.45 m.

Bed 5. Calcareous clayey siltstone with interbeds of fine-grained sandstone and reddish tuffs. Fossil content: fish scales, numerous radiolarians, and algae. Thickness: 1.5 m.

Bed 6. Calcareous sandstone, silty. Thickness: 0.2 m.

Bed 7-1. Grey mudstone, microlayered, platy. Concretions of brownish-grey limestone at the base and the top. Thickness: 1.0 m.

Bed 7-2, 7-3. Mudstone with silty interbeds, brownish-dark grey, platy. In the lower part of the bed, there is a 5-7 cm-thick bed of bioclastic limestone with rare unidentifiable fusulines, bryozoans, crinoids. In 7-2 concretions of limestone with numerous radiolarians Thickness: 0.8 m.

Bed 7-4, 7-5. Silty mudstone, grey, with carbonate nodules. Thickness: 0.8 m.

Artinskian Stage

Burtsevian horizon

Bed 8. Bioclastic limestone, coarse-grained, interpreted as a tempestite. Fossil content: abundant fusulines (8-1: *Boultonia* sp., *Schubertella* ex gr. *sphaerica* Suleimanov, *Fusiella schubertellinoides* Suleimanov, *Pseudofusulina* ? sp.; 8-2: *Boultonia* sp., *Schubertella* sp. A, *Schubertella* sp. B, *S. sphaerica chomatifera* Zolotova, *S. turaevkensis* Baryshnikov, *S. turaevkensis elliptica* Baryshnikov, *S. ex gr. kingi* Dunbar & Skinner, *S. ex gr. paramelonica* Suleimanov, *Mesoschubertella* sp. 1, *Pseudofusulina* sp. 1, *Pseudofusulina* sp. 2, *P. paraconcessa* Rauser, *P. ex gr. pedissequa* Vissarionova, *P. insignita* Vissarionova, *P. abortiva* Tchuvashov, *P. seleukensis*

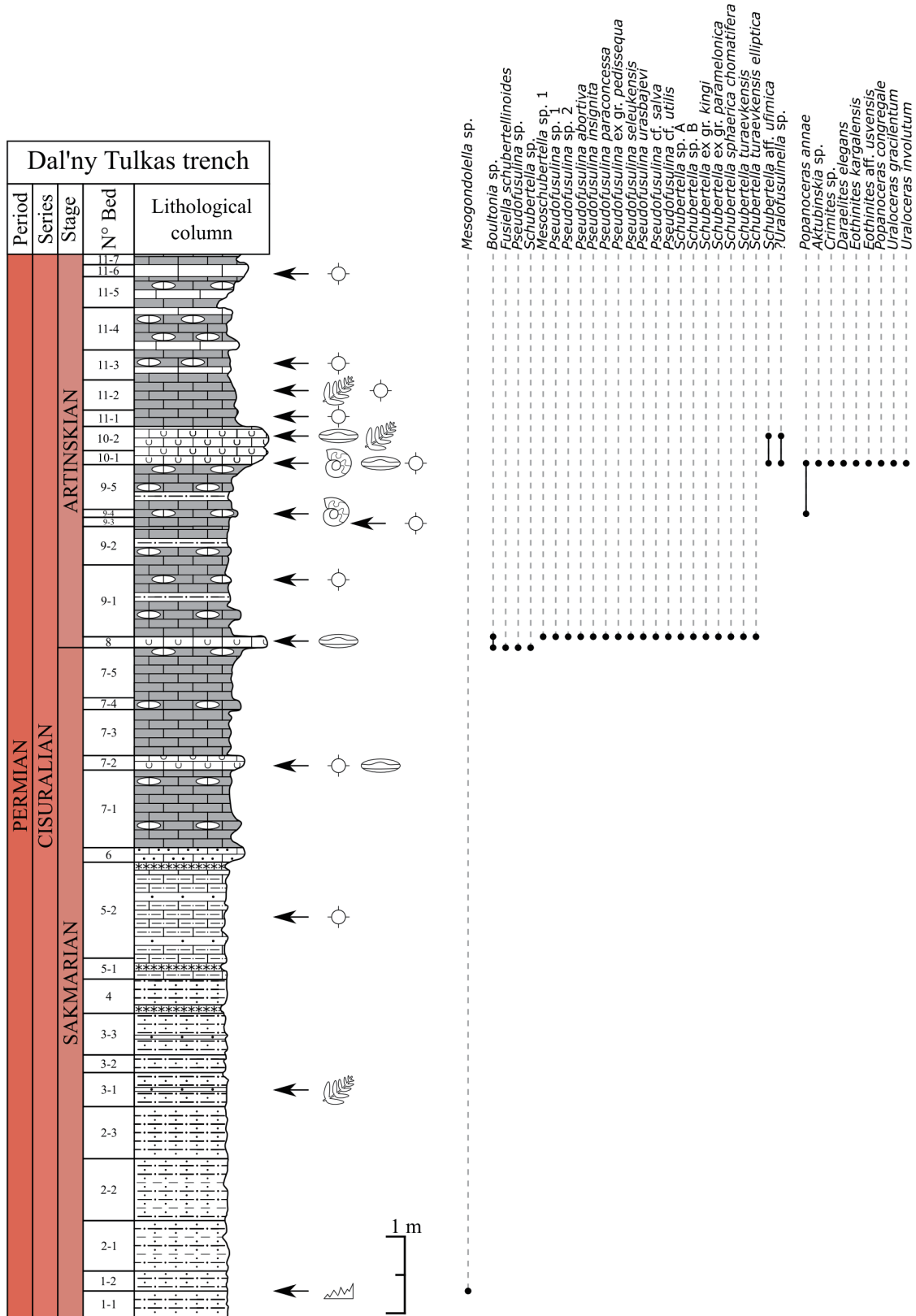


Fig. 5. Stratigraphic column with distribution of samples collected for conodonts, ammonoids, fusulines, and radiolarians in the Dal'ny Tulkas trench. See legend of Fig. 3 for lithology and fossil symbols.



Fig. 6. Photos of the Dal'ny Tulkas trench. A. general view of the trench and the section; B. Sakmarian part of the succession; C. Sakmarian-Artinskian boundary, bed 8.

Rauser, *P. urasbajevi* Rauser, *P. cf. utilis* Tchuvashov, *P. cf. salva* Vissarionova). Thickness: 0.15 m.

Bed 9. Dark grey mudstone with thin beds of siltstone and numerous limestone nodules. Fossil content: ammonoids (9-4: *Popanoceras annae* Ruzhencev), radiolarians. Thickness: 2.2 m.

Bed 10. Bioclastic limestone, grey, fine-grained, with interbeds of mudstone. Fossil content: large plant remains, fusulines (*Schubertella* aff. *ufimica* Baryshnikov, ?*Uralofusulinella* sp.), radiolarians, brachiopods, ammonoids [10-1: *Eothinites kargalensis* Ruzhencev, *Eothinites* aff. *usvensis* Bogoslovskaya, *Popanoceras annae* Ruzhencev, *P. congregale* Ruzhencev, *Daraelites elegans* Tchernow, *Uraloceras gracilentum* Ruzhencev, *U. involutum* (Voinova), *Crimites* sp., *Aktubinskia* sp.]. Thickness: 0.5 m.

Bed 11. Silty mudstone with nodules and interbeds of grey limestone. Fossil content: radiolarians, plant remains, and brachiopods. Thickness: 2.2 m.

Interpreted Sequence Stratigraphy

The Artinskian succession is associated with a transgressive systems tract and a maximum flooding surface in many global sections. This is best illustrated in the Raanes and Great Bear Cape formations in the Canadian Arctic (Beauchamp et al., 2021; Chernykh et al., 2020) where the base-Artinskian is correlated to a maximum flooding surface (MFS) based on the

local first occurrence of *Sweetognathus asymmetricus*. Having the boundary within or at the top (MFS) of a transgressive systems tract provides an easily identified physical stratigraphic correlation tool. The section at Dal'ny Tulkas has not been investigated in detail for the sequence stratigraphy, but it does exhibit features that can be interpreted as a sequence boundary and transgressive systems tract. For example, non-calcareous algae, plant remains, and *Calamites* have been recovered from beds 3 and 4 in the trench and bed 2 in the main section; also, bed 6 in the trench comprises calcareous sandstone. Units above bed 2 in the section and bed 6 in the trench (above lowest dashed line in Fig. 7) include carbonate mudstone, with increasingly diverse and abundant marine fossils. A little higher the base-Artinskian boundary is defined at the main section (solid red line in Fig. 7). Sedimentation appears to be uninterrupted throughout this transgressive interval, punctuated only by tempestites that delivered coarser bioclastic material to the slope during storms.

Biostratigraphy

The Dal'ny Tulkas section and trench have been studied extensively for biostratigraphic content. The following sections provide details regarding the occurrence and biostratigraphic utility of conodonts, ammonoids, fusulines, small foraminifers, palynomorphs, and radiolarians.

Conodonts

Conodonts are considered the primary biostratigraphic tool for this interval (Henderson, 2018), which makes it possible to clearly fix the desired boundary and carry out its global correlation with the appearance of the cosmopolitan form – *Sweetognathus asymmetricus* Sun and Lai, whose position in the chronomorphocline (Fig. 8) *Sw. binodosus* - *Sw. anceps* - *Sw. asymmetricus* is confirmed by the study of the Dal'ny Tulkas section (Henderson and Chernykh, 2021). The Dal'ny Tulkas section provides the best information with respect to conodonts of the genus *Sweetognathus* in the region (Chernykh, 2005, 2006).

In order to explain the value of these new data, it is useful to consider the previously published information about the development of this group of conodonts in the Usolka section (Chernykh and Chuvashov, 2004). The primitive form, *Sweetognathus expansus* (Perlmutter), in which the beginning of the carinal differentiation (Fig. 8) occurs, appears in middle to late Asselian. In latest Asselian to early Tastubian it evolves into *Sweetognathus* aff. *merrilli* (this form is significantly different from the type *Sw. merrilli* Kozur of mid-Asselian age; see Boardman et al., 2009; Petryshen et al., 2020) with carinal development forming rounded nodes in upper view (Fig. 8). Further evolution of this group leads to the appearance in the Tastubian horizon of such forms, which have few carinal nodes, but those nodes are laterally elongated with a tendency toward the bilobate dumbbell-like structure. These forms are referred to as the species *Sweetognathus binodosus* Chernykh (Fig. 8).

The special features of further evolution of this group during Sterlitamakian and Artinskian time are revealed in the trenched part of the Dal'ny Tulkas section. The development of the carina of Sterlitamakian representatives of the line *Sweetognathus*

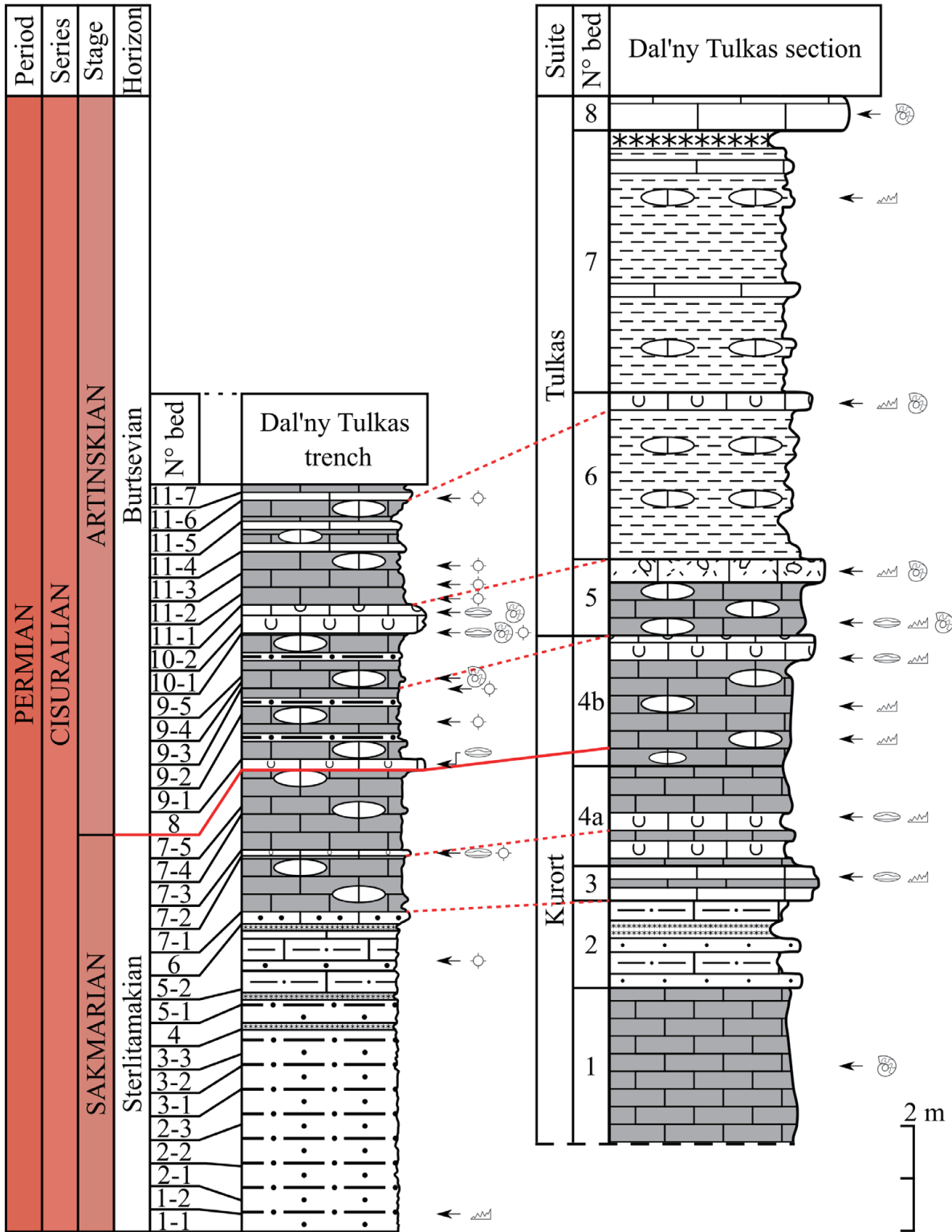


Fig. 7. Correlation of the Dal'ny Tulkas section and trench.

Asselian Stage		Sakmarian Stage		Artinskian Stage
Conodont Zone				
<i>postfusus</i>	<i>aff. merrilli</i>	<i>binodosus</i>	<i>anceps</i>	<i>asymmetricus</i>

Fig. 8. The evolutionary lineage: 1. *Sweetognathus expansus* (Perlmutter), (Usolka section, bed 21); 2. *Sw. aff. merrilli* Kozur (Usolka section, bed 26/2); 3. *Sw. binodosus* Chern. (Usolka section, bed 26/3); 4. *Sw. anceps* Chern. (D. Tulkas section, bed 4a); 5. transitional form from *Sw. anceps* to *Sw. asymmetricus* Sun and Lai (D. Tulkas section, bed 4b); 6. *Sw. asymmetricus* Sun and Lai (D. Tulkas, bed 4b).

expansus- *Sw. aff. merrilli* - *Sw. binodosus* continues in the direction of the differentiation of carinal nodes, that led to the appearance of *Sw. anceps* Chernykh (Fig. 9) that possesses dumbbell-like nodes. In addition to these forms, there appear forms that include fragmentary development of the pustulose, mid-carinal connecting ridge, which are considered as transitional to *Sw. asymmetricus*. Forms of *Sw. anceps* with the rudiments of mid-carinal pustulose ridge continue to be encountered above in the section until finally there appear specimens of *Sweetognathus* with fully developed dumbbell-like nodes and a complete middle pustulose connecting ridge. We identify such forms to the species *Sweetognathus asymmetricus* (Figs. 9, 10) whose representatives are widely known in many regions where deposits of Artinskian age are present. Proposals to use the appearance of *Sw. asymmetricus* (then identified as *Sw. whitei*, a form now known as a late Asselian homeomorph; see Rhodes, 1963, Riglos Suarez et al., 1987 and Holterhoff et al., 2013 for examples of the homeomorph; problems discussed in Henderson, 2018; lineages discussed in Petryshen et al., 2020) for determining the lower boundary of Artinskian Stage were noted previously by different researchers (Kozur, 1977; Mei et al., 2002; Ritter, 1986;

Wang et al., 1987); however, at the time there was insufficient knowledge about the early members of the evolutionary lineage of this group of conodonts. Forms referred to the independent species *Sweetognathus anceps*, also occur widely, but until now they were encountered together with the typical *Sw. asymmetricus*, and the majority of researchers identified those specimens, without the fully developed middle connecting ridge, as *Sweetognathus cf. whitei*. The transitional passage from *Sw. anceps* to *Sw. asymmetricus* is traced for the first time; these transitional forms indicate proximity to the boundary, but the point is recognized by the FAD of definite *Sw. asymmetricus*. We now have a complete picture of the development of these conodonts in the evolutionary lineage *Sweetognathus expansus* - *Sw. aff. merrilli* - *Sw. binodosus* - *Sw. anceps* - *Sw. asymmetricus* (Fig. 8). The emended definition as described by Henderson and Chernykh (2021) for *Sweetognathus asymmetricus* will need to be considered carefully given its importance for correlation of the Artinskian. Some previous correlations will need to be revised. For example, the cyclothem interval from Florence Limestone to Fort Riley Limestone in Kansas (Boardman et al., 2009) has long been correlated with the Artinskian because of the occurrence

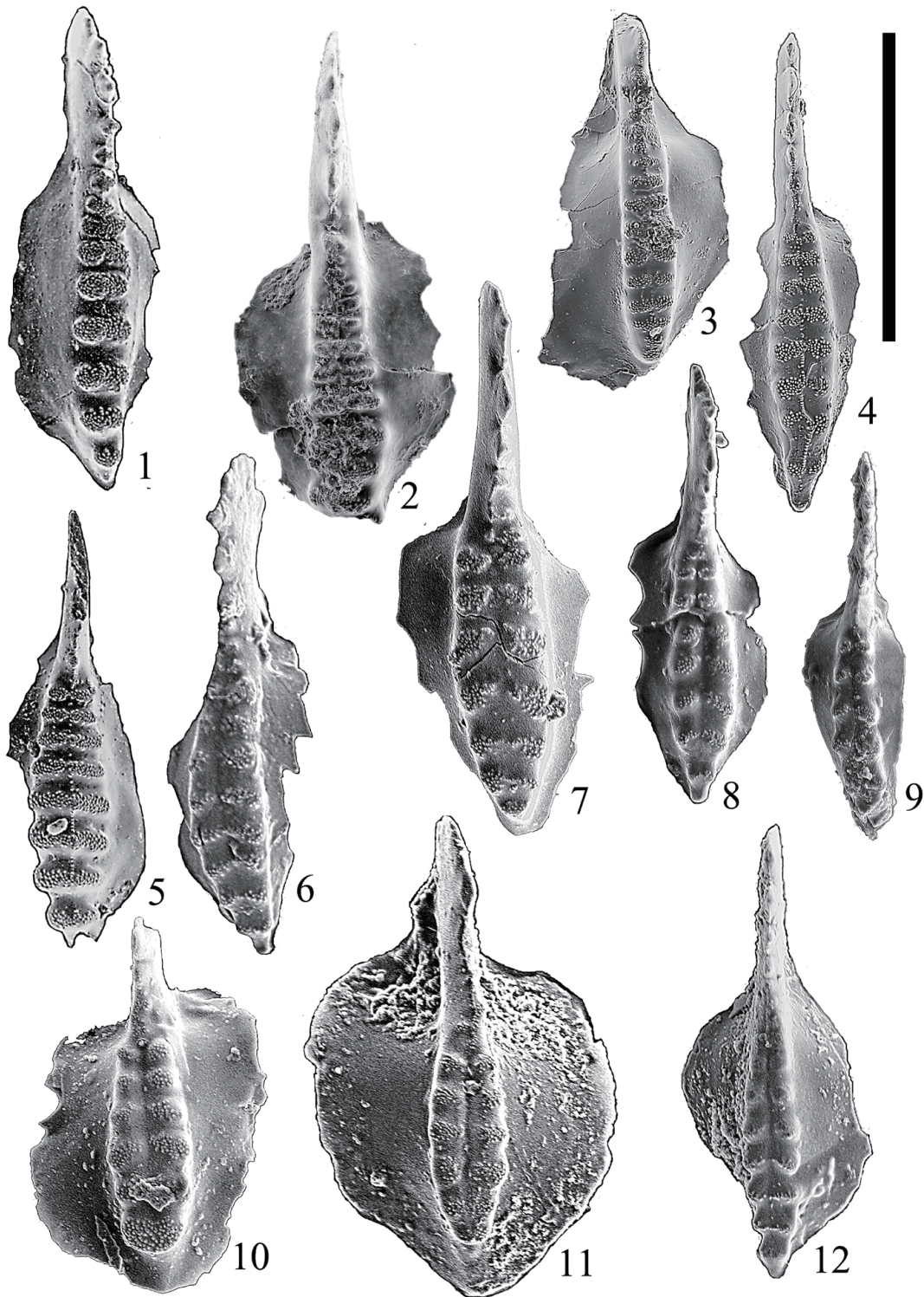


Fig. 9. Upper Sakmarian-Lower Artinskian conodonts in Dal'ny Tulkas section (x90). Scale bar: 500 μ m

1, 2. *Sweetognathus anceps* Chernykh, 2005: 1, holotype DT19-1, bed 5; lower part of Artinskian, *asymmetricus* Zone; 2, DT24, bed 4a; upper Sakmarian, Sterlitamakian horizon, *anceps* Zone. 3-5. *Sweetognathus asymmetricus* Sun and Lai, 2017: 3, DT-18a, transitional form from *Sweetognathus anceps* Chernykh to *Sw. asymmetricus* Sun and Lai, bed 4b; 4, DT-18b, typical specimen with a fully developed median ridge, bed 4b; 5, T-19-3, specimen with symmetrically built carina, bed 5, lower part of Artinskian, Burtsevian horizon, *asymmetricus* Zone. 6-8. *Sweetognathus obliquidentatus* (Chernykh), 1990: 6, holotype ZSP-1070/19v; 7, DT40-3; 8, T/19-1-5; bed 5; lower part of Artinskian, Burtsevian horizon, *asymmetricus* Zone. 9, 12. *Sweetognathus* aff. *ruzhencevi* (Kozur), 1976: 9, DT40-6; 12 – DT40-13; bed 5; lower part of Artinskian, Burtsevian horizon, *asymmetricus* Zona. 10, 11. *Sweetognathus gravis* Chernykh, 2006: 10 – DT40-10k; 11 – holotype U40-9b; bed 5; lower part of Artinskian, Burtsevian horizon, *asymmetricus* Zona.

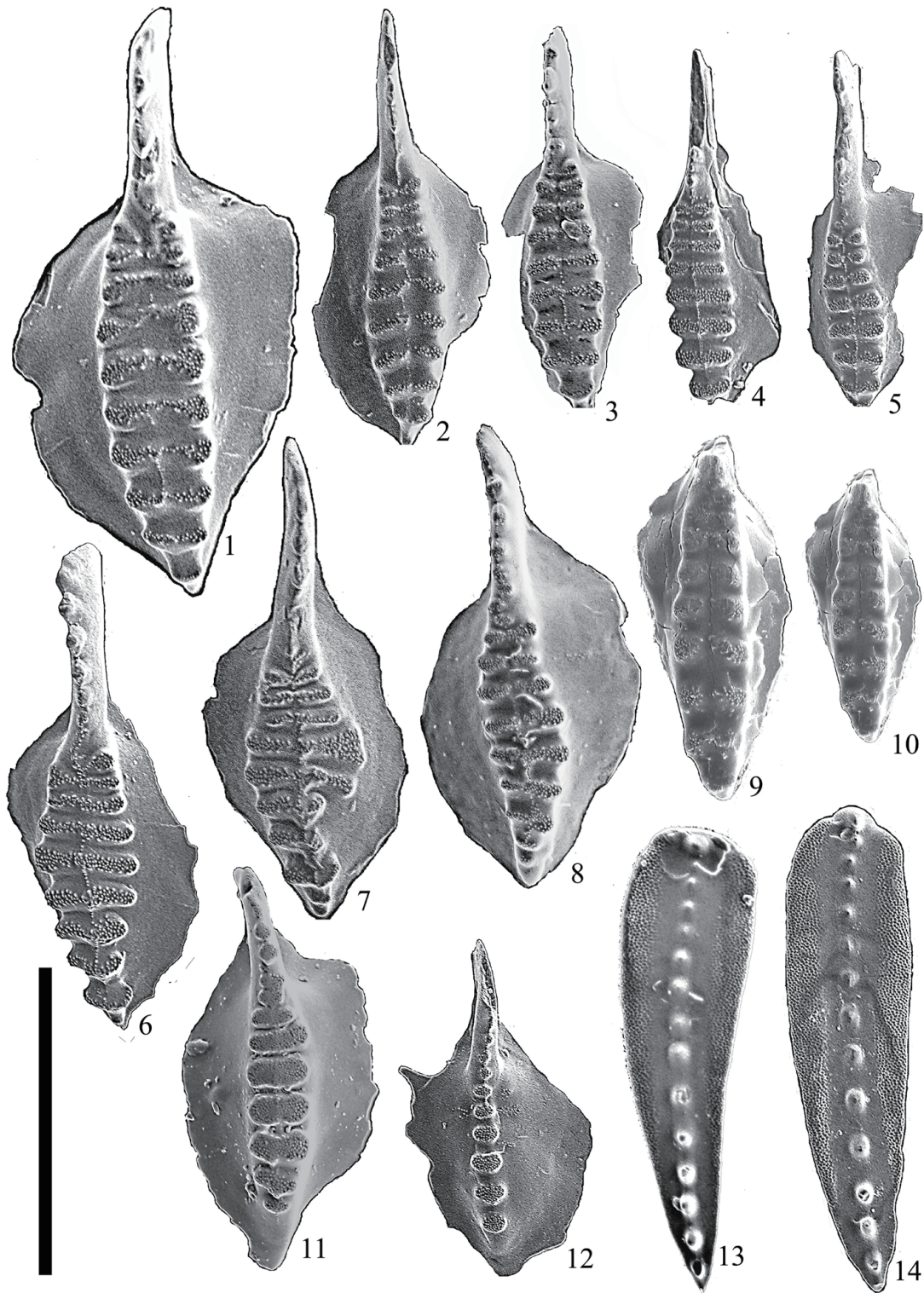


Fig. 10. Lower Artinskian conodonts in bed 10 (Artinskian, lower part of Iriginian horizon, clarki Zone in Dal'ny Tulkas section (x90). Scale bar: 500 μ m
1, 4-8. *Sweetognathus asymmetricus* Sun and Lai, 2017: 1, DT40-27, the relicts of the longitudinal middle ridge are visible; 4, DT40-29, the middle ridge is located above upper surface of carinal nodes; 5, DT40-17, the middle ridge is located lower upper surface of carinal nodes; 6, DT40-24; 7, DT40-19; 8, DT40-21. **2, 3.** *Sweetognathus* aff. *clarki* (Kozur), 1976: 2, DT40-18; 3, DT40-22, the relicts of the longitudinal middle ridge are visible. **9, 10.** *Sweetognathus clarki* (Kozur), 1976: 9, DT40-33; 10, DT40-32. **11, 12.** *Sweetognathus* aff. *binodosus* Chernykh, 2005: 11, DT40-23; 12, DT40-20. **13, 14.** *Mesogondolella laevigata* Chernykh, 2005: 13, U40-26; 14, holotype DT40-25.

of *Sweetognathus whitei*. However, it is now known that this taxon differs from *Sweetognathus asymmetricus* despite some similarity. The co-occurrence of *Sw. whitei* and *Streptognathodus florensis* supports a latest Asselian age; Chernykh (2006) reports *S. florensis* from the Usolka section of Russia exactly 1.1 metre below the GSSP for the base-Sakmarian stage (Chernykh et al., 2020). Other sections in which this taxonomic distinction has been made are described below.

The chronomorphocline *Sw. binodosus* - *Sw. anceps* - *Sw. asymmetricus* can also be recognized in transgressive facies of uppermost Raanes and lower Great Bear Cape formations (Beauchamp et al., 2021; Chernykh et al., 2020), southwest Ellesmere Island, Canadian Arctic (Henderson, 1988; Henderson, 1999; Beauchamp and Henderson, 1994; Mei et al., 2002), Riepetown Formation, Moorman Ranch, Nevada (Ritter, 1986), upper Riepe Springs Limestone, Elko County, Nevada (Read and Nestell, 2018), Buckskin Mountain Formation in Carlin Canyon, Nevada (Dehari, 2016), Ross Creek Formation in southeastern British Columbia (Henderson and McGugan, 1986), and many other regions. In South China, the chronomorphocline can be recognized in condensed and continuously deposited thin beds of slope carbonates, organic-rich mudstone or shale and wackestone in the Luodian (NSC) and Ziyun (Houhongchong or HHC) sections of Guizhou province. These slope deposits are correlated with the Liangshan Formation (or Liangshan Member in the basal part of the Chihhsia Formation) and the time represented by a hiatus between the Liangshan Formation and the Maping Formation in more proximal sections in South China. Chen (2011) illustrated well preserved specimens of *Sweetognathus binodosus* and *Sw. anceps* from 347 to 362 metres above the Luodian section base. Wang and Higgins (1989) and Wang (1994) also illustrated *Sw. binodosus* and *Sw. asymmetricus* from the Luodian section. Chen (2011) illustrated *Sw. asymmetricus* (*Sw. whitei* in his thesis) from -533 to -548 metres at the Houhongchong section in Ziyun. *Sweetognathus asymmetricus* was named based on its occurrence in beds 18-23 at the Tieqiao section (Guangxi Province) of south China, but this level, near the lithologic boundary between the Liangshan Member and the lower part of the main Chihhsia Formation, seems to be high in the range of the species (Wang et al., 1987; Shen et al., 2007; Sun et al., 2017; Zhang et al., 1988). The species, as currently understood, may have a long range, but the FAD level of *Sw. asymmetricus* is clearly recognized by being proximal to the *Sw. binodosus*-*Sw. anceps* lineage, with transitional forms from *Sw. anceps* and *Sw. asymmetricus* overlapping the boundary. At the Dal'ny Tulkas section, *Sw. asymmetricus* ranges at least as high as bed 13 (60 metres above bed 11; see Table 1) where it co-occurs with *Sw. clarki*, *Sw. aff. ruzhencevi*, and *Mesogondolella bisselli*.

Ammonoids

Little has been known about the ammonoids of the Dal'ny Tulkas. Previously, Boris Chuvashov and colleagues made collections at two levels of the lower part of the Artinskian stage (bed 5), in which M.F. Bogoslovskaya identified *Popanoceras annae* Ruzhencev, *P. tschernowi* Maximova, *P. congregale* Ruzhencev, *Kargalites* sp. and *Neopronorites skvorzovi* (Tchernow) (Chuvashov et al., 2002a, b). This assemblage dates

the host beds as early Artinskian. Rare specimens of Artinskian sp. are found here. In 2016, R.V. Kutygin searched for fossil cephalopods in the natural outcrop of the Dal'ny Tulkas, as well as in a trench dug by an excavator along this outcrop.

In the Sakmarian interval, ammonoids are very rare and unidentifiable specimens were found only in bed 1 of the section. At 1.6 m above the Sakmarian-Artinskian Stage boundary, a small accumulation of shells of *Popanoceras annae* Ruzhencev were found in clay-carbonate concretions in interbed 9-4 of bed 9 of the trench. This is the most common Artinskian ammonoid of the Southern Urals. The vertical interval of distribution of *Popanoceras annae* covers both substages of the Artinskian Stage; however most of the known specimens come from the lower substage (Aktastinian).

In the bioclastic limestone of the trench, many more young juvenile ammonoids are scattered 2.5 m above the Sakmarian-Artinskian boundary (bed 10-1 of the trench; Fig. 11; Table 1). Rare medium-sized and large ammonoid specimens are usually represented only by fragments. The collection of cephalopods is dominated by *Eothinites kargalensis* Ruzhencev, which is often found in the Aktastinian of the southern Urals. Among the *Eothinites*, several specimens have prominent transverse ornamentation (Figs. 11.4, 11.5), previously identified as *Eothinites* aff. *usvensis* Bogoslovskaya. Possessing ornamentation very similar to representatives of *E. usvensis* from the Urminskaya Formation (upper of part Artinskian) of the Middle Urals (Bogoslovskaya, 1962), the Tulkas specimens differ in the less evolute shell. In addition to *Eothinites*, the assemblage contains *Popanoceras annae*, *P. congregale*, and *Daraelites elegans* Tchernow, which characterize the Artinskian Stage of the Urals. Paragastrioceratids are rare; they are represented by small specimens of *Uraloceras involutum* (Voinova) and *U. gracilentum* Ruzhencev.

The species *Uraloceras involutum* is the most common of the Artinskian paragastrioceratids of the southern Urals, with the best finds occurring in the lower substage (Aktastinian). In addition to the Southern Urals, the species *Uraloceras involutum* is also known from the Urminskaya Formation of the Middle Urals (Bogoslovskaya, 1962), in the Kosva Formation of the Pechora Basin (Bogoslovskaya and Shkolin, 1998), in the upper Raanes ("Assistance") Formation of Ellesmere Island of the Canadian Arctic Archipelago (Nassichuk et al., 1966; Nassichuk, 1975), in the Jungle Creek Formation of the northern Yukon Territory (Nassichuk, 1971), in the Eagle Creek Formation of Alaska (Schiappa et al., 2005), as well as possibly in British Columbia and in Nevada (Schiappa et al., 2005).

A rare Aktastinian species of *Uraloceras gracilentum* has features of the oldest paragastrioceratids, expressed by unusually slow coiling for the genus *Uraloceras*. According to Ruzhencev (1956), the possible ancestor of *Uraloceras gracilentum* is the late Sakmarian species *Uraloceras limatulum* Ruzhencev, which probably belongs to a separate genus from *Uraloceras*. Also here the shells of species of the genera *Crimites* and *Aktubinskia* have been found, but poorly preserved.

In the natural outcrop of Dal'ny Tulkas section, ammonoids were collected from Bed 8. The ammonoids found in this locality belong to the families Daraelitidae, Pronoritidae,

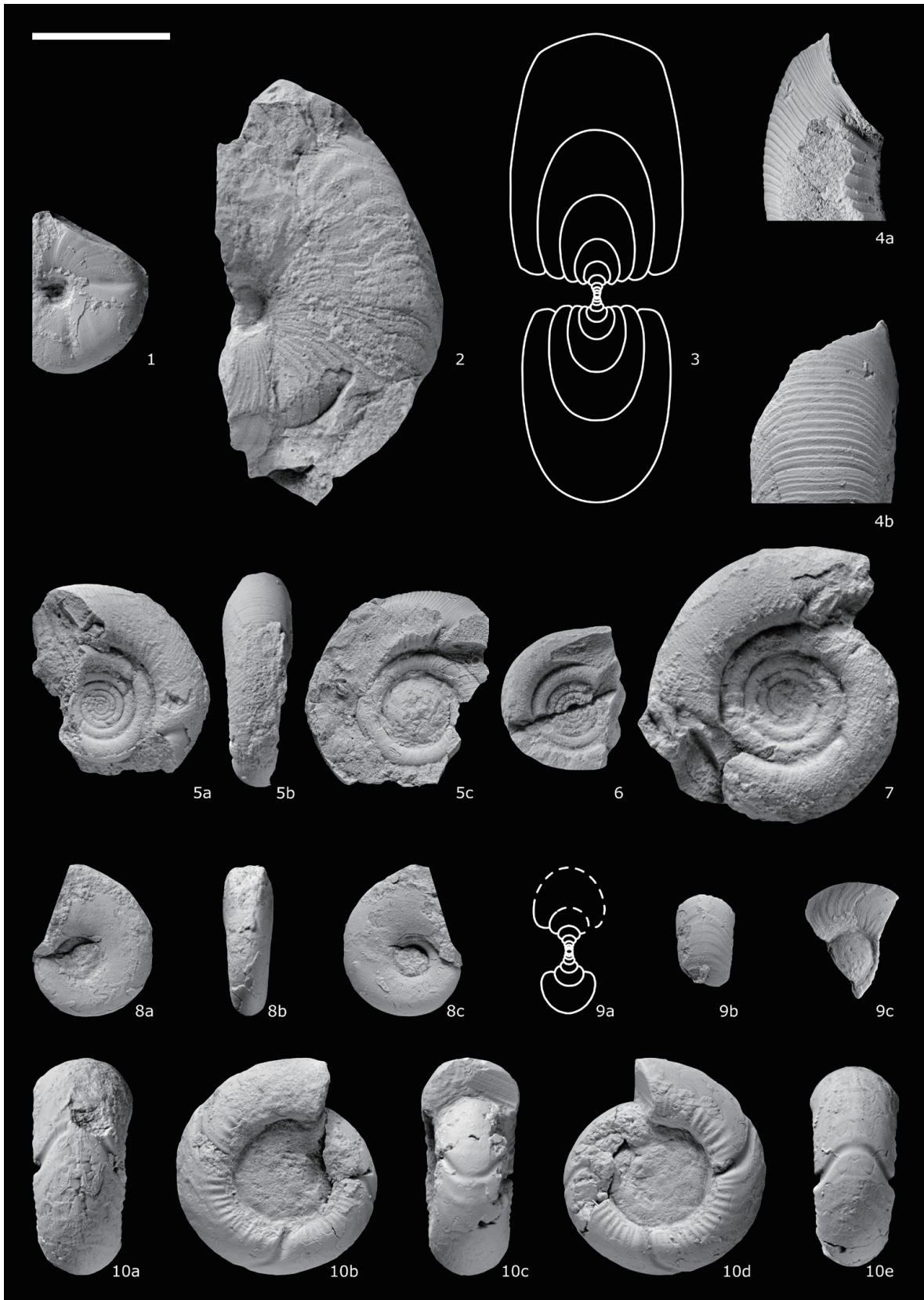


Fig. 11. Ammonoids from the Dal'ny Tulkas trench, bed 10-1. Scale bar: 10 mm for figs 1-3, 5-10; 5 mm for figs 4a-b.
 1. *Popanoceras congregale* Ruzhencev. 2-3. *Popanoceras annae* Ruzhencev. 4-5. *Eothinites* aff. *usvensis* Bogoslovskaya.
 6-7. *Eothinites kargalensis* Ruzhencev. 8. *Daraelites elegans* Tchernow. 9. *Uraloceras involutum* (Voinova). 10. *Uraloceras gracilentum* Ruzhencev.

Medlicottiidae, Agathiceratidae, Eothinitidae, Metalegoceratidae, Paragastrioceratidae, Marathonitidae, and Popanoceratidae. Earlier from the same location (Bed 8), Tamra Schiappa identified *Sakmarites postcarbonarius* (Karpinsky), *Agathiceras uralicum* (Karpinsky), *Kargalites typicus* (Ruzhencev), *Paragastrioceras* sp., and *Crimites subkrotowi* Ruzhencev (Chuvashov et al., 2013) (Table 1).

The ammonoid assemblage of the Dal'ny Tulkas section is typical of the lower Artinskian. Among ammonoids, a number of stratigraphically important genera, of which *Daraelites*, *Aktubinskia*, *Eothinites*, and *Popanoceras* have been recognized at Dal'ny Tulkas and appear in the Aktastinian. The entry of *Neopronorites skvorzovi*, *Uraloceras involutum*, *U. gracilentum*, *Popanoceras tschernowi* and *P. annae* are important indicators of the Sakmarian-Artinskian boundary. Considering the abundance of *Uraloceras involutum* in the lower part of the Artinskian stage in the southern Urals, and its wide geographical range, the interval of the Dal'ny Tulkas section containing lower Artinskian ammonoids is proposed to be designated as "Beds with *Uraloceras involutum*". The biostratigraphic value of Permian ammonoids is summarized in Leonova (2018).

Foraminifers

Dal'ny Tulkas section

Fusulines occurring with Sakmarian conodonts are represented by Sakmarian species as *Pseudofusulina callosa* Rauser, *P. callosa proconcavatas* Rauser, *P. jaroslavkensis fraudulentula* Kireeva, *P. cf. parajaroslavkensis* Kireeva, *P. blochini* Korzhenevski.

A redeposited assemblage of Sakmarian (Sterlitamakian) fusulines was found in the limestone which contains Artinskian conodonts: *P. aff. longa* Kireeva, *P. fortissima* Kireeva, *P. anostiata* Kireeva, *P. plicatissima* Rauser, *P. urdalensis abnormis* Rauser. Artinskian (Burtsevian) fusulines are found in carbonate mud matrix: *P. callosa*, *P. plicatissima*, *P. plicatissima irregularis* Rauser, *P. urdalensis* Rauser, *P. fortissima*, *P. concavatas* Vissarionova, *P. juresanensis* Rauser, *P. consobrina* Rauser, *P. paraconcessa* Rauser (Chernykh et al., 2015) (Table 1).

Dal'ny Tulkas trench

A new excavation needed for resampling of geochemical and paleontologic characteristics was carried out in 2016. Fusulines and small foraminifers were found in limestones at four levels. Fusulines are illustrated in figure 12 and small foraminifers are illustrated in figures 13 and 14; both are listed in Table 1.

Three complexes are distinguished in the trench. The first assemblage (bed 8-1) consists of 4 species of fusulines and 11 species of small foraminifers. Species of *Boultonia*, *Schubertella*, and *Pseudofusulina* are characteristic for the Sakmarian and the Artinskian. *Fusiella schubertellinoides* Suleimanov is typical for the upper Asselian-Sakmarian. Most small foraminifers species are Burtsevian (lower substage of Artinskian): *Dentalina particulata* Baryshnikov, *Geinitzina lysvaensis* Baryshnikov, *Nodosinelloides kislovi* (Koscheleva), *N. dualis* (Baryshnikov), *Howchinella* aff. *turrae* (Baryshnikov), *?Rectoglandulina* sp., *Postmonotaxinoides costiferus* (Lipina), *Endothyra lipinae lata* Zolotova. *Nodosariida* is predominant among them. There are *Rectoglandulina* and *Howchinella*, which appear at the base of

the Burtsevian (Baryshnikov et al., 1982).

The second assemblage (bed 8-2) consists of species of 5 genera of fusulines: *Boultonia*, *Schubertella*, *Pseudofusulina*, *Fusiella* and *Mesoschubertella*. Fusulines include the frequent and varied *Schubertellida*, which are characteristic for the Sakmarian and Artinskian. *Pseudofusulina paraconcessa*, *Ps. ex gr. pedissequa* Vissarionova, *Ps. abortiva* Tshuvashov, *Ps. seleukensis* Rauser, and *Ps. urasbajevi* Rauser are characteristic of the Artinskian. Generally the age of this assemblage is Artinskian. Among the 32 small foraminifer species of the second assemblage, in addition to the species from the first assemblage, there are *Langella*, Artinskian species - *Nodosinelloides bella kamaenis* (Baryshnikov), *N. jaborovensensis* (Koscheleva), *N. incebrata novosjolovi* (Baryshnikov), *Nodosinelloides netchaewi rasik* (Baryshnikov), *Endothyra soshkinae* Morozova, numerous *Postmonotaxinoides costiferus* (Lipina), *Bradyina* ex gr. *lucida* Morozova, *Br. lucida* Morozova, *Pseudobradyna compressa* Morozova, *Deckerella elegans multicamerata* Zolotova, *Hemigordiellina elegans* (Lipina), and the first *Hemigordius* sp. The Artinskian small foraminifers assemblages in the Urals are distinguished by the appearance of *Hemigordius*. The second assemblage also contains *Deckerella media bashkirica* Morozova, *D. elegans* Morozova, *Pseudobradyna compressa minima* Morozova, *Tetrataxis* ex gr. *conica* Ehrenberg, *T. plana* Morozova, *T. hemisphaerica* Morozova, *T. hemisphaerica elongata* Morozova, *T. lata* Spandel, characteristic of Sakmarian assemblages, and *Lateenoglobivalvulina spiralis* (Morozova), *Trepeilopsis* sp., and others of Cisuralian assemblages.

The third assemblage (bed 10) consists of fusulines: *Schubertella* aff. *ufimica* Baryshnikov, *?Uralofusulinella* sp. 2. Twenty-two small foraminifer species from the first and the second assemblages have been found in the third assemblage, and 15 species of small foraminifers appeared for the first time in the trench. These are Burtsevian-Irginian species - *Bradyina subtrigonalis* Baryshnikov, *Endothyranella protracta maxima* Baryshnikov, *Tetrataxis lata novosjolovi* Baryshnikov, *?Uralogordius* sp., *?Pachyphloia* sp., *Geinitzina richteri kasib* Koscheleva, *Nodosinelloides* ex gr. *netchaewi* (Tcherdynzev), *N. jazvae* Kosheleva and Cisuralian species - *Endothyra rotundata* Morozova, *E. symmetrica* Morozova, *E. lipinae* Morozova, *Pseudoagathammina regularis* (Lipina), *Pseudospira* cf. *vulgaris* (Lipina), and the upper Artinskian-lower Kungurian *Midiella ovatus minima* (Grozdilova).

All three small foraminifer assemblages are of early Artinskian age. They are similar in composition to early Yakhtashian assemblages from Turkey and northern Pamir (Filimonova, 2010). The first fusuline assemblage is of Sakmarian age, the second and third are Artinskian. The schubertellid-fusuline foraminiferal assemblages of late Asselian-Sakmarian age are replaced by typical Artinskian assemblages. Artinskian forms of foraminiferal communities are present throughout the entire boundary interval. Their diversity and abundance increase up section.

Palynology

The palynological succession of the beds above and below

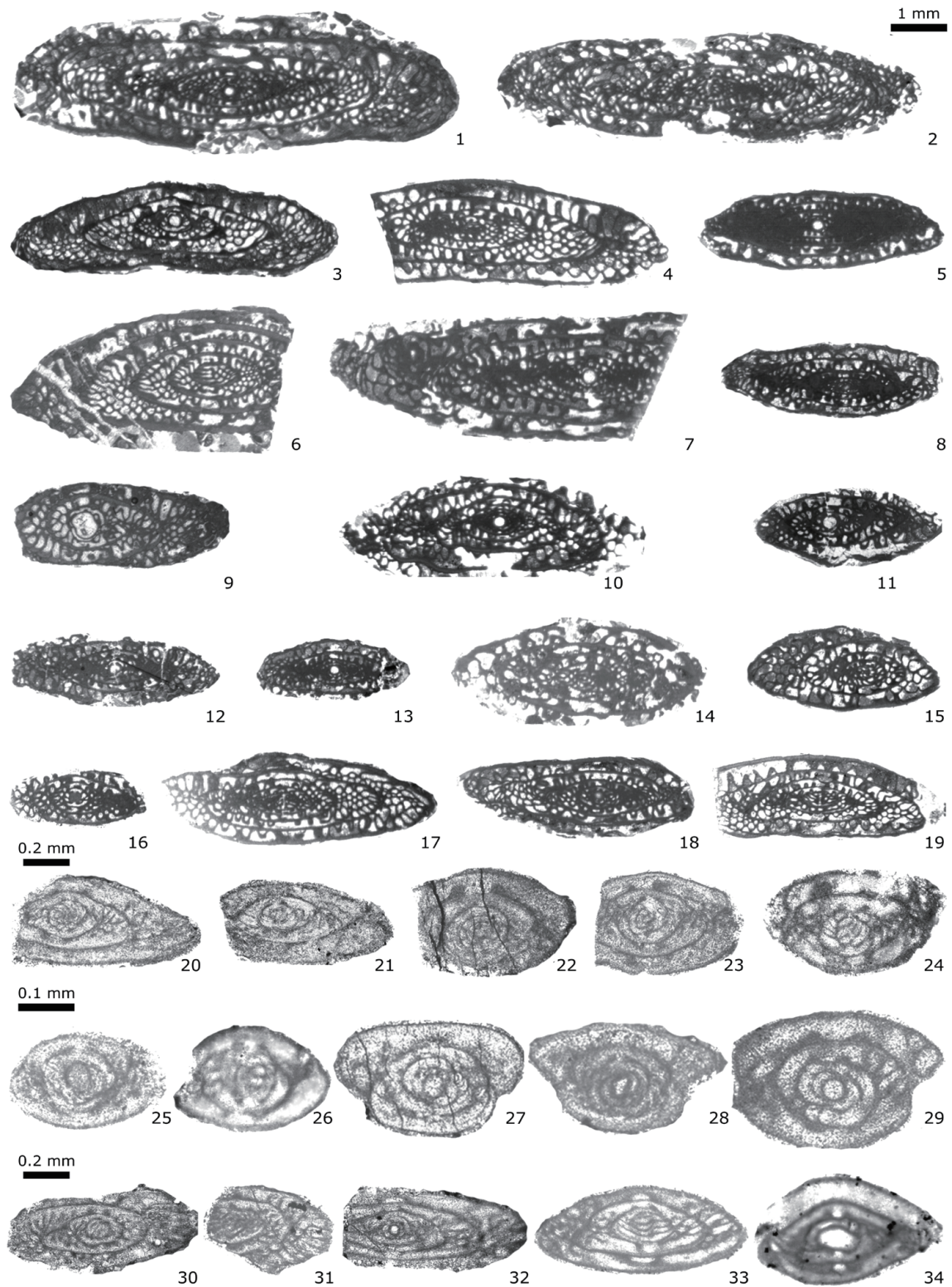


Fig. 12. Fusulines from Dal'ny Tulkas trench, beds 8-1, 8-2, 10. Scale bar: 1 mm for figs 1-19; 0.2 mm for figs 20-24, 30-34; 0.1 mm for figs 25-29.
1-2. *Pseudofusulina paraconcessa* Rauser, bed 8-2. **3-4.** *Pseudofusulina* ex gr. *pedissequa* Vissarionova, bed 8-2. **5.** *Pseudofusulina abortiva* Tchuvashov, bed 8-2. **6.** *Pseudofusulina* cf. *utilis* Tchuvashov, bed 8-2. **7.** *Pseudofusulina* cf. *salva* Vissarionova, bed 8-2. **8, 12-13.** *Pseudofusulina seleukensis* Rauser, bed 8-2. **9.** *Pseudofusulina* sp. 1, bed 8-2. **10-11.** *Pseudofusulina* ex gr. *seleukensis* Rauser, bed 8-2. **14-15.** *Pseudofusulina* sp. 2, bed 8-2. **16-19.** *Pseudofusulina urasbajevi* Rauser, bed 8-2. **20-21.** *Schubertella* ex gr. *kingi* Dunbar & Skinner, bed 8-2. **22-23.** *Schubertella* ex gr. *paramelonica* Suleimanov, bed 8-2. **24.** *Schubertella* sp. A, bed 8-2. **25-26.** *Schubertella* aff. *ufimica* Baryshnikov, bed 10. **27-29.** *Schubertella* sp. B; 27-28, bed 10; 29, bed 8-2. **30-31.** *Boultonia* sp.; 30, bed 8-1; 31, bed 8-2. **32.** *Fusiella schubertellinoides* Suleimanov, bed 8-1. **33.** *Mesoschubertella* sp. 1, bed 8-2. **34.** ?*Mesoschubertella* sp. 2, bed 10.

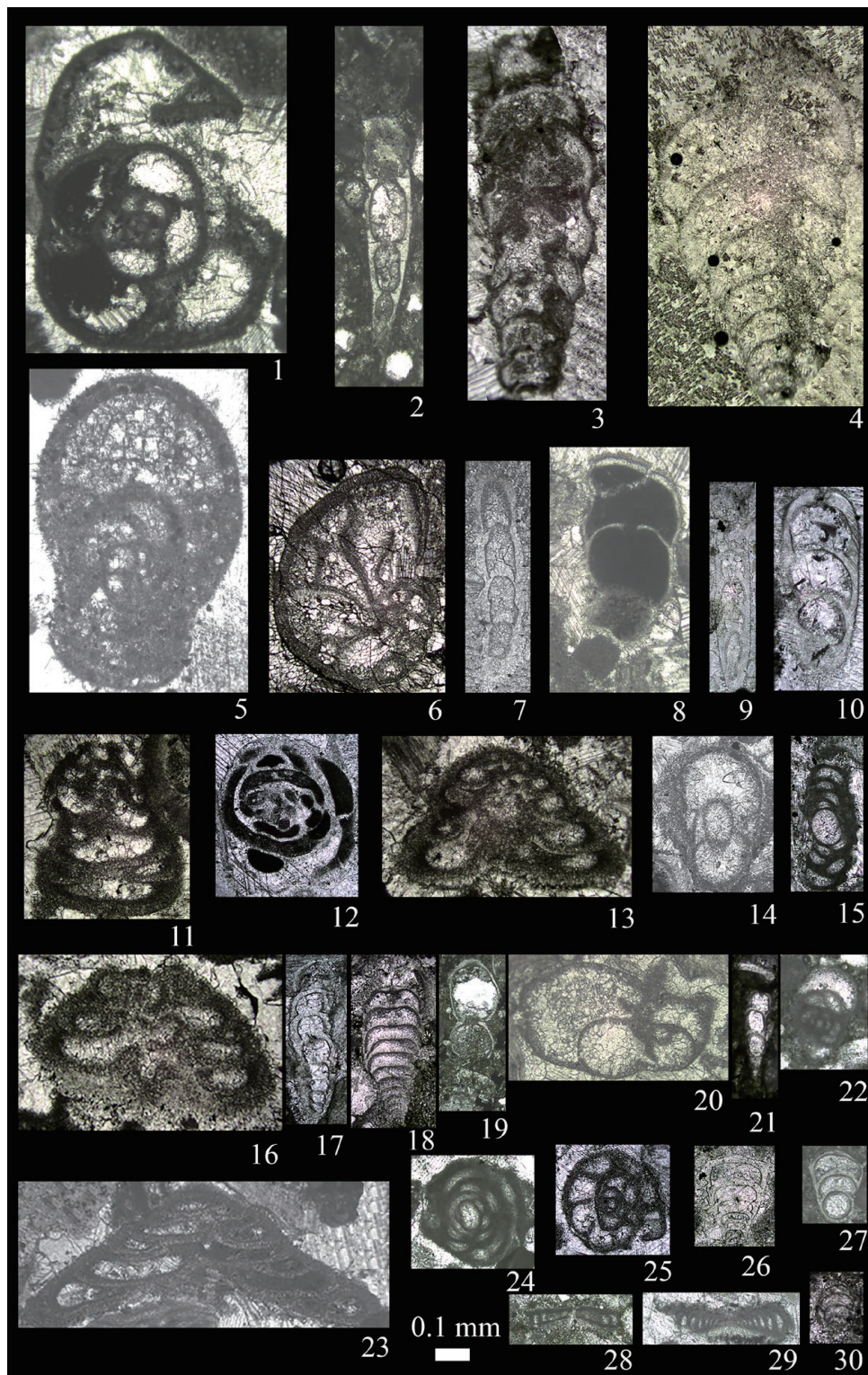


Fig. 13. Small foraminifers from the Dal'ny Tulkas trench, beds 8-1, 8-2. Scale bar: 0.1 mm.

1. *Bradyina lucida* Morozova, bed 8-2. 2. *Dentalina particulata* Baryshnikov, bed 8-1. 3. *Deckerella media bashkirica* Morozova, bed 8-2. 4. *Deckerella elegans multicamerata* Zolotova, bed 8-2. 5. *Pseudobradyna compressa* Morozova, bed 8-2. 6. *Globivalvulina* sp., bed 8-2. 7. *Dentalina particulata* Baryshnikov, bed 8-2. 8. *Nodosinelloides bella kamaensis* (Baryshnikov), bed 8-2. 9. *Nodosinelloides incebrata novosjolovi* Baryshnikov, bed 8-2. 10. *Nodosinelloides netchaewi rasik* (Baryshnikov), bed 8-2. 11. *Tetrataxis hemisphaerica elongata* Morozova, bed 8-2. 12. *Pseudoagathammina dublicata* (Lipina), bed 8-2. 13. *Tetrataxis lata* Spandel, bed 8-2. 14. *Pseudobradyna compressa minima* Morozova, bed 8-2. 15. *Hemigordius* sp., bed 8-2. 16. *Tetrataxis hemisphaerica* Morozova, bed 8-2. 17. *Nodosinelloides jaborovenski* Kosheleva, bed 8-2. 18. *Geinitzina spandeli* Tcherdynzev, bed 8-1. 19. *Nodosinelloides kislovi* (Kosheleva), bed 8-1. 20. *Lateenoglobivalvulina spiralis* (Morozova), bed 8-2. 21. *Nodosinelloides dualis* (Baryshnikov), bed 8-1. 22. *Endothyra lipinae lata* Zolotova, bed 8-1. 23. *Tetrataxis plana* Morozova, bed 8-2. 24. *Hemigordiellina elegans* (Lipina), bed 8-2. 25. *Endothyra soshkinae* Morozova, bed 8-2. 26. *Geinitzina lysvaensis* Baryshnikov, bed 8-1. 27. ?*Rectoglandulina* sp., bed 8-1. 28. *Postmonotaxinoides costiferus* (Lipina), bed 8-1. 29. *Postmonotaxinoides costiferus* (Lipina), bed 8-2. 30. *Howchinella* aff. *turae* (Baryshnikov), bed 8-1.

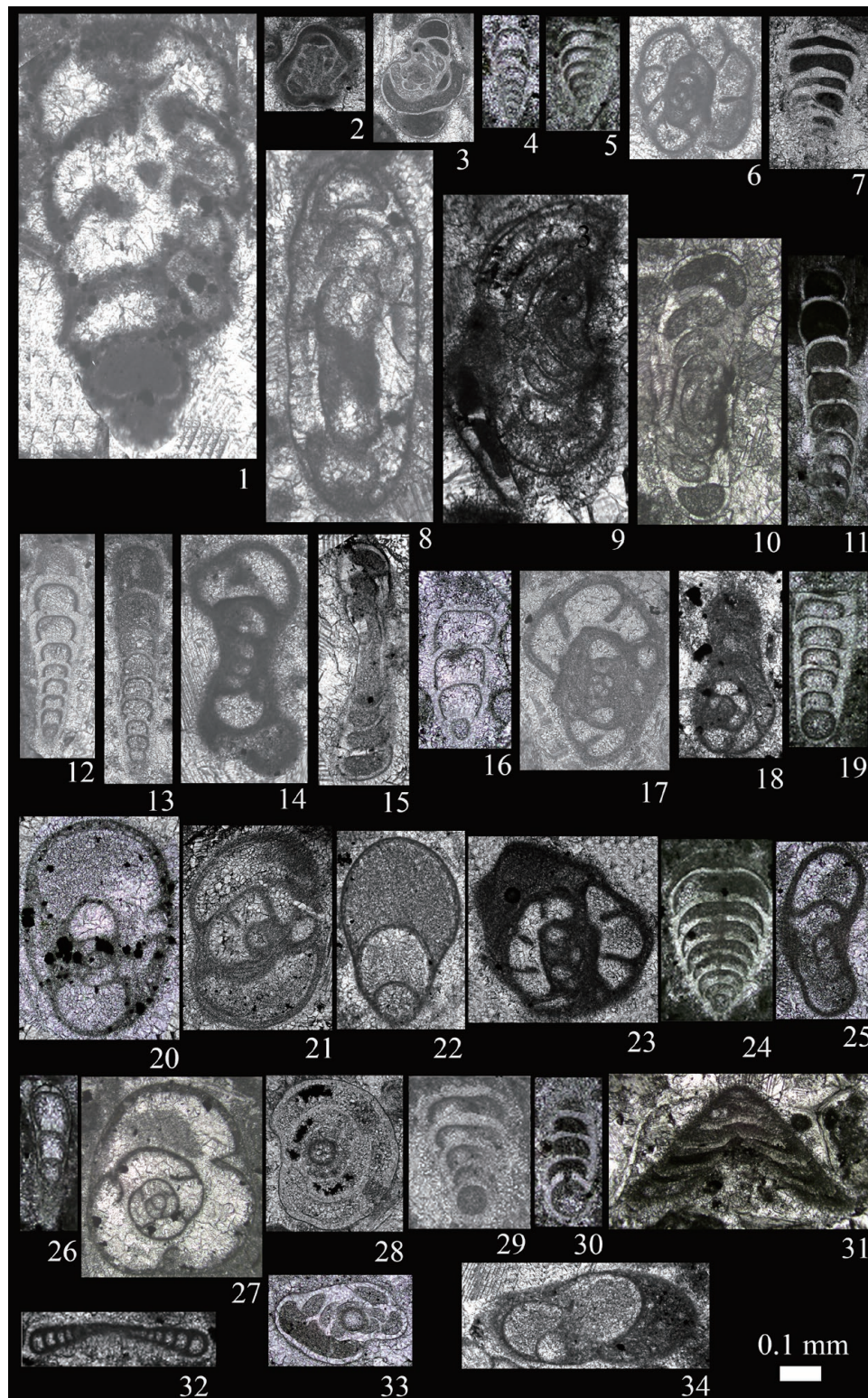


Fig. 14. Small foraminifera from the Dal'ny Tulkas trench, bed 10. Scale bar: 0.1 mm. 1. *Deckerella media bashkirica* Morozova. 2. *Hemigordiellina elegans* (Lipina). 3. *Pseudoagathammina dublicata* (Lipina). 4. *Howchinella* aff. *turae* (Baryshnikov). 5. *Geinitzina postcarbonica* Spandel. 6. *Endothyra rotundata* Morozova. 7. *Geinitzina richteri kasib* Koscheleva. 8-10. ?*Uralogordius* sp., 11. *Nodosinelloides bella kamaensis* (Baryshnikov). 12. *Nodosinelloides netchaewi* (Tcherdynzev). 13. *Nodosinelloides jaborovensis* Kosheleva. 14. *Endothyra symmetrica* Morozova. 15. *Hemigordius* sp. 16. *Nodosinelloides netchaewi rasik* (Baryshnikov). 17. *Endothyra soshkinae* Morozova. 18. *Endothyranella protracta maxima* Baryshnikov. 19. *Geinitzina lysvaensis* Baryshnikov. 20. *Pseudobradyna compressa* Morozova. 21. *Endothyra lipinae lata* Zolotova. 22. *Lateenoglobivalvulina spiralis* (Morozova). 23. *Endothyra rotundata* Morozova. 24. *Pachyphloia* sp. 25. *Pseudobradyna compressa minima* Morozova. 26. *Nodosinelloides dualis* (Baryshnikov). 27. *Bradyina subtrigonalis* Baryshnikov. 28. *Midiella ovatus minima* (Grozdilova). 29. *Geinitzina richteri kasib* Koscheleva. 30. ?*Langella* sp. 31. *Tetrataxis lata novosjolovi* Baryshnikov. 32. *Postmonotaxinoides costiferus* (Lipina). 33. *Pseudospira* cf. *vulgaris* (Lipina). 34. *Lateenoglobivalvulina spiralis* (Morozova).

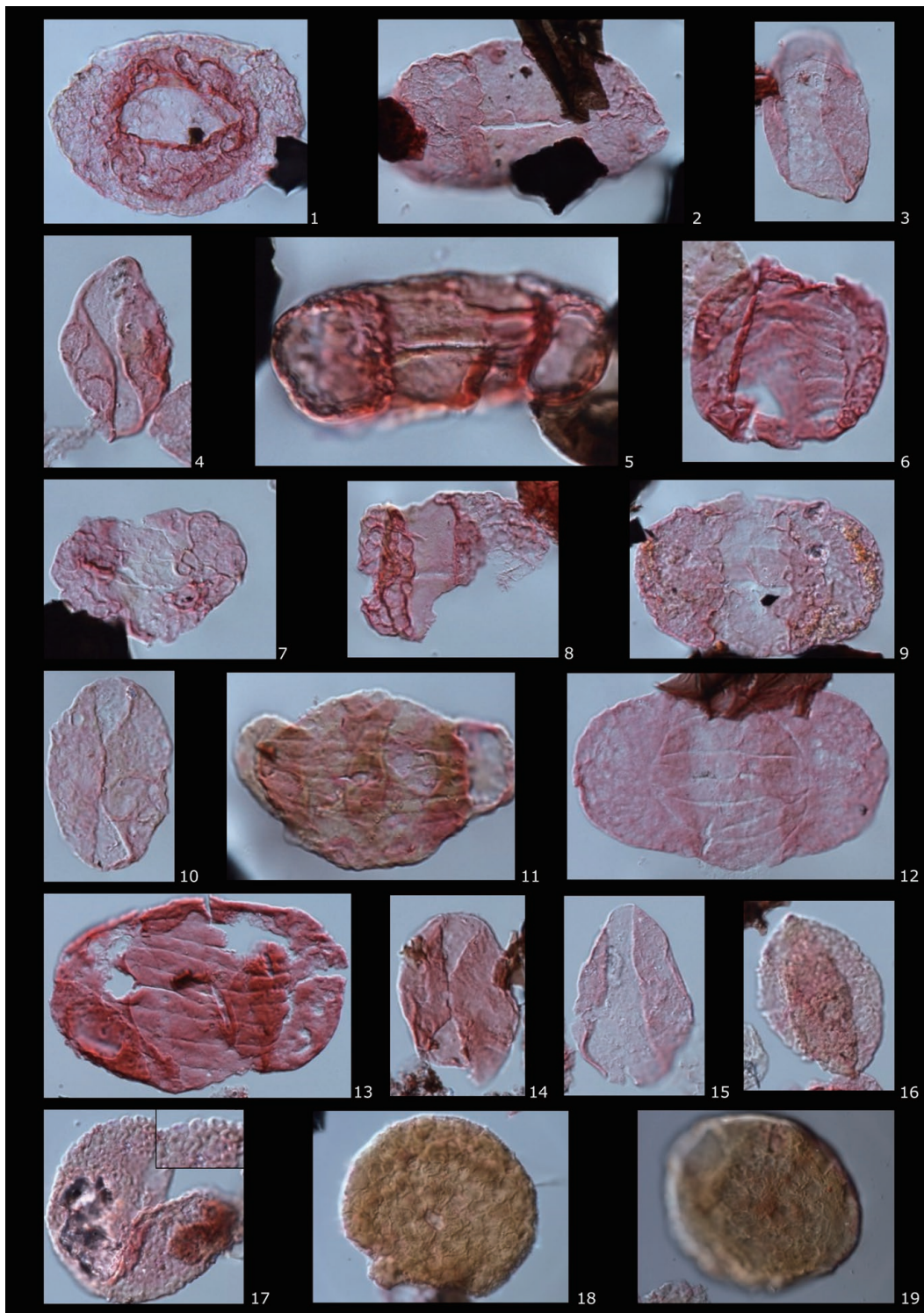


Fig. 15. Palynomorphs from the Dal'ny Tulkas natural exposure section. Slides are held in the collection of the BGS, Keyworth, Nottingham, NG12 5GG, UK. Locations of specimens are given first by England Finder code, then by BGS collections numbers. (MPA, MPK). The maximum dimension of each specimen is given in microns. **1.** *Potonieisporites grandis* Tshudy & Kosanke 1966, E44, MPA 56666, MPK 13629, 110 µm; **2.** *Limitsporites monstruosus* Lubert & Valts, F68/4, MPA 56666, MPK 13630, 95 µm; **3.** *Cycadopites ?glaber* (Lubert & Valts) Hart, E47, MPA 56666, MPK 13631, 50 µm; **4.** *Cycadopites ?glaber*, M57, MPA 56666, MPK 13632, 30 µm; **5.** *Limitsporites monstruosus*, D52/2, MPA 56666, MPK 13633, 55 µm; **6.** *Vittatina subsaccata* Samoilovich, D52/1, MPA 56666, MPK 13634, 45 µm. **7.** *Alisporites indarraensis* Segroves, D56/4, MPA 56666, MPK 13635, 50 µm; **8.** *Limitsporites monstruosus*, D52, MPA 56666, MPK 13636, 60 µm; **9.** *Protohaploxylinus* sp., S67, MPA 56666, MPK 13637, 65 µm; **10.** *Cycadopites ?glaber*, O60/1, MPA 56666, MPK 13638, 40 µm; **11.** *Hamiapollenites bullaeformis* (Samoilovich) Jansonius, N63/3, MPA 56666, MPK 13639, 65 µm; **12.** *?Complexisporites* sp., O61/4, MPA 56666, MPK 13640, 80 µm; **13.** *Protohaploxylinus* sp., L59/3, MPA 56659, MPK 13641, 90 µm; **14.** *Cycadopites ?glaber*, O60/1, MPA 56659, MPK 13642, 40 µm; **15.** *Cycadopites ?glaber*, O52/2, MPA 56659, MPK 13643, 40 µm; **16.** Algal palynomorph sp. A, M46/2, MPA 56659, MPK 13644, 60 µm; **17.** Algal palynomorph sp. A, O61/3, MPA 56659, MPK 13645, 60 µm (inset detail of ornament); **18.** *Azonalletes cf. compactus* Lubert, F51, MPA 56659, MPK 13646, 95 µm; **19.** *Azonalletes cf. compactus*, G57, MPA 56664, MPK 13647, 95 µm.

the proposed Artinskian GSSP at Dal'ny Tulkas was established in the natural exposure of the section and in the excavated trench (Fig. 2). Palynological data has been gathered from both sections; the first by Michael Stephenson and the second by M.V. Oshurkova (Chernyk pers. comm. 2021).

Dal'ny Tulkas section

Materials for study comprise samples collected by Michael Stephenson between June 25 and July 4, 2007 (Stephenson, 2007). Samples (mass <200g) were collected and processed using standard techniques (Wood et al. 1996) at the palynological laboratories of the British Geological Survey. The section sampled is shown in (Fig. 3) and consists of carbonate mudstone, siltstone and thin limestone.

The eleven samples yielded large amounts of organic residue including palynomorphs, sheet cellular material, woody material and amorphous organic matter. Palynomorphs were common in several samples, but were universally poorly preserved, showing signs of contemporaneous oxidation such that spore and pollen exine was near colourless and transparent in some cases. Saccate pollen was particularly poorly preserved with sacchi commonly separated from corpi. The poor preservation necessitated staining with Safranin O to improve possibility of determination.

The most diverse and best preserved of the samples are MPA 56664, 56659, 56663, 56666 and 56662 (Fig. 16). This sample range spans the proposed GSSP, which is within Bed 4 (Fig. 3).

Overall the samples are dominated by indeterminate non-

taeniate and taeniate bisaccate pollen (often detached corpi or sacchi), *Cycadopites* (mainly *C. ?glaber* (Luber & Valts) Hart) and *Vittatina* spp. (mainly *V. minima* Jansonius, *V. vittifera* (Luber & Valts) Samoilovich and *V. subsaccata* Samoilovich). ?Algal forms such as *Azonaletes* cf. *compactus* Luber and 'Algal palynomorph sp. A' (see Stephenson, 2007) are also locally common. Other taxa recorded include ?*Complexisporites* sp., *Alisporites indarraensis* Segroves, *Cordaitina* spp. (including *C. uralensis* (Luber & Valts) Samoilovich), *Crucisaccites ornatus* (Samoilovich) Dibner, *Florinites luberae* Samoilovich, *Hamiapollenites bullaeformis* (Samoilovich) Jansonius, indeterminate monosaccate pollen, *Knoxisporites* sp., *Limitsporites elongatus* Lele & Karim, *L. monstruosus* Luber & Valts, *Maculatasporites* sp., *Potonieisporites grandis* Tshudy & Kosanke, *Protohaploxypinus* spp., *Punctatisporites* sp. and *Sulcatisporites* spp. (Fig. 15).

'Algal palynomorph sp. A' is non-haplotypic and has a distinctive ornament of ring-like elements (Fig. 15). In the three lower samples, large ?algal palynomorphs (mean diameter approx. 100 µm) with an indistinct reticulate surface are very common, and are particularly conspicuous in slides because they do not absorb the Safranin O stain, remaining a translucent lemon yellow colour. For the present they are assigned to *Azonaletes* cf. *compactus*.

The lower part of the succession from beds 1, 2 and 3 appear to be dominated by probable algal palynomorphs such as *Azonaletes* cf. *compactus*, though indeterminate bisaccate pollen

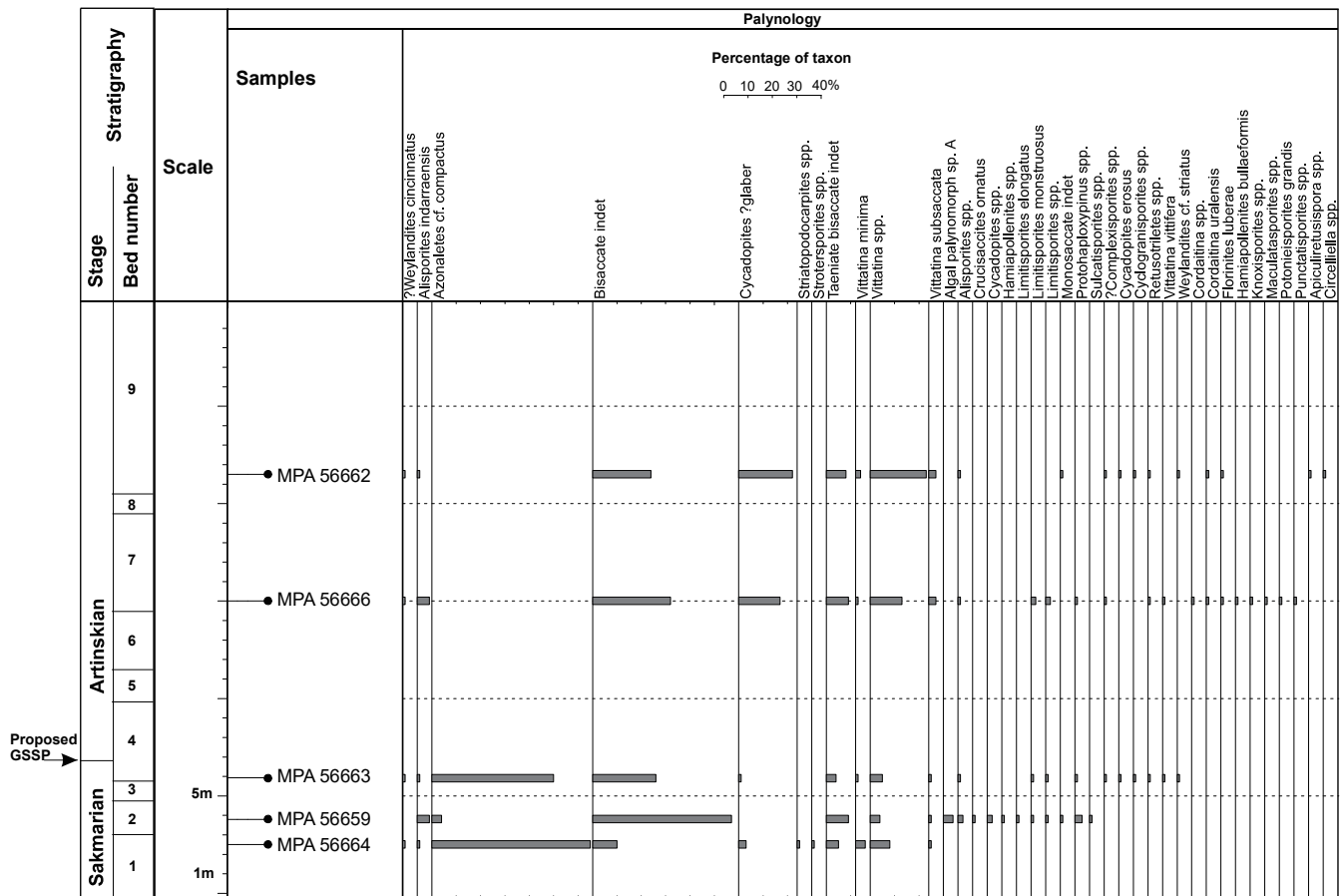


Fig. 16. Palynology of the Dal'ny Tulkas section.

are common, including taeniate indeterminate bisaccate pollen, as well as species of *Vittatina* are present.

Beds 7 to 9 contain very few algal palynomorphs such as *Azoniales* cf. *compactus*, and *Cycadopites* [mainly *C. ?glaber* (Luber and Valts) Hart] become more common above the proposed boundary level as do species of *Vittatina*.

Dal'ny Tulkas Trench

From beds 1 to 3 in the trench (Fig 5), M.V. Oshurkova reported common pollen such as *Vestigisporites* sp., *Hamiapollenites* sp., *Protohaploxypinus* sp., *Striatopodocarpites* spp. and *Vittatina vittifer*. Spores such as *Crassispora* sp., *Apiculatisporis* sp. and *Anaplanisporites* sp. are also present.

In beds 5 and 6, *Hamiapollenites* sp., *Protohaploxypinus* sp., and *Vittatina* spp. are again common in the trench.

Beds 7 to 9 contain *Crassispora* sp., *Cordaitina* spp. (including *C. rotata*), *Florinites luberae*, *Hamiapollenites* spp. (including *H. bullaeformis*), *Protohaploxypinus* sp., *Striatopodocarpites* spp., and *Vittatina* spp. (including *V. vittifer* and *V. striata*). A small number of *Weylandites* specimens were also recorded.

As a general comment on palynology for correlation of the base of the Artinskian, there are no markers among the spores and pollen that would provide a correlation point for the GSSP. However the probable algal taxa *Azoniales* cf. *compactus* appears to be very common below the proposed boundary and absent above (Fig. 16). Data on the wider stratigraphic occurrence of *Azoniales* cf. *compactus* and its biological affinity would help to decide whether it has any value as a palynological marker for the base of the Artinskian. The abundance of this taxon, in this case, coincides with proximity to the boundary. The role of Permian palynological biostratigraphy is summarized by Stephenson (2018).

Radiolarians

Numerous radiolarians of excellent preservation, represented by 32 species (Figs. 17, 18; Table 1), are found in the sediments associated with the Sakmarian-Artinskian boundary in the trench. In this assemblage, 16 species (50%) are common with radiolarians of other assemblages of the Southern Urals (Afanasieva, 2018).

The taxonomic composition of radiolarian assemblages has been revised for the Sakmarian-Artinskian boundary interval: (1) the total number of established radiolarian species has decreased; (2) the absolute and relative numbers of representatives of the class *Sphaerellaria* decreased; (3) the number of the species of the class *Stauraxonaria* decreased. However, on the other hand, the relative content of the class *Spumellaria* increased, and the species *Pseudoalbaillella scalprata* from the order *Albaillellaria* (class *Aculearia*) appeared.

The change in the taxonomic composition of radiolarians allows us to establish two assemblages: *Tetragregnon vimineum* (lower) and *Pseudoalbaillella scalprata* (upper). The quantitative ratio of taxa of higher rank (classes) reflects the characteristic of each assemblage.

Tetragregnon vimineum Assemblage. The terminal Sakmarian radiolarian assemblage is represented by 26 species (Figs. 17): *Sphaerellaria* – 13 species (50%), *Spumellaria* – five species (19.2%), *Stauraxonaria* – eight species (30.8%). Among the

radiolarians of this assemblage, 13 species are found only in the Sakmarian Stage. The association of radiolarians from the trench is considered characteristic of the *Tetragregnon vimineum* Assemblage within the range of the *Sweetognathus anceps* conodont zone.

Pseudoalbaillella scalprata Assemblage. The basal Artinskian radiolarian assemblage is represented by 19 species (Figs. 18): *Sphaerellaria* – nine species (47.4%), *Spumellaria* – five species (26.3%), *Stauraxonaria* – four species (21%), the bilaterally symmetrical species *Pseudoalbaillella scalprata* appears. Among the radiolarians of this assemblage, six species are characteristic only of the Artinskian Stage.

Bilaterally symmetrical radiolarians from the order *Albaillellaria* are of special note because they are extremely rare in the Southern Urals. *Pseudoalbaillella scalprata* was first described from the Lower Permian, Leonardian (upper Artinskian-Kungurian) deposits of the Havallah Formation in Nevada, USA (Holdsworth and Jones, 1980). Later, Murchey (in Stewart et al., 1986) noted that *P. scalprata* was found in the same sample with the conodont *Mesogondolella idahoensis*, the presence of which indicates an early Kungurian age (Lambert et al. 2007; Henderson et al., 2012; Wardlaw and Nestell, 2015; Nestell and Nestell, 2020).

The skeleton of *Pseudoalbaillella scalprata* is distinguished by a very short pseudoabdomen (25 µm), a wide conical apical cone and a wingspan of 70° (Holdsworth and Jones, 1980, fig. 1A). The specimen of *Ps. scalprata* found in the trench is characterized by the same parameters of the skeleton and a wingspan of 75°.

The species *Pseudoalbaillella scalprata* is very loosely interpreted by different researchers, both in terms of morphological features and age. The discovery of the species *Pseudoalbaillella scalprata* in the trench confirms the morphological features of this species (Holdsworth and Jones, 1980, fig. 1A), and clarifies the boundaries of its biostratigraphic distribution from the base of the Artinskian to the lower part of the Kungurian.

The association of radiolarians from the trench is considered as a characteristic assemblage of the *Pseudoalbaillella scalprata* Assemblage within the range of the *Sweetognathus asymmetricus* conodont zone.

A recent summary of Permian radiolarian biostratigraphy is provided by Zhang et al. (2018). However, unfortunately, none of the Lower Permian radiolarian zones has been established in the Southern Urals, since representatives of the genus *Pseudoalbaillella* are extremely rare in the Southern Urals. Nazarov and Ormiston (Nazarov and Ormiston, 1985, 1999; Nazarov, 1988) developed the first biostratigraphic scale based on Lower Permian radiolarians, comprising ten beds with characteristic faunas. These assemblages have been recognized in the territory of the Southern Urals and Western Mugodzhary.

At present, eighteen Early Permian radiolarian assemblages are recognized as valid based on the data for thirteen reference sections of the Greater Urals and Western Mugodzhary (Afanasieva, 2018, 2021). Two new assemblages (*Tetragregnon vimineum* and *Pseudoalbaillella scalprata*) complement the radiolarian biostratigraphic scale in the Southern Urals.

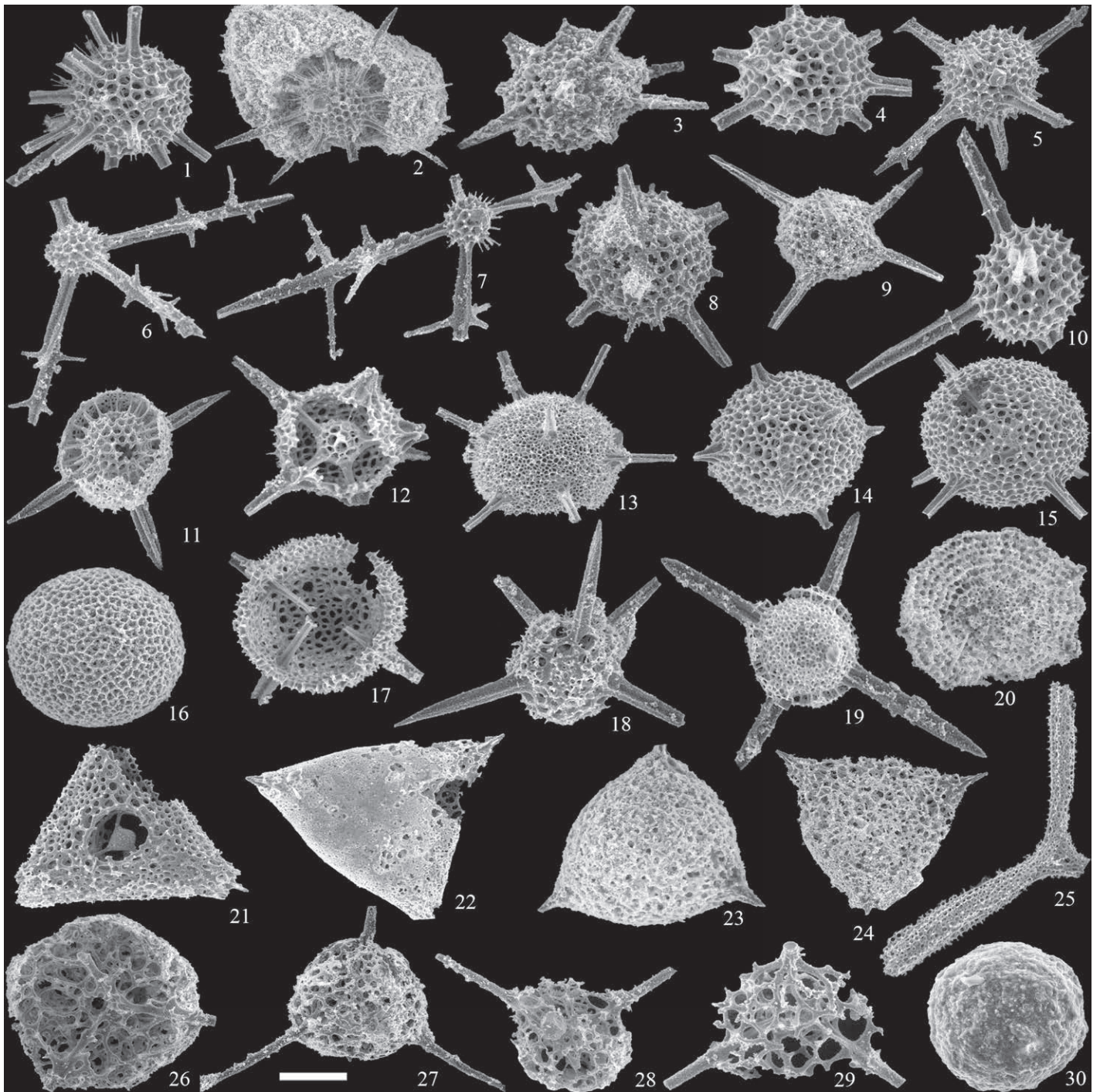


Fig. 17. Radiolarians from Dal'ny Tulkas trench, bed 7-2 (figs 1–19 and 21–29) and bed 5-2 (figs 20 and 30). 1-2. *Astroentactinia* sp. F: 1, bar 91 μm , 2, bar 132 μm . 3. *A. inscita* Nazarov in Isakova & Nazarov, bar 77 μm . 4. *A.* sp. G, bar 76 μm . 5. *Apophysiacus sakmaraensis* (Kozur & Mostler), bar 109 μm . 6-7. *A. praepynoclada* (Nazarov & Ormiston): 6, bar 92 μm , 7, bar 91 μm . 8. *Entactinia mariannae* Afanasieva & Amon, bar 92 μm . 9. *E. chernykhi* Afanasieva & Amon, bar 95 μm . 10. *E. dolichoacus* Nazarov in Isakova & Nazarov, bar 92 μm . 11. *Microporosa permica permica* (Kozur & Mostler), bar 92 μm . 12. *Helioentactinia* sp. I, bar 61 μm . 13. *H.* sp. B, bar 139 μm . 14. *H.* sp. D, bar 92 μm . 15. *H.* sp. C, bar 110 μm . 16. *Spongentactinia fungosa* Nazarov, bar 69 μm . 17. *S.* sp. A, bar 79 μm . 18. *S.* sp. H, bar 86 μm . 19. *Pluristratoentactinia* sp. J, bar 71 μm . 20. *Copicyntra fragilispinosa* Kozur & Mostler, bar 91 μm . 21. *Kozurispongus laqueus* (Nazarov & Ormiston), bar 109 μm . 22. *Latentidiota promiscua* (Nazarov & Ormiston), bar 108 μm . 23. *Nazarovispongus aequilateralis* (Nazarov in Isakova and Nazarov), bar 68 μm . 24. *N. pavlovi* Kozur, bar 137 μm . 25. *Latentifistula heteroextrema* Nazarov in Isakova and Nazarov, bar 141 μm . 26-27. *Tetragregnon sphaericus* Nazarov in Isakova and Nazarov: 26, bar 109 μm , 27, bar 137 μm . 28-29. *T. vimineum* Amon, Braun & Chuvashov: 28, bar 135 μm , 29, bar 91 μm . 30. *Palaeodiscalskexs* cf. *punctus* (Hinde), bar 80 μm .

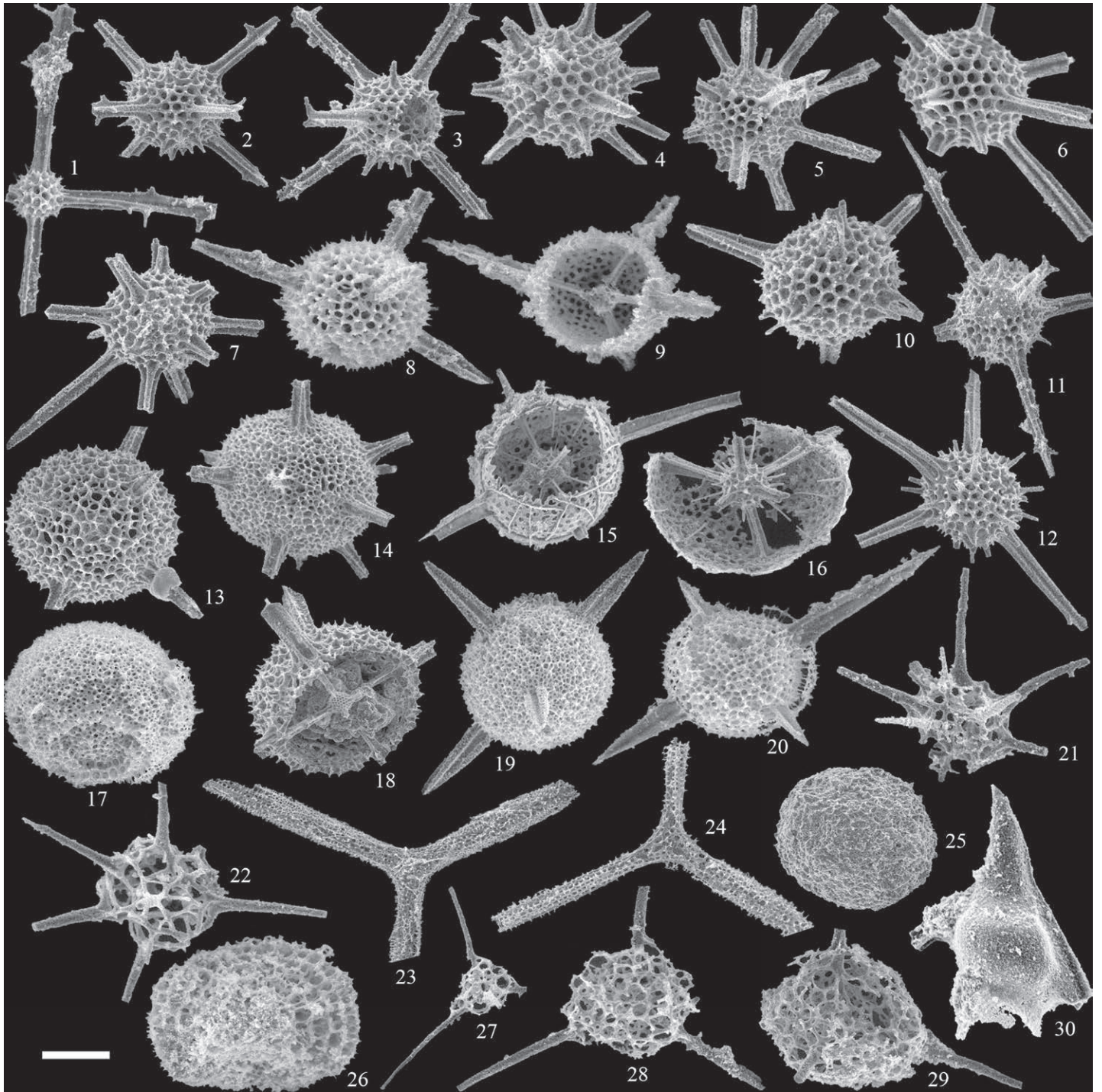


Fig. 18. Radiolarians from Dal'ny Tulkas trench, bed 10-1 (figs 2, 3, 5, 7, 11-14, 18, 19, and 23), bed 11-2 (figs 1, 4, 6, 8-10, 15, 16, 20-22, and 24-30), and bed 11-3 (fig. 17). **1.** *Apophysiacus praepycnoclada* (Nazarov & Ormiston), bar 90 μm . **2-3.** *A. sakmaraensis* (Kozur & Mostler): 2, bar 109 μm , 3, bar 91 μm . **4.** *Astroentactinia inscita* Nazarov in Isakova and Nazarov, bar 77 μm . **5-7.** *A. sp. G*: 5, 94 μm , 6, 68 μm , 7, 91 μm . **8-10.** *Bientactinosphaera sp. E*: 8, 59 μm , 9, 49 μm , 10, 69 μm . **11-12.** *Entactinia dolichoacus* Nazarov in Isakova and Nazarov: 11, bar 109 μm , 12, bar 95 μm . **13.** *Helioentactinia sp. C*, bar 103 μm . **14.** *H. sp. B*, bar 120 μm . **15-16.** *Paratriposphaera strangulata* (Nazarov & Ormiston): 15, bar 113 μm , 16, bar 91 μm . **17.** *Copicyntra fragilispinosa* Kozur & Mostler, bar 71 μm . **18.** *Spongentactinia sp. A*, bar 117 μm . **19.** *Pluristratoentactinia lusikae* Afanasieva, bar 89 μm . **20.** *P. sp. J*, bar 52 μm . **21-22.** *Secuicollecta amoenitas* Nazarov & Ormiston, bar 76 μm . **23-24.** *Latentifistula heteroextrema* Nazarov in Isakova and Nazarov: 23, bar 220 μm , 24, bar 166 μm . **25.** *Palaeodiscalexus cf. punctus* (Hinde), bar 135 μm . **26.** *Rectotortum fornicatum* Nazarov & Ormiston, bar 60 μm . **27-29.** *Tetragregon vimineum* Amon, Braun & Chuvashov, possible successive stages of skeleton formation, bar 122 μm . **30.** *Pseudoabaillella scalprata* Holdsworth & Jones, bar 69 μm .

U-Pb geochronology

Schmitz and Davydov (2012) carried out radiometric studies, based upon high-precision, isotope dilution-thermal ionization mass spectrometry (ID-TIMS) U-Pb zircon ages for interstratified volcanic ash beds in the paratratotype sections of the southern Urals, including in the Dal'ny Tulkas section. Here they selected ash tuffs at three levels (see black stars for levels in Fig. 3) - in the upper part of bed 2 (4m lower than base of Artinskian, in the upper part of bed 7 and in the base of bed 9 (2m higher than the previous sample).

In bed 2, of eight analyzed grains of zircon, six grains yielded a weighted mean $^{206}\text{Pb}/^{238}\text{U}$ date of 290.81 ± 0.09 Ma. Seven of eight analyzed grains from bed 7 produced a weighted mean $^{206}\text{Pb}/^{238}\text{U}$ date of 288.36 ± 0.10 Ma. And from the third interlayer of ash tuff (bed 9) all eight investigated grains gave a $^{206}\text{Pb}/^{238}\text{U}$ date of 288.21 ± 0.06 Ma. The three dated samples allow the calculation of a relatively constant accumulation rate through the lower portion of the section" (Schmitz and Davydov, 2012, p. 561). These zircons provided an interpolated geochronologic age of $290.1 \text{ Ma} \pm 0.2 \text{ Ma}$ (Schmitz and Davydov, 2012; Henderson et al., 2012) and $290.5 \text{ Ma} \pm 0.4 \text{ Ma}$ (Henderson and Shen, 2020) for the base-Artinskian. The radiometric ages determined from Dal'ny Tulkas sections will be of considerable value for correlations with non-marine Permian sections.

Strontium isotopes

Schmitz et al. (2009) in a presentation at the International Conodont Symposium indicated a consistent secular trend of $^{87}\text{Sr}/^{86}\text{Sr}$ isotopic ratios from conodont elements through the Early Permian. The $^{87}\text{Sr}/^{86}\text{Sr}$ ratio for the base-Artinskian is based on material from Dalny Tulkas and from Usolka was approximately 0.70765 (Schmitz et al., 2009). Strontium isotopes from individual conodont elements can be integrated with geochronologic ages to produce a time model. The strontium isotopic composition of seawater at the base of the Artinskian Stage is now calculated at $^{87}\text{Sr}/^{86}\text{Sr} = 0.70767$ (Chernykh et al., 2012); they also provided a description of the methodology used by Mark Schmitz. "Only well preserved specimens with colour alteration index <2.0 were measured. One to ten elements were pooled by genera and cleaned and partially dissolved. The undissolved portion was then completely dissolved in nitric acid and Sr separated on Sr-spec crown ether resin. Sr isotope ratios were measured by thermal ionization mass spectrometry (TIMS) with a reproducibility of $\pm .00001$." It was also indicated that a smoothed spline fit to these data with 95% confidence interval yielded a chronostratigraphic proxy with a resolution of about .5 Ma. The values provided in Chernykh et al. (2012; their fig. 8) were somewhat more radiogenic than brachiopods from the same sections for the interval Sakmarian-early Artinskian by Korte et al. (2006), but the reverse was true for brachiopods around the Carboniferous-Permian boundary from Usolka. All of these materials were considered to not be diagenetically altered. Future analyses will need to investigate these differences in order to enhance this method as a correlation tool. A summary figure of the Sr secular trend is also depicted in fig. 24.9 in GTS 2012.

Carbon isotope chemostratigraphy

A group of Chinese researchers with the participation of V.I. Davydov (USA, Boise State University) conducted a study of carbon and oxygen stable isotopes in the GSSP candidate sections of the South Urals – Usolka, Dal'ny Tulkas and Kondurovsky (Zeng et al., 2012). Basic results, obtained from the Dal'ny Tulkas section are provided below.

In the Dal'ny Tulkas section the curves of $\delta^{13}\text{C}$ and $\delta^{18}\text{O}$ display a general concurrent tendency of change with a rapid and sharp drop near the Sakmarian-Artinskian boundary and a long-term depletion in the subsequent interval of the Artinskian Stage (Fig. 19). The values of $\delta^{13}\text{C}$ present a dramatic depletion to approximately -16‰ . However, no similar $\delta^{13}\text{C}$ excursions around the Sakmarian-Artinskian boundary have been observed in other sections, including the Naqing and Zhongdi sections in South China analyzed by (Buggisch et al., 2011). These very negative values and concurrent trends in both carbon and oxygen isotopic compositions at Dal'ny Tulkas are attributed to diagenesis. Therefore this correlation technique is not currently of value for international correlation. Buggisch et al. (2011) showed an increase of about 1.5‰ from the upper part of the Sakmarian to the lower part of the Artinskian in the Naqing section and of about 3‰ in the Zhongdi and Kongshan succession in China. This positive trend - not observed in Dal'ny Tulkas - may provide the potential for correlation in other sections.

Paleomagnetic Stratigraphy

The Sakmarian-Artinskian boundary occurs within the long Kiaman superchron. Hounslow and Balabanov (2018) report a short normal polarity (C12n) within the upper Artinskian, but otherwise paleomagnetic data will not assist correlation of the boundary. This is confirmed in a paleomagnetic study of the Dal'ny Tulkas section by Balabanov et al. (2019). They demonstrate that the primary component of magnetization was well preserved, but no changes or reversals in the remanent magnetization were recognized in the boundary interval.

Gondwana Correlations

Correlation between the paleo-equatorial province in which the Permian Stage GSSPs are based and Gondwana has been historically difficult mainly because the conodonts on which Permian Stage GSSPs are based are largely absent from Gondwana basins (Mouro et al., 2020; Scomazzon et al., 2013, Stephenson 2016).

Australia has some of the best documented Permian basins in Gondwana, but most of the succession is nonmarine. Calibration of the local palynostratigraphic scheme (Price, 1997) to the global timescale was indirect and very difficult, having traditionally relied on correlations from relatively sparse, high-latitude, marine strata, within which ammonoids and conodonts are rare, fusulines are unknown, and much of the other fauna (brachiopods, bivalves) is endemic. Tie points are rare and often tenuous (Mantle et al., 2010). One example is the record of a single specimen of the ammonoid *Cyclolobus persulcatus* from the Cherrabun Member of the Hardman Formation, in the Canning

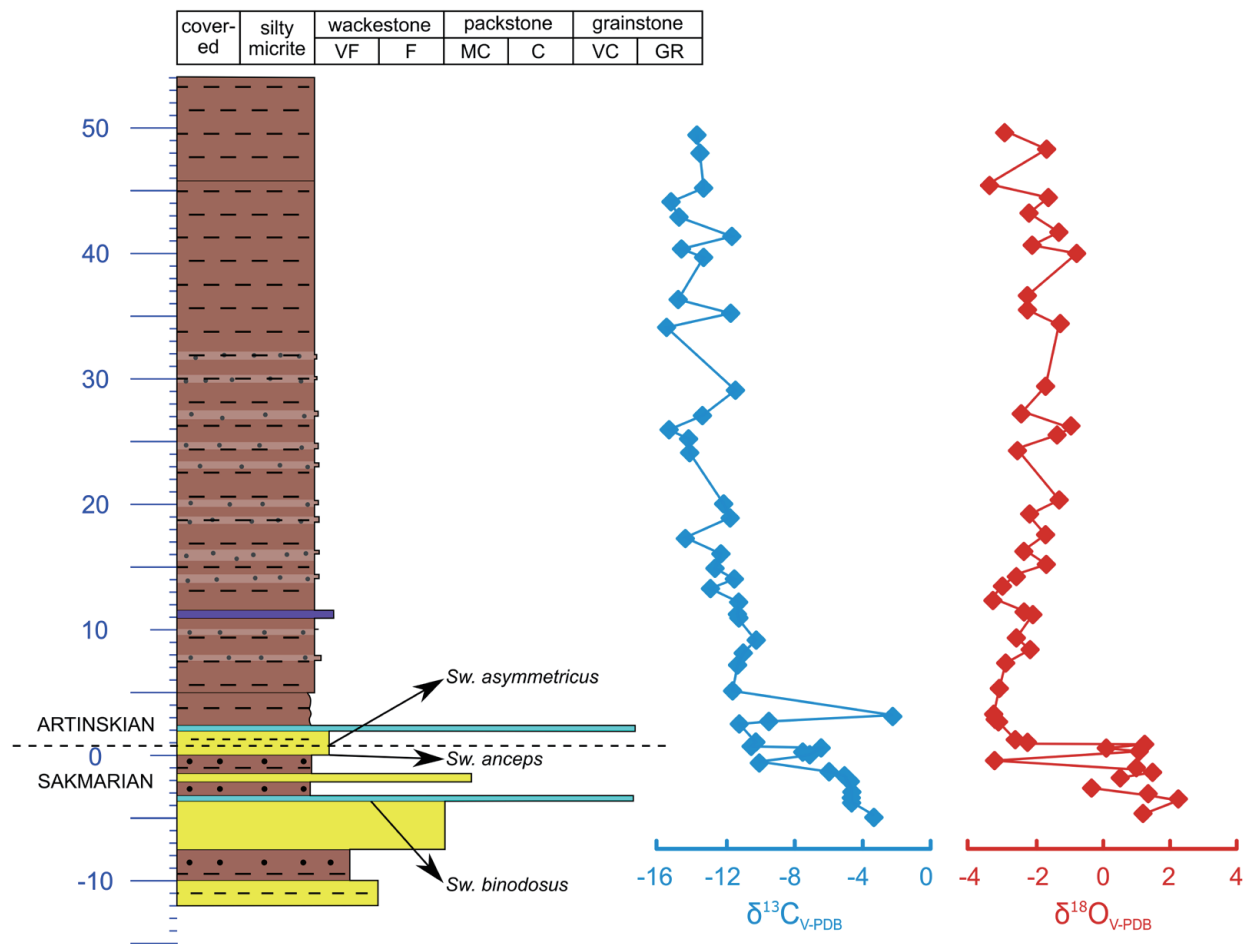


Fig. 19. Carbon and oxygen isotopic composition of the Dal'ny Tulkas section (modified from Zeng et al., 2012).

Basin, Western Australia (Foster and Archbold, 2001), dated as 'post-Guadalupian' by Glenister et al. (1990) and 'Capitanian–Dzhulfian' by Leonova (1998).

Recent advances in high-precision U-Pb CA-TIMS dating of Middle Permian to Lower Triassic sequences in eastern Australian Gondwana have seen major advances in the ability to date lithostratigraphic units (Metcalf et al. 2015; Bodorkos et al. 2016; Laurie et al. 2016, Nicoll et al. 2015). Based on these new dates, the Guadalupian-Lopingian/Capitanian-Wuchiapingian boundary is tentatively placed at the level of the Thirroul Sandstone in the lower part of the Illawarra Coal Measures in the Sydney Basin. The Wuchiapingian-Changhsingian boundary is at or close to the Kembla Sandstone horizon in the Illawarra Coal Measures, southern Sydney Basin, in the middle part of the Newcastle Coal Measures in the northern Sydney Basin, and in the middle of the Black Alley Shale in the southern Bowen Basin. However none of these dates allow the Dal'ny Tulkas Artinskian units to be correlated to Australia because the newly dated Australian units are all younger, but presumably correlative units may be found in the Pebbly Beach Formation of the Sydney Basin (Metcalf et al. 2015) and its associated brachiopods, bivalves, plants, abundant trace fossils and dropstones.

In South America, volcanic ash beds within the Cisuralian are much more common than in other Gondwana Permian basins and dates are becoming available, particularly for the Paraná Basin in

Brazil and the Tarija Basin of central Bolivia.

Dates from the Paraná Basin are now abundant (e.g. Cagliari et al. 2020; Rocha-Campos et al. 2006, 2007, 2019; Guerra Sommer et al. 2008a, b, c; Griffis et al. 2018, 2019; Simas et al. 2012; Santos et al. 2006; Jurigan et al. 2019), but vary greatly in precision. Those concentrating on the Vittatina costabilis palynological biozone are most relevant to the Dal'ny Tulkas section because several high precision CA-ID-TIMS radiometric dates (see Souza et al. 2021) indicate that the zone ranges in age from the Asselian to the early Artinskian, indicating in turn that the upper part of the Rio Bonito Formation is likely early Artinskian in age and similar in age to the Dal'ny Tulkas section. It should be noted that Paraná Basin rocks (Itarare Group) contain only Pennsylvanian and lowermost Asselian conodonts (Mouro et al., 2020; Scomazzon et al., 2013) so correlations can only be drawn using radiometric dates without the corroborating evidence of conodonts.

In this regard the Apillapampa section (Copacabana Formation) near Cochabamba, central Bolivia, is key to a more reliable correlation because it contains conodonts, fusulines and dated ash beds. Di Pasquo et al. (2015) quoted radiometric dates from six volcanic ash beds within the section; these dates were first presented in a talk by Henderson et al. (2009) based on analyses performed at Boise State University by J. Crowley and M. Schmitz. The six dates (cited as preliminary in Permian

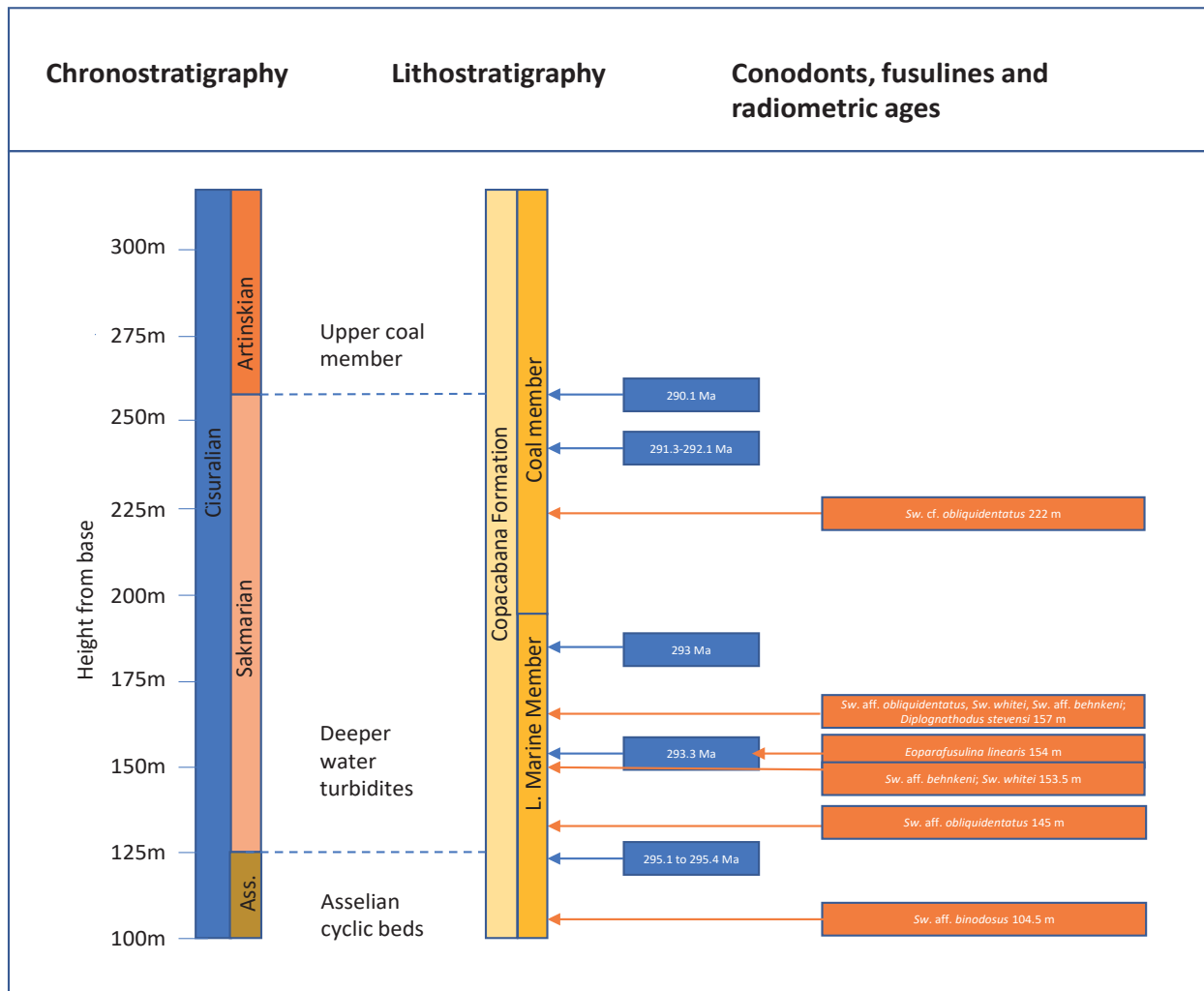


Fig. 20. Summary of relevant dates and conodont occurrences from the Apillapampa section (Copacabana Formation) (modified after di Pasquo 2015). Conodonts updated from those previously reported by Henderson et al. (2009). Dashed blue lines represent sequence boundaries.

ICS Newsletter Permophiles, 53, Supplement 1) are 298 (40 m), 295.2 (120 m), 293.3 Ma (154 m), 293 Ma (185 m), 291.6 Ma (242 m) and 290.1 Ma (262 m) (Fig. 20). These dates are CA-ID-TIMS dates, but the precision has not been published yet. These dates fix the upper Coal Member of the Copacabana Formation as late Sakmarian to early Artinskian. The presence of the conodont *Sweetognathus cf. obliquidentatus* corroborates this correlation. *Sweetognathus whitei* and *Sw. aff. behnkeni* occur lower in the section within turbidite facies; these taxa are typical of the late Asselian and early Sakmarian (Henderson, 2018; Petryshen et al., 2020). These taxa are the same reported by Suarez Riglos et al. (1987) from the Yaurichambi locality of the Copacabana Formation near La Paz, but the taxonomic identifications and relative age assignments have been revised.

Conclusion

The Dal'ny Tulkas section, as a candidate for the reference section (GSSP) of the Artinskian Stage, has the following characteristics necessary to substantiate its status.

1. The section is easily accessible and currently has a complete paleontological record for three key Permian biostratigraphic

groups of micro- and macrobiota — conodonts, ammonoids, and foraminifers.

2. In the section, the lower boundary of the Artinskian Stage was recorded according to the first appearance of the marker species *Sweetognathus asymmetricus* Sun and Lai in the continuous phylogenetic lineage of development of *Sweetognathus expansus* - *Sw. aff. merrilli* - *Sw. binodosus* - *Sw. anceps* - *Sw. asymmetricus*.

3. The ammonoids *Neopronorites skvorzovi*, *Uraloceras involutum*, *U. gracilentum*, and *Popanoceras annae* represent markers of the Sakmarian-Artinskian boundary.

4. The foraminiferal assemblages indicate that in the Sakmarian-Artinskian boundary interval of the Dal'ny Tulkas section, the schubertellid-fusuline assemblages of late Asselian-Sakmarian age are replaced by typical Artinskian forms. In the small foraminiferal assemblages throughout the entire boundary interval, there are Artinskian forms present with wide stratigraphic distribution.

5. Volcanic ash beds are present and geochronologic ages of zircons have been interpolated between 290.1 and 290.5 Ma.

6. A Sr isotopic ratio of .70767 provides additional means

for correlation. Unfortunately, carbon isotopic compositions are diagenetically altered and cannot be used for correlation.

7. A paleomagnetic study showed good preservation of the remanent magnetism, but no reversals were recognized in the boundary interval.

8. Numerous additional fossil groups have also been recorded from Dal'ny Tulkas including radiolarians, acritarchs, palynomorphs, brachiopods, fishes, and plant remains (algae and calamite trunks). The large diversity of fossils makes this section very attractive for paleontologists and for geotourism.

9. The base-Artinskian occurs within a transgressive systems tract and close to a major maximum flooding surface. This succession occurs above cyclic deposits and coupled with detailed biostratigraphy, it forms a recognizable sequence biostratigraphic signature and strong physical stratigraphic correlation tool.

10. Davydov et al. (2007) reported in *Permophiles* 50 that government agreement has been reached to protect all of the defined and proposed Cisuralian GSSP sites. The Dal'ny Tulkas site is now included in the Toratau Geopark and in the future may become one of the educational and tourist centres in the Republic of Bashkortostan, Russia.

Proposal

SPS proposes that the base-Artinskian GSSP be defined at 0.6 m above the base of bed 4b at the Dal'ny Tulkas section in the southern Urals of Russia (53.88847N and 056.51615E). This point corresponds to the First Appearance Datum of the conodont *Sweetognathus asymmetricus*, which is part of a well defined and widely distributed lineage. Additional markers for correlation include a geochronologic age interpolated between 290.1 and 290.5 Ma, a strontium isotopic ratio of .70767, and many additional fossils groups, particularly ammonoids and fusulines, but also including small foraminifers, radiolarians, and palynomorphs. Finally, the boundary occurs within a transgressive succession in many sections, near or at a maximum flooding surface, thereby forming a distinctive sequence biostratigraphic signature in the field.

References

Afanasieva, M.S., 2018. Early Permian Radiolarian Eco-Zones in the Great Urals, Northern Mygodzhary and Peri-Caspian Basin. In Nurgaliev, D., Barclay, M., Nikolaeva, S., and Silantiev, V. eds. Proceedings of Kazan Golovkinsky Stratigraphic Meeting 2017. Advances in Devonian, Carboniferous et Permian Research: Stratigraphy, Environments, Climate and Resources. Filodiritto, p. 11–18.

Afanasieva, M.S. 2021. Asselian and Sakmarian (Lower Permian) Radiolarian Ecozones in the South Urals, Russia. *Paleontological Journal*, v. 55, no. 8, p. 825–862.

Balabanov, Y.P., Sungatullin R.Kh., Sungatullina G.M., Kosareva L.R., Glukhov M.S. Yakunina P.G., Zhernenkov A.O., Antonenko V.V., and Churbanov A.A. 2019. Magnetostratigraphy of the Reference Sections of the Cisuralian Series (Permian System). In Nurgaliev D. et al. (eds.), Recent Advances in Rock Magnetism, Environmental Magnetism and Paleomagnetism, Springer Geophysics, pp. 317–342. Springer International Publishing AG, part of

Springer Nature 2019. https://doi.org/10.1007/978-3-319-90437-5_23

Baryshnikov, V.V., Zolotova, V.P. and Kosheleva, V.F., 1982. *Novye vidy foraminifer artinskogo yarusa Permskogo Priuralia* [New Species of Artinskian Foraminifers from the Permian Cis-Urals] Preprint No., UNTs AN SSSR, Sverdlovsk, 54 pp. [in Russian].

Beauchamp, B. and Henderson, C.M., 1994. The Lower Permian Raanes, Great Bear Cape and Trappers Cove formations, Sverdrup Basin, Canadian Arctic: stratigraphy and conodont zonation. *Bulletin of Canadian Petroleum Geology*, v. 42, no. 4, p. 562–597.

Beauchamp, B., Calvo Gonzalez, D., Henderson, C.M., Baranova, D.V., Wang, H.Y. and Pelletier, E. in press for 2021. Late Pennsylvanian–early Permian tectonically-driven stratigraphic sequences and carbonate sedimentation along northern margin of Sverdrup Basin (Otto Fiord Depression), Arctic Canada. In Henderson, C.M., Ritter, S., and Snyder, W.S. eds. *Late Paleozoic Tectonostratigraphy and Biostratigraphy of western Pangea*. SEPM Special Publication 113. doi: 10.2110/sepm.sp.113.

Boardman, D.R., Wardlaw, B.R. and Nestell, M.K. 2009. Stratigraphy and conodont biostratigraphy of uppermost Carboniferous and Lower Permian from North American Midcontinent. *Kansas Geological Survey Bulletin*, v. 255, 253 pp.

Bodorkos, S., Crowley, J., Holmes, E., Laurie, J., Mantle, D., McKellar, J., Mory, A., Nicoll, R., Phillips, L., Smith, T., Stephenson, M.H. and Wood, G. 2016. New dates for Permian palynostratigraphic biozones in the Sydney, Gunnedah, Bowen, Galilee and Canning basins, Australia. *Permophiles*, v. 63, p. 19–21.

Bogoslovskaya, M.F., 1962. Artinskian Ammonoids of the Central Urals: Proceedings of the Paleontological Institute of the Academy of Sciences of the USSR, v. 87 (Akad. Nauk SSSR, Moscow), p. 3–117 [in Russian].

Bogoslovskaya, A.F. and Shkolin, A.A., 1998. Ammonoidea. In Grunt, T.A., Esaulova, N.K. and Kanev, G.P. eds. *Biota of the East European Russia at the Early/Late Permian boundary: Moscow, Geos*, p.137–155 (in Russian).

Buggisch, W., Wang, X.D, Alekseev, A.S. and Joachimski, M.M., 2011. Carboniferous–Permian carbon isotope stratigraphy of successions from China (Yangtze platform), USA (Kansas) and Russia (Moscow Basin and Urals). *Palaeogeography, Palaeoclimatology, Palaeoecology*, v. 301, p. 18–38.

Cagliari, J., Schmitz, M.D., Lavina, E.L.C. and Netto, R.G., 2020. U-Pb CA-IDTIMS geochronology of the Late Paleozoic glacial and post-glacial deposits in southern Parana Basin. In EGU General Assembly 2020. <https://doi.org/10.5194/egusphereegu2020-12101>. Available at: (Accessed 21 May 2020).

Chen, J., 2011. Early Permian (Cisuralian) conodont biostratigraphy in southern Guizhou and global correlation: PhD thesis, Graduate University of Chinese Academy of Sciences, Nanjing, 225 pp.

Chernykh V.V., 2005. Zonal method in biostratigraphy, zonal conodont scale of the Lower Permian in the Urals. Institute of

Table 1. Distribution list of conodonts, ammonoids, fusulinids, and radiolarians from the Dal'ny Tulkas section and trench.

SECTION	Conodonts	Ammonoids	Fusulines
Bed 13	<i>Sweetognathus clarki</i> (Kozur), <i>Sw. asymmetricus</i> Sun & Lai, <i>Sweetognathus</i> aff. <i>ruzhencevi</i> , <i>Mesogondolella bisselli</i> (Clark & Behnken)		
Bed 10	<i>Sweetognathus clarki</i> (Kozur), <i>Sw. asymmetricus</i> Sun & Lai, <i>Sweetognathus</i> aff. <i>binodosus</i> , <i>Sw. aff. clarki</i> , <i>Mesogondolella laevigata</i> Chernykh; base Irginian		
Bed 9	<i>Mesogondolella bisselli</i> (Clark & Behnken); top Burtsevian		
Bed 8		<i>Sakmarites postcarbonarius</i> (Karpinsky), <i>Agathiceras uralicum</i> (Karpinsky), <i>Kargalites typicus</i> (Ruzhencev), <i>Paragastrioceras</i> sp., <i>Crimites subkrotowi</i> Ruzhencev	
Bed 7	<i>Mesogondolella bisselli</i> (Clark & Behnken)		
Bed 6	<i>Mesogondolella bisselli</i> (Clark & Behnken)	<i>Popanoceras annae</i> Ruzhencev, <i>P. tshernowi</i> Maximova, <i>P. congregale</i> Ruzhencev, <i>Kargalites</i> sp. and <i>Neopronorites skvorzovi</i> (Tchernow), rare <i>Artinskia</i> sp.	
Bed 5	<i>Sweetognathus gravis</i> Chernykh, <i>Sweetognathus obliquidentatus</i> (Chernykh), <i>Sweetognathus asymmetricus</i> Sun & Lai, <i>Mesogondolella bisselli</i> (Clark & Behnken)	<i>Popanoceras annae</i> Ruzhencev, <i>P. tshernowi</i> Maximova, <i>P. congregale</i> Ruzhencev, <i>Kargalites</i> sp. and <i>Neopronorites skvorzovi</i> (Tchernow), rare <i>Artinskia</i> sp.	<i>Pseudofusulina callosa</i> Rauser, <i>P. plicatissima</i> Rauser, <i>P. plicatissima irregularis</i> Rauser, <i>P. urdalensis</i> Rauser, <i>P. fortissima</i> Kireeva, <i>P. concavatus</i> Vissarionova, <i>P. juresanensis</i> Rauser, <i>P. consobrina</i> Rauser, <i>P. paraconessa</i> Rauser

Bed 4b	<p>Upper part - <i>Sweetognathus obliquidentatus</i> (Chernykh), <i>Mesogondolella bisselli</i> (Clark & Behnken) 1.2 m - <i>Sweetognathus obliquidentatus</i> Chernykh, <i>Sweetognathus asymmetricus</i> Sun & Lai, <i>Mesogondolella bisselli</i> (Clark & Behnken) 0.6 m - <i>Sweetognathus anceps</i> Chernykh, transitional form between <i>Sweetognathus anceps</i> and <i>Sweetognathus asymmetricus</i> Sun & Lai, <i>Sweetognathus asymmetricus</i> Sun & Lai, <i>Mesogondolella bisselli</i> (Clark & Behnken); base Bursevian</p>		<p><i>Pseudofusulina</i> aff. <i>longa</i> Kireeva, <i>P. fortissima</i> Kireeva, <i>P. anostiata</i> Kireeva, <i>P. plicatissima</i> Rauser, <i>P. urdalensis abnormis</i> Rauser</p>
Bed 4a	<p><i>Sweetognathus obliquidentatus</i> (Chernykh), <i>Sweetognathus anceps</i> Chernykh, transitional form between <i>Sweetognathus anceps</i> and <i>Sweetognathus asymmetricus</i> Sun & Lai, <i>Mesogondolella bisselli</i> (Clark & Behnken); top Sterliltamakian</p>		<p><i>Pseudofusulina callosa</i> Rauser, <i>P. callosa proconcavata</i> Rauser, <i>P. jaroslavkensis</i> <i>fraudulenta</i> Kireeva, <i>P. cf. parajaroslavkensis</i> Kireeva, <i>P. blochini</i> Korzhenevski</p>
Bed 3	<p><i>Sweetognathus obliquidentatus</i> (Chernykh)</p>		

TRENCH	Conodonts	Ammonoids	Fusulines	Small Foraminifers	Radiolarians
Bed 11-6					<p><i>Copicyntra fragilispinosa</i> Kozur & Mostler</p>
Bed 11-3					<p><i>Copicyntra fragilispinosa</i> Kozur & Mostler, <i>Rectotortum fornicatum</i> Nazarov et Ormiston.</p>

Bed 11-2					<p><i>Apophysiacus praepycnoclada</i> (Nazarov & Ormiston), <i>Apophysiacus sakmaraensis</i> (Kozur & Mostler), <i>Astroentactinia inscita</i> Nazarov in Isakova and Nazarov, <i>Astroentactinia</i> sp. G, <i>Bientactinosphaera</i> sp. E, <i>Entactinia dolichoacus</i> Nazarov in Isakova and Nazarov, <i>Helioentactinia</i> sp. C, <i>Latentifistula heteroextrema</i> Nazarov in Isakova and Nazarov, <i>Palaeodiscaleksus</i> cf. <i>punctus</i> (Hinde), <i>Paratriposphaera strangulate</i> (Nazarov & Ormiston), <i>Pluristratoentactinia</i> sp. J, <i>Pseudoalibaillella scalprata</i> Holdsworth & Jones, <i>Rectotormentum fornicatum</i> Nazarov & Ormiston, <i>Secuicollacta amoenitas</i> Nazarov & Ormiston, <i>Spongentactinia</i> sp. A, <i>Tetragregnon vimineum</i> Amon, Braun & Chuvashov.</p>
Bed 11-1					<p><i>Copicyntra fragilispinosa</i> Kozur & Mostler</p>
Bed 10		<p>(Bed 10-1) <i>Eothinites kargalensis</i> Ruzhencev, <i>Eothinites</i> aff. <i>usvensis</i> Bogoslovskaya, <i>Popanoceras annae</i> Ruzhencev, <i>P. congregale</i> Ruzhencev, <i>Daraelites elegans</i> Tchernow, <i>Uraloceras gracilentum</i> Ruzhencev, <i>U. involutum</i> (Voinova), <i>Crimites</i> sp., <i>Aktubinskia</i> sp.</p>	<p><i>Schubertella</i> aff. <i>ufimica</i> Baryshnikov, <i>?Uralofusulinella</i> sp.</p>	<p><i>Bradyina subtrigonalis</i> Baryshnikov, <i>Endothyranella protracta maxima</i> Baryshnikov, <i>Tetrataxis lata novosjolovi</i> Baryshnikov, <i>Pachyphloia</i> sp., <i>Geinitzina richteri kasib</i> Koscheleva, <i>Hemigordius</i> sp., <i>Nodosinelloides</i> ex gr. <i>netchaewi</i> (Tcherdynzev), <i>?Uralogordius</i> sp., <i>N. jazvae</i> Kosheleva, <i>Endothyra rotundata</i> Morozova, <i>E. symmetrica</i> Morozova, <i>E. lipinae</i> Morozova, <i>Pseudoagathammina regularis</i> (Lipina), <i>Pseudospira</i> cf. <i>vulgaris</i> (Lipina), <i>Midiella ovatus minima</i> (Grozdilova)</p>	<p><i>Apophysiacus praepycnoclada</i> (Nazarov & Ormiston), <i>Apophysiacus sakmaraensis</i> (Kozur & Mostler), <i>Astroentactinia inscita</i> Nazarov in Isakova and Nazarov, <i>Astroentactinia</i> sp. G, <i>Entactinia dolichoacus</i> Nazarov in Isakova and Nazarov, <i>Helioentactinia</i> sp. B, <i>Helioentactinia</i> sp. C, <i>Latentifistula heteroextrema</i> Nazarov in Isakova and Nazarov, <i>Pluristratoentactinia lusikae</i> Afanasieva, <i>Spongentactinia</i> sp. A, <i>Tetragregnon vimineum</i> Amon, Braun & Chuvashov.</p>
Bed 9-4		<p><i>Popanoceras annae</i> Ruzhencev</p>			

Bed 9-3					<i>Copicyntra fragilispinosa</i> Kozur et Mostler, <i>Pluristratoentactinia lusikae</i> Afanasieva.
Bed 9-1					<i>Copicyntra fragilispinosa</i> Kozur et Mostler
Bed 8-2			<i>Boultonia</i> sp., <i>Schubertella</i> sp. A, <i>Schubertella</i> sp. B, <i>S. sphaerica chomatifera</i> Zolotova, <i>S. turaevkensis</i> Baryshnikov, <i>S. turaevkensis elliptica</i> Baryshnikov, <i>S. ex gr. kingi</i> Dunbar & Skinner, <i>S. ex gr. paramelonica</i> Suleimanov, <i>Mesoschubertella</i> sp. 1, <i>Pseudofusulina</i> sp. 1, <i>Pseudofusulina</i> sp. 2, <i>P. paraconcessa</i> Rauser, <i>P. ex gr. pedissequa</i> Vissarionova, <i>P. insignita</i> Vissarionova, <i>P. abortiva</i> Tchuvashov, <i>P. seleukensis</i> Rauser, <i>P. urasbajevi</i> Rauser, <i>P. cf. utilis</i> Tchuvashov, <i>P. cf. salva</i> Vissarionova	<i>Langella</i> sp., <i>Dentalina particulata</i> Baryshnikov, <i>Hemigordius</i> sp., <i>Nodosinelloides incelebrata novosjolovi</i> (Baryshnikov), <i>N. netchaewi rasik</i> (Baryshnikov), <i>N. bella kamaenis</i> (Baryshnikov), <i>N. jaborovens</i> (Koscheleva), <i>Endothyra soshkinae</i> Morozova, <i>Bradyina lucida</i> Morozova, <i>Pseudobradyina compressa</i> Morozova, <i>P. compressa minima</i> Morozova, <i>Pseudoagathammina duplicata</i> (Lipina), <i>Deckerella elegans</i> Morozova, <i>D. elegans multicamerata</i> Zolotova, <i>D. media bashkirica</i> Morozova, <i>Hemigordiellina elegans</i> (Lipina), <i>Postmonotaxinoides costiferus</i> (Lipina), <i>Tetrataxis ex gr. conica</i> Ehrenberg, <i>T. plana</i> Morozova, <i>T. hemisphaerica</i> Morozova, <i>T. hemisphaerica elongata</i> Morozova, <i>T. lata</i> Spandel, <i>Lateenoglobivalvulina spiralis</i> (Morozova), <i>Trepeilopsis</i> sp., <i>Globivalvulina</i> sp.	
Bed 8-1			<i>Boultonia</i> sp., <i>Schubertella</i> sp., <i>Fusiella schubertellinoides</i> Suleimanov, <i>Pseudofusulina</i> sp.	<i>Dentalina particulata</i> Baryshnikov, <i>Geinitzina hysvaensis</i> Baryshnikov, <i>G. spandeli</i> Tcherdynzev, <i>Nodosinelloides kislovi</i> (Koscheleva), <i>N. dualis</i> (Baryshnikov), <i>Howchinella aff. turae</i> (Baryshnikov), <i>Postmonotaxinoides costiferus</i> (Lipina), <i>Endothyra lipinae lata</i> Zolotova, <i>?Rectoglandulina</i> sp.	

Bed 7-2					<i>Apophysiacus praepycnoclada</i> (Nazarov & Ormiston), <i>Apophysiacus sakmaraensis</i> (Kozur & Mostler), <i>Astroentactinia inscita</i> Nazarov in Isakova and Nazarov, <i>Astroentactinia</i> sp. F, <i>Astroentactinia</i> sp. G, <i>Entactinia chernykhii</i> Afanasieva & Amon, <i>Entactinia dolichoacus</i> Nazarov in Isakova and Nazarov, <i>Entactinia mariannae</i> Afanasieva & Amon, <i>Helioentactinia</i> sp. B, <i>Helioentactinia</i> sp. C, <i>Helioentactinia</i> sp. D, <i>Helioentactinia</i> sp. I, <i>Kozurispungus laqueus</i> (Nazarov & Ormiston), <i>Latentidiota promiscua</i> (Nazarov & Ormiston), <i>Latentifistula heteroextrema</i> Nazarov in Isakova and Nazarov, <i>Microporosa permica permica</i> (Kozur & Mostler), <i>Nazarovispungus aequilateralis</i> (Nazarov in Isakova and Nazarov), <i>Nazarovispungus pavlovi</i> Kozur, <i>Pluristratoentactinia</i> sp. J, <i>Spongentactinia fungosa</i> Nazarov, <i>Spongentactinia</i> sp. A, <i>Spongentactinia</i> sp. H, <i>Tetragregnon sphaericus</i> Nazarov in Isakova and Nazarov, <i>Tetragregnon vimineum</i> Amon, Braun & Chuvashov.
Bed 5-2					<i>Copicyntra fragilispinosa</i> Kozur & Mostler, <i>Palaeodiscaleksus</i> cf. <i>punctus</i> (Hinde)
Bed 1	<i>Mesogondolella</i> sp.				

- Geology and Geochemistry of RAN, Ekaterinburg, 217 pp. (in Russian)
- Chernykh, V.V., 2006. Lower Permian conodonts of the Urals. Institute of Geology and Geochemistry of RAN, Ekaterinburg, 130 pp. (in Russian)
- Chernykh, V.V., 2020. A brief review of the Dal'ny Tulkas Section (southern Urals, Russia) – potential candidate for a GSSP to define the base of the Artinskian stage in the global chronostratigraphic scale. *Permophiles*, v. 69, p. 9–14.
- Chernykh, V.V. and Chuvashov, B.I., 2004. Conodont biochronotype of Lower boundary of Sakmarian Stage. Annual-2003 of Institute of Geology and Geochemistry, Urals Branch of RAS. Ekaterinburg, UB RAS, p. 28–33. (In Russian).
- Chernykh, V.V., Chuvashov, B.I., Davydov, V.I. and Schmitz, M.D., 2012, Mechetlino Section: A candidate for the Global Stratotype and Point (GSSP) of the Kungurian Stage (Cisuralian, Lower Permian). *Permophiles*, v. 56, p. 21–34.
- Chernykh, V.V., Chuvashov, B.I., Davydov, V.I., Henderson, C.M., Shen, S., Schmitz, M.D., Sungatullina, G.M., Barrick, J.E. and Shilovsky, O.P., 2015. Southern Urals. Deep water successions of the Carboniferous and Permian. A Field Guidebook of XVIII International Congress on Carboniferous and Permian. Pre-Congress A3 Trip, August, 6-10, 2015. Kazan: Academy of Sciences of the Republic of Tatarstan Press, 88 pp.
- Chernykh, V.V., Chuvashov, B.I., Shen, S., Henderson, C.M., Yuan, D.X. and Stephenson, M.H., 2020. The Global Stratotype Section and Point (GSSP) for the base-Sakmarian Stage (Cisuralian, Lower Permian): Episodes, v. 43(4), p. 961–979. <https://doi.org/10.18814/epiugs/2020/020059>.
- Chuvashov, B.I., Chernykh, V.V., Bogoslovskaya, M.F., 2002a. Biostratigraphic Characteristic of Stage Stratotypes of the Permian System. *Stratigraphy and Geological Correlation*, v. 10, 4, p. 317–333.
- Chuvashov, B.I., Chernykh, V.V., Leven, E.Y., Davydov, V.I., Bowring, S., Ramezani, J., Glenister, B.F., Henderson, C.M., Schiappa, T.A., Northrup, C.J., Snyder, W.S., Spinosa, C.

- and Wardlaw, B.R., 2002b. Progress report on the base of the Artinskian and base of the Kungurian by the Cisuralian Working Group. *Permophiles*, no. 41, p. 13–16.
- Chuvashov, B.I., Chernykh, V.V., Shen, S. and Henderson, C.M., 2013. Proposal for the Global Stratotype Section and Point (GSSP) for the base-Artinskian Stage (Lower Permian): *Permophiles*, no. 58, p. 26–34.
- Chuvashov, B.I., Dyupina, G.V., Mizens, G.A. and Chernykh, V.V., 1990. Reference sections of the Upper Carboniferous and Lower Permian of western flank Urals and Preurals. Academy of Sciences, USSR, 369 pp. [in Russian]
- Davydov, V.I., Chuvashov, B. and Gareev, E., 2007. Report: Established and Proposed GSSPs of the Cisuralian Stages are Protected. *Permophiles*, no. 50, p. 18–22.
- Dehari, E., 2016. Upper Pennsylvanian–Lower Permian Carbonate Sedimentology and Conodont Biostratigraphy of the Strathearn and Buckskin Mountain formations, Carlin Canyon, Nevada [unpublished MSc thesis]: University of Calgary, Calgary, Alberta. 237 pp.
- di Pasquo, M., Grader, G.W., Isaacson, P., Souza, P.A., Iannuzzi, R. and Diaz-Martinez, E. 2015. Global biostratigraphic comparison and correlation of an early Cisuralian palynoflora from Bolivia. *Historical Biology*, v. 27, p. 868–897.
- Filimonova, T.V., 2010. Smaller Foraminifers of the Lower Permian from Western Tethys. *Stratigraphy and Geological Correlation*, v. 18, no. 7, p. 687–811.
- Foster, C.B. and Archbold, N.W., 2001. Chronologic anchor points for the Permian Early Triassic of the eastern Australian basins. In Weiss R.H. ed. *Contributions to geology and palaeontology of Gondwana in honour of Helmut Wopfner*. Geological Institute, University of Cologne, Germany, p. 175–199.
- Glenister, B.F., Baker, C., Furnish, W.M. and Dickins, J.M., 1990. Late Permian ammonoid cephalopod from Western Australia. *Journal of Paleontology*, v. 64, p. 399–402.
- Griffis, N.P., Montanez, I.P., Mundil, R., Richey, J., Isbell, J., Fedorchuk, N., Linol, B., Iannuzzi, R., Vesely, F., Mottin, T., Rosa, E., Keller, B. and Yin, Q.Z., 2019. Coupled stratigraphic and U-Pb zircon age constraints on the late Paleozoic icehouse-to-greenhouse turnover in south-central Gondwana. *Geology*, v. 47, p. 1146–1150.
- Griffis, N.P., Mundil, R., Montanez, I.P., Isbell, J., Fedorchuk, N., Vesely, F., Iannuzzi, R. and Yin, Q.Z., 2018. A new stratigraphic framework built on U-Pb single zircon TIMS ages with implications for the timing of the penultimate icehouse (Paraná Basin, Brazil). *Geological Society American Bulletin*, v. 130, p. 848–858.
- Guerra Sommer, M., Cazzulo-Klepzig, M., Menegat, R., Formoso, M.L.L., Basei, M.A.S., Barboza, E.G. and Simas, M.W., 2008a. Geochronological data from the Faxinal coal succession, southern Paraná Basin, Brazil: a preliminary approach combining radiometric U–Pb dating and palynostratigraphy. *Journal of South American Earth Sciences*, v. 25, p.246–256.
- Guerra-Sommer, M., Cazzulo-Klepzig, M., Santos, J.O.S., Hartmann, L.A., Ketzer, J.M., Formoso and M.L.L., 2008b. Radiometric age determination of tonsteins and stratigraphic constraints for the Lower Permian coal succession in southern Paraná Basin, Brazil. *International Journal of Coal Geology*, v. 74, p. 13–27.
- Guerra-Sommer, M., Cazzulo-Klepzig, M., Formoso, M.L.L., Menegat, R. and Mendonça, J.G., 2008c. U-Pb dating of tonstein layers from a coal succession of the southern Paraná Basin (Brazil): a new geochronological approach. *Gondwana Research*, v. 14, p. 474–482.
- Henderson, C.M., 1988. Conodont paleontology and biostratigraphy of the Upper Carboniferous to Lower Permian Canyon Fiord, Belcher Channel, Nansen, unnamed, and Van Hauen formations, Canadian Arctic Archipelago. Unpublished Ph.D. thesis, University of Calgary, Alberta, Canada, 287 pp.
- Henderson, C.M., 1999. Correlation of Cisuralian and Guadalupian stages in the Sverdrup Basin, Canadian Arctic Archipelago. XIV ICCP. Pander Society. Can. Paleontol. Conf. Abstrs. Calgary, p. 57–58.
- Henderson, C.M., 2018. Permian conodont biostratigraphy. In Lucas, S.G. and Shen S.Z. eds. *The Permian Timescale*. Geological Society, London, Special Publication 450, p. 119–142.
- Henderson, C.M., 2020. Are we ready yet to propose a GSSP for base-Artinskian and base-Kungurian? *Permophiles*, v. 69, p. 23–26.
- Henderson, C.M. and Chernykh, V.V., 2021. TO BE OR NOT TO BE *Sweetognathus asymmetricus*? *Permophiles*, v. 70, p. 10–13.
- Henderson, C.M., Davydov, V.I. and Wardlaw, B.R., 2012. The Permian Period. In Gradstein, F.M., Ogg, J.G., Schmitz, M.D. and Ogg, G.M. eds. *The Geological Timescale 2012*, vol. 2. Amsterdam, Elsevier, p. 653–680.
- Henderson, C.M. and McGugan, A., 1986. Permian conodont biostratigraphy of the Ishbel Group, southwestern Alberta and southeastern British Columbia. *Contributions to Geology*, University of Wyoming, v. 24. p. 219–235.
- Henderson, C.M. and Shen, S.Z., 2020. Chapter 24-The Permian Period. In Gradstein F.M., Ogg J.G., Schmitz M.D., and Ogg G.M. eds. *The Geologic Time Scale 2020*. v. 2. Elsevier, p. 875–902.
- Henderson, C.M., Schmitz, M., Crowley, J. and Davydov, V. 2009. Evolution and Geochronology of the *Sweetognathus* lineage from Bolivia and the Urals of Russia; Biostratigraphic problems and implications for Global Stratotype Section and Point (GSSP) definition. *Permophiles* v. 53, Supplement 1, p. 20–21.
- Henderson, C.M., Wardlaw, B.R., Davydov, V.I., Schmitz, M.D., Schiappa, T.A., Tierney, K.E., and Shen, S.Z., 2012. Proposal for base-Kungurian. *Permophiles*, v. 55, p. 8–34.
- Holdsworth, B.K. and Jones, D.L., 1980. Preliminary radiolarian zonation for Late Devonian through Permian time. *Geology*, v. 8, no. 6, p. 281–285.
- Holterhoff, P.F., Walsh, T.R. and Barrick, J.E., 2013. Artinskian (Early Permian) conodonts from the Elm Creek Limestone, a heterozoan carbonate sequence on the eastern shelf of the Midland Basin, West Texas, USA. In Lucas, S.G., Nelson, W.J. et al. eds. *The Carboniferous–Permian Transition*. New Mexico Museum of Natural History and Science Bulletin, v.

- 60, p. 109–119.
- Hounslow, M.W. and Balabanov, Y.P., 2018. A geomagnetic polarity timescale for the Permian calibrated to stage boundaries. In Lucas, S.G. and Shen S.Z. eds. *The Permian Timescale*. Geological Society, London, Special Publication 450, p. 61–103.
- Jurigan, I., Ricardi-Branco, F., Neregato, R. and Santos, T.J.S., 2019. A new tonstein occurrence in the eastern Paran' a Basin associated with the Figueira coalfield (Paran' a, Brazil): palynostratigraphy and U-Pb radiometric dating integration. *Journal of South America Earth Science*, v. 96, p. 1–18.
- Korte, C., Jasper, T., Kozur, H.W., and Veizer, J., 2006. ⁸⁷Sr/⁸⁶Sr record of Permian seawater. *Palaeogeography, Palaeoclimatology, Palaeoecology*, v. 240, p. 89–107.
- Kotlyar, G., Sungatullina, G. and Sungatullin, R., 2016. GSSPs for the Permian Cisuralian Series stages. *Permophiles*, v. 63, p. 32–37.
- Kozur H., 1977. Beitrage zur Stratigraphie des Perms. Teil I. Probleme der Abgranzung und Gliederung des Perms. Freiberg. Forschungsheft, C334. Leipzig, p. 85–161.
- Lambert, L.L., Wardlaw, B.R., and Henderson, C.M., 2007. *Mesogondolella* and *Jinogondolella* (Conodonta): Multielement definition of the taxa that bracket the basal Guadalupian (Middle Permian Series) GSSP. *Palaeoworld*, v. 16, p. 208–221.
- Laurie, J.R., Bodorkos, S., Nicoll, R.S., Crowley, J.L., Mantle, D.J., Mory, A.J., Wood, G.R., Champion, D.C., Holmes, E. and Smith, T.E., 2016. Calibrating the middle and late Permian palynostratigraphy of Australia to the geologic time-scale via U–Pb zircon CA-IDTIMS dating. *Australian Journal of Earth Sciences*, 63, 701–730.
- Leonova, T.B., 1998. Permian ammonoids of Russia and Australia. *Proceedings of the Royal Society of Victoria*, v. 110, p. 157–162.
- Leonova, T.B., 2018. Permian ammonoid biostratigraphy. In Lucas, S.G. and Shen, S.Z. eds. *The Permian Timescale*. Geological Society, London, Special Publication 450, p. 185–203.
- Mei, S.L., Henderson C.M. and Wardlaw B.R., 2002. Evolution and distribution of the conodonts *Sweetognathus* and *Iranognathus* and related genera during the Permian, and their implications for climate change. *Palaeogeography, Palaeoclimatology, Palaeoecology*, v. 180, p. 57–91.
- Metcalf, I., Crowley, J.L., Nicoll, R.S. and Schmitz, M., 2015. High-precision U-Pb CA-TIMS calibration of Middle Permian to Lower Triassic sequences, mass extinction and extreme climate-change in Australian Gondwana. *Gondwana Research*, v. 28, p. 61–81.
- Mouro, L.D., Alves M.L, Pacheco, F., Ricetti, J.H.Z., Scomazzon, A.K., Horodyski, R.S., Fernandes, A C. S., Carvalho, M.A., Weinschutz, L.C., Silva, M.S., Waichel, B.L. and Scherer, C.M.S., 2020. Lontras Shale (Paraná Basin, Brazil): Insightful analysis and commentaries on paleoenvironment and fossil preservation into a deglaciation pulse of the Late Paleozoic Ice Age. *Palaeogeography, Palaeoclimatology, Palaeoecology*, v. 555, p. 109850, <https://doi.org/10.1016/j.palaeo.2020.109850>.
- Nassichuk, W.W., 1971. Permian ammonoids and nautiloids, south eastern Eagle Plain, Yukon Territory. *Journal of Paleontology*, v. 45(6), p. 1001–1021.
- Nassichuk, W.W., 1975. The stratigraphic significance of Permian ammonoids on Ellesmere Island. In *Current Research, Part B*, Geological Survey of Canada, Paper 75-1b, p. 277–283.
- Nassichuk, W.W., Furnish, W.M. and Glenister, B.F., 1966. The Permian ammonoids of Arctic Canada; Geological Survey of Canada, Bulletin v. 131 p. 1–56.
- Nazarov, B.B. 1988. *Paleozoic Radiolaria. Practical Manual on Microfauna of the USSR*. Nedra, Leningrad, 231 pp. (In Russian).
- Nazarov, B.B. and Ormiston, A.R., 1985. Radiolarian from Late Paleozoic of the Southern Urals, USSR, and West Texas, USA. *Micropaleontology*, 30 (1), p. 1–54.
- Nazarov, B.B. and Ormiston, A.R. 1993. New biostratigraphically important Paleozoic Radiolaria of Eurasia and North America. *Micropaleontology, Special Publication*, v. 6, p. 22–60.
- Nestell, G.P. and Nestell, M.K., 2020. Roadian (earliest Guadalupian, Middle Permian) Radiolarians from the Guadalupe Mountains, West Texas, USA. Part I: Albaillellaria and Entactinaria. *Micropaleontology*, v. 66, no. 1, p. 1–50.
- Nicoll, R., McKellar, J., Ayaz, S.A., Laurie, J., Esterle, J., Crowley, J., Wood, G. and Bodorkos S., 2015. CA-IDTIMS dating of tuffs, calibration of palynostratigraphy and stratigraphy of the Bowen and Galilee basins. In Beeston J.W. ed. *Bowen Basin and Beyond*. Brisbane: Bowen Basin Symposium, 7-9 October 2015, p. 211–218.
- Park, Su-In, 1989. Microfossils of the Permo-Carboniferous Strata of Nongam Area in Mungyeong Coalfield. *Journ. Korean Earth Science Society*, v. 10 (1), p. 102–110
- Petryshen, W., Henderson, C.M., de Baets, K. and Jarochowska, E., 2020. Evidence of parallel evolution in the dental elements of *Sweetognathus conodonts*. *Proceedings of the Royal Society B*, 287, 20201922.
- Price, P.L., 1997. Permian to Jurassic palynostratigraphic nomenclature of the Bowen and Surat basins. In Green P., ed. *The Surat and Bowen Basins, southeast Queensland*. Brisbane: Queensland Department of Mines and Energy, p. 137–178.
- Read, M.T. and Nestell, M.K., 2018. Cisuralian (Early Permian) *Sweetognathid* conodonts from the upper part of the Riepe Springs Limestone, north Spruce Mountain ridge, Elko County, Nevada. In Over, D.J and Henderson, C.M. eds. *Conodont studies dedicated to the careers and contributions of Anita Harris, Glenn Merrill, Carl Rexroad, Walter Sweet, and Bruce Wardlaw*. *Bulletins of American Paleontology*, v. 395-396, p. 89–113.
- Rhodes, F.H.T., 1963. Conodonts from the topmost Tensleep sandstone of the Eastern Big Horn Mountains, Wyoming. *Journal of Paleontology*, v. 37 (2), p. 401–408.
- Riglos Suárez, M., Hünicken, M. A. and Merino, D., 1987. Conodont biostratigraphy of the Upper Carboniferous-Lower Permian rocks of Bolivia. In Austin, R.L. ed. *Conodonts: investigative techniques and applications*, British Micropalaeontological Society, Ellis Horwood Publishers, London, p. 317–325.

- Ritter, S. M., 1986. Taxonomic revision and Phylogeny of post-early crisis *bisselli-whitei* Zone conodonts with comments on Late Paleozoic diversity. *Geologica et Palaeontologica*, v. 20, p. 139–165.
- Rocha-Campos, A.C., Basei, M.A.S., Nutman, A.P. and Santos, P.R., 2006. SHRIMP U-Pb zircon geochronological calibration of the late Paleozoic Supersequence, Parana Basin, Brazil. In: South American Symposium on Isotope Geology, V, 2006, Punta del Este, p. 322–325.
- Rocha-Campos, A.C., Basei, M.A.S., Nutman, A.P. and Santos, P.R., 2007. SHRIMP U-Pb zircons ages of the late Paleozoic sedimentary sequence, Parana Basin, Brazil. In: Simposio sobre Cronoestratigrafia da Bacia do Parana, 4, 2007, Rio de Janeiro, Boletim de Resumos, p. 33
- Rocha-Campos, A.C., Basei, M.A.S., Nutman, A.P., Santos, P.R., Passarelli, C.R., Canile, F. M., Rosa, O.C.R., Fernandes, M.T., Santa Ana, H. and Veroslavsky, G., 2019. U-Pb zircon dating of ash fall deposits from the paleozoic paran basin of Brazil and Uruguay: a reevaluation of the stratigraphic correlations. *Journal of Geology*, v. 127, p. 167–182.
- Ruzhencev, V.E., 1956. Lower Permian ammonites of the Urals – Ammonites of the Artinskian Stage. *Trudy Paleontologicheskogo Instituta Akademii Nauk SSSR*, 60, p. 1–271.
- Santos, R.V., Souza, P.A., Alvarenga, C.J.S., Dantas, E.L., Pimentel, M.M., Oliveira, C.G. and Araujo, L.M., 2006. Shrimp U-Pb zircon dating and palynology of bentonitic layers from the Permian Irati Formation, Parana basin, Brazil. *Gondwana Research*, v. 9, p. 456–463.
- Schiappa, T.A., Hemmesch, N.T., Spinosa, C. and Nassichuk, W.W., 2005. Cisuralian ammonoid genus *Uraloceras* in North America. *Journal of Paleontology*, v. 79, no. 2, p. 366–377.
- Schmitz M.D. and Davydov V.I., 2012. Quantitative radiometric and biostratigraphic calibration of the Pennsylvanian–Early Permian (Cisuralian) time scale and pan-Euramerican chronostratigraphic correlation. *GSA Bulletin*, v. 124, no. 3–4, p. 549–577.
- Schmitz, M.D., Davydov, V.I. and Snyder, W.S., 2009. Permian–Carboniferous Conodonts and Tuffs: High precision marine Sr isotope geochronology. *Permophiles*, v. 53, Supplement 1 (ICOS 2009 Abstracts edited by C.M. Henderson and C. MacLean), p. 48.
- Scomazzon, A.K., Wilner, E., Purnell, M.A., Nascimento, S., Weinschütz, L.C., Lemos, V.B., de Souza, F.L. and da Silva, C.P., 2013. First report of conodont apparatuses from Brazil – Permian of Parana Basin, Itararé Group, Lontras Shale – Evidence of Gondwana deglaciation. In: Conodont from the Andes. 3rd International Conodont Symposium. Publicación Especial N° 13. Paleontological Note, p. 99–102.
- Shen, S.Z., Wang, Y., Henderson, C.M., Cao, C.Q. and Wang, W., 2007. Biostratigraphy and lithofacies of the Permian System in the Laibin-Heshan area of Guangxi, South China. *Palaeoworld*, v. 16, p. 120–139.
- Simas, M.W., Guerra-Sommer, M., Cazzulo-Klepzig, M., Menegat, R., Schneider Santos, J. O., Fonseca Ferreira, J.A. and Degani-Schmidt, I., 2012. Geochronological correlation of the main coal interval in Brazilian Lower Permian: radiometric dating of tonstein and calibration of biostratigraphic framework. *Journal of South American Earth Science*, v. 39, p. 1–15.
- Souza, P.A., Boardman, D.R., Premaor, E., Félix, C.M., Bender, R.R. and Oliveira, E.J., 2021. The Vittatina costabilis Zone revisited: New characterization and implications on the Pennsylvanian-Permian icehouse-to-greenhouse turnover in the Parana Basin, Western Gondwana, *Journal of South American Earth Sciences*, v. 106, <https://doi.org/10.1016/j.jsames.2020.102968>
- Stephenson, M.H., 2007. Preliminary results of palynological study of the Dal'ny Tulkas section, location of the proposed basal Artinskian GSSP. *Permophiles*, no. 50, p. 22–25.
- Stephenson, M.H. 2016. Permian palynostratigraphy: a global overview. In Lucas, S.G and Shen, S.Z. eds. *The Permian Timescale*. Geological Society, London, Special Publications, 450; p. 321–347.
- Stewart, J.H., Murchey, B., Jones, D.L., and Wardlaw, B.R., 1986. Paleontologic evidence for complex tectonic interlayering of Mississippian to Permian deep-water rocks of the Golconda allochthon in Tobin Range, north-central Nevada. *Geological Society of America Bulletin*, v. 97, p. 1122–1132.
- Suarez-Riglos, M., Hunicken, M.A. and Merino-Rodo D., 1987. Conodont biostratigraphy of the Upper Carboniferous–Lower Permian rocks of Bolivia. In Austin RL, editor. *Conodonts: investigative techniques and applications*. British Micropalaeontological Society. London: Ellis Horwood Publishers; p. 317–325.
- Sun, Y.D., Liu, X.T., Yan, J.X., Li, B., Chen, B., Bond, D.P.G. et al., 2017. Permian (Artinskian to Wuchiapingian) conodont biostratigraphy in the Tieqiao section, Laibin area, South China. *Palaeogeography, Palaeoclimatology, Palaeoecology*, v. 465, p. 42–63.
- Wang C.Y., Ritter S.M. and Clark D.L., 1987. The Sweetognathus complex in the Permian of China: implications for evolution and homeomorphy. *Journal of Paleontology*, v. 61, no. 5, p. 1047–1057.
- Wang, Z.H. & Higgins A.C., 1989. Conodont zonation of the Namurian–Lower Permian strata in South Guizhou, China. *Palaeontologia Cathayana*, v. 4, p. 261–325.
- Wang, Z.H., 1994. Early Permian conodonts from the Nashui section, Luodian of Guizhou. *Palaeoworld*, v. 4, p. 203–224.
- Wardlaw, B.R. and Nestell, M.K., 2015. Conodont faunas from a complete basinal succession of the upper part of the Wordian (Middle Permian, Guadalupian, West Texas). *Micropaleontology*, v. 61, p. 257–292.
- Wood, G.D., Gabriel, A.M. and Lawson, J.C. 1996. Palynological techniques – processing and microscopy. In Jansonius, J. and McGregor, D.C. eds. *Palynology: Principles and Applications*. American Association of Stratigraphical Palynologists Foundation, v. 1, p. 29–50.
- Zeng, J., Cao, C.Q., Davydov, V.I. and Shen, S.Z., 2012. Carbon isotope chemostratigraphy and implications of paleoclimatic changes during the Cisuralian (Early Permian) in the southern Urals, Russia. *Gondwana Research*, v. 21, p. 601–610.
- Zhang, L., Feng, Q.L. and He, W.H., 2018. Permian radiolarian biostratigraphy. In Lucas, S.G. and Shen, S.Z. eds. *The Permian Timescale*. Geological Society, London, Special Publications, 450; p. 321–347.

Permian Timescale. Geological Society, London, Special Publication, v. 450, p. 143–163.

Zhang, Z.H., Wang, Z.H. and Li, C.Q., 1988. Permian strata in South Guizhou. Guizhou People's Publishing House, Guiyang, 113 pp. (in Chinese).

Middle Kungurian (Early Permian) seaways in the southwestern USA

Spencer G. Lucas

New Mexico Museum of Natural History, 1801 Mountain Road N.W., Albuquerque, NM, 87104 USA
Email: spencer.lucas@state.nm.us

Charles Henderson

Department of Geoscience, University of Calgary, Calgary, Alberta, Canada T2N 1N4
Email: cmhender@ucalgary.ca

James E. Barrick

Department of Geosciences, Texas Tech University, Box 41053, Lubbock, TX 79409 USA
Email: Jim.Barrick@ttu.edu

Karl Krainer

Institute of Geology, University of Innsbruck, Innrain 52, Innsbruck, A-6020 Austria
Email: karl.krainer@uibk.ac.at

Introduction

In the southwestern USA (primarily the states of Arizona, New Mexico and Texas: Fig. 1), Lower Permian strata record a complex history of marine transgressions and regressions across part of equatorial western Pangea. However, the resulting epicontinental seaways have generally been little evaluated outside of local areas. This is because their regional distribution has been confounded by a lithostratigraphic nomenclature that changes across state lines and a lack of detailed biostratigraphic data by which to correlate the deposits of these seaways. We have recently obtained new conodont biostratigraphic data to provide more precise correlations that overcome the parochialism of local lithostratigraphic nomenclature to gain a more comprehensive understanding of the seaways that covered the American Southwest during part of middle Kungurian time.

Delaware Basin, Texas-New Mexico

In the Delaware Basin of West Texas-southeastern New Mexico (Fig. 1), the original unit stratotype of the Leonardian Series (Stage) of Adams et al. (1939) is the Leonard Formation in the Glass Mountains, now divided into the laterally equivalent Skinner Ranch and Hess formations overlain by the Cathedral Mountain Formation (Fig. 2).

Wardlaw and Nestell (2019) recently published the conodont biostratigraphy of the type Leonardian section, and Henderson (in Lucas et al., 2022) re-evaluated the taxonomic nomenclature and stratigraphic ranges of some of these conodonts. This re-

evaluation indicates that the base of the type Leonardian is of late Artinskian age, and, in the type Leonardian section, the base of the middle Kungurian (*Neostreptognathodus clinei* Zone) is at about the base of the Cathedral Mountain Formation (Fig. 2).

Midland Basin, Texas

On the eastern shelf of the Midland Basin of north-central Texas, placement of the base of the Leonardian has long been based primarily on Myers (1968), who documented the early Leonardian index fusulinid *Schwagerina crassitectoria* from the Talpa Limestone Member of the Clyde Formation (equivalent to strata in the upper part of the Wichita Group: Fig. 2). Most workers thus put the Leonardian base at or just below the stratigraphic level of the Talpa Limestone.

Placement of the base of the Kungurian in the Midland Basin is not well constrained, largely because the mostly nonmarine and very shallow marine facies have not produced index fossils. Generally, the Kungurian base is equated to the unconformity at the base of the Clear Fork Group (e.g., Ross, 1987; Ross and Ross, 1988), so the base of the Cathedral Mountain Formation likely correlates to a higher stratigraphic level in the dominantly nonmarine Clear Fork strata (Fig. 2). The most likely candidate from an event stratigraphic viewpoint is the Bullwagon Dolomite, which records a marine event across the Midland Basin and part of the Palo Duro Basin during and right after deposition of the Vale Formation (Nelson et al., 2013). However, there are no precise age data for the Bullwagon Dolomite; its only fossil record is of the nautiloid *Orthoceras* and long-ranging genera of bivalves and gastropods, such as *Aviculopecten*, *Myalina* and *Bellerophon* (Henderson, 1928). A more definite correlation of the Bullwagon Dolomite will require index fossils, so the correlation indicated here (Fig. 2) is very tentative.

Orogrande Basin, New Mexico

In the Orogrande Basin of central New Mexico, including its northern extent, which we term the Sierra-Bernalillo shelf (Fig. 1), much of the Lower Permian succession consists of strata of the Yeso Group (formerly formation) that have long been known to be deposits of shallow marine, evaporitic and arid coastal plain paleoenvironments equivalent to more “normal” marine strata in the Delaware Basin of West Texas and southeasternmost New Mexico (e.g., Mazzullo, 1995; Dinterman, 2001; Mack and Dinterman, 2002; Lucas et al., 2013). The Leonardian age assigned to the Yeso Group in the Delaware Basin of southeastern New Mexico has long been based on lithostratigraphic correlation of Yeso strata to much of the Leonardian Bone Spring Formation (Limestone), a slope-to-basinal carbonate-dominated unit.

The Yeso Group is a relatively thick unit (maximum thickness 1300m) that consists of three stratigraphically successive lithosomes that crop out across much of central and northern New Mexico: (1) a lower, mostly clastic lithosome, the De Chelly Sandstone (to the northwest, the southeastern edge of the DeChelly erg) and Arroyo de Alamillo Formation (to the southeast), deposits of an arid coastal plain with intercalated coastal sabkha deposits that developed between the De Chelly erg and the marine depositional environments of the Delaware Basin to the southeast; (2) a middle lithosome that is a complex,

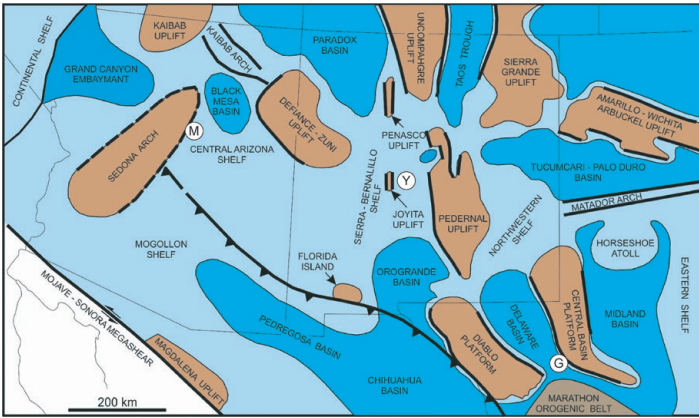


Fig. 1. Late Paleozoic paleo-tectonic map of Arizona, New Mexico and adjacent portions of Texas and other states (after Ross and Ross, 1985). Important locations in the text are indicated: G = Glass Mountains (Leonardian stratotype); M = Mogollon Rim near Payson, Arizona; Y = Yeso stratotype in Socorro County, New Mexico.

broadly cyclically-bedded succession of siltstone, gypsum and dolostone/dolomitic limestone, strata assigned to the Los Vallos Formation, the base of which is a thin interval of dolomitic limestone found across most of the Yeso outcrop belt, and interpreted as a significant event-stratigraphic horizon; and (3) the youngest lithosome, an interval of siliciclastic red beds, the Joyita Member of the Los Vallos Formation, deposited on an arid coastal plain, primarily by eolian, and subordinately by fluvial, processes (Baars, 1962; Mazzullo, 1995; Dinterman, 2001; Mack and Dinterman, 2002; Lucas and Zeigler, 2004; Lucas et al., 2005, 2013; Lucas and Krainer, 2012). The thin dolomitic limestone interval at the base of the Los Vallos Formation (Fig. 3A) is present across much of the Orogande Basin to as far north as the latitude of Belen, New Mexico (~ 34.7o N), and, north of that, it is laterally equivalent to siliciclastic strata (siltstone, sandstone) at the base of the San Ysidro Formation of the Yeso Group (Colpitts, 1989; Lucas et al., 1999, 2005, 2016; Lucas and Zeigler, 2004).

Lucas et al. (2022) document conodonts from the basal dolomitic limestone interval of the Torres Member of the Los Vallos Formation at Broken House Tank in the southern Caballo Mountains of Sierra County, New Mexico (cf. Lucas and Krainer, 2012). These conodonts are assigned to the lower part of the middle Kungurian *Neostreptognathodus clinei* Zone, where advanced *N. pnevi* and *N. clinei* co-occur (cf. Henderson, 2018) with *N. prayi*. These Yeso conodonts thus correlate the base of the Los Vallos Formation to the lower part of the Cathedral Mountain Formation in the type Leonardian section, but correlation to the uppermost Skinner Ranch cannot be discounted because of the lack of *N. clinei* in the Glass Mountains (Fig. 2).

Pedregosa Basin, Arizona, New Mexico and Mexico

The Pedregosa Basin was located in what is now southwestern New Mexico, southeastern Arizona and adjacent parts of the northern Mexican states of Chihuahua and Sonora (Fig. 1). It has a lithostratigraphic nomenclature different from correlative strata to the east and northeast in New Mexico. This nomenclature assigns the thick (> 2 km) upper Paleozoic section to the Naco Group composed of the (ascending) Pennsylvanian-Lower

Permian Horquilla Formation, and the Permian Earp, Colina, Epitaph, Scherrer and Concha formations (e. g., Gilluly et al., 1954; Zeller, 1965; Ross, 1973). Fusulinid and conodont age control indicate the youngest age of the Horquilla Formation is middle Wolfcampian (Nealian; Asselian), and fusulinids indicate an age of Roadian for the Concha Limestone (Ross, 1973; Wilde, 2006; Lucas et al., 2017).

The upper part of the Colina Limestone has yielded the Leonardian index ammonite *Perrinites hilli* (Sabins, 1957). An unpublished dissertation on conodonts from the Permian strata in the Pedregosa Basin by Butler (1972) has been analyzed by Henderson. It apparently documents records of *Neostreptognathodus pnevi* including advanced *N. pnevi* and one specimen that may be *N. clinei* (see Figure 6 in Butler, 1972) from the Colina Limestone. Other specimens could be assigned to *N. cf. lectulus* and one to *N. pequopensis*. Butler (1972) collected a series of samples throughout the extent of the Colina Limestone, but the collection numbers and University of Arizona curation numbers are not linked, and the collections appear to be lost. The conodonts suggest an early to early-middle Kungurian age. Thus, it is possible, but not certain, that the upper Colina Limestone correlates to the lower Cathedral Mountain Formation and to the basal Los Vallos Formation of the Yeso Group (Fig. 2). More analysis of the Colina conodonts is needed to confirm this.

Arizona shelf, Arizona

Permian strata deposited on the western part of the Arizona shelf are best exposed along the Mogollon Rim as a thick (up to 550 m), red-bed dominated section of the Supai Group south of Flagstaff that has a complex, local lithostratigraphic nomenclature (e.g., Blakey, 1979, 1989; Peirce, 1977, 1989). Marine strata of the Naco Formation below Supai Group red beds yield fusulinids and macroinvertebrates (primarily brachiopods) that indicate an age range of Middle-Late Pennsylvanian (Atokan-Virgilian) (e. g., Huddle and Dobrovlny, 1945; Brew, 1965, 1979). The Permian base is usually placed at the Naco-Supai contact, and this may

AGE		Mogollon Rim (Az)	Pedregosa Basin (Az-NM-Mx)	Orogande Basin (NM)	Delaware basin (TX)	Midland Basin (TX)	conodont zones
Leonardian	Cathedralian	upper Supai Group	Scherrer Formation	Yeso Group Los Vallos Formation Torres Member	Cathedral Mountain Formation	Clear Fork Group Chozza Formation	<i>N. bicar.</i>
			Epitaph Dolomite				
	Kungurian	Fort Apache Limestone	upper Colina Limestone			Bullwagon Dolomite	<i>N. pr.</i>
		Hessian	lower Supai Group	lower Colina Limestone	Arroyo de Alamillo Formation	Skinner Ranch/Hess formations	Vale Formation
upper Earp Formation	Arroyo Formation			<i>N. pequop.</i>			
	Sarginian	middle Earp sandstone			Wichita Group	<i>N. exsculptus</i>	

Fig. 2. Correlation of selected Leonardian strata in Arizona, New Mexico and Texas.

be a substantial unconformity between Virgilian and Leonardian strata (Lucas and Henderson, 2021).

The Fort Apache Limestone is a carbonate interval generally less than 20 m thick in the upper part of the Supai Group section along the Mogollon Rim (Figs. 2, 3B). Lucas and Henderson (2021) recently reported conodonts from the Fort Apache Limestone that include *Neostreptognathodus foliatus* and *N. clinei*, and lack *N. pnevi*. These conodonts are clearly of Kungurian age and were judged middle Kungurian, well above the base of the *N. clinei* Zone, by Lucas and Henderson (2021). However, it is also possible that they are a bit older within the *N. clinei* Zone (overlap of range of *N. clinei* and *N. foliatus*), which would correlate the Fort Apache Limestone to near the base of the Cathedral Mountain Formation, as shown here in Figure 2. The full range of the various Kungurian conodont taxa need to be tested with new samples. The Fort Apache Limestone has long been correlated to the Colina Limestone of the Pedregosa Basin based primarily on stratigraphic position and lithology (e.g., Sabins, 1957; Winters, 1963; Ross, 1973), a correlation that makes sense based on event stratigraphy. If those correlations are correct, then the Colina and Fort Apache are correlative to the Cathedral Mountain transgression. Further evaluation of the Fort Apache conodonts is planned and should more definitely determine their age within the Kungurian.

Kungurian seaways

The correlations reviewed here suggest the development of seaways from Arizona through Texas during middle Kungurian time correlative to the major transgression at the base of the Cathedral Mountain Formation in the Delaware Basin. Kerans et al. (2014, and other papers) have correlated numerous high frequency sequences (HFS) in the Guadalupe Mountains, including 8 in the Leonardian and 30 in the Guadalupian based on remarkable outcrop exposures. Correlating Leonardian HFS's into the Kungurian seaways will require additional study, but the upper Colina-Fort Apache-lower Torres correlation may constitute a single HFS transgressive succession or possibly two HFS events within the same systems tract. These seaways occupied the Delaware Basin (Cathedral Mountain Formation) and Orogrande Basin (lowermost strata of the Los Vallos Formation, Yeso Group), and quite possibly the Midland and Palo Duro basins (Bullwagon Dolomite), Pedregosa Basin (Colina Limestone) and Arizona shelf (Fort Apache Limestone). There thus was an extensive marine transgression across the American Southwest during middle Kungurian time, and this transgression is correlative to the Filippovian transgression in the Russian Urals and thus is likely a global eustatic event (cf. Ross and Ross, 1988). Nevertheless, more work is needed and planned to refine age assignments of Kungurian marine strata in the American Southwest to further delineate its Early Permian paleogeography and depositional history.

References

Adams, J. E., Cheney, M.G., Deford, R. K., Dickey, R. I., Dunbar, C. O., Hills, J. M., King, R. E., Lloyd, E. R., Miller, A. K, and Needham, C. E., 1939. Standard Permian section of North America. American Association of Petroleum Geologists

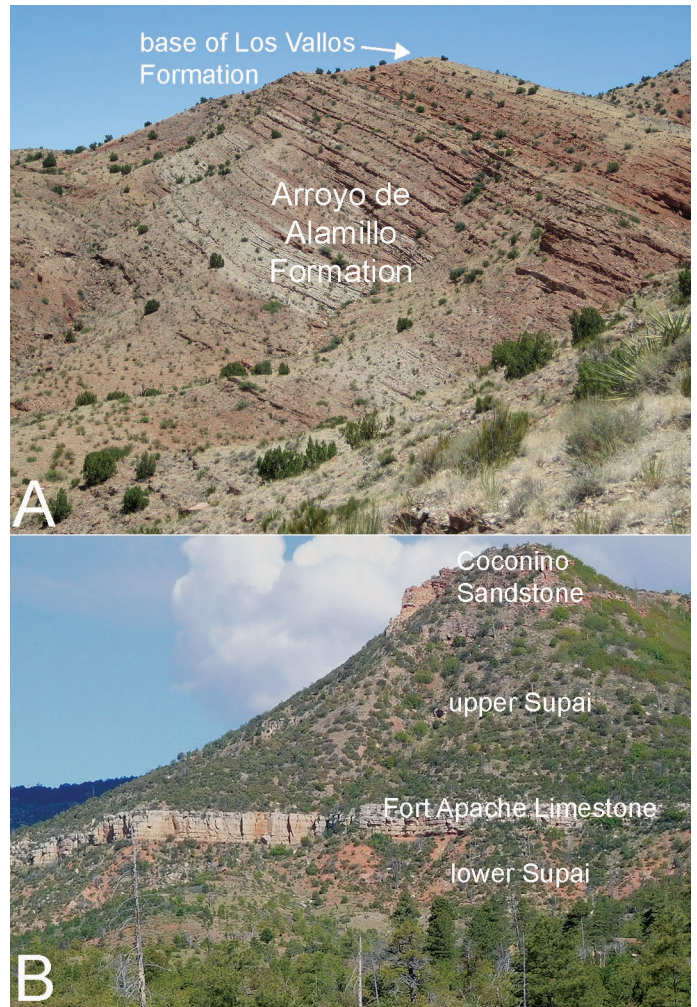


Fig. 3. Selected outcrops of Kungurian strata in New Mexico and Arizona. A, Part of Yeso Group section near the Yeso Group type section at Loma de las Cañas in Socorro County, New Mexico. B, Kungurian section at Tonto Creek on the Mogollon Rim in Gila County, Arizona.

Bulletin, v. 23, p. 1673–1681.

- Baars, D. L., 1962. Permian System of Colorado Plateau. American Association of Petroleum Geologists Bulletin, v. 46, p. 149–218.
- Blakey, R. C., 1979. Stratigraphy of the Supai Group (Pennsylvanian-Permian), Mogollon Rim, Arizona. In Beus, S. S. and Rawson, R. R. (eds.), Carboniferous stratigraphy in the Grand Canyon country northern Arizona and southern Nevada. American Geological Institute, Selected Guidebook Series No. 2, p. 89–104.
- Brew, D. C., 1965. Stratigraphy of the Naco Formation (Pennsylvanian) in central Arizona. Ph. D. thesis, Ithaca, Cornell University, 204 pp.
- Brew, D. C., 1979. Biostratigraphy of the Naco Formation (Pennsylvanian) in central Arizona. In Beus, S. S. and Rawson, R. R. (eds.), Carboniferous stratigraphy in the Grand Canyon country northern Arizona and southern Nevada. American Geological Institute, Selected Guidebook Series No. 2, p. 119–125.
- Butler, W. C., 1972. Permian conodonts from southeastern Arizona. Ph. D. thesis, Tucson, University of Arizona, 130 pp.

- Colpitts, R. M., Jr., 1989. Permian reference section for southeastern Zuni Mountains, Cibola County, New Mexico. New Mexico Geological Society, Guidebook 40, p. 177–180.
- Dinterman, P. A. 2001. Regional analysis of the depositional environments of the Yeso and Glorieta formations (Leonardian), New Mexico. M.S. thesis, Las Cruces, New Mexico State University, 165 pp.
- Gilluly, J., Cooper, J. A. and Williams, J. S., 1954. Late Paleozoic stratigraphy of central Cochise County, Arizona. U. S. Geological Survey, Professional Paper 266, 49 pp.
- Henderson, C. M. 2018. Permian conodont biostratigraphy. In Lucas, S. G. and Shen, S. Z. (eds.), The Permian timescale. Geological Society, London, Special Publications, v. 450, p. 119–142.
- Henderson, G. G. 1928. The geology of Tom Green County. University of Texas, Bulletin 2807, 116 pp.
- Huddle J. W. and Dobrovolsky, E., 1945. Late Paleozoic stratigraphy of central and northeastern Arizona. U. S. Geological Survey Oil and Gas Investigations Preliminary Chart 10.
- Kerans, C., Playton, T., Phelps, R., and Scott, S.Z., 2014. Ramp to rimmed shelf transition in the Guadalupian (Permian) of the Guadalupe Mountains, West Texas and New Mexico. SEPM Special Publication, no. 105, p. 26–49.
- Lucas, S. G. and Henderson, C. M., 2021. New age data for Permian strata on the Mogollon Rim, central Arizona, USA. Permophiles, no. 71, p. 18–21.
- Lucas, S. G., and Krainer, K., 2012. The Lower Permian Yeso Group in the Fra Cristobal and Caballo Mountains, Sierra County, New Mexico. New Mexico Geological Society Guidebook, no. 63, p. 377–394.
- Lucas, S. G., and Zeigler, K. E., 2004. Permian stratigraphy in the Lucero uplift, central New Mexico: New Mexico Museum of Natural History and Science Bulletin, v. 25, p. 71–82.
- Lucas, S. G., Krainer, K. and Colpitts, R. M., Jr., 2005. Abo-Yeso (Lower Permian) stratigraphy in central New Mexico. New Mexico Museum of Natural History and Science, Bulletin 31, p. 101–117.
- Lucas, S. G., Krainer, K., and Voigt, S., 2013, The Lower Permian Yeso Group in central New Mexico. New Mexico Museum of Natural History and Science Bulletin, v. 59, p. 181–199.
- Lucas, S. G., Henderson, C., Barrick, J. E. and Krainer, K., 2022. Conodonts and the correlation of the Lower Permian Yeso Group, New Mexico, USA. Stratigraphy, in press.
- Lucas, S. G., Krainer, K., Barrick, J. E., Vachard, D. and Ritter, S. M., 2017. Lithostratigraphy and microfossil biostratigraphy of the Pennsylvanian-lower Permian Horquilla Formation at New Well Peak, Big Hatchet Mountains, New Mexico, USA. Stratigraphy, v. 14, p. 233–246.
- Lucas, S. G., Rowland, J. M., Kues, B. S., Estep, J. W. and Wilde, G. L., 1999. Uppermost Pennsylvanian and Permian biostratigraphy at Placitas, New Mexico. New Mexico Geological Society, Guidebook 50, p. 281–292.
- Lucas, S. G., Krainer, K., Oviatt, C. G., Vachard, D., Berman, D. S. and Henrici, A. C., 2016. The Permian System at Abo Pass, central New Mexico (USA). New Mexico Geological Society Guidebook, v. 67, p. 313–350.
- Mack, G. H. and Dinterman, P.A., 2002. Depositional environments and paleogeography of the Lower Permian (Leonardian) Yeso and correlative formations in New Mexico. The Mountain Geologist, v. 39, p. 75–88.
- Mazzullo, S. J., 1995. Permian stratigraphy and facies, Permian basin (Texas-New Mexico) and adjoining areas in the Midcontinent United States. In Scholle, P. A., Peryt, T. M. and Ulmer-Scholle, D. S. (eds), The Permian of northern Pangaea Volume 2: Sedimentary basin and economic resources, Berlin, Springer-Verlag, p. 41–60.
- Myers, D. A., 1968. *Schwagerina crassitectoria* Dunbar and Skinner, 1937, a fusulinid from the upper part of the Wichita Group, lower Permian, Coleman County, Texas. U. S. Geological Survey Professional Paper, v. 600-B, p. 133–139.
- Nelson, W. J., Hook, R. W. and Chaney, D. S., 2013. Lithostratigraphy of the Lower Permian (Leonardian) Clear Fork Formation of north-central Texas. New Mexico Museum of Natural History and Science, Bulletin 60, p. 286–311.
- Peirce, H. W., 1977. Survey of uranium favorability of Paleozoic rocks in the Mogollon Rim and slope region—east central Arizona. State of Arizona Bureau of Geology and Mineral Technology, Circular 19, 60 pp.
- Peirce, H. W., 1989. Correlation problems of Pennsylvanian-Permian strata of the Colorado Plateau of Arizona. In Jenney, J. P. and Reynolds, S. J. (eds.), Geologic evolution of Arizona. Tucson, Arizona Geological Society Digest 17, p. 349–368.
- Ross, C.A., 1973, Pennsylvanian and early Permian depositional history, southeastern Arizona. American Association of Petroleum Geologists Bulletin, v. 57, p. 887–912.
- Ross, C. A., 1987. Leonardian Series (Permian), Glass Mountains, West Texas. Permian Basin Section SEPM, Publication 87–27, p. 25–33.
- Ross, C. A. and Ross, J. R. P., 1985. Paleozoic tectonics and sedimentation in West Texas, southern New Mexico, and southern Arizona. West Texas Geological Society, Publication 85–81, p. 221–230.
- Ross, C. A. and Ross, J. R. P., 1988. Late Paleozoic transgressive-regressive deposition. SEPM Special Publication 42, p. 227–247.
- Sabins, F. F., Jr., 1957. Stratigraphic relations in Chiuricahua and Dos Cabezas Mountains, Arizona. American Association of Petroleum Geologists Bulletin, v. 41, p. 466–510.
- Wardlaw, B. R. and Nestell, M. 2019. Conodont biostratigraphy of Lower Permian (Wolfcampian-Leonardian) stratotype sections of the Glass and Del Norte Mountains, West Texas, USA. AAPG Memoir, v. 118, p. 229–249.
- Wilde, G. L., 2006. Pennsylvanian-Permian fusulinaceans of the Big Hatchet Mountains, New Mexico. New Mexico Museum Natural History and Science, Bulletin 38, p. 1–311.
- Winters, S. S., 1963. Supai Formation (Permian) of eastern Arizona. Geological Society of America, Memoir 89, 99 pp.
- Zeller, R. A., Jr., 1965. Stratigraphy of the Big Hatchet Mountains, New Mexico. New Mexico Bureau of Mines and Mineral Resources, Memoir 16, 128 pp.

Update: improved palynological resolution in the latest Permian of the Levant

Michael H. Stephenson

British Geological Survey
 Email: mhste@bgs.ac.uk;
 Stephenson Geoscience Consulting
 Email: mikepalyno@me.com

Over much of the Middle East, the Lopingian is dominated by carbonate facies (the Khuff Formation and its equivalents the Dalan Formation in Iran and the Chia Zairi Formation in Iraq). Because carbonates tend to suppress the preservation of palynomorphs, the resolution of palynological biozonation schemes tend to become rather poor in the Lopingian and also make the position of the Permian-Triassic boundary difficult to determine by palynology alone in the Middle East. However in the northern parts of the region, in the Levant, the facies of the Lopingian are more siliciclastic with often very good palynological preservation through much of the Lopingian and Lower Triassic section. Work on these sequences including Stephenson & Powell (2013, 2014) and Stephenson and Korngreen (2020) have been able to apply some of the palynological schemes of the Arabian Peninsula to the Levant, and the favourable facies have allowed the extension of palynological biozonation schemes further into the Lopingian.

In Israel, the Lopingian is represented by the (upper) Arqov and (lower) Saad formations. Recent work on Cores 11 to 15 of the Makhtesh Qatan-2 borehole in the Negev, within the Arqov Formation suggest that at least part of the Arqov Formation can be

characterised by *Cedripites priscus*, *Reduviasporonites chalastus* and particularly *Pretricolpipoollenites bharadwajii*, while the Saad Formation contains a slightly less diverse assemblage lacking these three taxa (Stephenson and Korngreen, 2021). The first appearance of the tri-sulcate pollen *Pretricolpipoollenites bharadwajii* is approximately Changhsingian in age (Stephenson and Korngreen, 2021; Stephenson & Powell 2014) indicating that at least part of the Arqov Formation is Changhsingian.

Further north in the coastal plain of Israel, foraminifera from the Pleshet-1 and Gevim-1 boreholes suggest Midian (approx. Capitanian; Lucas and Shen 2018) and Djulfian (approx. Wuchiapingian; Lucas and Shen 2018) ages for the Saad and Arqov formations respectively (Labkovsky-Orlov 2004; Labkovsky-Orlov and Hirsch 2005).

In Jordan, the Umm Irna Formation is also likely to be Changhsingian in age.

Acknowledgments

Thanks to the staff of the core store of the Israel Geological Survey. Palynological samples were processed by Max Page of the British Geological Survey.

References

- Lucas, S. G. and Shen, S. Z. 2018. Permian chronostratigraphic scale. In Lucas, S.G., Shen, S.Z. (eds.), The Permian Timescale. Special Publications, 450. Geological Society, London, p. 21–50.
- Orlov-Labkovsky, O. and Hirsch, F. 2005. The Permian fusulinids in Israel. In: Hall, J.K., Krasheninnikov, V.A., Hirsch, F, Benjamini, C, and Flexer, A. (Eds.) Geological Framework of the Levant, Vol. II, The Levantine Basin and Israel, Edition:

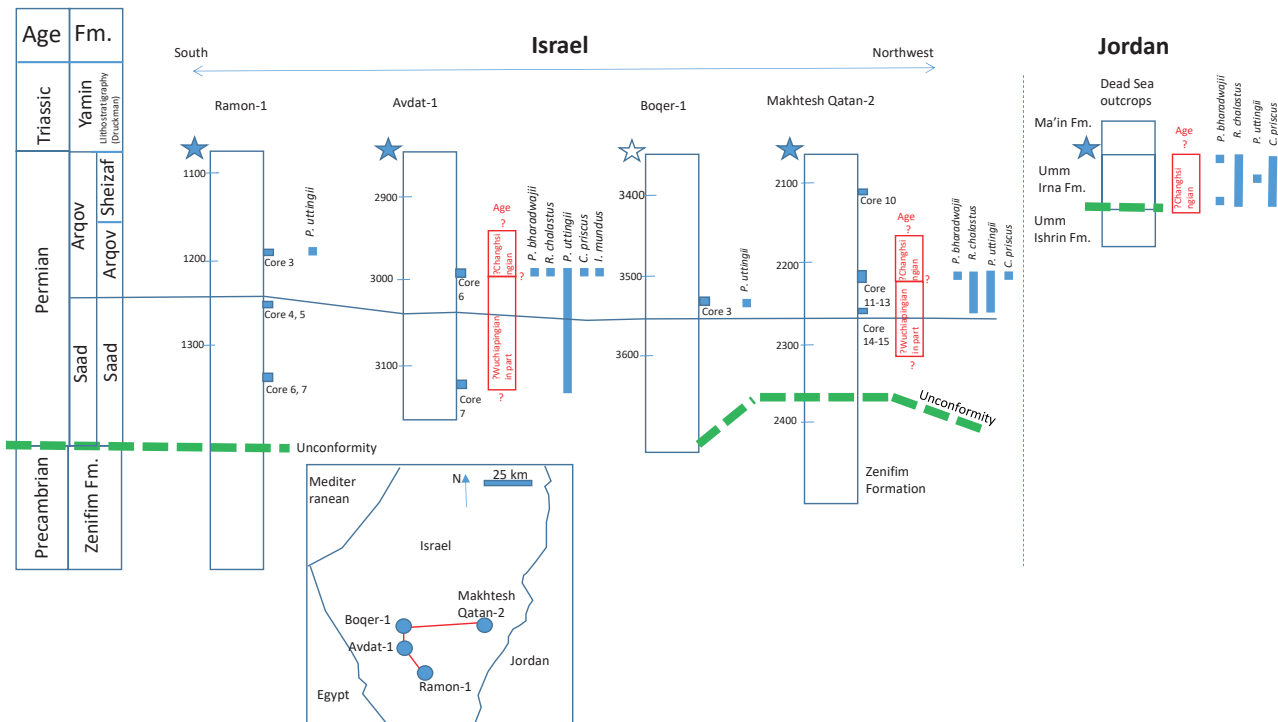


Fig. 1. Lithostratigraphy, palynology and biozones of Makhtesh Qatan-2; Ramon-1, Boqer-1, Avdat-1 and Jordanian Dead Sea outcrops; solid star indicates Permian-Triassic boundary depth, blank star indicates approximate depth of Permian-Triassic boundary. Summarised from data in Stephenson and Korngreen (2020, 2021)

1, Chapter: 18B, Publisher: Historical Productions-Hall, Jerusalem, p. 317–330.

Orlov-Labkovsky, O. 2004. Permian fusulinids (foraminifera) of the subsurface of Israel: taxonomy and biostratigraphy. *Rev. Espan. Micropaleontol.*, v. 36, p. 389–406.

Stephenson, M. H. and Korngreen, D. 2020. Palynological correlation of the Arqov and Saad formations of the Negev, Israel, with the Umm Irna Formation of the eastern Dead Sea, Jordan, *Review of Palaeobotany and Palynology*, v. 274, 104153

Stephenson, M. H. and Korngreen, D. 2021. Palynology of the Permian of the Makhtesh Qatan-2, Ramon-1 and Boqer-1 boreholes Arqov Formation, Negev, Israel. *Rivista Italiana di Paleontologia e Stratigrafia*, v. 127, no. 3.

Stephenson, M. H. and Powell, J H. 2013. Palynology and alluvial architecture in the Permian Umm Irna Formation, Dead Sea, Jordan. *GeoArabia*, v. 18, p. 17–60.

Stephenson, M. H. and Powell, J H. 2014. Selected spores and pollen from the Permian Umm Irna Formation, Jordan, and their stratigraphic utility in the Middle East and North Africa. *Rivista Italiana di Paleontologia e Stratigrafia*, v. 120, p. 145–156.

Call to the Permian community: Identifying an enigmatic sedimentary structure from the Bromacker

Frank Scholze

Friedrich Schiller University Jena, Institute for Geoscience, Burgweg 11, 07749 Jena, Germany.
Email: Frank.Scholze@uni-jena.de

Anna Pint

Friedrich Schiller University Jena, Institute for Geoscience, Burgweg 11, 07749 Jena, Germany.
Email: Anna.Pint@uni-jena.de

Peter Frenzel

Friedrich Schiller University Jena, Institute for Geoscience, Burgweg 11, 07749 Jena, Germany.
Email: Peter.Frenzel@uni-jena.de

Introduction

Herein, we present an enigmatic sedimentary structure from the Tambach Sandstone Member (Tambach Formation, Early Permian; Fig. 1) that was collected during recent field activities at Bromacker in the Thuringian Forest Basin (Free State of Thuringia, central Germany). From the authors' current knowledge, this new specimen hardly compares to other sedimentary structures known previously from the Tambach Formation. We hope that feedbacks from the Permophiles readership will help identifying this enigmatic sedimentary structure.

Geologic setting

Lower Permian (Artinskian; Schneider et al., 2020) red-bed sediments of the Tambach-Dietharz (sub-) basin, as part of the

Thuringian Forest Basin, are well-exposed through quarries, a palaeontological excavation site, and drill core sections (e.g., Martens et al., 2009) at the Bromacker grassland and forest area (Fig. 2A–C). The Bromacker is an outcrop area that is located about 2 km north to the city centre of Tambach-Dietharz (Fig. 2A). The red-beds at the Bromacker belong lithostratigraphically to the Tambach Sandstone Member (Tambach Formation, Upper Rotliegend 1 Subgroup, Rotliegend Group; see Fig. 1). Due to spectacular finds of both tetrapod body fossils (e.g., *Diadectes*, *Orobates*, *Dimetrodon*, *Eudibamus*, and others) and tetrapod tracks and footprints, the Tambach Sandstone Member at the Bromacker can be designated as a fossil Lagerstätte (Martens,

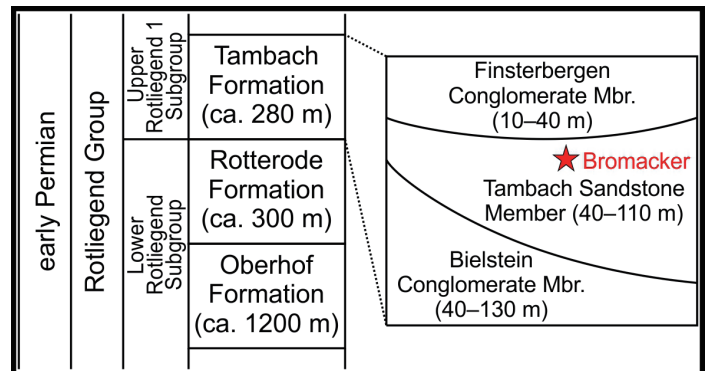


Fig. 1. Stratigraphy of the study area with generalized thickness values (e.g., Lütznier et al., 2012). The Tambach Formation is subdivided lithostratigraphically into the Bielstein Conglomerate, the Tambach Sandstone, and the Finsterbergen Conglomerate members. The red asterisk marks the position of the Bromacker outcrop section in the Tambach Sandstone Member.

2018). Fossil invertebrates, invertebrate traces, and plant remains occur as well. The richness in fossils and excellent preservation of many fossils makes this site appealing to a wider audience triggering science communication and geotouristic interest. Thus, selected fossils are displayed along the so-called saurian discovery trail, a hiking path with, e.g., 3D-reconstructions of *Dimetrodon* (Fig. 2D) and other early tetrapods.

Previous sedimentological studies characterise the Tambach Formation as sedimentary deposits of a small hydrologically closed intramontane upland basin (Eberth et al., 2000) in a semi-arid, temporary wet palaeoclimate (e.g., Roscher and Schneider, 2006). An absence of true aquatic vertebrate fossils (i.e., fishes) may indicate a phase of pronounced terrestrial habitat conditions (e.g., Martens et al., 2005). Occurrences of well-preserved sedimentary structures at the Bromacker include desiccation cracks, rain drop imprints, small-sized load casts, tool and scour marks, water level marks, ripples, and intraformational clayey rip-up clasts. Variable lithologies of the Tambach Sandstone Member are interpreted as deposits of a fluvial facies, which includes both a variable sandy channel (sub-) facies for the 'Bromacker Sandstone' (an informal local stratigraphic unit in the sense of Martens et al., 2009) and a finer grained, thin-bedded flood plain (sub-) facies for the 'Bromacker horizon' (sensu Martens et al., 2009). The thicker-bedded deposits of the sandy channel (sub-) facies of the 'Bromacker Sandstone' involve multiple facies architectures of fluvial sandstones, such as massive beds, slightly horizontal bedding, and channel-shaped beds with internal through-shaped cross bedding. In particular,

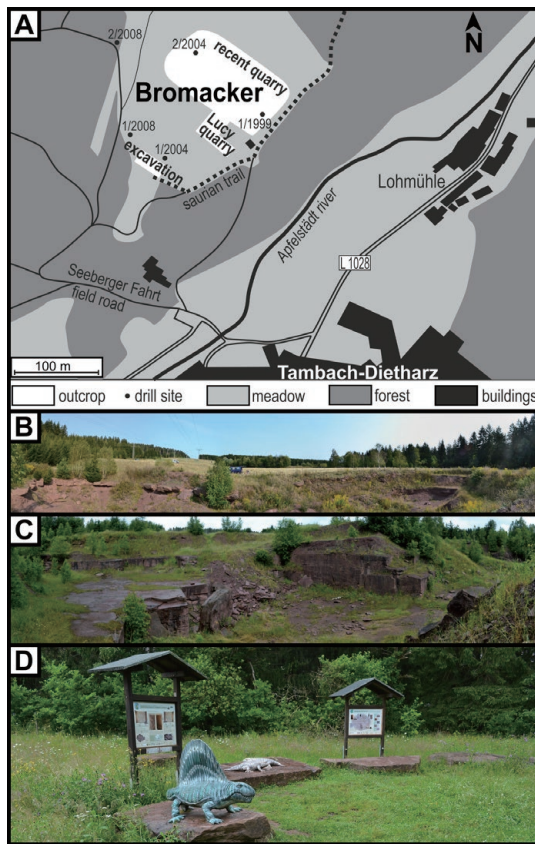


Fig. 2. The Bromacker area. A. Geographic map showing the localities of quarries, drill sites, and the excavation. B–C. Outcrop sections photographs of the excavation site (Fig. B; width about 50 m) and the still active quarry (Fig. C; width about 60 m in front of the photograph) both in viewing direction north, showing fine- to medium-grained sandstones of the Tambach Sandstone Member (Tambach Formation, Rotliegend Group; early Permian). D. Station of the geotouristic path along the Bromacker site, displaying boards and 3D-reconstructions of Bromacker fossils (i.e., Dimetrodon in front, Seymouria in the background).

massive and slightly horizontally bedded sandstones at the Bromacker can be interpreted as sheet flood deposits, possibly as result of temporary strong precipitation (e.g., Schneider and Gebhardt, 1993).

Material and methods

The specimen reported herein was found by the authors in the present day quarry at the Bromacker. The quarry is still considered as an active one, although mining has paused since several years. The herein reported material consists of a single rock slab of red coloured, fine- to slightly medium-grained sandstone that corresponds lithostratigraphically to the so-called ‘Bromacker Sandstone’ in the sense of Martens et al. (2009). The ‘Bromacker Sandstone’ is an about 8.50 m thick informal local unit within the Tambach Sandstone Member. The rock slab shows a greyish coloured patina, due to recent surface weathering. In the laboratory of the Institute of Geoscience in the University of Jena, the slab was cleaned with water and a soft brush to remove mud and small recent vegetation remnants. The sedimentary structure on the rock slab was photographed with a Nikon DX digital camera and a Nikkor AF-S macro lens under an artificial (LED) shallow angle light. Interestingly, due to both a strong LED illumination and a short distance between the digital camera

and the photographed slab, its predominantly greyish weathering colour turned apparently into a red colour on the digital photographs. The latter colour is more similar to the original red rock colour of freshly exposed sandstones of the Tambach Sandstone Member. Different camera focus images were stacked vertically using the raster image software Adobe Photoshop 22 (Figs. 3A, C, D) and became mounted to figures using the vector graphic software Corel DRAW 21. A Keyence VHX-6000 digital microscope was used for relief measurements (Fig. 4).

Results

The red coloured, fine- to medium-grained sandstone slab measures about 40x20x8 cm. The lower side of the slab bears desiccation cracks and a poorly preserved specimen of the ichnotaxon *Tambia spiralis* (Müller 1956) as a hyporelief. The enigmatic sedimentary structure described herein is located at

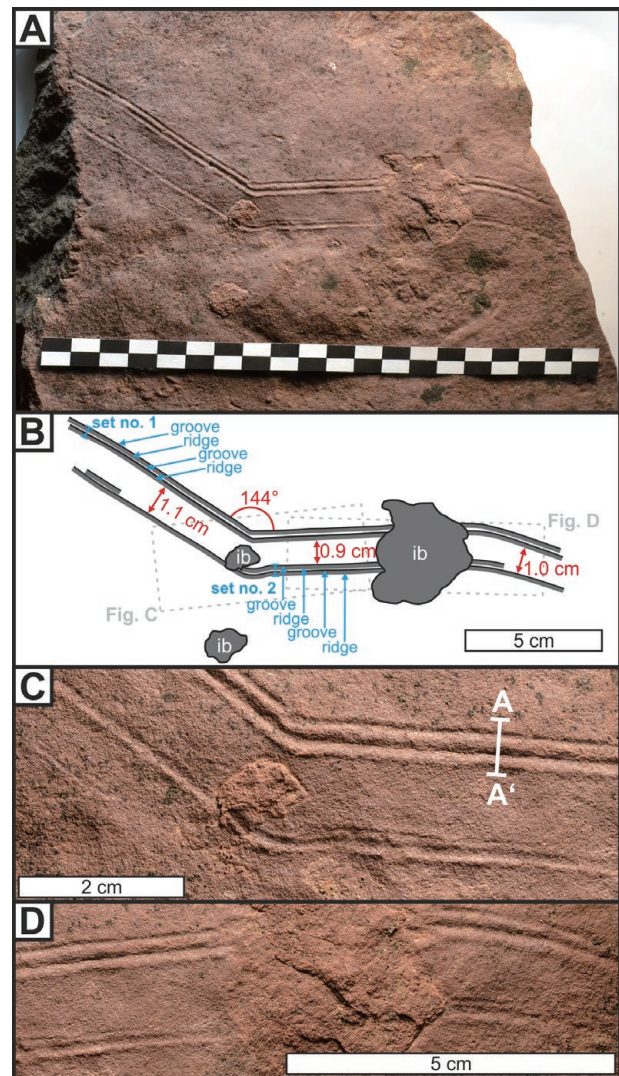


Fig. 3. Pictures of the sandstone slab with the enigmatic linear sedimentary structure. A: Overview showing the total size of the structure; scale bar 20x1 cm. B: Line drawing of the sedimentary structure and its measurement values; the structure consists of two linear sets that are each composed of concave grooves and convex ridges; assumed invertebrate burrows (‘ib’) are highlighted in grey. C–D: Close-ups on the parallel grooves and ridges around invertebrate burrows; for measurement values of the A–A’ cross section see Fig. 4.

the upper side of the slab. Composite length of the structure measures 19 cm; however, it is breaking off at the margins of the sandstone slab and, therefore, the sedimentary structure had been longer initially. The structure is preserved as concave epirelief on a distinct bedding plane that is almost completely composed of fine-grained sandstone rich in quartz and some alkali feldspar with a very low amount of smaller mica, whereas medium-sized grains occur in lesser extent.

The enigmatic sedimentary structure consists of two almost parallel linear sets, which are each composed of grooves and ridges (Fig. 3A). The spacing between these two sets measures 0.9–1.1 cm (Fig. 3B). The respective sets count one to two grooves and one to three ridges, one or two of them distinct. In set no. 2, the grooves are weaker developed than in set no. 1 or even absent locally (Fig. 3B). In well-preserved parts of a single set, it can be observed that the sand arrangement of a convex ridge results directly from the formation of its corresponding concave groove. In cross section, a groove has a similar width of about 0.5 mm as an adjacent ridge, but the ridges can be broader as well with up to ca. 2 mm width. The furrows cut max. about 200 μm into the surface, the ridges elevate up to ca. 180 μm above (Fig. 4). Set no. 2 comprises shallower furrows of around 160 μm depth and ridges of ca. 80 μm elevation. Each of the two sets is composed of both rather straight intervals and a slightly curved interval recognisable on the right side of Fig. 3A, B and D. A noticeable kink has an angle of 144° (Fig. 3B). Remarkably, this kink occurs in a corresponding position in both sets.

Finally, assumed invertebrate burrows (see ‘ib’ in Fig. 3B) of different diameters disturb either one set (Fig. 3C) or two sets (Fig. 3D) of grooves and ridges, while further assumed invertebrate burrows also occur outside the enigmatic sedimentary structure on the same bedding plane. The burrows do not penetrate the sandstone slab. The largest burrow (Fig. 3D) has a maximum diameter of ca. 3.7 cm and interrupts the grooves and ridges, the smaller with a diameter of ca. 1.1 cm at the kink of the linear sediment structure (Fig. 3C) shows a partly hidden continuation of the shallower groove. The contours of the burrows are irregular to rounded; their orientation seems to be perpendicular to the bedding plane. In contrast to the bedding plane with the sedimentary structure discussed here, the burrows are brighter in colour, are broken at their surface and contain a slightly coarser sand.

Discussion

Based on the authors’ field observations at the Bromacker, most invertebrate trace fossils had been primarily generated on thin layers (mud drapes) of clayey to fine-sandy siltstone that were later covered and preserved as convex hyporelief on the bottom side of the directly overlying fine-grained sand layer, whereas the primary underlying mud drapes (with the original concave epirelief of the invertebrate trace fossils) were usually not preserved in the surface outcrops. This does particularly account for the frequently occurring (invertebrate?) trace fossil *Tambica spiralis* as well as frequent abiotic sedimentary structures, such as rain drop imprints (see, e.g., Scholze, 2020: fig. 7). Certain intervals of the enigmatic sedimentary structure described herein show morphological similarities to certain invertebrate

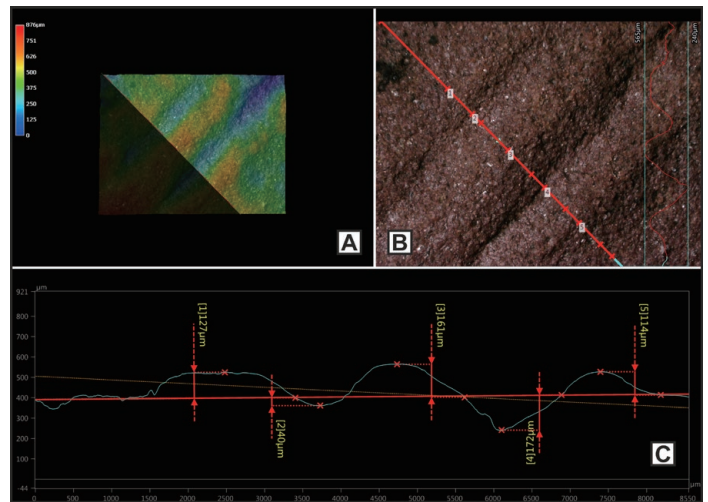


Fig. 4. A 3D-model of the linear sedimentary structures of set no. 1 positioned at cross section A–A’ in Fig. 3C. A. Colour coded elevation model. B. Cross section through the furrows and ridges of set no. 1. Numerals give reference points of measurements. C. Cross section of the linear structures in set no. 1 with elevation measurements referring to the slab surface around set no. 1.

traces that are composed of parallel grooves and ridges. Based on comparison to literature, both straight and curved arranged, two- to three-grooved traces of *Diplopodichnus* Brady 1947 might be like a single set interval of the enigmatic sedimentary structure described herein. However, parallel grooves separated by ridges as described by Brady (1947) do not correspond to the presence of two parallel sets that are composed of up to two grooves and ridges as it can be observed here (Fig. 3). Although (invertebrate?) trace fossil occurrences at the Bromacker had also been published by Müller (1969), Martens (1975, 1982), and Martens et al. (1981), none of the traces described therein compares to the enigmatic structure of the present study. Tetrapod tracks occur at the Bromacker as well (e.g., Voigt and Haubold, 2000); however, morphologies of tetrapod tail traces (e.g., Fichter, 1998: plates 14–16) are less complex than the groove/ridge assemblage that occurs parallel in two sets of the presented slab. Concluding, the sedimentary structure documented here is not a trace fossil by our opinion.

Several abiotic sedimentary structures from the Tambach Formation have been described previously either from the Bromacker section (e.g., Eberth et al., 2000; Martens, 2007) or from other localities of the Tambach Formation (e.g., Lützner, 1981) in the Tambach-Dietharz sedimentary basin. More recently, Scholze (2021) differentiated between syn-sedimentary (e.g., ripples) and post-sedimentary (e.g., tool marks) structures that can be found in the Tambach Sandstone Member at the Bromacker. Occurrences of parallel marks with several centimetres lengths and 1 mm widths were mentioned previously from the Bromacker but neither figured nor interpreted (Martens et al., 1981: p. 78). Partially, curved scratches figured by Scholze (2022: fig. 2) are morphologically similar to some intervals of the enigmatic sedimentary structure described in the present paper. In analogy to the formation mechanisms that are known from recent scratch circles (e.g., Müller, 1983), wind-induced movements of plants anchored by their roots may have caused circular to slightly curved scratches on its surrounding sandy bedding plane. Plant fossils occur at the Bromacker (e.g., Barthel and Rößler, 1994),

but their remains are often poorly preserved. There are also no indications that plant remains (e.g., root traces) are preserved on the herein reported rock slab bearing the enigmatic sedimentary structure.

The strict parallel arrangement of furrows points to a drag mark of an object pulled or pushed over the soft sediment. An object floating in water and touching the ground seems to be the most probable explanation of the structure reported herein. The similar sediment volumes lost in the furrows and accumulated in accompanying ridges point to a drag mark on soft sediment under water as well. The object had two pairs of sharply pointed structures causing the furrows on both sides of the double lineatures with a total width of at least 1.5 cm. These pointed structures had a distance of at least 2 mm in each pair. The object was moving almost straight changing the direction of movement at the kink, maybe caused by a gust of wind. A change in water currents could not cause such a sudden change of moving direction. The object should be rigid and distinctively larger than its appearing width drawn by the drag marks, because of the straight furrows and nearly constant distance between both sets of furrows. The sharp corner and constant width point to a stop of the drift and rotation of the object before the drift continued in another direction. Furthermore, a large area exposed to the wind should have been above the water surface to drive the continuous and mainly straight movement.

Conclusions and Call for Feedback

The groove and ridge components of the enigmatic sedimentary structure (Fig. 3) resemble an arrangement of sedimentary marks that might be characteristic for a drag mark caused by a drifting object in shallow water above soft sediment. The fact that groove/ridge assemblages occur in two parallel sets makes its designation as invertebrate trace fossil unlikely, although some intervals within a single set of the documented sedimentary structure show affinities to *Diplopodichnus*-like traces. The drifting object could have been a wooden plant fragment moved by wind. A carcass is unlikely, because it is not rigid enough for such a stable drag mark.

For further discussions of this enigmatic sedimentary structure, the authors kindly call the *Permophiles* readership to comment on the present report. Email feedbacks to the group of authors are highly welcome.

Acknowledgements

This present report contributes to the Bromacker Project (2020–2025), funded by the BMBF (German Federal Ministry of Education and Research). We thank all our project and cooperation partners for support in joint field activities and scientific discussions.

References

Barthel, M. and Rößler, R., 1994. Calamiten aus dem Oberrotliegend des Thüringer Waldes. - Was ist "Walchia imbricata"? Veröffentlichungen des Naturhistorischen Museums Schleusingen, v. 9, p. 69–80.
 Brady, L. F., 1947. Invertebrate Tracks from the Coconino Sandstone of Northern Arizona. *Journal of Paleontology*, v.

21, p. 466–472.
 Eberth, D. A., Berman, D., Sumida, S. S. and Hopf, H., 2000. Lower Permian terrestrial paleoenvironments and vertebrate paleoecology of the Tambach basin (Thuringia, Central Germany): The upland holy grail. *Palaios*, v. 15, p. 293–313.
 Fichter, J., 1998. Bericht über die Bergung einer 20 t schweren Fährtenplatte aus dem Tambacher Sandstein (Unter Perm) des Thüringer Waldes und erste Ergebnisse ichnologischer Studien. *Philippia*, v. 8, p. 147–208.
 Lützner, H., 1981. Sedimentation der variszischen Molasse im Thüringer Wald. *Schriftenreihe für geologische Wissenschaften*, v. 17, p. 1–217.
 Lützner, H., Andreas, D., Schneider, J. W., Voigt, S. and Werneburg, R., 2012. Stefan und Rotliegend im Thüringer Wald und seiner Umgebung. *Schriftenreihe der Deutschen Gesellschaft für Geowissenschaften*, v. 61, p. 418–487.
 Martens, T., 1975. Zur Taxonomie, Ökologie und Biostratigraphie des Oberrotliegenden (Saxon) der Tambacher Mulde in Thüringen. *Freiberger Forschungshefte C*, v. 309, p. 115–133.
 Martens, T., 1982. Zur Stratigraphie, Taxonomie, Ökologie und Klimaentwicklung des Oberrotliegenden (Unteres Perm) im Thüringer Wald (DDR). *Abhandlungen und Berichte des Museums der Natur Gotha*, v. 11, p. 33–57.
 Martens, T., 2007. Die Bedeutung der Sedimentmarken für die Analyse der Klimatelemente im kontinentalen Unterperm. *Zeitschrift für geologische Wissenschaften*, v. 35, p. 177–211.
 Martens, T., 2018. Scientific importance of the Fossilagerstätte Bromacker (Germany, Tambach Formation, Lower Permian) - vertebrate fossils. *Cuvillier Verlag, Göttingen*, 47 p.
 Martens, T., Schneider, J. and Walter, H., 1981. Zur Paläontologie und Genese fossilführender Rotsedimente - Der Tambacher Sandstein, Oberrotliegendes, Thüringer Wald. *Freiberger Forschungshefte C*, v. 363, p. 75–100.
 Martens, T., Berman, D. S., Henrici, A. C. and Sumida, S. S., 2005. The Bromacker Quarry - The most important locality of Lower Permian terrestrial vertebrate fossils outside of North America. *New Mexico Museum of Natural History and Science Bulletin*, v. 30, p. 214–215.
 Martens, T., Hahne, K. and Naumann, R., 2009. Lithostratigraphie, Taphozonien und Geochemie des Tambach-Sandsteins im Typusgebiet der Tambach-Formation (Thüringer Wald, Oberrotliegend, Unteres Perm). *Zeitschrift für geologische Wissenschaften*, v. 37, p. 81–119.
 Müller, A. H., 1956. Über problematische Lebensspuren aus dem Rotliegenden von Thüringen. *Berichte der Geologischen Gesellschaft in der Deutschen Demokratischen Republik für das Gesamtgebiet der geologischen Wissenschaften*, v. 1, p. 147–154.
 Müller, A. H., 1969. Über ein neues Ichnogenus (*Tambia* n.g.) und andere Problematica aus dem Rotliegenden (Unterperm) von Thüringen. *Monatsberichte der Deutschen Akademie der Wissenschaften zu Berlin*, v. 11, p. 922–931.
 Müller, A. H., 1983. Potentielle Pseudofossilien: 1. Scharrkreise und ähnliche Sedimentmarken durch wind- oder wasserbewegte Organismenreste. *Freiberger Forschungshefte C*, v. 384, p. 130–137.
 Roscher, M. and Schneider, J. W., 2006. Permo-Carboniferous

- climate: Early Pennsylvanian to Late Permian climate development of central Europe in a regional and global context. Geological Society, London, Special Publications, v. 265, p. 95–136.
- Schneider, J. and Gebhardt, U., 1993. Litho- und Biofaziesmuster in intra- und extramontanen Senken des Rotliegend (Perm, Nord- und Ostdeutschland). Geologisches Jahrbuch A, v. 131, p. 57–98.
- Schneider, J. W., Lucas, S. G., Scholze, F., Voigt, S., Marchetti, L., Klein, H., Opluštil, S., Werneburg, R., Golubev, V. K., Barrick, J. E., Nemyrovska, T., Ronchi, A., Day, M. O., Silantiev, V. V., Rößler, R., Saber, H., Linnemann, U., Zharinova, V. and Shen, S. Z., 2020. Late Paleozoic-early Mesozoic continental biostratigraphy – links to the Standard Global Chronostratigraphic Scale. Palaeoworld, v. 29, 186–238.
- Scholze, F., 2020. Die Paläotemperatur am Bromacker: Auswertung geochemischer Analysedaten zu kontinentalen Rotliegend-Sedimentgesteinen aus dem frühen Perm in Thüringen. Beiträge zur Geologie von Thüringen Neue Folge, v. 26, p. 253–272.
- Scholze, F., 2021. Sedimentology of the Bromacker (Thuringian Forest Basin, Germany; early Permian): Classification of sedimentary structures. Abstracts, 2nd DGGV Early Career Sedimentologist Meeting.
- Scholze, F., 2022. A digital photograph collection of sedimentary structures from the Bromacker reveals a new interesting specimen. Proceedings of the Kazan Golovkinsky Stratigraphic Meeting 2021, in press.
- Voigt, S. and Haubold, H., 2000. Analyse zur Variabilität der Tetrapodenfährte *Ichniotherium cottae* (Pohlig, 1885) aus dem Tambacher Sandstein (Rotliegend, Unter-Perm, Thüringen). Hallesches Jahrbuch für Geowissenschaften B, v. 22, p. 17–58.

Celebrating the 180th anniversary of the establishment of the Permian System – report on Kazan Golovkinsky Stratigraphic Meeting 2021

Joerg W. Schneider

Technical University Bergakademie Freiberg,
Institute of Geology, Dept. Palaeontology and Stratigraphy
Bernhard-von-Cotta-Str. 2, D-09599 Freiberg, Germany
Institute of Geology and Petroleum Technologies, Kazan (Volga Region) Federal University,
Kremlyovskaya str. 18, 420008 Kazan, Russia
E-mail: Joerg.Schneider@geo.tu-freiberg.de

Vladimir V. Silantiev

Institute of Geology and Petroleum Technologies, Kazan (Volga Region) Federal University,
Kremlyovskaya str. 18, 420008, Kazan, Russia
E-mail: vsilant@gmail.com

Milyausha N. Urazaeva

Institute of Geology and Petroleum Technologies, Kazan (Volga

Region) Federal University,
Kremlyovskaya str. 18, 420008, Kazan, Russia
E-mail: urazaeva.m.n@mail.ru

Veronika V. Zharinova

Institute of Geology and Petroleum Technologies, Kazan (Volga Region) Federal University,
Kremlyovskaya str. 18, 420008, Kazan, Russia
E-mail: nika_zharinova@mail.ru

Ilja Kogan

Technical University Bergakademie Freiberg,
Institute of Geology, Dept. Palaeontology and Stratigraphy
Bernhard-von-Cotta-Str. 2, D-09599 Freiberg, Germany
Institute of Geology and Petroleum Technologies, Kazan (Volga Region) Federal University,
Kremlyovskaya str. 18, 420008 Kazan, Russia
E-mail: i.kogan@gmx.de

The Kazan Golovkinsky Meeting 2021 was dedicated to the 180 anniversary of the establishment of the Permian System by the Scottish geologist Sir Roderick Impey Murchison in 1841, as a result of two excursions (1840, 1841) to Russia together with the French palaeontologist Édouard de Verneuil and the Baltic-German-Russian geologist and zoologist Alexander Graf von Keyserling (Silantiev et al., 2021). Invited by Tsar Nicholas I and starting from Moscow, they visited the outcrops of the Russian Platform in the surroundings of the towns Vladimir, Kazan, and Perm. In a first report on the results of the expedition, Murchison (1841a, b) introduced the name Permian for the observed widespread deposits of red-coloured conglomerates, sandstones, and siltstones, intercalated with marine carbonate rocks (Fig. 1; Sennikov, 2020; Benton and Sennikov, 2021).

Unfortunately, the meeting had to be held online because of the Covid pandemic and no excursion to the classical Permian outcrops near Kazan was possible. Nevertheless, numerous interesting talks and posters spanning the whole range of “Sedimentary Earth Systems: Stratigraphy, Paleoclimate, Geochronology, Petroleum Resources”, as reflected by the meeting subtitle, were presented to the international audience.

The abstract volume contains 70 contributions, 32 of which focus to the Permian (21 are in English). For the link to the abstract volume see below. Permian stratigraphy is discussed, e.g., by T.A. Grunt for the Permian Kapp Starostin Formation and the so far unresolved issues of its age and the correlation with Spitsbergen; by T.A. Leonova in the light of Permian ammonoid research and its importance for defining stratigraphic units and boundaries; and by E. Malysheva et al. who studied the Permian-Triassic boundary in marine deposits in the Barents Sea. L.G. Porokhovnichenko and co-authors discuss the age of a fossil flora from the Late Paleozoic of the Verkhoyanye region (NE Russia); new non-ammonoid cephalopods of the Early Permian Shakh-Tau reef in Bashkortostan are reported by A.Y. Shchedukhin; interesting Permian-Triassic non-marine bivalves from the volcanic succession of the Siberian Flood-Basalt Province are reported by V.V. Silantiev and co-authors; V.V. Zharinova describes conchostracans from the Late Permian and

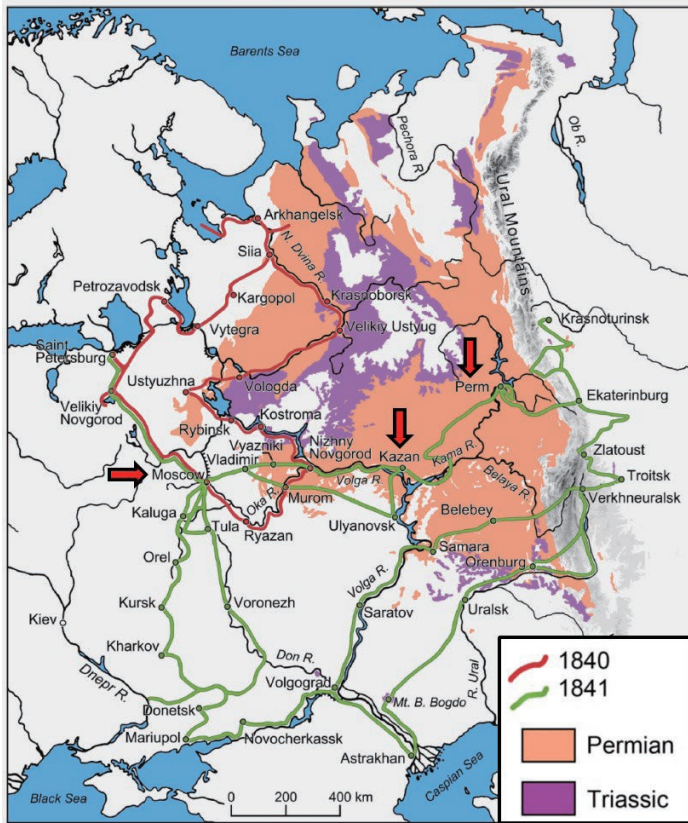


Figure 1. Routes of the expedition of Murchison across Russia in 1840 and 1841, modified from Benton and Sennikov (2021).

Early Triassic of Eastern Europe and Siberia; A.S. Bakaev et al. (in Russian) discuss the age of the non-marine fossil lagerstätte Kuyeda-Klyuchiki in the southern part of the Perm Krai, which is famous for fishes, amphibians, reptiles, insects, and plants; A.S. Biakov (in Russian) investigates the influence of the Permian mass extinction on inoceramid-like bivalves in NE Asia.

Several contributions address Permian fauna and flora. M.A. Naumcheva discusses indications of sexual dimorphism in smooth Permian freshwater ostracods from the Vladimir region of the East European Platform; A.S. Bakaev and I. Kogan report on the enigmatic discordichthyiform fishes endemic to the Middle and Late Permian of European Russia; B.I. Morkovin and co-authors describe recently discovered new localities of Lower Triassic terrestrial vertebrates, mainly temnospondyl labyrinthodonts, some reptiles and fishes, in the Komi Republic of Russia. Two contributions by N.S. Bukhman and L.M. Bukhman concern plant remains from the Middle Permian of the Volga-Ural region, and the abstract of D.N. Miftakhutdinova and R.V. Kutugin provide information on Permian-Triassic marine trace fossils of the Southern Verkhoyansk region in Yakutia in relation to the end-Permian crisis.

Abstracts dedicated to sedimentology and climatology of Permian non-marine deposits are that of F.A. Mouraviev and co-authors on paleosols from the upper Kazanian red beds of the Sentyak reference section in the Lower Kama region, which indicate a humid climate during the Kazanian; that the abstract of F. Scholze gives an overlook on the so far known sedimentary structures and invertebrate ichnia of the Lower Permian Tambach

Sandstone with the world-famous tetrapod skeleton and trackway lagerstätte at the Bromacker in the Thuringian Forest basin of Germany.

Two abstracts of A.M. Fetisova and co-authors (in Russian) deal with magnetostratigraphy at the PT-boundary in the Orenburg region as well as in the East European Platform in general. This is especially interesting in the light of the recently published new data on the magnetostratigraphy of the Meishan section in South China, challenging the traditional views on the magnetostratigraphic scale of the Permian-Triassic boundary interval (Zhang et al., 2021). The abstract of A.V. Chistyakova and co-authors reports on the geochronology and provenience of detrital zircons in Permian-Triassic transitional sections of the Orenburg region which point with a 530 Ma age on a source area in the Proto-Ural-Timan orogen.

Questions of economic geology are discussed in the contributions by I.R. Rakhimov on chromite-bearing Upper Permian (Kazanian) sandy sediments of the Southern Pre-Urals, and of N.N. Ryabinkina and co-authors on the Permian coals of the Pechora basin and their importance for the use of coal mine methane, liquid fuel, and for various components for the production of electrode products for metallurgy.

Apart from the recent research questions and results, in the opening talk of the meeting, V.V. Silantiev, J.W. Schneider and co-authors provided an outline of the history of the Permian System in Russia and Central Europe, comparing Murchison's (1841a,b) concept of the Permian and that of Marcou (1859) with his Dyas, as well as the opinions of leading European geologists of this time, such as Geinitz (1861). Within this contribution, V.K. Golubev pointed out that, with a marine lower and a terrestrial upper part, the Russian Permian represents a kind of "mirror image" of the West European Permian whose lower part is continental while the upper part is marine.

The absolute highlight of the meeting celebrating the 180th anniversary of the establishment of the Permian system in Russia was the announcement by the International Subcommittee on Permian Stratigraphy (SPS) secretary, Prof. Yichun Zhang, that the call to vote on the Global Stratotype Section and Point (GSSP) defining the base of the Artinskian Stage of the Permian System had been sent to the SPS Voting Members on 18th October 2021, just the day of the opening session of the Golovkinsky Stratigraphic Meeting 2021 (Fig. 2). The call was based on Chernykh et al. (2021) in Permophiles no. 71, August 2021. Right now, as the SPS vote for the base of the Artinskian Stage was in favour of the Dal'ny Tulkas section in the southern Urals of Russia, the proposal has been forwarded to ICS for voting and ratification.

After the conference, a special issue of the journal "Uchenye Zapiski Kazanskogo Universiteta" was published (<https://kpfu.ru/uz-eng-ns-2021-3.html>) that includes 15 articles, seven of which are dedicated to the Permian system. The abstract volume is available under <https://dspace.kpfu.ru/xmlui/bitstream/handle/net/166390/Golovkinsky-2021.pdf>.

We thank the international scientific organizing committee of the conference in 2021 and look forward to future collaboration. The next Golovkinsky stratigraphic meeting will be held in Kazan in autumn 2022, hopefully in person.

Standard Global Chronostratigraphic Scale			Age (Ma)	Russia				
System	Series	Stage		System	Series	Stage	Substage	Radioisotopic date
Triassic			*	Triassic				
Permian	Lopingian	Changhsingian	*	Upper (Tatarian)	Vyatkian	Upper	★253,95	
		Wuchiapingian	*			Lower		
	Guadalupian	Capitanian	*		Severodvinian	Upper		
		Wordian	*			Lower		
		Roadian	*	Kazanian	Upper			
		Kungurian	*		Lower			
	Cisuralian	Artinskian	*	Lower (Cisuralian)	Ufimian			
		Sakmarian	*		Kungurian			
		Asselian	*		Artinskian			
			*		Sakmarian	★290,50 ★291,10		
	*		Asselian	★296,69 ★298,05 ★298,49 ★299,22 ★298,92				
Carboniferous				Carboniferous				

Figure 2. Stratigraphic chart of the Permian System in European Russia. Standard Global Chronostratigraphic Scale and numerical ages for stage boundaries based on International Chronostratigraphic Chart v 2021/7 (Cohen et al., 2013). Ratified GSSPs are indicated by black asterisks. General Stratigraphic Scale of Russia is given according to the 'Stratigraphic Code of Russia' (2019) and Schneider et al. (2020). Stratigraphic positions of the radioisotopic ages are indicated by red asterisks: the Vyatkian radioisotopic date is according to Davydov et al. (2020); the Asselian and Sakmarian radioisotopic dates are according to Chernykh et al. (2020).

References

Benton, M. J., and Sennikov, A. G., 2021. The naming of the Permian System. *Journal of the Geological Society*: jgs2021-037 <http://dx.doi.org/10.1144/jgs2021-037>

Chernykh, V.V., Chuvashov, B.I., Shen, S.Z., Henderson, C.M., Yuan, D.X., and Stephenson, M.H., 2020. The Global Stratotype Section and Point (GSSP) for the base-Sakmarian Stage (Cisuralian Lower Permian). *Episodes*, v. 43, no.4, p. 961–979.

Chernykh, V.V., Henderson, C.M., Kutugin, R.V., Filimonova, T.V., Sungatullina, G.M., Afanasieva, M.S., Isakova, T.N., Sungatullin, R.Kh., Stephenson, M.H., Angiolini, L., and Chuvashov, B.I., 2021. Proposal for the Global Stratotype Section and Point (GSSP) for the base-Artinskian Stage

(Lower Permian). *Permophiles*, no. 71, p. 45–72.

Cohen, K. M., Finney, S. C., Gibbard, P. L., and Fan, J.X., 2013. The ICS International Chronostratigraphic Chart. *Episodes*, v. 36 p. 199–204. (Updated: <https://stratigraphy.org/ICSchart/ChronostratChart2021-07.pdf>)

Davydov, V.I., Arefiev, M.P., Golubev, V.K., Karasev, E.V., Naumcheva, M.A., Schmitz, M.D., Silantiev, V.V., Zharinova, V.V., 2020. Radioisotopic and biostratigraphic constraints on the classical Middle-Upper Permian succession and tetrapod fauna of the Moscow Syncline, Russia. *Geology*, v. 48, no. 7, p. 742–747. DOI: 10.1130/G47172.1

Geinitz, H.B., 1861. *Dyas oder die Zechsteinformation und das Rothliegende*. Heft 1. Die animalischen Ueberreste der Dyas. 130 pp., 23 pl., Verlag Wilhelm Engelmann (Leipzig).

Marcou, J., 1859. *Dyas et Trias: ou le nouveau grès rouge en Europe dans l'Amérique du Nord et dans l'Inde*, 63 pp.

Murchison, R.I., 1841a. *Observations géologiques sur la Russie*. (Lettre adressée à son Excellence Monsieur G. Fischer de Waldheim, Conseiller d'état actuel, etc. etc. etc.). *Bulletin de la Société des Naturalistes de Moscou*, v. 13, p. 901–909. (Also reprinted as: *Geological observations in Russia*. Mr. Murchison's letter to Mr. Fischer von Waldheim. *Gorniy Zhurnal*, no. 1841 (4, 11–12), p. 160–169 [in Russian])

Murchison, R.I., 1841b. First sketch of some of the principal results of a second geological survey of Russia, in a letter to M. Fischer. *Philosophical Magazine and Journal of Science*, Series 3, v. 19, p. 417–422.

Schneider, J.W., Lucas, S.G., Scholze, F., Voigt, S., Marchetti, L., Klein, H., Opluštil, S., Werneburg, R., Golubev, V.K., Barrick, J.E., Nemyrovska, T., Ronchi, A., Day, M.O., Silantiev, V.V., Rößler, R., Saber, H., Linnemann, U., Zharinova, V., and Shen, S.-Z., 2020. Late Paleozoic–early Mesozoic continental biostratigraphy — Links to the Standard Global Chronostratigraphic Scale. *Palaeoworld*, v. 29, p. 186–238.

Sennikov, A.G., 2020. The expedition of R.I. Murchison to Vyazniki town. *Priroda*, 2020, p. 55–69 [in Russian]. <https://doi.org/10.7868/S0032874X20100075>

Silantiev, V.V., Sennikov, A.G., Golubev, V.K., and Schneider, J.W., 2021. Outline of the history of the Permian System in Russia and Central Europe. *Golovkinsky Stratigraphic Meeting 2021, Sedimentary Earth Systems: Stratigraphy, Paleoclimate, Geochronology, Petroleum Resources and Sixth All-Russian Conference "Upper Paleozoic of Russia"*, October 18–22, 2021, Kazan, Russia, Abstract volume, p. 56–60.

Stratigraphic Code of Russia 2019, VSEGEI Press, St. Petersburg, 93 pp. [in Russian].

Zhang, M., Quin, H. F., He, K., Hou, Y.F., Zheng, Q.F., Deng, C.L., He, Y., Shen, S.Z., Zhu, R.X., and Pan, Y.X., 2021. Magnetostratigraphy across the end-Permian mass extinction event from the Meishan sections, southeastern China: *Geology*, v. 49, no. 11, p. 1289–1294, <https://doi.org/10.1130/G49072.1>.

Extended abstracts of the projects funded by SPS

Correlating the continental end-Permian biome collapse (Lopingian) across eastern Australia

Chris Mays

Background

The end-Permian extinction event (EPE; 252 million years ago) was the most extreme mass extinction in Earth's history (Stanley, 2016) and has been linked to rapid, planet-scale warming (Frank et al., 2021). The Australian stratigraphic record offers a globally unique opportunity to explore the severity and pace of terrestrial carbon sinks in response to this hyperthermal event across a broad latitudinal range. The Bowen, Sydney and Tasmania basins of eastern Australia collectively represent a ~2500 km north-south transect (Fig. 1) of contemporaneous continental depositional environments and floras during the Late Permian and Early Triassic (palaeolatitudes: ~45–75°S). From the Sydney Basin, our team has built a robust chronostratigraphic framework (Fig. 2), with which we have reconstructed the timeline of continental environmental and floral changes in the region (Fielding et al., 2019, 2021; Mays et al., 2020, 2021b; Vajda et al., 2020; McLoughlin et al., 2021). More recently, we have successfully applied our chronostratigraphic scheme to the Bowen Basin to constrain the ages of the climatic and floristic changes (Frank et al., 2021). The poorly studied Tasmania Basin is the highest palaeolatitude Permian–Triassic basin of Australia, and can provide chronostratigraphic and biogeographic links between Antarctica and the other basins of eastern Australia.



Hypotheses

'Polar refugium': Plant extinction patterns from other hyperthermal events (end-Triassic, mid-Cretaceous) have revealed a greater rate of relict taxon survival at high latitudes

(Bomfleur et al., 2018). As such, the degree of EPE floristic change was likely suppressed in the high-latitude Tasmania Basin, compared to the lower latitude Sydney & Bowen basins.

'Diachronous aridification': the change in climate that precipitated this change was likely time transgressive, with more severe drying occurring later at higher latitudes (McLoughlin et al., 1997). The plant fossil record should reflect this diachronous change, with more wetland taxa surviving into the post-EPE interval at higher latitudes.

Aim

The goal of this project is to compare the timing and amplitude of the end-Permian event and concurrent ecological collapse across eastern Australia. The collected samples will form the basis for the highest latitude region of a broad, ~2500 km north-south transect. This study will: 1, constrain the chronostratigraphy of the uppermost Permian and Lower Triassic of the Tasmania Basin; 2, test the 'polar refugium' and 'diachronous aridification' hypotheses outlined above; and 3, facilitate further correlations of uppermost Permian and lowermost Triassic strata between localities across greater Gondwana (Antarctica, India, southern Africa).

Methods

Broad data trends of the Upper Permian and Lower Triassic will be revealed by moderate resolution (1–10 m) bore core sampling in the Tasmania Basin, Tasmania (cores: MPT-3, TDM Bothwell East). Preliminary data from these cores have constrained the target intervals, and ensured that the preservation quality of the spore-pollen assemblage is sufficient for correlation. Higher-resolution (1–10 cm) sampling of these cores and the outcrop successions at Cygnet and Adventure Bay (Fig. 1B), will target the EPE and early post-extinction intervals. Cores are held at the publicly accessible Mornington Core Library (Mineral Resources Tasmania, MRT).

Field and core library data collection will include lithological logs and sediment sampling for: palynomorphs, palynofacies, plant meso-/macrofossils, stable isotopes (C, N), geochemical climate proxies (chemical index of alteration) and radiogenic isotope ages (volcaniclastic facies will be especially targeted for

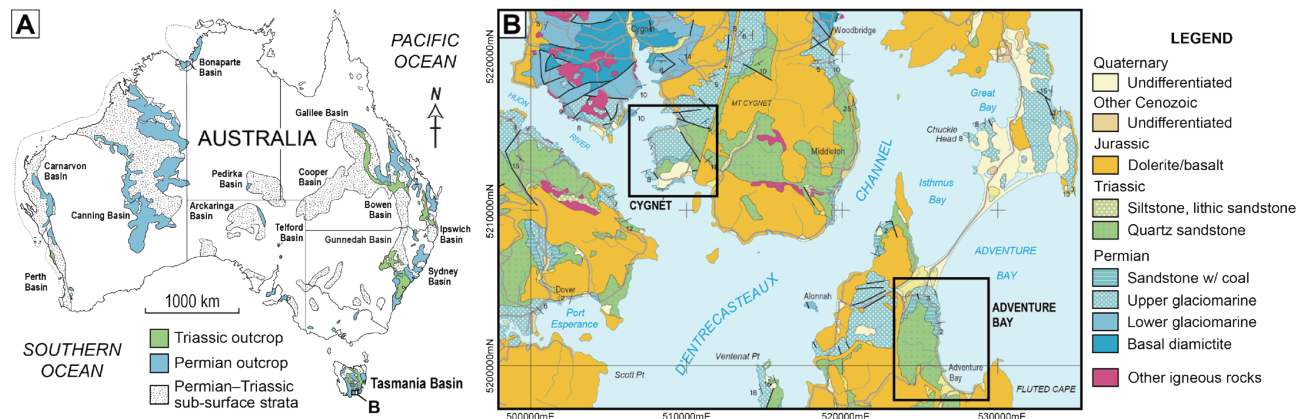


Fig. 1. Geological maps of Australia, indicating the distributions of Permian and Triassic strata. A, Australian basins with Permian and/or Triassic strata, from Mays et al. (2021a). B, Detail of the southern Tasmania Basin, including the target outcrop localities, from Forsyth et al. (2005).

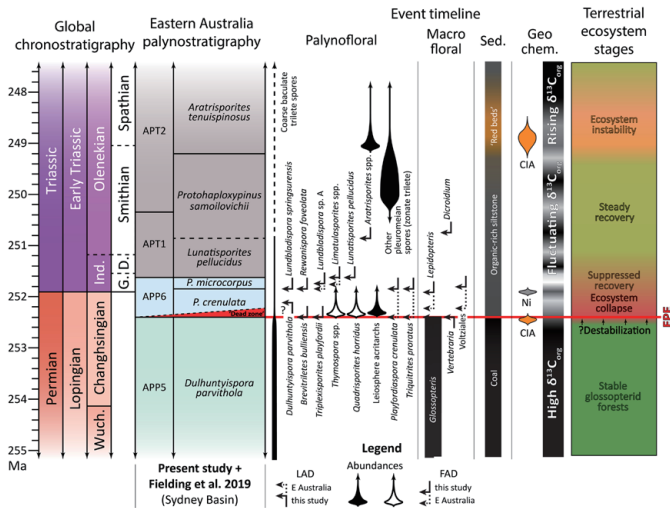


Fig. 2. Timeline of Permian–Triassic floral and palynological bioevents, geochemical and sedimentological features, as recorded from eastern Australian basins. FAD—first appearance datum; LAD—last appearance datum; CIA—chemical index of alteration; sed.—sedimentary facies. From Mays et al. (2020).

high precision CA-IDTIMS dating to provide the optimal age constraints on the succession). The severity of floral overturn will be measured by quantitative palynology (abundance, concurrent last appearances), palynofacies and macrofloral assemblage data.

References

Banks, M.R. and Naqvi, I.H., 1967. Some formations close to the Permo-Triassic boundary in Tasmania. *Papers and Proceedings of the Royal Society of Tasmania*, v. 101, p. 17–30.

Fielding, C.R., Frank, T.D., Vajda, V., McLoughlin, S., Mays, C., Tevyaw, A.P., Winguth, A., Winguth, C., Nicoll, R.S., Bocking, M. and Crowley, J.L., 2019. Age and pattern of the southern high-latitude continental end-Permian extinction constrained by multiproxy analysis. *Nature Communications*, v. 10, p. 385.

Fielding, C.R., Frank, T.D., Tevyaw, A.P., Savatic, K., Vajda, V., McLoughlin, S., Mays, C., Nicoll, R.S., Bocking, M. and Crowley, J.L., 2021. Sedimentology of the continental end-Permian extinction event in the Sydney Basin, eastern Australia. *Sedimentology*, v. 68, p. 30–62.

Forsyth, S.M., Clarke, M.J., Calver, C.R., Everard, J.L., McClenaghan, M.P., Corbett, K.D. and Vicary, M.J., 2005. *Geology of Southeast Tasmania, Digital Geological Atlas 1:250 000 Scale Series 2012.1*. MRT, Hobart.

Frank, T.D., Fielding, C.R., Winguth, A.M.E., Savatic, K., Tevyaw, A., Winguth, C., McLoughlin, S., Vajda, V., Mays, C., Nicoll, R., Bocking, M. and Crowley, J.L., 2021. Pace, magnitude, and nature of terrestrial climate change through the end Permian extinction in southeastern Gondwana. *Geology*, v. 49, p. 1089–1095.

Mays, C., Vajda, V., Frank, T.D., Fielding, C.R., Nicoll, R.S., Tevyaw, A.P., McLoughlin, S., 2020. Refined Permian–Triassic floristic timeline reveals early collapse and delayed recovery of south polar terrestrial ecosystems. *GSA Bulletin* v. 132, p. 1489–1513.

Mays, C., Vajda, V., McLoughlin, S., 2021a. Permian–Triassic non-marine algae of Gondwana—distributions, natural affinities and ecological implications. *Earth-Science Reviews*, v. 212, p. 103382.

Mays, C., McLoughlin, S., Frank, T.D., Fielding, C.R., Slater, S.M., Vajda, V., 2021b. Lethal microbial blooms delayed freshwater ecosystem recovery following the end-Permian extinction. *Nature Communications*, v. 12, p. 5511.

McLoughlin, S., Lindström, S., Drinnan, A.N., 1997. Gondwanan floristic and sedimentological trends during the Permian–Triassic transition: new evidence from the Amery Group, northern Prince Charles Mountains, East Antarctica. *Antarctic Science*, v. 9, p. 281–298.

McLoughlin, S., Nicoll, R.S., Crowley, J.L., Vajda, V., Mays, C., Fielding, C.R., Frank, T.D., Wheeler, A., Bocking, M., 2021. Age and paleoenvironmental significance of the Frazer Beach Member—A new lithostratigraphic unit overlying the end-Permian extinction horizon in the Sydney Basin, Australia. *Frontiers in Earth Science*, v. 8, p. 600976.

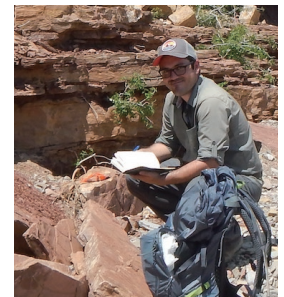
Stanley, S.M., 2016. Estimates of the magnitudes of major marine mass extinctions in earth history. *Proceedings of the National Academy of Sciences*, v. 113, E6325–E6334.

Vajda, V., McLoughlin, S., Mays, C., Frank, T., Fielding, C.R., Tevyaw, A., Lehsten, V., Bocking, M., Nicoll, R.S., 2020. End-Permian (252 Mya) deforestation, wildfires and flooding—an ancient biotic crisis with lessons for the present. *Earth and Planetary Science Letters*, v. 529, p. 1089–1095.

Correlation between the Cisuralian successions of the Robledo Mountains (New Mexico) and the Carnic Alps (Austria) integrating conodont and foraminifer biostratigraphy

Daniel Calvo Gonzalez

Department of Geoscience,
University of Calgary, Calgary,
Alberta T2N 1N4, Canada
Email: dcalvogo@ucalgary.ca



Introduction

New biostratigraphic data from the Robledo Mountains and Apache Dam formations of New Mexico and from the Lower Permian succession of the Carnic Alps, have allowed us to revisit the age interpretation of Cisuralian strata in these two locations (Fig. 1). Newly published conodont biostratigraphic data, updated taxon identifications and relevant globally distributed foraminifer taxa have been used to further support the new age interpretations.

Robledo Mountains

The upper Paleozoic succession in the Robledo Mountains, New Mexico, is composed of cyclic and non-cyclic, mixed limestone-sandstone strata of the Horquilla, Shalem Colony, Community Pit, Robledo Mountains, and Apache Dam

formations. The Shalem Colony, Community Pit, Robledo Mountains, and Apache Dam formations comprise the Hueco Group, which conformably overlies the Horquilla Formation. The current age interpretation of that succession is mostly based on fusulinid and small foraminifer biostratigraphy, and rarely on conodont data. The foraminifer and conodont assemblages of the Horquilla Formation are predominantly characteristic of the Pennsylvanian (Bashkirian-Gzhelian or Morrowan-lower Wolfcampian). A few age diagnostic conodont specimens were previously retrieved from the mid-lower and uppermost intervals of the Horquilla Formation in the Robledo Mountains section (Krainer et al., 2015). In the uppermost part of the formation, specimens include *S. binodosus*, *S. elongatus*, *S. conjunctus*, and possibly *S. wabaunensis* (Krainer et al., 2015). Due to taxonomic revisions specimens labelled 1, 4, and 5 on Figure 25 of Krainer et al. (2015) as *S. conjunctus* and *S. binodosus* are here reinterpreted as *S. longus*; specimen labelled 2 originally interpreted as *S. conjunctus* is here reinterpreted as *S. grandis*; and specimen labelled 6 originally named *S. binodosus* is here interpreted as *S. paraisolatus* (C. Henderson 2021, pers. comm., 5 January 2021). This conodont assemblage is characteristic of the early Asselian *Streptognathodus glenisteri* Zone (Henderson, 2018), and hence indicates that the contact between the Horquilla and the overlying Shalem Colony formations in the Robledo Mountains is earliest Asselian. The conodont assemblage of the Shalem Colony Formation is limited to single occurrences of *S. invaginatus* and *S. elongatus* (Kozur and LeMone, 1995; Krainer and Lucas, 1995). Kozur and LeMone originally identified *S. invaginatus* and *S. elongatus* (currently identified as *S. longus*) and *Sweetognathus expansus* from strata that they interpreted to belong to the upper Hueco Formation in a section located in NW1/4 NW1/4, 30 within the Prehistoric Trackways National Monument. However, these taxa are interpreted as early Asselian indicating that the formation is misidentified because the upper Hueco Formation is much younger. Currently, these strata are interpreted to be equivalent to the lower Shalem Colony Formation as shown by Krainer et al. (2015). Therefore, we infer that the lower Shalem Colony Formation is of early Asselian age based on the presence of *S. invaginatus*, *S. longus* and *Sw. expansus*. Several conodont species were reported from the lower and middle sections of the overlying Robledo Mountains Formation. Kozur and LeMone (1995) identified specimens from two brachiopod- and crinoid-

rich samples, sample A and B respectively. Sample A yielded conodonts identified as *Sw. primus* transitional to *Sw. merrilli posterus*, *Sw. primus*, and *Sw. merrilli posterus*. Sample B yielded elements from *Sw. merrilli posterus* transitional to *Sw. merrilli merrilli* and *Sweetognathus* n. sp. B, which we interpret as the real *Sweetognathus whitei* (Fig. 8.13 of Kozur and LeMone). These two samples were collected at a level correlative to the crinoid- and brachiopod-rich limestone beds observed in our Branson Canyon section (Fig. 2). Additional specimens in Lucas et al. (1995) were identified by Bruce Wardlaw as *Sw. expansus*, *Hindeodus excavatus*, and *Neostreptognathodus clarki* from the middle interval of the Robledo Mountains Formation (named Robledo Mountains Member at the time); these specimens were not illustrated. No conodont occurrences have previously been reported in the overlying Apache Dam Formation, the youngest unit of the Hueco Group in the Robledo Mountains.

In this study, three limestone samples collected in the Robledo Mountains Formation and two in the Apache Dam Formation at the Branson Canyon section yielded age-diagnostic conodonts. The stratigraphically lowest sample (#286) is a packstone rich in echinoids and large bivalves located at 55.4 m (Fig. 2) that yielded *Sweetognathus* aff. *merrilli*, *Sweetognathus posterus*, *Sweetognathus posterus* transitional to *Sw. binodosus*, and *Hindeodus* sp. (Fig. 3.2-3.6). We raise Kozur's subspecies to species rank as *Sw. posterus* because it may not be related to *Sw. merrilli*. The sample is located near the top of the first crinoid-rich interval in the section immediately below the fourth red bed of the formation. The second sample (#274) was collected at an outcrop ~ 1.5 km north of Branson Canyon. The sampled interval is equivalent to red bed 4 of the formation (Fig. 2). This sample yielded a broken fragment of *Mesogondolella* sp., interpreted as the deepest water specimen in the section (Fig. 3.1.) The third sample (#295) was retrieved from a brachiopod- and echinoderm-rich limestone bed located on the mesa immediately north of where the Branson Canyon section was measured. The limestone bed is equivalent to the brachiopod- and crinoid-rich limestone beds found in the Branson Canyon section between 81.6 and 85 m (Fig. 2). This sample yielded *Sweetognathus sulcatus* (Fig. 3.8), *Hindeodus* sp. (Figure 3.7, 3.9), *Sweetognathus posterus* transitional to *Sw. binodosus* (Fig. 3.10), and *Sw. posterus* (Fig. 3.11-3.12). Sample 4 (#296) from the Apache Dam Formation was collected from thin marl interbeds composed of a heterozoan fauna (bryozoans, echinoderms, brachiopods, and ostracods) observed approximately 20 m above the formation base. This sample yielded *Sweetognathus* cf. *anceps* (Fig. 2; Fig. 3.15). Sample 5 (#294) was collected from a limestone located in the uppermost interval of the formation at Branson Canyon, approximately 28 m above the formation base. This sample yielded a juvenile *Diplognathodus stevensi* (Fig. 3.13) and juvenile *Sweetognathus* sp. (Fig. 2; Fig. 3.14).

Samples #286 and #295 yield conodonts that we would refer to the Sakmarian in general agreement with Kozur and LeMone (1995) who suggested a Sterlitamakian (upper Sakmarian) age for a comparable fauna. Based on this evidence, we provisionally place the Asselian-Sakmarian boundary interval in proximity to the first occurrence of *Sweetognathus sulcatus* in the Robledo Mountains Formation. Therefore the Shalem Colony

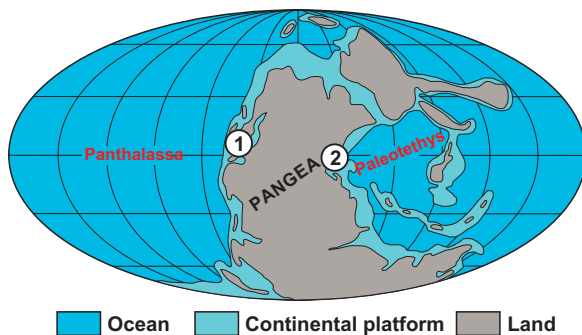


Fig. 1. Paleogeographic map showing the location of the measured sections during the Early Permian. 1. Robledo Mountains (New Mexico); 2. Carnic Alps (Austria).

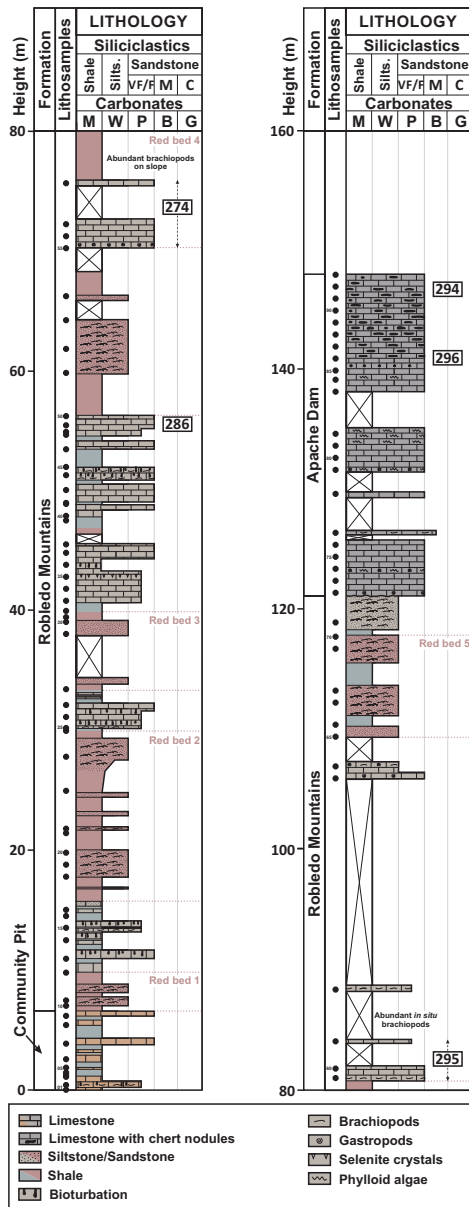


Fig. 2. Branson Canyon section measured in the Robledo Mountains showing the location of samples where conodont specimens were found. Siliciclastic grain sizes: VF/F=Very fine-fine; M=Medium; C=Coarse; Dunham carbonate classification: M=Mudstone; W=Wackestone; P=Packstone; B=Boundstone; G=Grainstone.

and Community Pit formations are interpreted to be Asselian age. The occurrence of *Sw. posterus* transitional to *binodosus* further supports a Sakmarian age. The occurrence of a specimen with a well-developed pustulose central ridge (Fig. 3.15) in the heterozoan marl beds of the Apache Dam is comparable to a specimen named by Chernykh (2006) as *Sweetognathus anceps* (his plate XIV, fig.14) from the basal Artinskian *Sw. asymmetricus* Zone of Russia. We refer to it as *Sweetognathus cf. anceps* and interpret it to be late Sakmarian-early Artinskian. We provisionally place the Sakmarian-Artinskian boundary near the contact between the Robledo Mountains and the Apache Dam formations. The exact location of the stage boundary may correspond to a maximum flooding surface within a third-order

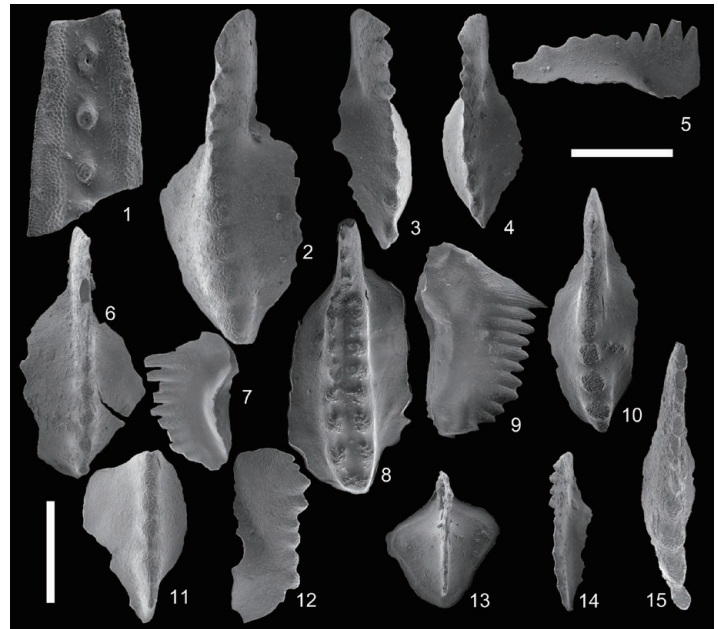


Fig. 3. Plate of conodonts found in the Branson Canyon section in the Robledo Mountains. Robledo Mountains Formation: 3.1. *Mesogondolella* sp., sample 274, ~ 70-75 m interval; 3.2-3.6. *Sweetognathus posterus*, sample 286, 55.4 m; 3.7. *Hindeodus* sp., sample 295, ~ 81.6-85 m; 3.8. *Sweetognathus sulcatus*, sample 295, ~ 81.6-85 m; 3.9. *Hindeodus* sp., sample 295, ~ 81.6-85 m; 3.10. *Sweetognathus posterus* transitional to *Sw. binodosus*, sample 295, ~ 81.6-85 m; 3.11-3.12. *Sweetognathus posterus*, sample 295, ~ 81.6-85 m; Apache Dam Formation: 3.13. *Diplognathodus stevensi*, sample 294, 146.7 m; 3.14. *Sweetognathus* sp., sample 294, 146.7 m; 3.15. *Sweetognathus cf. anceps*, sample 296, 140.7 m. Scale bar is 200 μ m.

sequence represented by the Apache Dam Formation, comparable to the stage boundary reported by Beauchamp et al. (submitted for publication) in the Butte Basin, NE Nevada, within the Buckskin Mountain Formation. This interpretation would be further supported by the presence of *Diplognathodus stevensi* in the Apache Dam Formation at Branson Canyon.

The newly interpreted age of the formations in the Robledo Mountains is further supported by key small foraminifer taxa. An Asselian age is indicated by the presence of *Geinitzina postcarbonica* from the basal Community Pit Formation to lower half of the Robledo Mountains Formation (Lucas et al. 2015). This taxon is reported from the upper Nansen Formation in Arctic Canada, currently interpreted as middle-late Asselian based on conodont faunas (Pinard and Mamet, 1998; Beauchamp et al., 2021), and in the Kapp Duner Formation in offshore Arctic Norway, also interpreted as Asselian (Groves and Wahlman, 1997). Additionally, this taxon is also found in the lower Chihisia Formation (Hua-Zhang and Erwin, 2002). *Amphoratheca* sp., reported from the middle section of the Robledo Mountains Formation by Lucas et al. (2015), is present in the Crouse limestone of Kansas (Groves and Boardman, 1999) as part of the Crouse cyclothem, interpolated to be 296.6-296.2 Myr (Henderson, 2018). The Crouse Limestone includes a middle Asselian conodont assemblage, including *Sweetognathus expansus* and *Streptognathodus constrictus* (Boardman et al., 2009). Other occurrences of *Amphoratheca* (*A. robusta* and *A. iniqua*) include Asselian strata of the Belcher Channel and Nansen formations in the Canadian Arctic (Pinard and Mamet,

1998), and *A. iniqua* in mid-Asselian strata of the Kapp Duner Formation (Groves and Wahlman, 1997). *Tezaquina clivuli* is found in the mid-upper interval of the Shalem Colony Formation (Lucas et al. 2015). This taxon is also found in Asselian and older strata from the Nansen, Belcher Channel, and Mount Bayley formations in the Canadian Arctic (Pinard and Mamet, 1998), and in Asselian and Gzhelian strata of the Kapp Duner Formation (Groves and Wahlman, 1997). *Nodosinelloides longa* is present in the upper Horquilla, Shalem Colony (?), and lowermost Community Pit formations (Krainer et al., 2015; Lucas et al., 2015). In the Canadian Arctic, it ranges between Kasimovian and Asselian strata of the upper Nansen, Belcher Channel, and Mount Bayley formations (Pinard and Mamet, 1998). This taxon is also reported from the Asselian strata of the Sezym Formation in the northern Urals (Inkina, 2019). Finally, *Climacammina* sp. is present in the Shalem Colony Formation (Lucas et al., 2015), in the middle-upper Asselian of Norway (Groves and Wahlman, 1997), in the Asselian cyclothems of Kansas (Groves and Boardman, 1999), and in Bashkirian-Asselian strata of the Nansen Formation in the Canadian Arctic including *C. magna*, *C. procera*, *C. durabilis*, *C. rara*, and *C. grandis* (Pinard and Mamet, 1998).

Carnic Alps

Upper Paleozoic rocks in the Carnic Alps include cyclic strata of the Pennsylvanian Auernig Group, cyclic to non-cyclic strata of the Lower Permian Rattendorf Group, and non-cyclic deposits of the Lower Permian Trogkofel Group. Of relevance to this study, the Lower Permian Rattendorf and Trogkofel groups are composed of the Schulterkofel, Grenzland, Zweikofel and Zottachkopf formations, and of the Trogkofel and Goggau limestones, respectively (Krainer et al., 2019). The Schulterkofel, Grenzland, and Zweikofel formations are interpreted to record glacio-eustatic sea-level changes in the form of cyclothems, whereas the Zottachkopf, Trogkofel Limestone, and Goggau Limestone are widely considered to be non-cyclic. Conodont occurrences in the Cisuralian succession of the Carnic Alps are rare despite great efforts to sample these strata in the quest to retrieve age diagnostic microfauna (Forke, 1995; Forke, 2002; Krainer and Schaffhauser, 2012 and references therein). A limited number of conodonts were retrieved from the shallow water facies of the Zweikofel and Zottachkopf formations, and from the reefal and “Sonderfazies” (basin facies) within the massive limestone of the overlying Trogkofel Formation at the Zweikofel massif. Forke (2002) and Davydov et al. (2013) illustrated the same conodont specimen in two different stratigraphic levels in the lower interval of the Zweikofel Formation or the uppermost interval of the Grenzland Formation. The specimen illustrated by these authors is characterized by the absence of a longitudinal connecting ridge, high-standing, dumbbell-shaped nodes, and narrow grooves. It was identified as *Sweetognathus anceps* by Davydov et al. (2013) and as *Sweetognathus* sp. aff. *whitei* by Forke (2002). Davydov et al. (2013) position the specimen in unit 9 of the upper Grenzland Formation whereas Forke (2002) illustrates the same element in the lower Zweikofel Formation some 30 m above the Grenzland-Zweikofel contact, both at the type section of the Zweikofel Formation. It is

noteworthy that a similar specimen was illustrated by Read and Nestell (2019a) from the upper member of the Riepe Spring Limestone at Spruce Mountain, Nevada, in an interval that also contained *Eoparafusulina linearis*, *Pseudoschwagerina robusta*, *Alaskanella* sp., and *Schwagerina glassensis*. Read and Nestell (2019a) named this Nevadan specimen *Sweetognathus binodosus*. In our study, the specimen illustrated by Davydov et al. (2013) and Forke (2002) is reinterpreted as *Sweetognathus binodosus* transitional to *Sw. anceps*. The overlying lower interval of the non-cyclic Zottachkopf Formation yielded diagnostic specimens at the Trogkar section (Forke 1995). The well-bedded, grey to red-coloured limestone strata in this locality contain elements of *Sweetognathus* aff. *whitei*, *Sweetognathus inornatus*, and *Neogondolella* cf. *bisselli*. Forke (1995) also reported *Sweetognathus* sp. and *Diplognathodus expansus* in the overlying, massive to bedded strata of the Trogkofel Formation. After examination of the illustrated specimens reported by Forke at Trogkar, the authors herein agree with the interpretation of the lower occurrence of *Sw. aff. whitei* in the section as *Sw. whitei*, however the second occurrence of *Sweetognathus* aff. *whitei*, *Sweetognathus inornatus*, and *Diplognathodus expansus* are reinterpreted as *Sweetognathus anceps*, *Sweetognathus binodosus*, and *Diplognathodus stevensi*, respectively. The Trogkofel Formation also yielded a juvenile form of *Neostreptognathodus* cf. *pequopensis* in the marl facies (referred to as “Sonderfazies” or basin facies) at the type section of the Zweikofel Formation at Zweikofel massif (Forke 2002). Similar forms of the latter species are also identified as a homeomorph of *N. pequopensis* in the upper Riepe Springs of Nevada (Read and Nestell, 2018).

The reinterpretation of the ages of this Cisuralian succession in the Carnic Alps is further supported by key small foraminifer taxa found in several locations where successions abundant in conodont and foraminifer biostratigraphic data provide a strong age diagnosis. The Asselian age of the Zweikofel Formation and possibly of the lowermost Zottachkopf Formation is further supported by the presence of *Biwaella omiensis* in the upper interval of the Zweikofel Formation at Zweikofel massif, and in the red-coloured limestone beds of the lowermost Zottachkopf Formation at locality “Höhe 2004” (Davydov et al., 2013). A different species of this genus, *Biwaella americana*, is present in the lower upper member of the Riepe Spring Limestone in Nevada (Read and Nestell, 2019a). This occurrence is significant because it occurs below the first occurrence of *Sweetognathus binodosus*, *Sweetognathus anceps*, and *Eoparafusulina linearis* in the Riepe Spring Limestone. These taxa are considered biomarkers for the Sakmarian and therefore the *B. americana* found in this locality is older and likely Asselian. *Biwaella* sp. is also present in the upper Nansen Formation immediately below the cyclic lowermost Raanes Formation in the Canadian Arctic (Beauchamp et al., 2021). The age of the lowermost Raanes Formation is interpreted as late Asselian due to the first appearance of *Mesogondolella dentiseparata*. Higher up in the lower Raanes Formation, the first appearance of *Mesogondolella monstra* and *Sweetognathus binodosus* suggests the Asselian-Sakmarian contact occurs immediately above the last cyclothem observed in the formation (Beauchamp et al.,

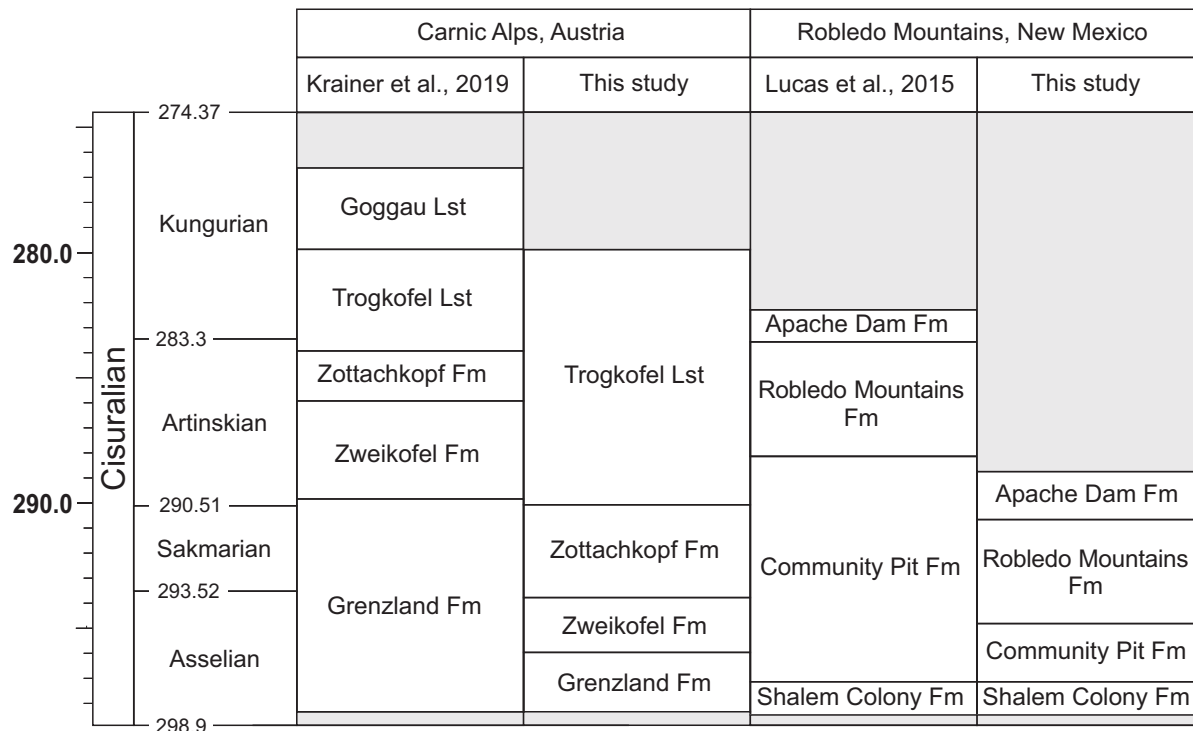


Fig. 4. Stratigraphic chart showing the previous and our current age interpretations of Cisuralian formations in the Robledo Mountains, New Mexico, and the Carnic Alps, Austria.

2021). Another species of *Biwaella*, *B. provecta* is present in the Asselian uppermost Maping Formation in the Tieqiao section in Laibin (Shen et al., 2007). This occurrence is reported from an interval approximately 40 m below the contact with the Chihhsia Formation, currently interpreted as Sakmarian (Sun et al., 2017). This is in accordance with the proliferation of this genus across the Tethys and Panthalassa oceans during the Asselian and Sakmarian reported by Read and Nestell (2019b). *Cribrogenerina gigas* was reported from the Zweikofel and Zottachkopf formations in the Carnic Alps (Krainer et al., 2019). This taxon was also identified in the Nansen and Mount Bayley formations in the Canadian Arctic (Pinard and Mamet, 1998) and in offshore Norway by Groves and Wahlman (1997). *Amphorateca* sp. is present in the Carnic Alps in the Zweikofel Formation (Krainer et al., 2019). This taxon is also reported in the Nansen Formation in the Canadian Arctic, and in the Crouse and Wreford cyclothem of Kansas, interpreted to be 296.6-296.2 and 295.8-295.4 My, respectively (Henderson 2018). Lastly, *Tezaquina* cf. *clivuli* is present in the Auernig Formation and in the Zweikofel Formation (Krainer et al., 2019). As mentioned previously, this taxon is also found in Asselian and older strata in the Canadian Arctic and Norway.

Based on this evidence, the Asselian-Sakmarian boundary is interpreted as occurring in proximity to the first occurrence of *Sweetognathus binodosus* and above the only occurrence of *Sweetognathus whitei* in the lowermost Zottachkopf Formation at locality "Höhe 2004". Therefore, the Schulterkofel, Grenzland, and Zweikofel formations are herein reinterpreted as Asselian (Fig. 4). The absence of conodont biostratigraphic data from the Zottachkopf, aside from those reported at locality "Höhe 2004", inhibits the interpretation of the ages of this formation and the

Trogkofel Formation. Based on the presence of *Diplognathodus stevensi* and *Neostreptognathodus* cf. *pequopensis* in the lower Trogkofel Formation, the Sakmarian-Artinskian boundary interval is placed near the base of this formation at Trogkar and the Zweikofel massif.

Conclusions

In conclusion, key foraminifer taxa, new conodont data, and the reinterpretation of previously collected conodont specimens suggest that the Lower Permian successions of the Robledo Mountains and the Carnic Alps may be older than currently correlated. In the Robledo Mountains, the Asselian-Sakmarian boundary interval is reinterpreted to be in proximity to the first occurrence of *Sweetognathus sulcatus* in the Robledo Mountains Formation. We interpret the lower half of the Robledo Mountains, Shalem Colony, and Community Pit formations as Asselian. The Sakmarian-Artinskian boundary is herein placed at the base or within the lower interval of the Apache Dam Formation (Fig. 4). In the Carnic Alps, the Grenzland and Zweikofel formations are reinterpreted to be Asselian instead of Asselian-Sakmarian and lower-middle Artinskian, respectively. In this study, the Asselian-Sakmarian boundary is placed within the lowermost Zottachkopf Formation at locality "Höhe 2004". The Zottachkopf is here interpreted to be latest Asselian-late Sakmarian. The lowermost Trogkofel Formation at Trogkar and the Zweikofel massif is here interpreted to be latest Sakmarian-earliest Artinskian (Fig. 4).

Acknowledgments

Foremost, the author would like to thank PhD co-supervisors Drs. Benoit Beauchamp and Charles M. Henderson for their support and guidance in the field, their devotion and generous

time providing insightful discussions and generating new ideas, and for editing of this abstract. This project was funded by co-supervisors' Discovery Grants provided by the Natural Science and Engineering Research Council of Canada (NSERC). The Subcommittee on Permian Stratigraphy also provided generous financial support. Additional funding support was provided by the University of Calgary. The author also thanks Dr. Spencer Lucas for his aid in the field and subsequent discussions, and Drs. Lucia Angiolini and Yichun Zhang for their assistance during the funding application process and submission of this abstract.

References

- Beauchamp, B., Calvo Gonzalez, D., Henderson, C.M., Baranova, D.V., Wang, H.Y. and Pelletier, E. 2021 (in press). Late Pennsylvanian–Early Permian tectonically-driven stratigraphic sequences and carbonate sedimentation along northern margin of Sverdrup Basin (Otto Fiord Depression), Arctic Canada. In Henderson, C.M., Ritter, S. and Snyder, W.S., eds. Late Paleozoic Tectonostratigraphy and Biostratigraphy of Western Pangea. SEPM Special Publication, no. 113, <https://doi.org/10.2110/sepm.113>.
- Beauchamp, B., Henderson, C.M., Dehari, E., Waldbott von Bassenheim, D., Elliott, S. and Calvo Gonzalez, D., (accepted). Late Pennsylvanian–Early Permian stratigraphic sequences and carbonate sedimentation, Carlin Canyon, Nevada (Basin and Range, USA). in Henderson, C.M., Ritter, S. and Snyder, W.S. (eds). Late Paleozoic Tectonostratigraphy and Biostratigraphy of Western Pangea. SEPM Special Publication no. 113.
- Boardman, D.R., Wardlaw, B.R., and Nestell, M.K., 2009. Stratigraphy and conodont biostratigraphy of the uppermost Carboniferous and Lower Permian from the North American Midcontinent. Kansas Geological Survey, Bulletin, v. 255 (parts A and B), 146 pp.
- Davydov, V., Krainer, K. and Chernykh, V., 2013. Fusulinid biostratigraphy of the Lower Permian Zweikofel Formation (Rattendorf Group; Carnic Alps, Austria) and Lower Permian Tethyan chronostratigraphy. Geological Journal, v. 48, no. 1, p. 57–100.
- Forke, H.C., 1995. Biostratigraphie (Fusuliniden; Conodonten) und Mikrofazies im Unterperm (Sakmar) der Karnischen Alpen (Naßfeldgebiet, Österreich). Jahrbuch der geologischen Bundesanstalt, v. 138, no. 2, p. 207–297.
- Forke, H.C., 2002. Biostratigraphic subdivision and correlation of uppermost Carboniferous/Lower Permian sediments in the Southern Alps: Fusulinoidean and conodont faunas from the Carnic Alps (Austria/Italy), Karavanke Mountains (Slovenia), and Southern Urals (Russia). Facies, v. 47, no. 1, p. 201–275.
- Groves, J.R. and Wahlman, G.P., 1997. Biostratigraphy and evolution of Late Carboniferous and Early Permian smaller foraminifers from the Barents Sea (offshore Arctic Norway). Journal of Paleontology, v. 71, no. 5, p. 758–779.
- Groves, J.R. and Boardman, D.R., 1999. Calcareous smaller foraminifers from the Lower Permian Council Grove Group near Hooster, Kansas. The Journal of Foraminiferal Research, v. 29, no. 3, p. 243–262.
- Groves, J.R., 2000. Suborder Lagenina and other smaller foraminifers from uppermost Pennsylvanian–lower Permian rocks of Kansas and Oklahoma. Micropaleontology, p. 285–326.
- Groves, J.R., Altiner, D. and Rettori, R., 2003. Origin and early evolutionary radiation of the Order Lagenida (Foraminifera). Journal of Paleontology, v. 77, no. 5, p. 831–843.
- Henderson, C.M., 2018. Permian conodont biostratigraphy. in Lucas S.G. and Shen S.Z. (eds). The Permian Timescale. Geological Society, London, Special Publications, v. 450, no. 1, p. 119–142.
- Pan, H. Z. and Erwin, D.H., 2002. Gastropods from the Permian of Guangxi and Yunnan provinces, south China. Journal of Paleontology, v. 76 (sp56), p. 1–49.
- Inkina, N.S., 2019. New Data on the Sezym Formation (Lower Permian, Polar Urals). Doklady Earth Sciences, v. 489, no. 1, p. 1269–1272.
- Kozur, H. and LeMone, D.V., 1995. The Shalem Colony section of the Abo and upper Hueco members of the Hueco Formation of the Robledo Mountains, Doña Ana County, New Mexico: Stratigraphy and new conodont-based age determinations. In Lucas S.G. and Heckert A.B., eds. Early Permian Footprints and Facies. New Mexico Museum of Natural History and Science: Bulletin, v. 6, p. 39–55.
- Krainer, K. and Schaffhauser, M., 2012. The type section of the Lower Permian Zweikofel Formation (Rattendorf Group; Carnic Alps, Austria). Austrian Journal of Earth Sciences, v. 105, no. 3, p. 61–79.
- Krainer, K., Lucas, S.G., Vachard, D., Barrick, J.E. and DiMichele, W.A., 2015. The Pennsylvanian–Permian section at Robledo Mountain, Doña Ana County, New Mexico, USA. in Lucas S.G. and DiMichelle, W.A.(eds). Carboniferous–Permian Transition in the Robledo Mountains, Southern New Mexico. New Mexico Museum of Natural History and Science: Bulletin, v. 65, p. 9–41.
- Krainer, K., Vachard, D. and Schaffhauser, M., 2019. Early Permian (Yakhtashian; Artinskian–Early Kungurian) foraminifers and microproblematica from the Carnic Alps (Austria/Italy), v. 73, Geologische Bundesanstalt.
- Lucas, S.G., Anderson, O.J., Heckert, A.B. and Hunt, A.P., 1995. Geology of Early Permian tracksites, Robledo Mountains, south-central New Mexico. in Lucas S.G. and Heckert A.B. (eds). Early Permian Footprints and Facies. New Mexico Museum of Natural History and Science: Bulletin, v. 6, p. 13–32.
- Lucas, S.G., Krainer, K., Vachard, D. and DiMichele, W.A., 2015. The Lower Permian Hueco Group, Robledo Mountains, New Mexico (USA). in Lucas S.G. and DiMichelle, W.A.(eds). Carboniferous–Permian Transition in the Robledo Mountains, Southern New Mexico. New Mexico Museum of Natural History and Science: Bulletin, v. 65, p. 43–95.
- Pinard S. and Mamet B., 1998. Taxonomie des petits Foraminifères du Carbonifère Supérieur–Permien Inférieur du Bassin de Sverdrup, Arctique Canadien, Palaeontographica Canadiana 15. Geological Association of Canada, St Johns, Newfoundland. 253 pp.
- Read, M.T. and Nestell, M.K., 2018. Cisuralian (Early Permian) Sweetognathid conodonts from the upper part of the Riepe

- Spring Limestone, North Spruce Mountain Ridge, Elko County, Nevada. in Over D. J. and Henderson C.M.(eds). Conodont Studies Dedicated to the Careers and contributions of Anita Harris, Glen Merrill, Carl Rexroad, Walter Sweet and Bruce Wardlaw. *Bulletins of American Paleontology*, v. 395–396, p. 89–113.
- Read, M.T. and Nestell, M.K., 2019a. Lithostratigraphy and fusulinid biostratigraphy of the Upper Pennsylvanian-Lower Permian Riepe Spring Limestone at Spruce Mountain Ridge, Elko County, Nevada, USA. *Stratigraphy*, v. 16, no. 4, p. 195–247.
- Read, M.T. and Nestell, M.K., 2019b. Global Distribution of the Fusulinacean Genus *Biwaella*. *Paleontological Journal*, v. 53, no. 9, p. 946–949.
- Shen, S.Z., Wang, Y., Henderson, C.M., Cao, C.Q. and Wang, W., 2007. Biostratigraphy and lithofacies of the Permian System in the Laibin–Heshan area of Guangxi, South China. *Palaeoworld*, v. 16, no. 1–3, p. 120–139.
- Sun, Y.D., Liu, X.T., Yan, J.X., Li, B., Chen, B., Bond, D.P.G., Joachimski, M.M., Wignall, P.B., Wang, X. and Lai, X.L., 2017. Permian (Artinskian to Wuchapingian) conodont biostratigraphy in the Tieqiao section, Laibin area, South China. *Palaeogeography, Palaeoclimatology, Palaeoecology*, v. 465, p. 42–63.

Everything on track(s): Upcoming excavation for an exceptional Middle to Late Permian ichnofauna in central Germany

Daniel Falk^{1,2}

¹School of Biological, Earth and Environmental Sciences, University College Cork, Distillery Fields, North Mall, T23 TK30, Cork, Ireland.

²Environmental Research Institute, University College Cork, Cork, Ireland.



Permian tetrapods are of high relevance for the correlation of Permian non-marine strata (Lucas 2018). However, an incomplete fossil record of tetrapod body fossils hampers the research progress on e.g., detailed biostratigraphy. Tetrapod trace fossils may close that gap as they are more common than skeletal remains and could expand the known stratigraphic and/or geographic ranges of their assumed trackmaker groups. The Middle to Late Permian Hornburg Formation (Germany) reveals a rich fossil content including promising tetrapod traces (Buchwitz et al. 2019, Buchwitz et al. 2020, Falk 2013, 2014, Falk et al. 2015). This is exceptional for central Europe.

In this project we aim at a palaeontological excavation and sedimentological documentation in an abandoned quarry in the state of Saxony-Anhalt (Germany). We will collect and scientifically describe vertebrate and invertebrate trace fossils and try to verify our previous findings for global Permian biostratigraphy.

Middle to Late Permian terrestrial fossiliferous deposits are

rare in the Euramerican area of Europe and North America. In fact, extended fossiliferous surface outcrops exist only in the Lodève Basin (France), and the Argana Basin (Morocco) but their exact chronostratigraphic ages remain uncertain (Schneider et al. 2020). In Germany, these sediments are nearly exclusively known from drilling cores (Legler et al. 2008); hence the fossil record is sparse. In contrast, more than 14 surface outcrops expose fan and playa sediments of the Hornburg Formation in the Hornburg Basin (Hoyningen-Huene 1960, Falk et al. 1979, Falk 2014). Magnetostratigraphic, cyclostratigraphic, tectono- and climate-stratigraphic data indicate a Late Middle to Early Late Permian age for those beds (e.g., Gebhardt and Lützner 2012), which are partly very rich in vertebrate and invertebrate traces (Buchwitz et al. 2020) (Fig. 1). The successions represent an exceptional window into the continental environments and biotas of the Euramerican Permian Pangean palaeoequatorial northern trade wind zone. The comprehensive analysis of the Hornburg Formation's litho- and biofacies patterns will advance the knowledge of evolution and adaptation of tetrapods during a pronounced aridisation of palaeoequatorial Pangea and support a new reconstruction of the depositional environment.

The Hornburg Formation's successions comprise seven lithological members (Mb) in two to three cycles (Fig. 1): (1) Unteres Quarzitkonglomerat Mb and (2) Blankenheim Sandstein Mb of the Lower Cycle; the Upper Cycle comprises (3) Oberes Quarzitkonglomerat Mb, (4) Rundkörniger Sandstein Mb, (5) Feinkörniger Sandstein Mb, (6) Blättertton Mb (Fig. 2) and (7) Mischkörniger Sandstein Mb. The conglomerates and sandy siltstones of 1–3 represent alluvial fan to braid plain system deposits. They are laterally and vertically overlain by sandy and silty braid plain and evaporitic sand flat deposits (4–5). Aeolian transport is indicated by bimodal sandstones and spatially restricted, well-sorted sandstones, which have been fluvial redeposited (5). They are overlain by fossiliferous lacustrine, fine clastic deposits (6) including laminated claystones, evaporitic horizons and halite pseudomorphs, and intercalated channel sandstones (Fig. 2). An additional sedimentary cycle may be indicated by (7).

The Blättertton Mb is outstanding in its rich ichnofauna. A few tetrapod footprints and short trackways were reported as *Dromopus*, *?Amphisauropus* and recently as *Capitosauroides*; the latter are often accompanied by numerous tetrapod swimming traces (Buchwitz et al. 2020). Furthermore, jellyfish imprints, conchostracans with biostratigraphic potential (Müller 1973, Schneider and Scholze 2018), and about 21 different arthropod ichnotaxa were reported from at least two locations (Walter 1983). However, poor preservation of tetrapod tracks (Fig. 2) made ichnotaxonomic determination of many historical specimens impossible; determinations of invertebrate trace fossils show insufficient use for biostratigraphy (Minter et al. 2007). Acquisition of specimens is difficult, as former fossiliferous sites are not accessible anymore or depleted in tetrapod track bearing horizons. In 2013, a prospecting excavation in the laminated clay-, silt- and sandstone-dominated beds of an abandoned quarry in Wolferode, Saxony-Anhalt (Germany, Figs 1, 2) by the Technical University Bergakademie Freiberg and the Geological Survey of Saxony-Anhalt revealed first trace fossils including a variety of

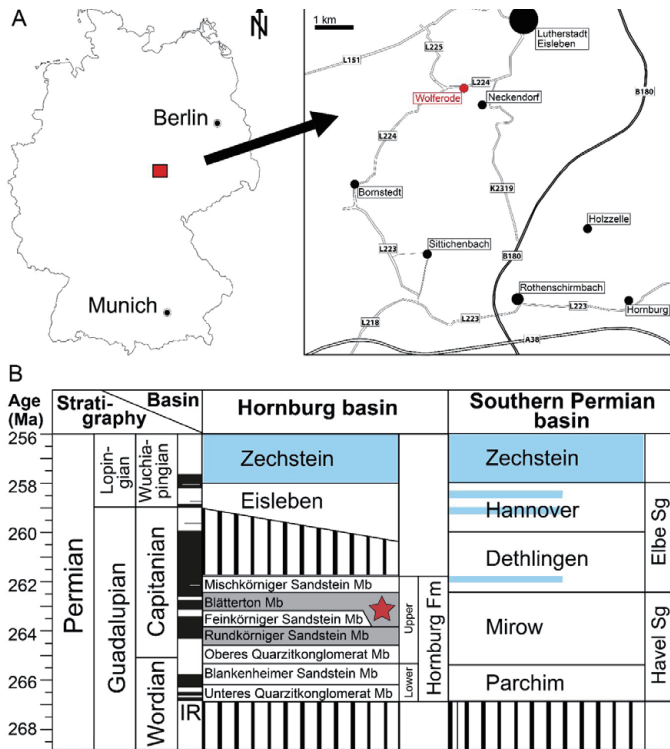


Fig. 1: Location and stratigraphy of the Middle to Upper Permian Hornburg Formation, modified after Buchwitz et al. (2020). A, Geographical position of the excavation site (Wolferode, Saxony-Anhalt, Germany); B, schematic lithostratigraphic successions of the Hornburg basin and Southern Permian basin (after Gebhardt and Lützner 2012); a prospecting excavation was performed in fossiliferous strata highlighted with a star, excavation will take place in strata marked with grey colour, marine ingressions are marked with light blue colour. Map data based on OpenStreetMap; magnetostatigraphy after Hounslow and Balabanov (2018).

tetrapod tracks, tetrapod scratch marks, jellyfish impressions and arthropod tracks. The NE corner of the quarry exposes promising laminated claystone layers rich in jellyfish imprints and arthropod traces with a high potential for well-preserved tetrapod traces and is of particular interest for a bed-by-bed excavation of the about 6 m thick strata in summer to –autumn 2022.

The detailed documentation will include photogrammetry of bedding surfaces and trace fossils (Mallison and Wings 2014).

The project will be conducted by collaborators from Germany (Geological Survey of Saxony-Anhalt, Museum of Natural History Magdeburg, Technical University Bergakademie Freiberg) and Ireland (University College Cork). The excavation will greatly contribute to the tasks of the “Nonmarine-Marine Correlation Working Group” of the Subcommissions on Carboniferous Stratigraphy (SCCS), Permian Stratigraphy (SPS), and Triassic Stratigraphy (STS). We are thankful for the dedicated effort of the numerous scientists that lay the foundation for this research over the last decades. Daniel Falk is grateful for the awarded research grants by the European Association of Vertebrate Palaeontologists (EAVP) and the Subcommission of Permian Stratigraphy (SPS) as well as for substantial funding by the other collaborator institutions. He thanks Prof. Maria E. McNamara (University College Cork, Ireland) for her support and acknowledges his funding from the Irish Research

Council (Government of Ireland Postgraduate Scholarship GOIPG/2018/3354). A special thanks is given to Dipl.-Ing. (FH) Jürgen Waschkuhn, who owns the quarry and kindly permits access and excavations.

The entire project including this article is a team effort and would not be possible without the scientific expertise, experience and support from all team members including:

M. Buchwitz³, B.-C. Ehling⁴, U. Gebhardt⁴, J. W. Schneider^{5,6}

³ Museum für Naturkunde Magdeburg, Otto-von-Guericke-Str. 68–73, 39108 Magdeburg, Germany.

⁴ Landesamt für Geologie und Bergwesen Sachsen-Anhalt, Köthener Str. 38, 06118 Halle (Saale), Germany.

⁵ TU Bergakademie Freiberg, Institut für Geologie, Bernhard-von-Cotta-Straße 2, 09596 Freiberg, Germany.

⁶ Kazan Federal University, Institute of Geology and Petroleum Technologies, Kremlyovskaya Street 18, Kazan, Russia.

References

Buchwitz, M., Marchetti, L., Jansen, M., Falk, D., Trostheide, F. and Schneider, J. W., 2020. Ichnotaxonomy and trackmaker assignment of tetrapod tracks and swimming traces from the Middle Permian Hornburg Formation of Saxony-Anhalt (Germany). *Annales Societatis Geologorum Poloniae*, v. 90, p. 291–320. http://www.asgp.pl/90_3_291_320_Buchwitz_et_al

Buchwitz, M., Klein, H., Falk, D. and Wings, O., 2019. Overview of the Permian and Triassic tetrapod trackway localities in Saxony-Anhalt, Germany. in Buchwitz, M., Falk, D., Klein, H., Mertmann, D., Perl, A. and Wings, O. (eds.), 3rd

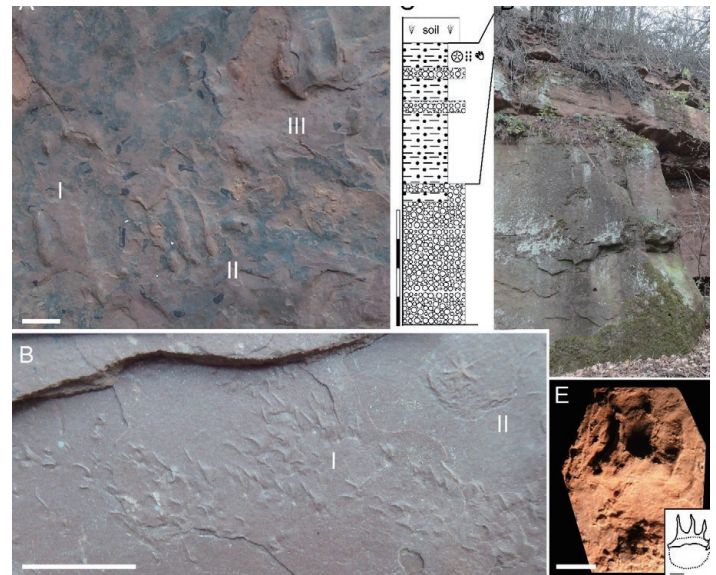


Fig. 2. Lithology and trace fossils of the Wolferode quarry (Hornburg Formation Upper Cycle). A, tetrapod swimming traces (I–III), indetermined, cast, WfG-71; B, arthropod trackways, indetermined (I) and freshwater jellyfish *Medusina limnica* (II), cast, WfG-165A; C, D, schematic lithological profile and photograph of the profile section in the abandoned quarry in Wolferode, where the excavation will take place in 2022; E, tetrapod track, incomplete, indetermined, cast, WfG-16; textures: bubbles – fine to coarse grained sandstone, poorly sorted, partly bimodal; dash-dot – laminated silt and clay stones, Upper beds yield trace fossils, scales: 10 mm (A, B, D, E) and 4 m (C).

- International Conference of Continental Ichnology (ICCI 2019), Abstract Volume and Field Trip Guide. Hallesches Jahrbuch für Geowissenschaften, v. 46, p. 4–5.
- Falk, D., Schneider, J. W., Gebhardt, U. and Walter, H., 2017. The Ichnofauna of a singular Middle to Late Permian Playa Lake in Europe (Upper Hornburg Fm., Saxony-Anhalt, Germany). Second International Conference of Continental Ichnology (ICCI-2017). in Bordy, E. M. (ed.), Second International Conference of Continental Ichnology (ICCI-2017), Abstract Book. University of Cape Town, South Africa, p. 23–24.
- Falk, D. Schneider, J. W., Gebhardt, U., and Ehling, B.C., 2015. Trace fossil record and sedimentology of the “Blätterton” facies of the Hornburg Formation, Saxony-Anhalt (Late Guadalupian, Permian). in Lagnaoui, A., Belahmira, A. and Saber, H. (eds.), First International Congress on Continental Ichnology (ICCI-2015), Proceeding of Abstracts. Chouaib Doukkali University El Jadida, Morocco, p. 25.
- Falk, D., 2014. Sedimentologie, Paläontologie und Environment-Rekonstruktion der Hornburg-Formation des südlichen Permbeckens (spätes Guadalupian, Permian). Institut für Geologie. TU Bergakademie Freiberg, MSc thesis: 237 pp. [German]
- Falk, D., 2013. Kartierung der Rotliegend Klastite und Pyroklastite am Hornburger Sattel (Hornburg-Formation, Sachsen-Anhalt). Institut für Geologie – Bereich Paläontologie/Stratigraphie and Landesamt für Geologie und Bergwesen Sachsen-Anhalt. TU Bergakademie Freiberg, Fakultät für Geowissenschaften, Geotechnik und Bergbau, Geological Mapping Report: 138 pp. [German]
- Falk, F., Ellenberg, J., Grumbt, E. and Lütznier, H., 1979. Zur Sedimentation des Rotliegenden im Nordteil der Saale-Senke – Hallesche bis Hornburger Schichten. Hallesches Jahrbuch für Geowissenschaften, v. 4, p. 3–22. [German]
- Gebhardt, U. and Lütznier, H. (2012): Innervariscische Rotliegendebcken und Norddeutsches Becken – Fragen ihrer stratigraphischen Verknüpfung. in Deutsche Stratigraphische Kommission, Stratigraphie von Deutschland X. Rotliegend. Teil 1: Innervariscische Becken. Schriftenreihe der Deutschen Gesellschaft für Geowissenschaften, v. 61, p. 732–747. [German]
- Hounslow, M. W. and Balabanov, Y. P., 2018. A geomagnetic polarity timescale for the Permian, calibrated to stage boundaries. Geological Society London, Special Publications, v. 450, p. 61–103.
- Hoyningen-Huene, E. Von, 1960. Das Permokarbon im östlichen Harzvorland. Freiburger Forschungshefte C, v. 93, p. 1–116. [German]
- Legler, B., Schneider, J. W., Gebhardt, U., Merten, D. and Gaupp, R., 2011. Lake deposits of moderate salinity as sensitive indicators of lake level fluctuations: Example from the Upper Rotliegend saline lake (Middle–Late Permian, Northeast Germany). Sedimentary Geology, v. 234, p. 56–69.
- Lucas, S. G., 2018. Permian tetrapod biochronology, correlation and evolutionary events. Geological Society London, Special Publications, v. 450, p. 405–444.
- Mallison, H. and Wings, O., 2014. Photogrammetry in paleontology – a practical guide. Journal of Paleontological Techniques, v. 12, p. 1–31.
- Minter N. J., Braddy S. J. and Davis, R. B., 2007. Between a rock and a hard place: arthropod trackways and ichnotaxonomy. Lethaia, v. 40, p. 365–375.
- Müller, A. H., 1973. Zur Taphonomie und Ökologie rezenter und fossiler limnischer Hydromedusen. Zeitschrift für Geologische Wissenschaften, v. 1, p. 1475–1480. [German]
- Schneider, J. W. and Scholze, F., 2018. Late Pennsylvanian–Early Triassic conchostracan biostratigraphy: a preliminary approach. Geological Society, London, Special Publications, v. 450, p. 365–386.
- Schneider, J. W., Lucas, S. G., Scholze, F., Voigt, S., Marchetti, L., Klein, H., Opluštil, S., Werneburg, R., Golubev, V. K., Barrick, J. E., Nemyrovska, T., Ronchi, A., Day, M. O., Silantiev, V. V., Rößler, R., Saber, H., Linnemann, U., Zharinova, V. and Shen, S. Z., 2020. Late Paleozoic-early Mesozoic continental biostratigraphy – links to the Standard Global Chronostratigraphic Scale. Paleoworld, v. 29, p. 186–238.
- Walter, H., 1983. Zur Taxonomie, Ökologie und Biostratigraphie der Ichnia limnisch-terrestrischer Arthropoden des mitteleuropäischen Jungpaläozoikums. Freiburger Forschungshefte C, v. 382, p. 146–193. [German]

Stratigraphic gap associated with the Permian-Triassic succession in the continental deposits of SW Europe: time constraints, stratigraphic correlations and paleogeography inferences

Joan Lloret^{1,2}

1 Instituto de Geociencias (CSIC, UCM), Madrid, Spain. Universidad Complutense, Madrid, Spain.

2 Departamento de Geodinámica, Estratigrafía y Paleontología, Facultad de Ciencias Geológicas, Universidad Complutense, Madrid, Spain.

Email: jolloret@ucm.es



Stratigraphic gaps are present in most continental basins and the amount of missing time and strata are often difficult to estimate due to the scarcity of high-resolution chronostratigraphic data. Where fossils are absent or rare precise stratigraphic correlation is also difficult. Moreover, when a stratigraphic gap/hiatus occurs over a wide area, it further complicates the analysis of the geological record. The sedimentary record of the post-Variscan continental basins located in SW Europe (N-NE Spain, S-SE France, Sardinia and other surrounding areas) is never continuous, giving rise to complex stratigraphic relationships between the different regions and, sometimes, also between contiguous basins. In particular, one of the most striking evidence in this domain, is a ubiquitous and long-lasting gap in the sedimentary record between the ?early-middle Guadalupian and the earliest Triassic as remarked in various papers in the last twenty years (e.g. Bourquin et al., 2007, 2011; Linol et al., 2009;

Cassinis et al., 2012; Gretter et al., 2015; Lloret et al., 2021).

Since now, the significance of this gap has not been explained in detail, especially in a regionally large area. The gap makes regional lithostratigraphic correlations difficult with neighboring areas where the sedimentary record is more continuous. However elucidation of the stratigraphic gap is crucial to understanding the evolution of Pangea during this time interval.

This stratigraphic gap seems to show a different inception and duration in the SW European basins. In Spain, its lowermost limit is represented by the top of different units (Fig. 1); the Sotres Formation, in the Cantabrian Mountains (middle Kungurian; López-Gómez et al., 2019a, b), the top of the Upper Red Unit in the E Pyrenees (Kungurian-?Wordian; Lloret et al., 2018), the top of the Lower Red Unit in the Central Pyrenees (Artinskian-middle Kungurian; Mujal et al., 2016), the P3 Formation in Minorca (Wordian-?Changhsingian; Ramos, 1995, Bercovici et al., 2009 or middle Artinskian-Changhsingian; Matamales-Andreu et al., 2021a) and the Asa Formation in Majorca (lower Permian; Matamales-Andreu et al., 2021b). In the SE of France, the uppermost Permian units below the unconformity are represented by the La Motte Formation (Fig. 1) in Provence (Wordian; Durand, 2006, Gand and Durand, 2006) and the La Lieude Formation in Lódève (Roadian-Wordian; Michel et al., 2015). In Sardinia, the uppermost Permian sedimentary record before the unconformity is the Cala del Vino Formation (latest Kungurian-Roadian; Citton et al. 2019).

The lowermost post unconformity beds are the the Cicera Formation (Fig. 1) in the Cantabrian Mountains (late Anisian-Ladinian; López-Gómez et al., 2019a), the Palanca de Noves Formation in the Pyrenees (Olenekian; Lloret et al., 2020), and the Son Serralta Formation in Majorca (Olenekian-Anisian; Matamales-Andreu et al., 2021b). The basal Triassic sedimentary record in SE France (Lódève and Provence) and Sardinia was ascribed to the Early Triassic (Smithian-Spathian) for the Port Issol and Porticciolo Formations respectively (Fig.1; Cassinis et al., 2003; Durand, 2006; Linol et al., 2009; Bourquin et al., 2011).

The goal of this project is to estimate and constrain the duration and age of the unconformity through the most precise dating of its youngest pre-unconformity beds and oldest post-unconformity beds in selected key sections, trying to ascertain its possible significance. Although some basins have been recently revisited providing new and more precise stratigraphical data, other ones, as in the case of the Permian-Early Triassic continental succession in the Basque Country (N Spain), still need detailed revision. Our aim is to reach the proposed objectives following these steps: a) a careful review of the unconformity in the more recent literature, gathering all the relevant fossil or radiometric data: a regional chronostratigraphic correlation chart will be provided on the basis of this information; b) a refined stratigraphic correlation of the SW European region and surrounding areas; c) a reconstruction of the palaeogeography of SW Europe during this gap in this near-equator region belt; d) a state-of-the-art and critic analysis on the possible causes of this major gap/hiatus.

References

- Bercovici, A., Díez, J.B., Broutin, J., Bourquin, S., Linol, B., Villanueva-Amadoz, U., López-Gómez, J. and Durand, M., 2009. A palaeoenvironmental analysis of Permian sediments in Minorca (Balearic Islands, Spain) with new palynological and megafloral data. *Review of Palaeobotany and Palynology*, v. 158, p. 14–28. <https://doi.org/10.1016/j.revpalbo.2009.07.001>
- Bourquin, S., Marc Durand, M., Díez, JB., J. Broutin, J. and Fluteau, F. 2007. The Permian-Triassic boundary and lower Triassic sedimentation in western European basins: an overview. *Journal of Iberian Geology*, v. 33, p. 221–236.
- Bourquin, S., Bercovici, A., López-Gómez, J., Díez, J.B., Broutin, J., Ronchi, A., Durand, M., Arché, A., Linol, B. and Amour, F., 2011. The Permian–Triassic transition and the onset of Mesozoic sedimentation at the northwestern peri-Tethyan domain scale: Palaeogeographic maps and geodynamic implications. *Palaeogeography, Palaeoclimatology, Palaeoecology*, v. 299, p. 265–280. <https://doi.org/10.1016/j.palaeo.2010.11.007>
- Cassinis, G., Durand, M. and Ronchi, A., 2003. Permian-Triassic continental sequences of Northwest Sardinia and South Provence: stratigraphic correlations and palaeogeographical implications. *Bollettino Società Geologica Italiana Volume speciale*, p. 119–129.
- Cassinis, G., Perotti, C.R. and Ronchi, A., 2012. Permian continental basins in the Southern Alps (Italy) and perimediterranean correlations. *International Journal of Earth Sciences (Geol Rundsch)*, v. 101, p. 129–157. <https://doi.org/10.1007/s00531-011-0642-6>
- Citton, P., Ronchi, A., Maganuco, S., Caratelli, M., Nicosia, U., Sacchi, E. and Romano, M., 2019. First tetrapod footprints from the Permian of Sardinia and their palaeontological and stratigraphical significance. *Geological Journal*, v. 54, p. 2084–2098. <https://doi.org/10.1002/gj.3285>
- Durand, M., 2006. The problem of the transition from the Permian to the Triassic Series in southeastern France: comparison with other Peritethyan regions. *Geological Society, London, Special Publications*, v. 265, p. 281–296. <https://doi.org/10.1144/GSL.SP.2006.265.01.13>
- Gand, G. and Durand, M., 2006. Tetrapod footprint ichnoassociations from French Permian basins. Comparisons with other Euramerican ichnofaunas. *Geological Society, London, Special Publications*, v. 265, p. 157–177. <https://doi.org/10.1144/GSL.SP.2006.265.01.07>
- Gretter, N., Ronchi, A., López-Gómez, J., Arche, A., De la Horra, R., Barrenechea, J. and Lago, M., 2015. The Late Palaeozoic-Early Mesozoic from the Catalan Pyrenees (Spain): 60Myr of environmental evolution in the frame of the western peri-Tethyan palaeogeography. *Earth-Science Reviews*, v. 150, p. 679–708. <https://doi.org/10.1016/j.earscirev.2015.09.001>
- Linol, B., Bercovici, A., Bourquin, S., Díez, J.B., López-Gómez, J., Broutin, J., Durand, M. and Villanueva-Amadoz, U., 2009. Late Permian to Middle Triassic correlations and palaeogeographical reconstructions in south-western European basins: New sedimentological data from Minorca (Balearic Islands, Spain). *Sedimentary Geology*, v. 220, p. 77–94. <https://doi.org/10.1016/j.sedgeo.2009.06.003>

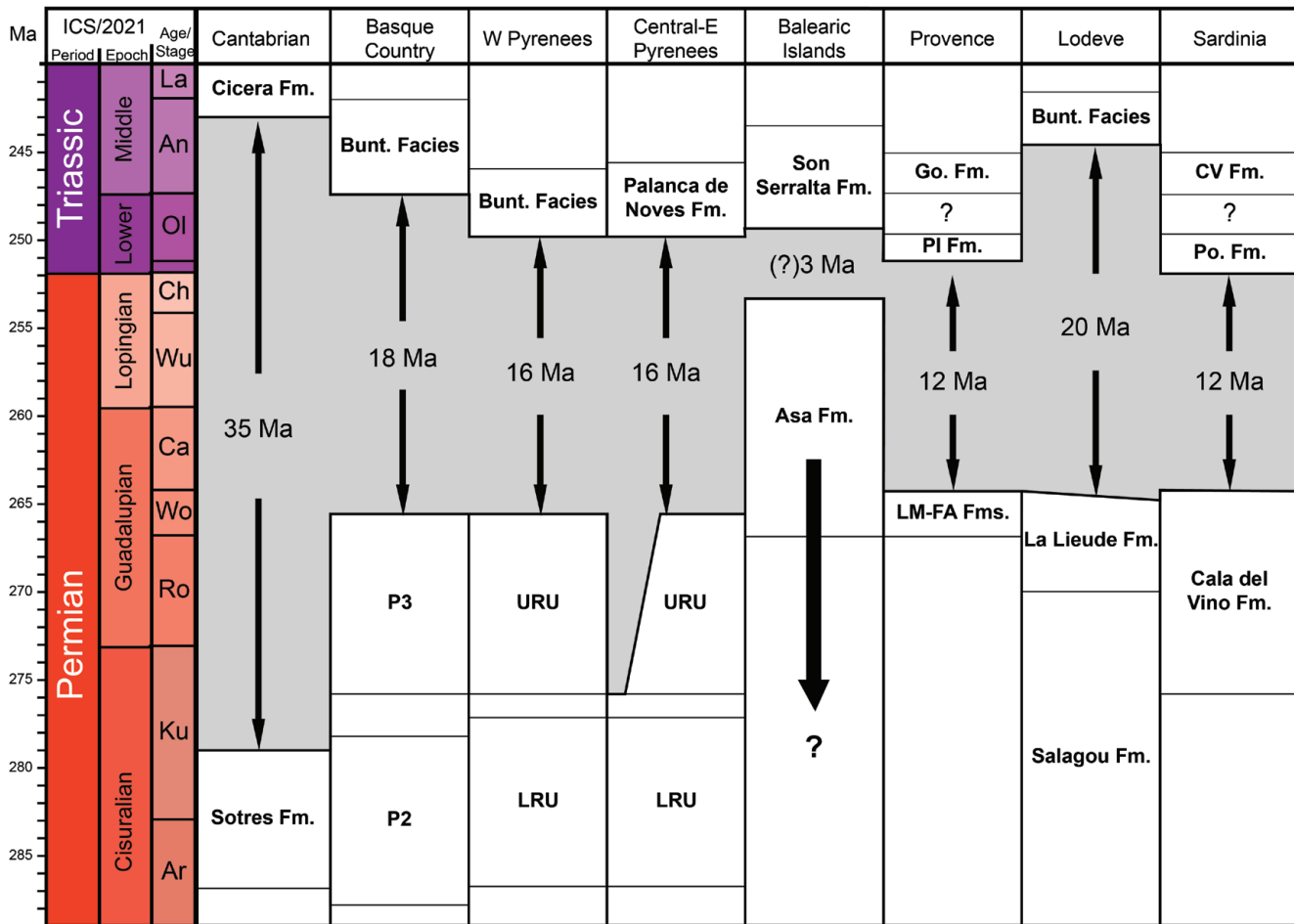


Fig. 1. Chronostratigraphic scheme of the SW European stratigraphic units concerning the Permian-Triassic stratigraphic gap. The age of the units are referenced in the text

Lloret, J., Ronchi, A., López-Gómez, J., Gretter, N., De la Horra, R., Barrenechea, J.F. and Arche, A., 2018. Syn-tectonic sedimentary evolution of the continental late Palaeozoic-early Mesozoic Erill Castell-Estac Basin and its significance in the development of the central Pyrenees Basin. *Sedimentary Geology*, v. 374, p. 134–157. <https://doi.org/10.1016/j.sedgeo.2018.07.014>

Lloret, J., De la Horra, R., Gretter, N., Borrueal-Abadía, V., Barrenechea, J.F., Ronchi, A., Diez, J.B., Arche, A. and López-Gómez, J., 2020. Gradual changes in the Olenekian-Anisian continental record and biotic implications in the Central-Eastern Pyrenean basin, NE Spain. *Global and Planetary Change*, v. 192, p. 103252. <https://doi.org/10.1016/j.gloplacha.2020.103252>

Lloret, J., López-Gómez, J., Heredia, N., Martín-González, F., de la Horra, R., Borrueal-Abadía, V., Ronchi, A., Barrenechea, J.F., García-Sansegundo, J., Galé, C., Ubide, T., Gretter, N., Diez, J.B., Juncal, M. and Lago, M., 2021. Transition between Variscan and Alpine cycles in the Pyrenean-Cantabrian Mountains (N Spain): Geodynamic evolution of near-equator European Permian basins. *Global and Planetary Change*, v. 207, p. 103677. <https://doi.org/10.1016/j.gloplacha.2021.103677>

López-Gómez, J., Alonso-Azcárate, J., Arche, A., Arribas, J., Fernández Barrenechea, J., Borrueal-Abadía, V., Bourquin, S., Cadenas, P., Cuevas, J., De la Horra, R., Díez, J.B., Escudero-Mozo, M.J., Fernández-Viejo, G., Galán-Abellán, B., Galé, C., Gaspar-Escribano, J., Gisbert Aguilar, J., Gómez-Gras, D., Goy, A., Gretter, N., Heredia Carballo, N., Lago, M., Lloret, J., Luque, J., Márquez, L., Márquez-Aliaga, A., Martín-Algarra, A., Martín-Chivelet, J., Martín-González, F., Marzo, M., Mercedes-Martín, R., Ortí, F., Pérez-López, A., Pérez-Valera, F., Pérez-Valera, J.A., Plasencia, P., Ramos, E., Rodríguez-Méndez, L., Ronchi, A., Salas, R., Sánchez-Fernández, D., Sánchez-Moya, Y., Sopena, A., Suárez-Rodríguez, Á., Tubía, J.M., Ubide, T., Valero Garcés, B., Vargas, H. and Viseras, C., 2019a. Permian-Triassic Rifting Stage, in: Quesada, C., Oliveira, J.T. (Eds.), *The Geology of Iberia: A Geodynamic Approach*. Springer International Publishing, Cham, p. 29–112. https://doi.org/10.1007/978-3-030-11295-0_3

López-Gómez, J., Martín-González, F., Heredia, N., de la Horra, R., Barrenechea, J.F., Cadenas, P., Juncal, M., Diez, J.B., Borrueal-Abadía, V., Pedreira, D., García-Sansegundo, J., Farias, P., Galé, C., Lago, M., Ubide, T., Fernández-Viejo, G. and Gand, G., 2019b. New lithostratigraphy for the Cantabrian Mountains: A common tectono-stratigraphic

evolution for the onset of the Alpine cycle in the W Pyrenean realm, N Spain. *Earth-Science Reviews*, v. 188, p. 249–271. <https://doi.org/10.1016/j.earscirev.2018.11.008>

Matamales-Andreu, R., Roig-Munar, F.X., Oms, O., Galobart, À. and Fortuny, J., 2021a. A captorhinid-dominated assemblage from the palaeoequatorial Permian of Menorca (Balearic Islands, western Mediterranean). *Earth and Environmental Science Transactions of the Royal Society of Edinburgh*, v. 112, p. 125–145. <https://doi.org/10.1017/S1755691021000268>

Matamales-Andreu, R., Peñalver, E., Mujal, E., Oms, O., Scholze, F., Juárez, J., Galobart, À., and Fortuny, J., 2021. Early–Middle Triassic fluvial ecosystems of Mallorca (Balearic Islands): Biotic communities and environmental evolution in the equatorial western peri-Tethys. *Earth-Science Reviews*, v. 222, p. 103783. <https://doi.org/10.1016/j.earscirev.2021.103783>.

Michel, L.A., Tabor, N.J., Montañez, I.P., Schmitz, M.D. and Davydov, V.I., 2015. Chronostratigraphy and Paleoclimatology of the Lodève Basin, France: Evidence for a pan-tropical aridification event across the Carboniferous–Permian boundary. *Palaeogeography, Palaeoclimatology, Palaeoecology*, v. 430, p. 118–131. <https://doi.org/10.1016/j.palaeo.2015.03.020>

Mujal, E., Fortuny, J., Oms, O., Bolet, A., Galobart, À. and Anadón, P., 2016. Palaeoenvironmental reconstruction and early Permian ichnoassemblage from the NE Iberian Peninsula (Pyrenean Basin). *Geological Magazine*, v. 153, p. 578–600. <https://doi.org/10.1017/S0016756815000576>

Ramos, A., 1995. Transition from alluvial to coastal deposits (Permian–Triassic) on the Island of Mallorca, western Mediterranean. *Geological Magazine*, v. 132, p. 435–447. <https://doi.org/10.1017/S001675680002149X>

papers at numerous national and international conferences, conducted research in Nevada and Idaho, West Texas, Mexico, Italy, Palau, Ellesmere Island, Southern Ural Mountains, Kazakhstan/Russia, Siberia, and developed and led a geology field camp in Sardinia. He continued to organize this field experience for students and teach Historical Geology as Professor Emeritus for the Department of Geosciences well after he retired from BSU in 2003.

Claude was born in 1937 in Baunei, Sardinia. He immigrated to the USA with his mother Giuseppina Cabras in 1948 and in 1961 graduated with a Geology degree from City College of New York. He met his soon to be wife Jean Vitarelli while attending City College where she was studying to be a nurse. Upon graduation Claude was drafted into the U.S. Army and served from September 1961 through September 1963 as a Terrain Analyst. He requested and was granted an early discharge (1 month) so that he could marry the love of his life, Jean. They were married in August of 1963 and moved to Iowa City, Iowa so Claude could pursue a Ph.D. in Geology at the University of Iowa. At the University of Iowa, Claude studied under William Furnish and Brian Glenister investigating the Xenodiscidae ammonoids. He completed his Ph.D. dissertation on Permian ammonoids in 1968, titled “The Xenodiscidae, Permian Otoceratacean Ammonoids” (Spinosa, 1968). Most notable from this detailed taxonomic study, was the compilation of a phylogenetic tree for the Xenodiscidae and Araxoceratinae, two evolutionary lineages originating from *Paraceltites elegans* Girty, 1908. Since publication of this study (Spinosa et al., 1975), the figure illustrating this evolutionary succession is commonly reprinted in Historical Geology textbooks and used as an example of gradualism in Permian invertebrates (Levin, 1978 and subsequent editions). After graduating from the University of Iowa, Claude taught for a short time at the University of Indiana

Memorial to Claude Spinosa
17 July 1937 – 5 September 2021

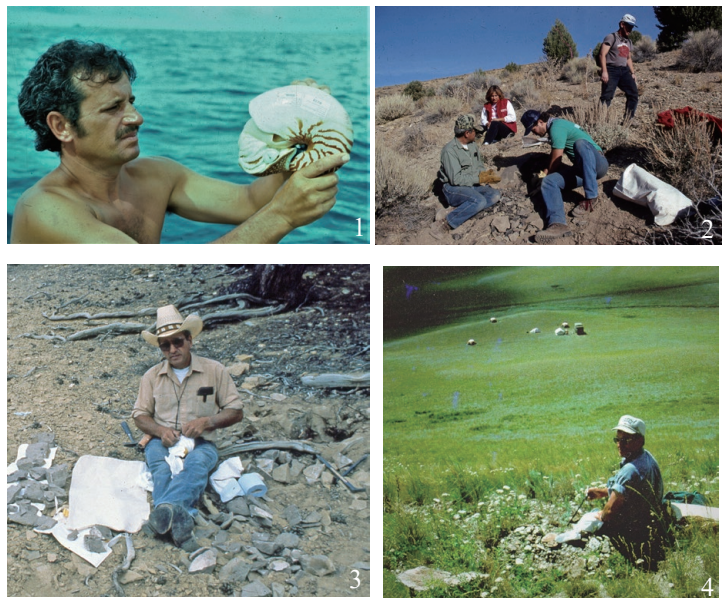
Tamra A. Schiappa

Department of Geography, Geology and the Environment
 Slippery Rock University
 Slippery Rock, PA 16057
 Email: tamra.schiappa@sru.edu

Walter Snyder

Department of Geosciences
 Boise State University
 Boise, Idaho 83725
 Email: walter.snyder@boisestate.edu

Claude Spinosa, 84, professor, mentor, advisor, ammonoid paleontologist and friend passed away on 5 September 2021 in Sandpoint, Idaho. He served as a member, titular (voting) member, and secretary of the Permian Subcommittee for much of his career, helping to formalize the Permian Time Scale. He was an inspiring teacher for 33 years at Boise State University (BSU), Boise, Idaho. During his tenure at BSU, he led countless student field trips, advised many graduate theses, presented



1. Claude trapping *Nautilus* cf. *N. Pompilius* off coast of Palau, summer of 1977. 2. Claude with students collecting ammonoids in Nevada, spring 1987. 3. Claude collecting Artinskian ammonoids, Beck Springs, Nevada, summer 1987. 4. Claude collecting ammonoids at the Aktasty section, southern Ural Mountains, Russia during a summer 1991 field conference.

prior to moving to Boise to teach at BSU.

In the fall of 1970, Claude joined the Geology faculty at Boise State University. He became a full professor and served as chairperson of the Department of Geosciences several times during his career. Claude along with Walt Snyder formed the Permian Research Institute at BSU, obtained numerous NSF grants to support his efforts of understanding the life habits of the Nautilus, refine the Permian Time Scale, and understand the biostratigraphy and paleogeography of the western margin of Pangaea. As Professor of Geology at BSU, he helped to advance the Department of Geosciences by starting a Masters in Geology program which laid the foundation for the addition of the current Ph.D. program. He was instrumental in collaborations with international scientists, both through his work with the Permian Subcommittee and by inviting many to come and study at BSU to refine and formalize the base of the Permian System.

Claude made many contributions to the International Stratigraphic Commission, serving as a titular (voting) member and secretary for the Permian Subcommittee for approximately 20 years. He began as a co-editor of the Compendium of Permophiles Volume 1, July 1978-May 1981. He is listed as a member and contributing author in 1986 publishing Permian

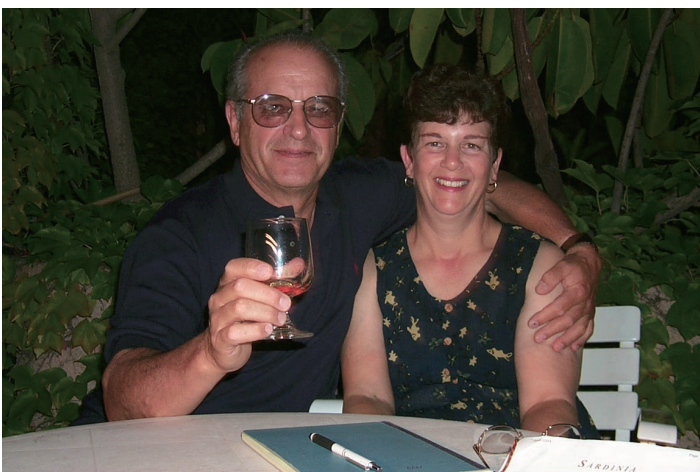
Ammonoid Uraloceras in North America its Global Significance with W.W. Nassichuk in Newsletter 10 page 9. Claude published many other articles as main author or co-author (e.g., Numbers 25, 26) throughout his participation with the Permian Subcommittee and even upon retirement from BSU. He was one of many co-authors to propose Aidaralash as GSSP for the base of the Permian System (Davydov et al., 1995), working on the proposal until it was ratified. He was instrumental along with Brian Glenister, Bruce Wardlaw, and others in establishing the three series/epoch nomenclatural scheme for the Permian System proposing that the Guadalupian become the Middle Permian Series (Glenister et al., 1999). He became secretary of the Permian Subcommittee in June 1996 (No. 28) replacing John Utting and served until 1999 when he was replaced by Charles Henderson. Claude always seemed to be at the forefront of technology and as secretary in 1996 (Vol. No. 28) he digitized *Permophiles* and made it available to the Permian community on the internet adding colored images. Claude encouraged many of his graduate students to publish in *Permophiles* including Tamra Schiappa, Dora Gallegos, Dale Kerner and Michael Dunn. In 2003, Claude stepped down from his position as titular member and became an honorary member.

His relationship with Brian Glenister continued well after he graduated with his Ph.D., serving together on the Permian Subcommittee, traveling to international meetings, and working long hours on figures for publication until they were just right. Claude spent many hours perfecting sutures and reformatting text for the revised treatise on ammonoids. Included in this volume, dedicated to the memory of William Furnish 1912-2007, are systematic descriptions of Carboniferous and Permian ammonoids, prepared by William M. Furnish, Brian F. Glenister, Jürgen Kullmann, and Zhou Zuren. Orders Goniatitida and Prolecanitida are included, along with a stratigraphic range chart to the genus level, references, and index. All the sutures and range charts imaged in this compendium were redrawn and produced by Claude under Brian Glenister's watchful eye.

Claude published and presented over 50 papers in paleontology. Most of his research was dedicated to Permian ammonoids. While at Iowa he developed research relationships with fellow colleagues William Nassichuk and Bruce Saunders, coauthoring research papers on North American Permian ammonoids and the *Nautilus* cf. *N. pompilius* from the Pacific Ocean around Palau, respectively. William Nassichuk and Claude spent several research expeditions together on Ellesmere, Island resulting in several publications (Nassicuk and Spinosa, 1970; 1972). Claude also spent many summers traveling to Palau to trap and tag Nautilus, to understand their life habits and develop a better understanding of ammonoids. This research resulted in many co-authored papers on topics including sexual dimorphism (Saunders and Spinosa, 1978), predation (Saunders, Spinosa, and Davis, 2010), and migration patterns (Saunders and Spinosa, 1979). His research excursions to Palau piqued his curiosity and he developed a small, closed-circulation aquarium at Boise State that was designed to observe nautilus behavior and to help educate students about research (Spinosa, 2010). Claude also studied ammonoids found closer to home. He spent many hours conducting field trips to Nevada and to eastern Idaho to study



Claude with Brian Glenister, Tatyana Leonova, and student, in Aktubinsk, during summer 1991 field conference.



Claude and Jean Spinosa at dinner during 1999 Sardinia field conference.



Claude with Tamra Schiappa at Lake Pend Oreille, Sandpoint, Idaho in 2016.



Claude on Lake Pend Oreille, Sandpoint, Idaho.

Permian ammonoids faunas. He involved many undergraduate and graduate students in these research endeavors resulting in several theses and publications on Permian ammonoid taxonomy (e.g., Spinosa et al., 1991; Spinosa and Nassichuk, 1994; Schiappa et al., 1995, Schiappa, 1993; Hemmesch, 2004). In addition, he fostered many senior and graduate theses on regional biostratigraphy and stratigraphy of the southern Urals and Nevada.

After retiring, Claude continued to teach for BSU and interact with his colleagues and students. Eventually he moved to northern Idaho to live in the house he and Jean built on Lake Pend Oreille. Claude loved spending time with his brother, Bob, his three sons, John, Mike and Dan, his daughters-in-law and grandchildren. Over the years, he spent countless hours camping and fishing with his sons and friends, and always had a good story about one of his adventures to share. He loved entertaining friends and family and was very generous with his time. Many a home-cooked meal was shared with fine wine around the table with Claude discussing the Permian, the latest politics, a good book, a fishing tale, or proper ways to peel garlic or prepare the

pasta. Claude was a teacher, advisor, mentor, colleague, and friend to so many people that it is difficult to capture that feeling in writing. He is deeply missed by many.

References

- Davydov, V.I., Glenister, B.F., Spinosa, C., Ritter, S.M., Chernykh, V. V., Wardlaw, B.R. and Snyder, W.S., 1995. Proposal of Aidaralash as GSSP for the Base of the Permian System, *Permian*, no. 26, p.3–9.
- Glenister, B. F., Wardlaw, B. R., Lambert, L. L., Spinosa, C., Bowring, S.A., Erwin, D.H., Menning, M. and Wilde, G.L., 1999. Proposal of Guadalupian and Component Roadian, Wordian and Capitanian Stages as International Standards for the Middle Permian, *Permian*, no. 34, p. 3–11.
- SeriesThe Guadalupian: Proposed International Standard for a Middle Permian Series: *International Geology Review*, v. 34, p. 857–888.
- Hemmesch, N. T., 2004. The Cisuralian Ammonoid Genus *Uraloceras*, Unpubl. (Masters Thesis, Boise State University).
- Nassichuk, W. W., and Spinosa, C., 1970. *Helicoprion* sp., a Permian elasmobranch from Ellesmere island, Canadian Arctic. *Journal of Paleontology*, v. 44, no. 6, p. 1130–1132.
- Nassichuk, W. W., and Spinosa, C., 1972. Early Permian (Asselian) ammonoids from the Hare Fiord Formation, northern Ellesmere Island. *Journal of Paleontology*, v. 46, no. 4, p. 536–544.
- Saunders, W. B., and Spinosa, C., 1978. Sexual dimorphism in *Nautilus* from Palau. *Paleobiology*, v. 4, no.3, p. 349–358.
- Saunders, W. B., and Spinosa, C., 1979. *Nautilus* movement and distribution in Palau, western Caroline Islands. *Science*, v. 204 (4398), 1199–1201.
- Saunders, W. B., Spinosa, C., and Davis, L. E., 2010. Predation on *Nautilus*. In *Nautilus* Springer, Dordrecht, p. 201–212.
- Schiappa, T. A., 1993. Selected Early Permian ammonoids from Portuguese Springs, White Pine County, Nevada. Unpubl. (Master's thesis, Boise State University).
- Schiappa, T. A., Spinosa, C., and Snyder, W. S., 1995. *Nevadoceras*, a new Early Permian *Adrianitid* (Ammonoidea) from Nevada. *Journal of Paleontology*, v. 69, no. 6, p. 1073–1079.
- Spinosa, C., 1968. The *Xenodiscidae*, Permian otoceratacean ammonoids. Unpubl. (Doctoral dissertation, Ph. D. dissertation, Univ Iowa).
- Spinosa C., 2010. A Small, Closed Aquarium System for *Nautilus*. In: Saunders W.B., Landman N.H. (eds) *Nautilus. Topics in Geobiology*, v. 6. Springer, Dordrecht. p. 585–594.
- Spinosa, C., Furnish, W. M., and Glenister, B. F., 1975. The *Xenodiscidae*, Permian Ceratitoid Ammonoids. *Journal of Paleontology*, v. 49 (2), p. 239–283.
- Spinosa, C., and Nassichuk, W. W., 1994. The Permian ammonoid *Demarezites Ruzhencev* from the Phosphoria Formation, Idaho. *Journal of Paleontology*, v. 68 (5), p. 1036–1040.
- Spinosa, C., Nassichuk, W. W., Snyder, W. S., and Gallegos, D. M., 1991. Paleogeologic implications of high latitude and middle latitude affinities of the ammonoid *Uraloceras* in Cooper, J.D. and Stevens, C. H.(eds). *Paleozoic*,

- Paleogeography of the Western United States -Vol. II, Pacific Section, SEPM, v. 67, p. 839–846.
- Levin, Harold L. and King, David T., 2016. *The Earth Through Time*, 11th edition, Wiley Publishing, 608 pages.
- Seldon, Paul A. (ed.) 2009. *Treatise on Invertebrate Paleontology: Part L (Revised) Mollusca 4, v. 2, Carboniferous and Permian Ammonoidea*, 258 p.
-

SUBMISSION GUIDELINES FOR ISSUE 73

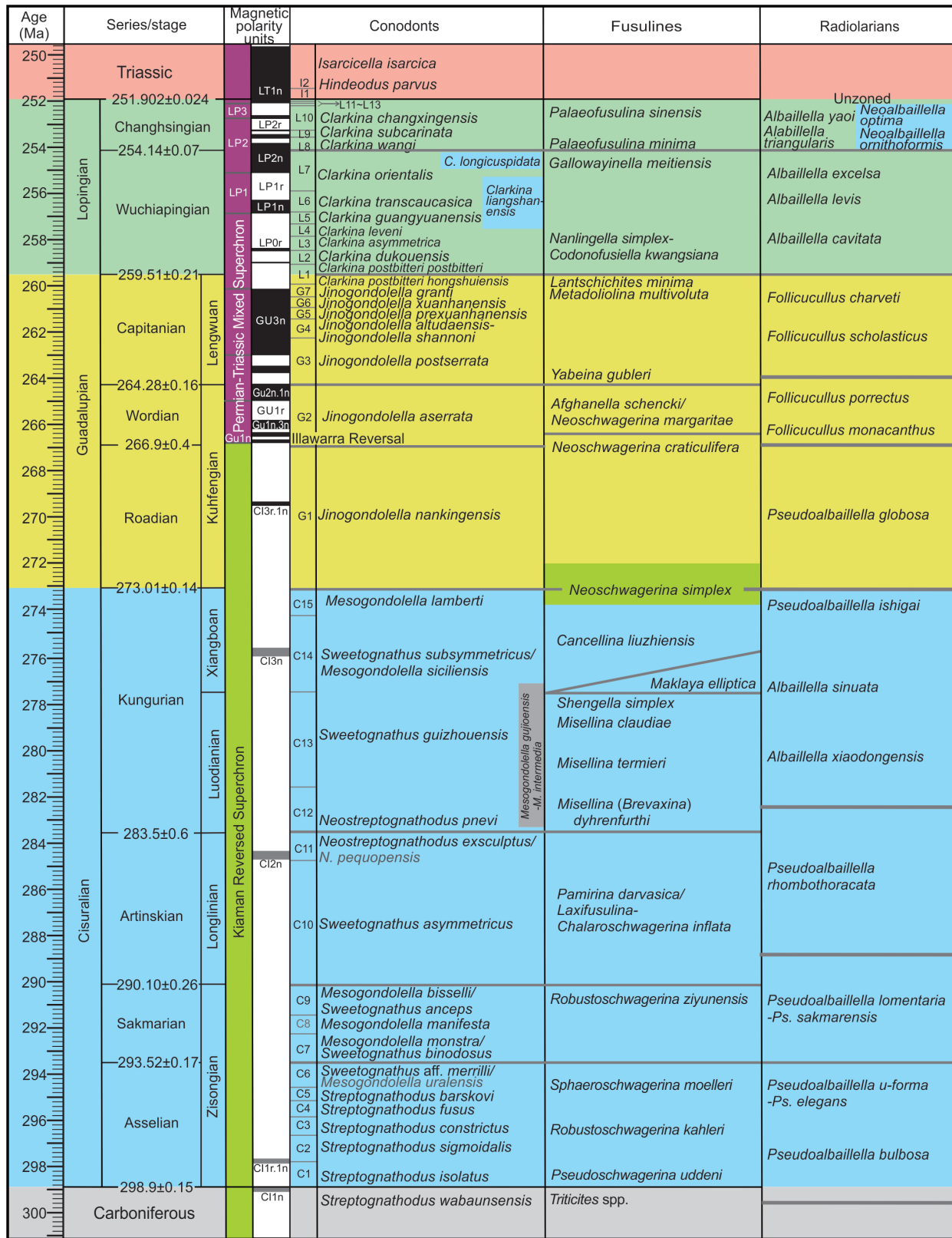
It is best to submit manuscripts as attachments to E-mail messages. Please send messages and manuscripts to Yichun Zhang's E-mail address. Hard copies by regular mail do not need to be sent unless requested. To format the manuscript, please follow the TEMPLATE that you can find on the SPS webpage at <http://permian.stratigraphy.org/>.

Please submit figures files at high resolution (600dpi) separately from text one. Please provide your E-mail addresses in your affiliation. All manuscripts will be edited for consistent use of English only.

Prof. Yichun Zhang (SPS secretary)

Nanjing Institute of Geology and Palaeontology, Chinese Academy of Sciences, Nanjing, Jiangsu, 210008, P.R.China, Email: yczhang@nigpas.ac.cn

The deadline for submission to Issue 73 is July, 31th, 2022



High-resolution integrative Permian stratigraphic framework (after Shen et al., 2019. Permian integrative stratigraphy and timescale of China. Science China Earth Sciences 62(1): 154-188. Guadalupian ages modified after (1) Shen et al., 2020. Progress, problems and prospects: An overview of the Guadalupian Series of South China and North America. Earth-Science Reviews, 211: 103412 and (2) Wu et al., 2020, High-precision U-Pb zircon age constraints on the Guadalupian in West Texas, USA. Palaeogeography, Palaeoclimatology, Palaeoecology, 548: 109668. Lopingian ages modified after Yang et al., 2018, Early Wuchiapingian cooling linked to Emeishan basaltic weathering? Earth and Planetary Science Letters, 492: 102-111.